UNIVERSIDADE DE LISBOA
FACULDADE DE CIÊNCIAS

Effect of major Cenozoic palaeoceanographic events on coccolithophore morphotypes: climatically induced changes in *C. pelagicus* s.l. (CliMorph)

" Documento Definitivo"

Doutoramento em Ciências do Mar

Gonçalo Abreu Prista

Tese orientada por:
Professor Doutor Mário Cachão
Doutora Áurea Narciso

Documento especialmente elaborado para a obtenção do grau de doutor

2018

UNIVERSIDADE DE LISBOA
FACULDADE DE CIÊNCIAS

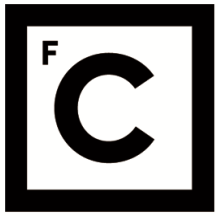

Ciências
ULisboa

Effect of major Cenozoic palaeoceanographic events on coccolithophore morphotypes: climatically induced changes in *C. pelagicus* s.l. (CliMorph)

Doutoramento em Ciências do Mar

Gonçalo Abreu Prista

Tese orientada por:

Professor Doutor Mário Cachão
Doutora Áurea Narciso

Júri:

Presidente:

- Doutora Maria da Conceição Pombo de Freitas, Professora Catedrática, Faculdade de Ciências da Universidade de Lisboa

Vogais:

- Doutora Giuliana Villa, Professore Associato, Dipartimento di Scienze Chimiche, della Vita e della Sostenibilità Ambientale da Università degli Studi di Parma (Itália)
- Doutora Maria Teresa Drago Pereira, Investigadora Auxiliar, Instituto Português do Mar e da Atmosfera (IPMA)
- Doutora Anabela Tavares Campos Oliveira, Técnica Superior, na qualidade de individualidade de reconhecida competência na área científica, Instituto Hidrográfico
- Doutor Mário Albino Pio Cachão, Professor Associado com Agregação, Faculdade de Ciências da Universidade de Lisboa (orientador)
- Doutora Ana de Jesus Branco de Melo de Amorim Ferreira, Professora Auxiliar, Faculdade de Ciências da Universidade de Lisboa

Documento especialmente elaborado para a obtenção do grau de doutor

Fundação para a Ciência e Tecnologia do Ministério da Ciência, Tecnologia e Ensino Superior SFRH/BD/95593/2013

2018

To my family, thank you so much for your support, and especially to my sons, sorry for every time dad was away, physically or emotionally…

ACKNOWLEDGMENTS

I start by thanking Verónica, my wife. It wasn't always easy, especially because we were both doing a PhD. But somehow we managed, while bringing two new souls to this world! Thank you for the support, for the good and the bad moments, for sharing this road with me.

Now I need to thank my parents. Without them this wouldn't be possible. Not only for their occasional help with daily routines, and for their encouragement, but also for the financial support, something that is more or less indispensable for a PhD student in Portugal.

I need to thank Professor Jorjintje Henderiks of the Uppsala University, Sweden, for the Eocene-Oligocene transition samples and for being available to receive me for a short period in her lab. Six weeks of learning, experiencing a completely different way of living and working in academia. Thank you.

To Professor Giuliana Villa, from the University of Parma, a special thanks! I can only regret not being able to stay there for a longer period. I truly felt at home there. Thank you for your kindness, for your teachings and, of course, for the Miocene samples. I also extend my thanks to Giovanna Ianelli who so kindly prepared all the samples and always met me with a wonderful smile. Grazie Giovanna.

A special thanks to Silvério Figueiredo, Centro Português de Geo-História e Pré-História and Professor at Instituto Politécnico Tomar, for the time spent measuring 4.000 coccoliths just to test a hypothesis.

I want to thank Professor Ana Amorim from the University of Lisbon who was always available to help with my PhD project, for giving me access to the Algoteca, and for sharing her incredible knowledge on algae biology. Also to Vera Veloso who gave support to my coccolithophores cultures, taught me how to prepare and maintain them, allowing for my culture experiences to be viable.

To my colleagues Catarina Guerreiro, who stayed for a short period at the nanolab, for the great conversations and for sharing an excellent TV taste, and Sofia Pereira, for the stress release talks in the paleolab. I have an enormous respect for you Sofia!

Katia and Gianluca! Grazie dal profondo del mio cuore! I couldn't imagine or expect nothing even close to these guys to receive me in Parma! Thank you Katia for all your support at the University, and to both of you for showing me around and for not letting me procrastinate at home! I'm the one failing now, but in 2019 I won't fail to visit you!

To my cousin/brother/oldest friend Rogério: thank you for all the motivation you gave me, for being an inspiration in so many aspects and for pushing me forward in the difficult moments. And we know they were a few. Obrigado meu irmão!

To Zé thank you so much for precious moments during these past years, and for always keeping my mind sharp! You truly know how to stimulate critical thinking. You were also crucial to my beekeeping adventure, sharing it with me, which has become my mind therapy and way of keeping sane. Thank you my brother!

I cannot forget my graduation companions and long time friends Fernando and Renato. They also did the PhD journey recently and I hope I help them as much as they helped me. They have been helping me since our first year of the graduation, even when they don't even realise.

It would be impossible to forget Professor Rui Agostinho, my former master thesis co-supervisor. Thank you Professor for your energy, your help with models ideas, with the computer, and so many other things. You're someone I look up to since we started working together back in 2010.

I saved my supervisors for last on purpose. I have the privilege of working with Professor Mário Cachão since 2010. He was one of my master thesis supervisors and since then I have learned a lot. In the end I'm starting to think he has gained more then me, after all he managed to pull me from Sirenia into these invisible unicellular algae… Lets just say that he won this round, but we will get back to the big league! Thank you for everything Professor. I consider myself extremely lucky for having you not only as a supervisor, but also as a Professor for so long.

Finally to my co-supervisor Áurea Narciso, PhD. I will always regard you not only as an astonishing professional, but most of all as a human being of extremely rare qualities. You have an amazing scientific richness, great teaching qualities and an assertive soul. You were my PhD guardian angel. Thank you so much for everything.

Gonçalo Abreu Prista foi bolseiro de doutoramento da Fundação para a Ciência e Tecnologia do Ministério da Educação e Ciência.

SFRH/BD/95593/2013

Summary

The Cenozoic (past 65 Ma) is characterized by an overall cooling climatic trend punctuated by warming events. The biosphere underwent progressive adaptations towards a cooler world while also being affected by periods of global warming. Thus, the Cenozoic emerges as a fundamental time interval to study how species respond to opposite trends of climate change.

Coccolithophores constitute a major component of planktonic communities throughout the world's oceans, being among the main primary producers, and playing a distinct role in the oceans' ecosystems. They're a good proxy on palaeotemperature estimation, have a significant role on the global carbon and sulphur cycles, which arises from the fact that they're among the most important pelagic calcifying organisms in the modern ocean, accounting up to 20% of total carbon fixation.

Biological populations evolve with respect to the distribution of organism size and other phenotypic traits by differential fitness. How a phenotypic character like body size evolves over time and what environmental factors influence phenotypic change are fundamental questions of biology and palaeontology.

Coccoliths are produced intracellularly, so that their final proportions are attained prior to being extruded to the coccosphere. The size of coccoliths, preserved in the fossil record, is therefore an intrinsic property of a particular (morpho)species or ecophenotype.

Coccolith morphometry has great potential in palaeoceanographic studies addressing questions such as taxonomy, biostratigraphy and palaeoecology of calcareous nannoplankton.

In this work a new tool – IMMA – was developed to study microevolution on coccolithophores, having *C. pelagicus* s.l. as targeted species. With more than 60 Ma of evolution and a wide geographic distribution, this coccolithophore species is ideal for studies of microevolution on coccolithophores. Its morphotypes can be related to a variety of palaeoceanographic conditions.

IMMA allowed for the observation of *C. pelagicus* s.l. morphological plasticity in high-resolution Quaternary samples, and provided interesting resulting in older Cenozoic periods, opening new important discussions on coccolithophores morphometry.

Keywords: Coccolithophores; *Coccolithus pelagicus* s.l.; Morphometry; Microevolution; Morphological plasticity; Cenozoic; IMMA

Resumo

Os cocolitóforos (divisão Haptophyta) cobrem as suas células com estruturas calcárias (os cocólitos) pelo menos durante uma fase do seu ciclo de vida. Estas algas marinhas originaram-se no final do Triásico (~225 milhões de anos), evoluindo desde então e compreendendo hoje aproximadamente 200 morfospécies na subclasse monofilética Calcihaptophydae. Têm um dos mais abundantes e contínuos registos fósseis desde há ~225 milhões de anos, o que os torna em ferramentas ideais para estudos de biostratigrafia, evolução e paleoceanografia em sedimentos do Mesozoico e do Cenozoico.

Os cocolitóforos são uma das componentes principais das comunidades planctónicas dos oceanos, estando entre os principais produtores primários e desempenhando um papel particular nos ecossistemas, especialmente no seu envolvimento nos ciclos do enxofre e do carbono. Sendo dos mais importantes organismos pelágicos calcários têm um papel directo nas trocas gasosas oceano-atmosfera, podendo ser responsáveis pela fixação de 20% do carbono nalguns sistemas. Os cocólitos são produzidos intracelularmente, o que significa que as suas dimensões finais são adquiridas antes de serem expelidos da célula para a cocosfera. O tamanho dos cocólitos é desta forma uma propriedade intrínseca de uma particular morfoespécie ou ecofenótipo.

As populações biológicas evoluem em relação à distribuição do tamanho do organismo e outras características fenotípicas por aptidão diferencial. Um caractere fenotípico como o tamanho corporal evolui ao longo do tempo. Que factores ambientais influenciam mudanças fenotípicas são questões fundamentais da Biologia e, quando aplicada ao registo fóssil, da Paleontologia.

Coccolithus pelagicus s.l. está presente no registo fóssil desde o início do Cenozoico (Paleocénico inferior) e, na actualidade, o seu tamanho foi já demonstrado estar relacionado geneticamente com duas subespécies existentes, uma mais pequena *C. pelagicus* ssp. *pelagicus* (<10μm) e outra maior *C. pelagicus* ssp. *braarudii* (>10μm). Isto significa que a morfometria dos cocolitóforos pode ser usada como um proxy para a sua variabilidade genética ao longo do registo fóssil. O foco na morfometria permite assim abordar questões de paleoecologia e evolução deste grupo.

A morfometria de cocólitos tem um enorme potencial em estudos paleoceanográficos, desde questões de taxonomia, à biostratigrafia ou à paleoecologia, tal como tem sido demonstrado por diversos trabalhos. No caso da taxonomia de cocolitóforos fósseis

esta é de facto baseada fundamentalmente na morfologia da fase heterococolítica do ciclo de vida e, ao nível da espécie, em pequenas ou micro variações do tamanho e forma.

O tamanho dos cocólitos é relevante nas rotinas de identificação de certas espécies de nanofósseis calcários. Mas foi também demonstrado o potencial de diferentes morfótipos como *proxies* para a influência de massas de água e correntes oceânicas distintas. Ou ainda o diâmetro das cocosferas como reflexo de comportamentos de crescimento num estudo com Coccolithus sp. do Paleocénico-Eocénico.

Apesar do uso transversal da morfometria em estudos de paleoceanografia, a metodologia habitual, devido ao seu carácter empírico, apresenta limitações no que respeita observações genéticas/evolucionárias em curto espaço de tempo. Ou seja, a plasticidade de uma dada espécie para responder/adaptar-se a perturbações climáticas. Acrescenta-se as estas limitações o facto de os estudos actuais não estarem estruturados para observar reacções das espécies a eventos climáticos a escalas temporais curtas.

Com o potencial para a taxonomia ou a biostratigrafia bem explorado e já bem implementado, estão criadas as condições para avançar evolutivamente na morfometria. E esta, apesar de estar a ser usada para caracterizações mais gerais das morfoespécies, pode também ser uma ferramenta para estudar a sua plasticidade morfológica.

A tecnologia actual aplicada a imagens obtidas de microscópios ópticos ou electrónicos permite estimar tamanhos pelo menos até à décima do micrómetro. No entanto continua a ser comum nos métodos de morfometria categorizar os cocólitos em intervalos morfométricos de 1μm, definindo os limites dos morfótipos à unidade. Esta resolução à unidade não parecer ser suficiente para observar padrões de microevolução em morfoespécies, tanto no registo fóssil como em amostras actuais. Efectivamente diversos estudos têm demonstrado variações à décima do micro como resposta a pressões ambientais por parte dos cocolitóforos.

O Cenozoico corresponde aos últimos 65 milhões de anos e é caracterizado por uma tendência global de arrefecimento, pontuada por eventos de aquecimento. A biosfera passou por adaptações progressivas afectas ao arrefecimento, enquanto teve de ser capaz de lidar com períodos de aquecimento. Desta forma o Cenozoico emerge como um intervalo de tempo fundamental em estudos às respostas de espécies e ecossistemas a forçamentos opostos da evolução climática.

Com mais de 60 milhões de anos de evolução e uma distribuição geográfica ubíqua, Coccolithus pelagicus (Wallich) é uma espécie ideal para estudos desta natureza. Presente ao longo de todo o Cenozoico, os morfótipos desta alga marinha calcária unicelular têm sido relacionados com diversas condições paleoceanográficas.

Um novo método, denominado Integrated Multivariate Morphon Analysis (IMMA) é proposto neste trabalho para a determinação de morfótipos com uma resolução de 0,1μm. Os resultados são validados por modelos de populações teóricas geradas. Ao aumentar a resolução na definição dos limites dos morfótipos, este novo método mostra potencial para documentar padrões de microevolução em cocolitóforos e permite o uso dos cocólitos para seguir alterações paleoambientais em escalas temporais curtas.

Após a construção do modelo com base em populações teóricas utilizou-se o IMMA para reanalisar dados de *Coccolithus pelagicus* s.l. de duas amostragens do Holocénico e uma que cobre desde o Miocénico Superior até ao Holocénico. Os resultados sugerem que tanto *C. pelagicus* ssp. *braarudii* como *C. pelagicus* ssp. *pelagicus* apresentam plasticidade morfológica em resposta a alterações paleoambientais, principalmente variações do regime de afloramento costeiro na costa oeste de Portugal e das condições paleoceanográficas no Atlântico Norte associadas a períodos glaciares.

O IMMA foi aplicado também a dois conjuntos de amostras, um da Transição Eocénico-Oligocénico (TEO) e outro no Óptimo Climático do Miocénico e sua transição (OCM+T), na procura de respostas às inúmeras dúvidas sobre as adaptações e respostas do *C. pelagicus* s.l. à evolução climática do Cenozoico. Este método foi capaz de produzir dados morfométricos coerentes com o conhecimento actual da morfometria do *C. pelagicus* s.l.. No entanto devido à baixa resolução e ao reduzido número de amostras, não foi observada plasticidade morfológica além de variações aritméticas simples (média, mediana, máximo, mínimo).

No caso do TEO o intervalo coberto pelas amostras teve também influência nos resultados, já que estas estavam totalmente dentro do(s) evento(s) climático(s). Obter mais amostras para aumentar a resolução ou para estender o intervalo coberto aos períodos imediatamente adjacentes à fase de perturbação seria necessário para permitir melhor extracção de informação dos dados e, eventualmente, observar plasticidade morfológica.

O IMMA demonstrou ser capaz de detectar plasticidade morfológica em amostras de alta resolução do Quaternário, bem como microvariações no tamanho dos cocólitos/morfótipos em amostras do EOT ao longo do intervalo estudado. Novos passos foram dados e identificaram-se claramente os futuros passos de forma a solucionar mais problemas em torno de estudos de microevolução com fósseis de nanoplâncton calcário.

Palavras-chave: Cocolitóforos; *Coccolithus pelagicus* s.l.; Morfometria; Microevolução; Plasticidade morfológica; Cenozoico; IMMA

De acordo com o disposto no artigo 31º do Regulamento de Estudos Pós-Graduados da Universidade de Lisboa, Despacho nº 2950/2025, publicado no Diário da República - 2ª Série - nº 57 – 23 de Março de 2015, foram utilizados nesta dissertação resultados incluídos nos seguintes artigos:

Prista, G., Narciso, A., Cachão, M. Integrated Multivariate Morphon Analysis – a new approach into the microevolutionary morphometric patterns of coccolithophores [Manuscript in preparation].

Prista, G., Narciso, A., Cachão, M. Reassessing *Coccolithus pelagicus* s.l. data with IMMA – morphological plasticity of *C. p. braarudii* in the West coast of Portugal [Manuscript in preparation].

Prista, G., Agostinho, R.J., Cachão, M. 2015. Observing the past to better understand the future: a synthesis of the Neogene climate in Europe and its perspectives on present climate change. Open Geosci. 7, 65-83 doi:10.1515/geo-2015-0007

No cumprimento do disposto da referida deliberação, o autor esclarece serem da sua responsabilidade, exceto quando referido em contrário, a execução das experiências que permitiram a elaboração dos resultados apresentados, assim como a interpretação e discussão dos mesmos. Durante o presente doutoramento, foram ainda produzidos resultados incluídos em outros artigos publicados/ submetidos em revistas internacionais, nomeadamente:

Prista, G., Cachão, M. 2019. Use of mussels to study coastal calcareous nannoplankton associations: case study from the West coast of Portugal. J. Nannoplankton Res. Special Issue 4, 55-61

Personal reflection

Academy is the last organized place we have to teach millions of adults to doubt authority, to look things up, to weigh ideas and evidence, to argue in a nonviolent fashion, to do the hard work of changing their own minds […] the academy is also the last place… where truly independent research can be conducted […].
Alice Dreger (2017)

I decided to write this preface because I believe that it is fundamental for everyone, especially for a PhD student, to take the eye patches that narrow the focus and attention into their work and look around, see, reflect and to build a critical view of, at least, their bubble in this world. You can see this as an exercise towards the suggestion placed by Edwards & Roy (2017) in their paper that beyond conventional goals of achieving quantitative metrics, a PhD program should also be viewed as an exercise in building character, with some emphasis on the ideal of practicing science as service to humanity.

It is critical, in my own opinion, that a PhD student develops an idea of what is the present state of science. Not the state of the art of its own field of research, but how science in general is evolving and functioning globally. There is no point in being part of the scientific community and merely specialize yourself in a *nannodot* of knowledge. For societies to properly function and evolve, individuals must have a critical knowledge of it. Otherwise we'll be no more than working ants in a giant colony.

Science is probably the last bastion of true freethinking, but is being swallowed by this *make-money-get-profit* world. Science and scientists are becoming more and more detached from the pure curiosity that once drove them, and they are embracing this notion of profitable science, which means that an idea must first be sold in order to be explored. XXI century scientists need more marketing skills than actual scientific capabilities, since for a scientist to be able to develop research in his field, he must first sell it to get funding. This, of course, comes with a price.

In naturally profitable scientific fields the price is lower, and usually consists on adjusting the direction of a certain study to the best economical outcome. In present market and economic laws this outcome usually fits with lowest possible costs to highest possible value. But what about when there is no direct profit? Fundamental science, for example. To be able to sell it in order to get funding a scientist is

frequently forced to bend or adjust the true reality of it. And it doesn't matter how hard he will then fight to ignore the distortions used in the marketing plan. His focus, his scientific agenda is forever deviated.

We are embracing, in science and as scientists, the same values and rules of the financial markets. We have transformed it into the monetisation of science (see Horton, 2016). This means that no longer the primary goal of science is to increase knowledge for the growth and prosperity of mankind but to obtain profits and be economically strong, under present neoliberal economical principles.

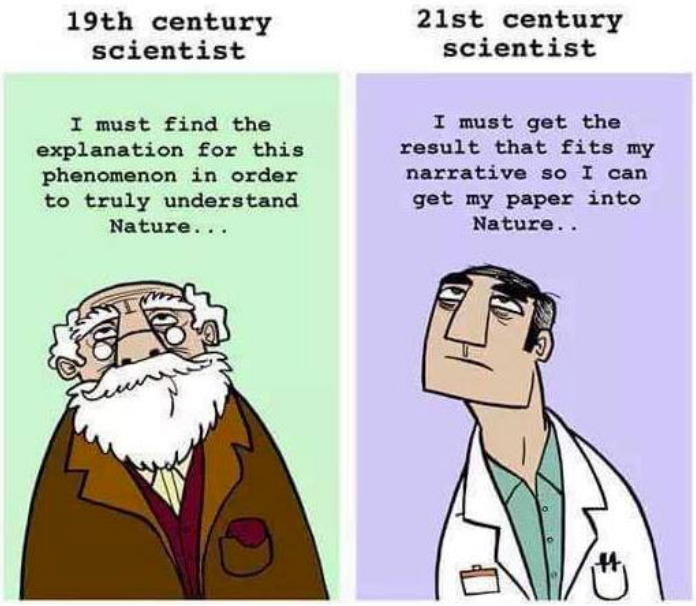

Figure from Pedromics, a creation of Pedro Veliça, researcher at Karolinska Institue, Sweden

We are moving away from what science should be. It is like we, the scientists, decided to forget the teachings of our great predecessors that fought, even when what was expecting them was to be burned alive, for a free thinking and exploration of our Universe, battling against all dogmas and absolute truths.

This view is supported by evidence, like any scientific idea should be. Today it is mainly the number of publications, instead of their quality, that evaluates researchers. This method, which has been growingly criticised, managed to produce some truly disturbing consequences.

Van Noorden (2011) brings the effects of this system during the first decade of the 21st century. Scientific papers publishing increased 44% during this period. However retractions increased by 1.000%! And nearly half of them are for misconduct! The problem is still growing. In 2016 around 650 retractions were accounted, which was similar to 2015 numbers. Unfortunately, instead of meaning it was stabilizing, 2017 closed with over 1.000 retractions (data from Retraction Watch).

The problem of evaluating researchers by their number of publications, and worst, of generating a tremendous pressure on scientists to publish, is not only the increase

of misconduct, but also the decrease of scientific quality. Both Richard Horton and John Ioannidis state that nearly half of what is currently published is most likely untrue (Ioannidis, 2005; Horton, 2015).

Fanelli (2009) published a study with frightening results showing that, on average, 1.97% of scientists admitted to have fabricated, falsified or modified data or results at least once, and up to 33.7% admitted other questionable research practices. In surveys asking about the behaviour of colleagues, admission rates were 14.1% for falsification, and up to 72% for other questionable research practices. It is highly curious to note that misconduct was reported more frequently by medical/pharmacological researchers than others in this study.

But the problem does not end here. Horton (2015) also discusses the responsibilities of the journals and editors in this new publishing reality, with thousands of scientific journals desperate to gain their share of the now highly profitable scientific publishing market. Marcovitch (2010) talks about the effects of Impact Factor for the selection of papers by editors, favouring certain types of studies, known for being highly cited, and neglecting low citable articles regardless of the quality of each.

And what about open access? In principle it is a good idea but the question is how to achieve it. The competition and the primary focus on profits are so deeply entangled that quality, ethics and truth is frequently left aside. Bohannon (2013) gives us the results of submitting a flawed paper to 304 open access journals, with more than half accepting it.

But probably the best deceiving paper ever submitted was the one by Neuroskeptic, a neuroscientist that uses this pseudonym to write a blog in Discovery Magazine. Testing predatory journals, he wrote a paper about midi-chlorians, with references such as Palpatine (1957), and authored by Lucas McGeorge and Annette Kin. In the words of the author, the manuscript is an absurd mess of factual errors, plagiarism and movie quotes. Even so, 4 of the 9 journals that received the manuscript accepted it, and 3 published it online before receiving the publication fees (see http://blogs.discovermagazine.com/neuroskeptic).

“Over the last 50 years the incentives for academic scientists have become increasingly perverse in terms of competition for research funding, development of quantitative metrics to measure performance, and a changing business model for higher education itself. If a critical mass of scientists become untrustworthy, a tipping

point is possible in which the scientific enterprise itself becomes inherently corrupt and public trust is lost, risking a new dark age with devastating consequences for humanity" (Edwards & Roy, 2017). They present an 11-page article on how this new business model academia is putting the very science at risk. In the conclusions they make a series of suggestions that, although defend the values science should stand for, are perhaps a bit naive for modern human society values.

This desperate scenario of obtaining funding and publishing papers generated a completely new scientific communication strategy, which is now putting at risk centuries of work from the scientific community to create trust in the general public. Instead of bringing science to the public, of teaching and sharing knowledge, scientists and the academia are turning into preachers, presenting dogmas and absolute truths, rejecting discussions and using persuasion as a way of spreading the message. This can actually be seen between scientists, with climate science being probably the best example of a scientific field where no longer scientific discussions are tolerated. Either you defend climate change or you're against it. Something I have only seen in religion before…

Fiske & Dupree (2014) talk about this communication problem. Although they use climate science as an example of good communication (and I agree regarding the transmission of the message to the general public), they state, "rather than persuading, we and our audiences are better served by discussing, teaching, and sharing information".

There is in fact a dark path for science that we have already started to cross. From the transformation of science into a business model and the now giant world of scientific publishing, to the pressure and demand over students and researchers, we scientists are the first to be harming science. Maybe we should listen more to the ones that are trying to warn us about future consequences of this road. Maybe we could listen to one of the last great names alive, Peter Higgs. In an interview to The Guardian on December 6, 2013, Higgs told, "today I wouldn't get an academic job. It's as simple as that. I don't think I would be regarded as productive enough". But the Nobel Prize, with only 20 publications in his entire career, did not stop here. He also stated, "it's difficult to imagine how I would ever have enough peace and quiet in the present sort of climate to do what I did in 1964". An interview worth reading.

Claude Huriet said it all in a recent article in European Scientist (2018): scientific publication is not an end in itself. It should not be confused with an advertising approach, let alone comparative advertising in a competitive context. “Content” is supposed to contribute, for cognitive or fundamental research, to the advancement of knowledge, and to the improvement of the human condition, based on what we call applied research.

On a personal experience, I exposed my thoughts on this subject once, during an official PhD evaluation meeting performed by the PhD Evaluation Commission. My inquisitors then asked me if I had rich parents. One should always keep in mind that the problem is never in who makes the rules, but in who obeys.

I wanted to become a scientist for as long as I can remember. Questioning the Universe, exploring our world and digging to understand all that surrounds us is what drives my character since childhood. It breaks my heart to see science and scientists working not to question absolute truths, but yet to create them.

“Science is but a perversion of itself unless it has as its ultimate goal the betterment of humanity.”
Quote unofficially attributed to Nikola Tesla

References

Bohannon, J., 2013. Who’ s Afraid of Peer Review ? Sci. Mag. 342, 60–65. doi:10.1126/science.342.6154.60

Dreger, A., 2017. Take Back the Ivory Tower - democracy depends on having a public capable of thinking. Chron. Rev. - Chron. High. Educ. 1–12.

Edwards, M.A., Roy, S., 2017. Academic Research in the 21st Century: Maintaining Scientific Integrity in a Climate of Perverse Incentives and Hypercompetition. Environ. Eng. Sci. 34, 51–61. doi:10.1089/ees.2016.0223

Fanelli, D., 2009. How many scientists fabricate and falsify research? A systematic review and meta-analysis of survey data. PLoS One 4. doi:10.1371/journal.pone.0005738

Fiske, S.T., Dupree, C., 2014. Gaining trust as well as respect in communicating to motivated audiences about science topics. Proc. Natl. Acad. Sci. 111, 13593–13597. doi:10.1073/pnas.1317505111

Horton, R., 2015. Offline: What is medicine’s 5 sigma? Lancet 385, 1380. doi:10.1016/S0140-6736(15)60696-1

Horton, R., 2016. Offline: The crisis in scientific publishing. Lancet 388, 322. doi:10.1016/S0140-6736(16)31132-1

http://blogs.discovermagazine.com/neuroskeptic/2017/07/22/predatory-journals-star-wars-sting/#.W3VE-dhKjYV (accessed August 16th 2018)

https://www.theguardian.com/science/2013/dec/06/peter-higgs-boson-academic-system (accessed August 15th 2018)

Huriet, C., 2018. Publish or perish: How to burst the bubble of scientific publication inflation? 20th September 2018 https://www.europeanscientist.com/en/features/publish-or-perish-how-to-burst-the-bubble-of-scientific-publication-inflation/

Ioannidis, J.P.A., 2005. Why most published research findings are false. PLoS Med. 2, 0696–0701. doi:10.1371/journal.pmed.0020124

Marcovitch, H., 2010. Editors, publishers, impact factors, and reprint income. PLoS Med. 7, 7–8. doi:10.1371/journal.pmed.1000355

Van Noorden, R., 2011. Science publishing: The trouble with retractions. Nature 478, 26–28. doi:10.1038/478026a

PREFACE

The Earth is a tiny insignificant dot in the Universe with a precious (and rare – at current knowledge) cargo: life! Among the millions of species that evolved in this small planet over the past 3.77 (or 4.28) billion years (Dodd et al., 2017), one has dedicated the last few thousand years trying to understand this apparent rare organisation of matter. Having appeared in the final seconds of the one-year Universe calendar, *Homo sapiens* took its curiosity beyond any other species on Earth and has unlocked several mysteries about life emergence and evolution.

Our focus and need to understand our world and the Universe, i.e., to comprehend the Cosmos, lead us from the geocentric and God creation to the infinite Universe and evolution. Although there are many names to remember and thanks for this social and culture change, like several thinkers of the Ancient Greek, or disperse scientists of Medieval and Renascent Europe, most of all with need to be grateful to all mankind. In the end it is the work of every single being that define society direction and promote its evolution.

In fact, societies evolution is not so different from biological evolution. Societies are a living super organism, constantly changing and under continuous pressure, which, from time to time, faces a more turbulent period. We tend to call them revolutions. In truth, these are periods of adaptation and evolution, when something gets "extinct" and something new emerges (with human societies nothing gets truly extinct, because culture makes sure that nothing gets completely lost). Just like Earth: a dynamic planet, continuously changing, where species are under permanent environmental pressure, facing periods of great challenge to life. These periods are in fact the moments when life is put to test and species must, by facing extinction, demonstrate their adaptation skills, i.e., their plasticity[1].

How species adapt and evolve in a continuously changing environment is probably the question that gave birth to biology as a scientific field. Nearly 160 years after Charles Darwin (1809-1882) and Alfred Russel Wallace (1823-1913) discussions and publications, and over 200 years after Jean Baptiste Lamarck (1744-1829) hypothesis,

[1] In life also, nothing gets truly extinct. A species may disappear, even a family or an entire group, but the evolutionary traits continue. Otherwise there would be extremely more profound differences between species and the recovery from major extinction events would not only take more time, but it would produce results far different from the previous life forms.

studies regarding evolution and adaptation of species are still a major area in biology, with the increase in scientific knowledge generating some answers and many new questions.

I. GENERAL INTRODUCTION

CHAPTER 1

General Introduction, Work Objectives and Thesis Organization

1.1 Introduction

Understanding evolution demands studies of both current and past species. This requires the skills and focus of different disciplines, Biology and Geology. Present species are almost strictly the Biology goal while past species, which evidences are brought to us as fossilized remains (body fossils) or evidences of their activity (trace fossils) are the focus of Palaeontology, a field that merges Geology with Biology.

Coccolithophores, unicellular algae that cover their cells with calcified scales (coccoliths), are commonly subjected to evolutionary studies since it presents an almost continuous fossil record since the limit between the Triassic to the Jurassic (Bown et al., 2004) with several taxa appearing along the Cenozoic epochs, many still extant, making them ideal tools for biostratigraphic, evolutionary and palaeoceanographic studies of Mesozoic and Cenozoic sediments (see references in Frada et al., 2010). They currently comprise ~200 morphospecies within the monophyletic subclass Calcihaptophycidae (de Vargas et al., 2007).

Thus, coccolithophores are able to provide good and consistent (micro)fossil data (Micropalaeontology), together with extant living data (Biology). They are also short life cycle organisms, meaning short time generations, an advantage for Biology that is able to observe adaptations to environmental changes, either in lab cultures (Daniels et al., 2014; Sheward et al., 2014, 2016) or in the field (Renaud & Klaas, 2001), but a disadvantage for Palaeontology, since morphological responses to environmental changes in short time periods raise a challenge regarding samples resolution. As shown in previous works (e.g. Reitan et al., 2012), the long-term Cenozoic record does not reveal any influence of long-term climate change on morphology of *Cocolithus pelagicus*, although morphological and palaeogeographical changes are

observed in the fossil record. This raises the question at what time scales would climate have an effect, if not on a million-year time scale? This is certainly due to short life cycle/generation time, which would imply, assuming a capable genetic plasticity, adaptations on a much shorter (biological) time scale.

Although the generation time presents a great challenge for palaeontological evolutionary studies in coccolithophores, the continuous fossil record together with the several extant species are major advantages that define this group as a strong choice for this type of work. Moreover, there are many species present today that have an abundant and continuous fossil record since different Cenozoic epochs.

Coccolithophores constitute a major component of planktonic communities throughout the world's oceans. They are currently very fashionable among climate scientists, being among the main open ocean primary producers, and playing a distinct role in the oceans' ecosystems (see Balch, 2018 for a review). They're a good proxy on palaeotemperature estimation (e.g. Henderiks & Bollmann, 2004) and also have a significant role on the global carbon and sulphur cycles (and therefore climate regulation) through direct involvement in ocean-atmosphere gas exchange (Malin & Steinke, 2004), which arises from the fact that they're among the most important pelagic calcifying organisms in the modern ocean (Baumann et al., 2005), accounting up to 20% of total carbon fixation in some systems (Poulton et al., 2007). However, although information on the life cycle of coccolithophores has increased in recent decades, it still lags considerably behind the state of knowledge for other important marine phytoplankton, notably the diatoms and the dinoflagellates, as pointed out by Frada et al. (2018).

Coccolithus pelagicus s.l. is one of the most interesting species that evolved during the Cenozoic. Its fossil record appears since the beginning of the Cenozoic (65 million years ago) and still thrives in the oceans today, namely off the Portuguese coast. This means that due to its genetic plasticity, *C. pelagicus* s.l. managed to survive and adapt to several dramatic changes that occurred since the extinction of the non-avian Dinosaurs, namely the Palaeocene-Eocene Thermal Maximum (see Sexton et al., 2011; Cope & Winguth, 2011), the Eocene Optimum Climates (see Höntzsch et al., 2011; Barke et al., 2012; Witkowski et al., 2012), the Eocene-Oligocene Transition and the beginning of the Antarctic glaciations (see DeConto et al., 2008; Héran et al., 2010; Cotton & Pearson, 2011; Houben et al., 2012), the Miocene

Optimum Climate (see Böhme, 2003; You et al., 2009; Böhme et al., 2011; Prista et al., 2015) and the beginning of the North Hemisphere continental glaciations and the present Glacial Era (see Raymo 1994; DeConto et al., 2008; Naafs et al., 2010), to name the most important and with global impact events (see Zachos et al., 2001, 2008 for a broad discussion on Cenozoic climate events).

Biological populations evolve both the geno- and the phenotype. In this last case it may include the organism size in addition or separate from other morphological traits by differential fitness. How a phenotypic character like body size evolves over time and what environmental factors influence phenotypic change are fundamental questions of Biology and crucial in Palaeontology (Reitan et al., 2012).

Coccolithophores produce two types of coccoliths: heterococcoliths and holococcoliths. The first are formed of crystal-units of variable shape and size, typically arranged in cycles with radial symmetry, while the last are coccolith formed of numerous minute (<0.1 μm) crystallites, all of which may, or may not, be identical (Braarud et al., 1955). Heterococcoliths are typical of the nonmotile diploid stage, while holococcoliths occur in the haploid motile form, but asexual reproduction can occur in both stages (see Taylor et al., 2017; Balch, 2018 for reviews).

Heterococcoliths are produced intracellularly, so that their final proportions are attained prior to being extruded to the coccosphere. The size of heterococcoliths, preserved in the fossil record, is therefore an intrinsic property of a particular (morpho)species or ecophenotype (e.g. Westbroek et al., 1994; Young et al., 1999; Young & Henriksen, 2003).

Coccolithus pelagicus s.l. is present throughout the entire Cenozoic and its size was demonstrated to be genetically related to different subspecies, with a present-day smaller form *C. pelagicus* spp. *pelagicus* and an intermediate form *C. pelagicus* spp. *braarudii* (Saez et al., 2003; Vargas et al., 2004). This means that morphometry of coccolithophores can be used as a proxy of their genetic variability along the fossil record. Focusing on morphometrics, both palaeoecology and evolution of coccolithophores can be addressed simultaneously (e.g. Read et al., 2013). Thus, coccolith morphometry has great potential in palaeoceanographic studies to address taxonomy, biostratigraphy and palaeoecology of calcareous nannoplankton.

Previous work on *C. pelagicus* s.l. revealed the importance of its coccolith morphometry. Morphotypes have been shown to have potential as a

palaeoceanographic proxy for the influence of distinct ocean water masses, currents and oceanographic mechanisms (Parente et al., 2004). More recently, fossil *Coccolithus* sp. was used to show that the diameter of coccospheres also provides a powerful tool for interpreting growth behaviour during the Palaeocene-Eocene (Gibbs et al., 2013). The latter study also pointed to the possibility of low adaptation capability to abrupt environmental disturbances.

Although morphometry has been widely used in palaeoceanographic studies, the usual methodology, due to its discrete empirical nature, shows limitations regarding short-term genetic/evolutionary observations, i.e. the fast-evolving plasticity of a certain species to respond/adapt to climate perturbations. Arising from these limitations, present studies don't allow observation of how a certain species reacts to short-scale climatic events, meaning that current methodologies for fossil record data are limited in extracting morphological plasticity data. Most statistical methods, varying from simple histogram analysis (e.g. Mattioli et al., 2004; Thibault, 2010) to more complex mixture analysis (e.g. Suchéras-Marx et al., 2010), don't allow the identification, at least not without significant assumptions (e.g. normal distribution) on the morphological pattern of the potential different morphotypes within a population. To address this limitation a multivariate statistical morphometrical tool (MMA) was developed to identify different placolith morphotypes regarding maximum coccolith length in the Quaternary and applied to Quaternary Northeast Atlantic offshore *C. pelagicus* s.l. data (Parente et al., 2004; Narciso et al., 2006) (see Fig. 1.1 regarding types of coccoliths and *C. pelagicus* s.l. morphometry).

Summarizing, *C. pelagicus* s.l. was selected to be the focus of this work due to its presence since the beginning of the Cenozoic until today, its good morphometric knowledge, the fact that it is robust and easily distinguished in calcareous nannoplankton samples, as well as current knowledge that shows morphological differences and responses of this species to environmental changes and conditions.

An also important concept to define is plasticity. According to Price et al. (2003) different environments directly induce changes in an individual's behaviour, morphology and physiology. Such changes are collectively termed phenotypic plasticity.

It is widely acknowledged that recent global changes in climate have had notable effects on the behaviour and distribution of numerous plant and animal species (e.g.

Parmesan & Yohe, 2003; Root et al., 2003; Thomas et al., 2004). This means that adaptive phenotypic plasticity can work in very short time scales. For example, Charmantier et al. (2008) studied the phenotypic adaptations of *Parus major* in the UK over a half-century period. Regarding fossil morphological plasticity studies, Hughes (1991) studied the morphological plasticity of *Dikelocephalus minnesotensis* (trilobite) over a 2 Ma period. The measurements of over 2.500 specimens showed morphological plasticity in 23 characters. However, studying coccolithophores fossils doesn't make it possible to directly observe these variations. We can, nonetheless, observe morphometric variations within a morphospecies (the definition of a species based on its morphological traits – the oldest concept to describe different species).

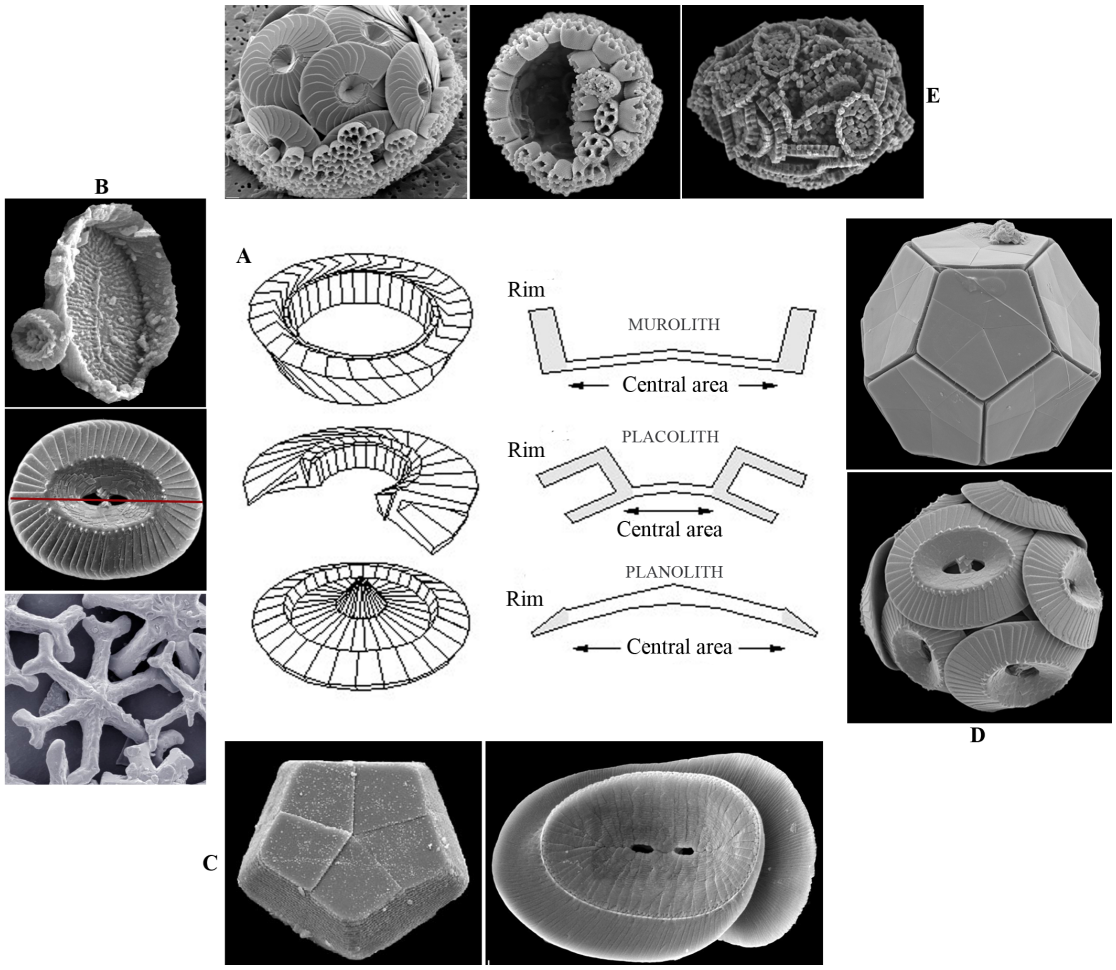

Figure 1.1 – A – types of coccoliths according to structure: murolith with a rim and a simple shield; placoliths with a rim and a double shield; planolith with no or very small rim and simple shield. B – examples of coccoliths, from top to bottom: *Pontosphaera plana* (murolith), *Coccolithus pelagicus* (placolith) and *Discoaster exilis* (planolith). C – examples of coccoliths according to shape: left – *Braarudosphaera bigelowii* – pentalith (belonging to planoliths) and right – *Helicosphaera carteri* – helicolith (belonging to placoliths). D – examples of coccospheres, bottom *C. pelagicus*, top *B. bigelowi*. E – holococcoliths from *C. pelagicus* (right) and *Calcidiscus leptoporus* (middle). On the left an image showing holo and heterococcoliths of *C. leptoporus* at the same time, representing a moment of transition in the life cycle (source Nannotax3.com). The red line over *C. pelagicus* placolith represents the morphometric parameter studied in this work.

Using these observations, it is possible to determine which morphotypes evolve as a response to which environmental changes. The morphological plasticity of *C. pelagicus* s.l. that will be analysed consists in its morphometric variations, and how certain morphotypes (that can't be determined without performing the morphometric studies) behave. In this work only the length of the larger axis of *C. pelagicus* s.l. was analysed, since this parameter has been shown to reflect the environmental conditions in culture (Daniels et al., 2014; Sheward et al., 2014, 2016) and field (Renaud & Klaas, 2001) studies, either of *C. pelagicus* s.l. or the related *Calcidiscus leptoporus*.

Phenotypic plasticity is usually defined as a property of individual genotypes to produce different phenotypes when exposed to different environmental conditions, biotic or abiotic (Agrawal, 2001; Pigliucci et al., 2006), which represents the potential for an organism to produce a range of different, relatively fit phenotypes in multiple environments (DeWitt et al., 1998). Morphological plasticity corresponds to changes in morphology that are ecological significant, under two conditions: 1) the changes must have an impact in fitness in that environment; 2) they must differ across environmental conditions for some ecological reason (Travis, 1994).

This means that *C. pelagicus* s.l. may have different morphotypes as response to different environmental conditions, and that these would be observable in its heterococcolith size, i.e. through morphometry. However, one must consider the possibility of being different (sub)species. The morphometry of coccolithophores reflects the variations of the cells size, since the heterococcoliths are produced intracellularly, so that their final proportions are attained prior to being extruded to the coccosphere (Young et al., 1999). The size of coccoliths, preserved in the fossil record, is therefore an intrinsic property of a particular morphospecies or ecophenotype (e.g. Westbroek et al., 1984; Young et al., 1999; Young & Henriksen, 2003). One must keep in mind one other and simpler possibility for the different morphotypes. Since coccolith size reflects the cell size, they can be showing the cell sizes that occur under certain conditions. Meaning that cell size may vary as a response to temperature, nutrients and/or solar radiation, simply by being able to grow more in, e.g., higher nutrients conditions. Houdan et al. (2006) show that *C. pelagicus* diploid phase (the one that produce the microfossils we observe in the geological record) is highly competitive in nutrient rich media. Smaller phytoplankton species have a surface-area-to-volume ratio that provides effective acquisition of nutrient

solutes and photons, as well as hydrodynamic resistance to sinking (Li et al., 2009). On the other hand, a vacuole with nutrient reserves is common in algal cells, and this vacuole volume increases cell volume (Malone, 1980). Recently, size variation was found to occur as a response to nutrient availability in coccolithophore laboratorial cultures (Daniels et al., 2014; Sheward et al., 2014, 2016). This could be one explanation for the results found by Parente et al. (2004), with three morphotypes, presenting different sizes, in different oceanographic realms:

- The cold-water form is the smallest one, and found in polar waters, having a high surface-area-to-volume ratio in a highly rich environment;
- The intermediate form, found in upwelling regions, may require a vacuole for downwelling seasons, poor in nutrients, and presenting a larger form;
- The largest form, the subtropical form, is found in less rich with no upwelling waters, which can increase the necessity of large vacuoles, increasing cell size.

A promising, but largely unexplored, factor is the potential for the morphological variation of a species to affect its susceptibility to extinction. Greater variation, or a wider range of forms, might afford a species more ecological flexibility during environmental perturbations or permit it to inhabit a greater geographic range, an attribute that is known to promote survivorship (Lloyd & Gould 1993; Payne & Finnegan 2007; Jablonski 2008). Kolbe et al. (2011) found that veneroid bivalves that were more variable morphologically survived the regional Plio-Pleistocene extinction in Florida. Since *C. pelagicus* s.l. has been present throughout the entire Cenozoic, it is expected to have a high morphological plasticity, in order to survive all the Cenozoic climate perturbations.

1.2 Work Objectives and Thesis Organization

This proposal aims to answer the main following palaeo(oceanographic) questions:

1) What were the responses of *C. pelagicus* s.l. to certain climatic events of the Cenozoic?

2) What kind of morphological plasticity can be extracted from palaeontological data and does the data reflect the known variations in extant *C. p. pelagicus* and *C. p. braarudii*?
3) Can our method for *C. pelagicus* s.l. morphometry be applied to all Cenozoic?

To address these questions, we will use an already developed statistical analysis, the Multivariate Morphometric Analysis (MMA) for coccolith morphometry studies (Narciso et al., 2006). MMA allows identification of one or more morphotypes within a certain species by analysing time-stack morphometric data, a type of 4D histogram defined for a certain high-resolution time interval.

The method's main limitation, however, is related to the predefinition of size-intervals (morphons) during data tabulation as common histogram analysis, which makes the method dependent of the observer's subjectivity. For these reasons we intend to introduce a new criterion in the definition of morphotype size limits that may be both statistically robust and independent of the tabulation size intervals and limits of the morphons themselves.

This new method, here named Integrated Multivariate Morphometric Analysis (IMMA), will allow to study small-scale (less than 1 micron) changes in size of morphotypes and aims to document high-resolution subtle plasticity of *C. pelagicus* s.l. to climate change.

Summarizing, we will study *C. pelagicus* s.l. morphometric variation during selected climatic events of the Cenozoic, as a measure of accessing its genetic and (palaeo)ecological plasticity, using an updated morphometric methodology. Answering these questions will be a step in understanding evolution and increasing our knowledge of life. Also, if future scenarios of oceanographic condition changes occur in the regions inhabited by *C. pelagicus* s.l. (namely North Atlantic – subpolar waters and Azores, and West Atlantic – from Benguela Current to Iberia West coast) this work could be crucial to predict how it will respond to such perturbations.

The thesis will be structured into article like chapters, with each chapter containing its own references and annexes when needed (Annexes numbered after the Chapter they belong to – there is no Annex-1). In Section II the new methodology, IMMA, will be addressed, detailing it and presenting tests performed with theoretical populations. A discussion notes on Principal Components Analysis and Factor

Analysis, as well as the use of rotations with these statistical methods, is present in the chapter annex.

Section III presents *C. pelagicus* s.l. morphometry. The first chapter presents a reassessment of previously studied Quaternary samples from the North and Northeast Atlantic – MD95-2040 (West Iberia), DSDP608 (North Central Atlantic) and GeoB5559-2 (Canary Islands). The second chapter presents IMMA applied to older Cenozoic periods (Eocene-Oligocene transition and the Miocene Optimum Climate) and the effects of low resolution, low number of samples and samples exclusively from highly perturbed time intervals.

Section IV presents a general discussion together with reflections on IMMA improvements and traditional morphometric methodologies (namely if morphometry should be done in a fixed minimum number of specimens per sample, or if it should be performed on a minimum area of the slides).

References

Agrawal, A.A., 2001. Phenotypic plasticity in the interactions and evolution of species. Science 294, 321–6. doi:10.1126/science.1060701

Balch, W.M., 2018. The ecology, biogeochemistry, and optical properties of coccolithophores. Ann. Rev. Mar. Sci. 10, 71–98. doi:10.1146/annurev-marine-121916-063319

Barke, J., van der Burgh, J., van Konijnenburg-van Cittert, J.H. a., Collinson, M.E., Pearce, M. a., Bujak, J., Heilmann-Clausen, C., Speelman, E.N., van Kempen, M.M.L., Reichart, G.-J., Lotter, A.F., Brinkhuis, H., 2012. Coeval Eocene blooms of the freshwater fern Azolla in and around Arctic and Nordic seas. Palaeogeogr. Palaeoclimatol. Palaeoecol. 337–338, 108–119. doi:10.1016/j.palaeo.2012.04.002

Baumann, K.-H., Andruleit, H., Böckel, B., Geisen, M., Kinkel, H., 2005. The significance of extant coccolithophores as indicators of ocean water masses, surface water temperature, and palaeoproductivity: a review. Paläontologische Zeitschrift 79, 93–112. doi:10.1007/BF03021756

Böhme, M., 2003. The Miocene Climatic Optimum: evidence from ectothermic vertebrates of Central Europe. Palaeogeogr. Palaeoclimatol. Palaeoecol. 195, 389–401. doi:10.1016/S0031-0182(03)00367-5

Böhme, M., Winklhofer, M., Ilg, A., 2011. Miocene precipitation in Europe: Temporal trends and spatial gradients. Palaeogeogr. Palaeoclimatol. Palaeoecol. 304, 212–218. doi:10.1016/j.palaeo.2010.09.028

Bown, P.R., Lees, J.A., Young, J.R., 2004. Calcareous nannoplankton evolution and diversity through time, in: Thierstein, H.R., Young, J.R. (Eds.), Coccolithophores: From Molecular Processes to Global Impact. Springer Berlin Heidelberg, pp. 481–508. doi:10.1007/978-3-662-06278-4_18

Braarud, T., Deflandre, G., Halldal, P., Kamptner, E., 1955. Terminology, nomenclature, and systematics of the Coccolithophoridae. Micropaleontology 1, 157–159.

Charmantier, A., McCleery, R.H., Cole, L.R., Perrins, C., Kruuk, L.E.B., Sheldon, B.C., 2008. Adaptive phenotypic plasticity in response to climate change in a wild bird population. Science 320, 800–3. doi:10.1126/science.1157174

Cope, J.T., Winguth, A., 2011. On the sensitivity of ocean circulation to arctic freshwater input during the Paleocene/Eocene Thermal Maximum. Palaeogeogr. Palaeoclimatol. Palaeoecol. 306, 82–94. doi:10.1016/j.palaeo.2011.03.032

Cotton, L.J., Pearson, P.N., 2011. Extinction of larger benthic foraminifera at the Eocene/Oligocene boundary. Palaeogeogr. Palaeoclimatol. Palaeoecol. 311, 281–296. doi:10.1016/j.palaeo.2011.09.008

Daniels, C.J., Sheward, R.M., Poulton, A.J., 2014. Biogeochemical implications of comparative growth rates of *Emiliania huxleyi* and *Coccolithus* species. Biogeosciences 11, 6915–6925. doi:10.5194/bg-11-6915-2014

de Vargas, C., Aubry, M.-P., Probert, I., Young, J., 2007. Origin and Evolution of Coccolithophores: From Coastal Hunters to Oceanic Farmers, in: Falkowski, P., Knoll, A.H. (Eds.), Evolution of Aquatic Photoautotrophs. Elsevier, pp. 251–286. doi:10.1016/B978-0-12-370518-1.50013-8

DeConto, R.M., Pollard, D., Wilson, P.A., Pälike, H., Lear, C.H., Pagani, M., 2008. Thresholds for Cenozoic bipolar glaciation. Nature 455, 652–656. doi:10.1038/nature07337

DeWitt, T.J., Sih, A., Wilson, D.S., 1998. Costs and limits of phenotypic plasticity. Trends Ecol. Evol. 13, 77–81.

Dodd, M.S., Papineau, D., Grenne, T., Slack, J.F., Rittner, M., Pirajno, F., O'Neil, J., Little, C.T.S., 2017. Evidence for early life in Earth's oldest hydrothermal vent precipitates. Nature 543, 60–64. doi:10.1038/nature21377

Frada, M., Young, J., Cachão, M., Sílvia Lino, A.M., Narciso, Á., Ian Probert, C. de V., 2010. A guide to extant coccolithophores (Calcihaptophycidae, Haptophyta) using light microscopy. J. Nannoplankt. Res. 31, 58–112.

Frada, M.J., Bendif, E.M., Keuter, S., Probert, I., 2018. The private life of coccolithophores. Perspect. Phycol. 1–20. doi:10.1127/pip/2018/0083

Gibbs, S.J., Poulton, A.J., Bown, P.R., Daniels, C.J., Hopkins, J., Young, J.R., Jones, H.L., Thiemann, G.J., Dea, S.A.O., Newsam, C., 2013. Species-specific growth response of coccolithophores to Palaeocene – Eocene environmental change. Nat. Geosci. 6, 1–5. doi:10.1038/ngeo1719

Henderiks, J., Bollmann, J., 2004. The Gephyrocapsa sea surface palaeothermometer put to the test: comparison with alkenone and foraminifera proxies off NW Africa. Mar. Micropaleontol. 50, 161–184. doi:10.1016/S0377-8398(03)00070-7

Héran, M.-A., Lécuyer, C., Legendre, S., 2010. Cenozoic long-term terrestrial climatic evolution in Germany tracked by $\delta^{18}O$ of rodent tooth phosphate. Palaeogeogr. Palaeoclimatol. Palaeoecol. 285, 331–342. doi:10.1016/j.palaeo.2009.11.030

Höntzsch, S., Scheibner, C., Guasti, E., Kuss, J., Marzouk, A.M., Rasser, M.W., 2011. Increasing restriction of the Egyptian shelf during the Early Eocene? — New insights from a southern Tethyan carbonate platform. Palaeogeogr. Palaeoclimatol. Palaeoecol. 302, 349–366. doi:10.1016/j.palaeo.2011.01.022

Houben, A.J.P., van Mourik, C.A., Montanari, A., Coccioni, R., Brinkhuis, H., 2012. The Eocene–Oligocene transition: Changes in sea level, temperature or both? Palaeogeogr. Palaeoclimatol. Palaeoecol. 335–336, 75–83. doi:10.1016/j.palaeo.2011.04.008

Houdan, A., Probert, I., Zatylny, C., Véron, B., Billard, C., 2006. Ecology of oceanic coccolithophores. I. Nutritional preferences of the two stages in the life cycle of *Coccolithus braarudii* and *Calcidiscus leptoporus*. Aquat. Microb. Ecol. 44, 291–301. doi:10.3354/ame044291

Hughes, N.C., 1991. Morphological plasticity and genetic flexibility in a Cambrian trilobite. Geology 19, 913. doi:10.1130/0091-7613(1991)019<0913:MPAGFI>2.3.CO;2

Jablonski, D., 2008. Extinction and the spatial dynamics of biodiversity. Proc. Natl. Acad. Sci. U. S. A. 105, 11528–11535.

Kolbe, S.E., Lockwood, R., Hunt, G., 2011. Does morphological variation buffer against extinction? A test using veneroid bivalves from the Plio-Pleistocene of Florida. Paleobiology 37, 355–368. doi:10.1666/09073.1

Li, W.K.W., McLaughlin, F. a, Lovejoy, C., Carmack, E.C., 2009. Smallest algae thrive as the Arctic Ocean freshens. Science 326, 539. doi:10.1126/science.1179798

Lloyd, E.A., Gould, S.J., 1993. Species selection on variability. Proc. Natl. Acad. Sci. U. S. A. 90, 595–599.

Malin, G., Steinke, M., 2004. Dimethyl sulfide production: what is the contribution of the coccolithophores?, in: Thierstein, H.R., Young, J.R. (Eds.), Coccolithophores: From Molecular Processes to Global Impact. Springer Berlin Heidelberg, pp. 127-164

Mattioli, E., Pittet, B., Young, J.R., Bown, P.R., 2004. Biometric analysis of Pliensbachian-Toarcian (Lower Jurassic) coccoliths of the family Biscutaceae: intra- and interspecific variability versus palaeoenvironmental influence. Mar. Micropaleontol. 52, 5–27. doi:10.1016/j.marmicro.2004.04.004

Narciso, A., Cachão, M., Abreu, L. De, 2006. *Coccolithus pelagicus* subsp. *pelagicus* versus *Coccolithus pelagicus* subsp. *braarudii* (Coccolithophore, Haptophyta): A proxy for surface subarctic Atlantic waters off Iberia during the last 200 kyr. Mar. Micropaleontol. 59, 15–34. doi:10.1016/j.marmicro.2005.12.001

Parente, Á., 2006. Morfometria aplicada ao cocolitóforo *Coccolithus pelagicus* (*s.l.*) à escala do Atlântico Norte, para os últimos 6 Ma. Implicações paleoceanográficas e paleoecológicas da presença de distintos morfótipos. Tese de Doutoramento, Universidade de Lisboa.

Parente, A., Cachão, M., Baumann, K., Abreu, L. De, Ferreira, J., 2004. Morphometry of *Coccolithus pelagicus s.l.* (Coccolithophore, Haptophyta) from offshore Portugal, during the last 200 kyr. Micropaleontology 50, 107–120.

Parmesan, C., Yohe, G., 2003. A globally coherent fingerprint of climate change impacts across natural systems. Nature 421, 37–42. doi:10.1038/nature01286

Payne, J.L., Finnegan, S., 2007. The effect of geographic range on extinction risk during background and mass extinction. Proc. Natl. Acad. Sci. U. S. A. 104, 10506–11. doi:10.1073/pnas.0701257104

Pigliucci, M., Murren, C.J., Schlichting, C.D., 2006. Phenotypic plasticity and evolution by genetic assimilation. J. Exp. Biol. 209, 2362–7. doi:10.1242/jeb.02070

Poulton, A.J., Adey, T.R., Balch, W.M., Holligan, P.M., 2007. Relating coccolithophore calcification rates to phytoplankton community dynamics: Regional differences and implications for carbon export. Deep. Res. Part II Top. Stud. Oceanogr. 54, 538–557. doi:10.1016/j.dsr2.2006.12.003

Price, T.D., Qvarnström, A., Irwin, D.E., 2003. The role of phenotypic plasticity in driving genetic evolution. Proc. Biol. Sci. 270, 1433–40. doi:10.1098/rspb.2003.2372

Raymo, M., 1994. The Initiation of Northern Hemisphere Glaciation. Annu. Rev. Earth Planet. Sci. 22, 353–383. doi:10.1146/annurev.earth.22.1.353

Read, B. a, Kegel, J., Klute, M.J., Kuo, A., Lefebvre, S.C., Maumus, F., Mayer, C., Miller, J., Monier, A., Salamov, A., Young, J., Aguilar, M., Claverie, J.-M., Frickenhaus, S., Gonzalez, K., Herman, E.K., Lin, Y.-C., Napier, J., Ogata, H., Sarno, A.F., Shmutz, J., Schroeder, D., de Vargas, C., Verret, F., von Dassow, P., Valentin, K., Van de Peer, Y., Wheeler, G., Dacks, J.B., Delwiche, C.F., Dyhrman, S.T., Glöckner, G., John, U., Richards, T., Worden, A.Z., Zhang, X., Grigoriev, I. V, 2013. Pan genome of the phytoplankton Emiliania underpins its global distribution. Nature 499, 209–213. doi:10.1038/nature12221

Reitan, T., Schweder, T., Henderiks, J., 2012. Phenotypic evolution studied by layered stochastic differential equations. Ann. Appl. Stat. 6, 1531–1551. doi:10.1214/12-AOAS559

Renaud, S., Klaas, C., 2001. Seasonal variations in the morphology of the coccolithophore *Calcidiscus leptoporus* off Bermuda (N . Atlantic). J. Plankton Res. 23, 779–795. doi:10.1093/plankt/23.8.779

Root, T.L., Price, J.T., Hall, K.R., Schneider, S.H., Rosenzweig, C., Pounds, J.A., 2003. Fingerprints of global warming on wild animals and plants. Nature 421, 57–60. doi:10.1038/nature01309.1.

Saez, A.G., Probert, I., Geisen, M., Quinn, P., Young, J.R., Medlin, L.K., 2003. Pseudo-cryptic speciation in coccolithophores. Proc. Natl. Acad. Sci. U. S. A. 100, 7163–7168. doi:10.1073/pnas.1132069100

Sexton, P.F., Norris, R.D., Wilson, P. a, Pälike, H., Westerhold, T., Röhl, U., Bolton, C.T., Gibbs, S., 2011. Eocene global warming events driven by ventilation of oceanic dissolved organic carbon. Nature 471, 349–52. doi:10.1038/nature09826

Sheward, R.M., Daniels, C.J., Gibbs, S.J., 2014. Growth rates and biometric measurements of coccolithophores (*Coccolithus pelagicus*, *Coccolithus braarudii*, *Emiliania huxleyi*) during experiments, PANGAEA. doi:10.1594/PANGAEA.836841

Sheward, R.M., Poulton, A.J., Gibbs, S.J., Daniels, C.J., Bown, P.R., 2016. Physiology regulates the relationship between coccosphere geometry and growth phase in coccolithophores. Biogeosciences Discuss. 14, 1493–1509. doi:10.5194/bg-14-1493-2017

Suchéras-Marx, B., Mattioli, E., Pittet, B., Escarguel, G., Suan, G., 2010. Astronomically-paced coccolith size variations during the early Pliensbachian (Early Jurassic). Palaeogeogr. Palaeoclimatol. Palaeoecol. 295, 281–292. doi:10.1016/j.palaeo.2010.06.006

Taylor, A.R., Brownlee, C., Wheeler, G., 2017. Coccolithophore Cell Biology: Chalking Up Progress. Ann. Rev. Mar. Sci. 9, 283–310. doi:10.1146/annurev-marine-122414-034032

Thibault, N., 2010. Biometric analysis of the Arkhangelskiella group in the upper Campanian-Maastrichtian of the Stevns-1 borehole, Denmark: Taxonomic implications and evolutionary trends. Geobios 43, 639–652. doi:10.1016/j.geobios.2010.06.002

Thomas, C.D., Cameron, A., Green, R.E., Bakkenes, M., Beaumont, L.J., Collingham, Y.C., Erasmus, B.F.N., De Siqueira, M.F., Grainger, A., Hannah, L., Hughes, L., Huntley, B., Van Jaarsveld,

A.S., Midgley, G.F., Miles, L., Ortega-Huerta, M. a, Peterson, a T., Phillips, O.L., Williams, S.E., 2004. Extinction risk from climate change. Nature 427, 145–8. doi:10.1038/nature02121

Travis, J., 1994. Evaluating the Adaptative Role of Morphological Plasticity, in: Wainwright, P.C., Reilly, S.M. (Eds.), Ecological Morphology: Integrative Organismal Biology. University of Chicago Press, Chicago, p. 367.

Vargas, C., Sáez, A.G., Medlin, L.K., Thierstein, H.R., 2004. Super-Species in the calcareous plankton, in: Thierstein, H.R., Young, J.R. (Eds.), Coccolithophores: From Molecular Processes to Global Impact. Springer Berlin Heidelberg, pp. 271-298

Westbroek, P., de Jong, E.W., van der Wal, P., Borman, a. H., de Vrind, J.P.M., Kok, D., de Bruijn, W.C., Parker, S.B., 1984. Mechanism of Calcification in the Marine Alga *Emiliania huxleyi* [and Discussion]. Philos. Trans. R. Soc. B Biol. Sci. 304, 435–444. doi:10.1098/rstb.1984.0037

Witkowski, J., Bohaty, S.M., Mccartney, K., Harwood, D.M., 2012. Enhanced siliceous plankton productivity in response to middle Eocene warming at Southern Ocean ODP Sites 748 and 749. Palaeogeogr. Palaeoclimatol. Palaeoecol. 326–328, 78–94. doi:10.1016/j.palaeo.2012.02.006

You, Y., Huber, M., Müller, R.D., Poulsen, C.J., Ribbe, J., 2009. Simulation of the Middle Miocene Climate Optimum. Geophys. Res. Lett. 36, 1–5. doi:10.1029/2008GL036571

Young, J., Davis, S., Bown, P., Mann, S., 1999. Coccolith ultrastructure and biomineralisation. J. Struct. Biol. 126, 195–215. doi:10.1006/jsbi.1999.4132

Young, J.R., Henriksen, K., 2003. Biomineralization Within Vesicles: The Calcite of Coccoliths. Rev. Mineral. Geochemistry 54, 189–215. doi:10.2113/0540189

Zachos, J., Pagani, M., Sloan, L., Thomas, E., Billups, K., 2001. Trends, rhythms, and aberrations in global climate 65 Ma to present. Science 292, 686–93. doi:10.1126/science.1059412

Zachos, J.C., Dickens, G.R., Zeebe, R.E., 2008. An early Cenozoic perspective on greenhouse warming and carbon-cycle dynamics. Nature 451, 279–83. doi:10.1038/nature06588

II. IMMA DEVELOPMENT

CHAPTER 2

Integrated Multivariate Morphon Analysis – a new approach into the microevolutionary morphometric patterns of coccolithophores

Abstract

Although current digital techniques can estimate sizes at least to the decimal of the micron morphometric methods commonly tabulate coccoliths into integer morphometric intervals. Since studies evidence morphometric changes up to the decimal of the micron in response to environmental pressures the 1μm size resolution may not be enough to follow microevolutionary patterns on morphospecies boundaries on both fossil and extant coccolithophores.

A new morphometric method, denominated Integrated Multivariate Morphon Analysis (IMMA) is proposed to determine morphotypes with a resolution of 0.1μm. Results are validated by model-generated theoretical data. By increasing the boundary definition of the morphotypes to the decimal point this new method allows: 1) to document microevolutionary patterns in coccolithophores and 2) to trace short time palaeoenvironmental changes.

Keywords: Morphometry; Coccolithophores; IMMA; Microevolution; Theoretical model

2.1 Introduction

Coccolithophores, the predominant phytoplankton group within the broader oceanic calcareous nannoplankton, are the main producers of identifiable calcareous nannofossils, commonly used as palaeoenvironmental proxies and markers of oceanographic processes (e.g., Ziveri et al., 2004; Silva et al., 2008; Guerreiro et al., 2013) due to their exceptional fossil record in both open ocean (Ziveri et al., 2004) and continental shelf/slope sediments (Cachão & Moita, 2000; Guerreiro et al., 2005, 2015).

Although advances on the understanding of hetero-holo coccolithophore life cycles, taxonomy of extant taxa, particularly those with fossil record, is still mainly based on the heterococcolith (hereafter simply referred as coccolith) life cycle stage, namely the crystallographic pattern of sets of minute low-Mg calcite crystallites and their overall morphology. At species level certain distinctions are made based on fine variations in size and shape (Jordan & Green, 1994). This has been successfully applied to the fossil record and compares well with findings from other research disciplines such as cell physiology and more recently molecular genetics (Sáez et al., 2003; Young et al., 2005).

The usefulness of measurements on coccolith morphological parameters, i.e. coccolith morphometry, is based on the fact that coccoliths are produced intracellularly, and so have their final proportions prior to being extruded to the coccosphere (Westbroek et al., 1984; Young et al., 1999; Young & Henriksen, 2003). Hence their dimensions may be considered an intrinsic property of a particular species or ecophenotype. This method was already used to address questions such as taxonomy, biostratigraphy and palaeoecology of several calcareous nannoplankton (e.g. Samtleben, 1980; Backman & Hermelin, 1986; Young, 1990; Wei, 1992; Baumann, 1995; Knappertsbusch, 2000; Colmenero-Hidalgo et al., 2002; Parente et al., 2004; Narciso et al., 2006; Faucher et al., 2017).

The main goal of the present study is focused on a better definition of morphotype/morphospecies size boundaries by increasing its resolution to the decimal of the micron in such a way that is independent of the initial limits and length interval by which sizes (commonly the maximum length of an elliptical placolith or the diameter of a round coccolith) are tabulated.

Current morphometric methods commonly tabulate coccoliths into 1μm morphometric intervals. Morphotypes boundaries are thus generally defined by integers although modern digital techniques allow to estimate sizes at least to the decimal of the micron. This current methodological limitation implies that eventual palaeoenvironmental and/or evolutionary decimal changes may not be disclosed. However, studies with batch cultures, as well as with natural extant assemblages report decimal variations in coccolith size in response to changes in the environment, mainly nutrients (see Renaud & Klaas, 2001; Daniels et al., 2014; Sheward et al., 2014, 2016). So, in order to understand microevolutionary adaptations of coccolithophores to continuous variations in their marine palaeoenvironments, based on high to ultra-high resolution sets of core samples, one need to further improve current morphometric tools, namely to detail robust decimal shifts in coccolith-based morphotype boundaries.

In this work a new morphometric method able to determine morphotypes with a resolution of 0.1μm is presented and discussed. It uses model generated theoretical data to compute morphometric matrixes for validation. This method is a development of the Multivariate Morphon Analysis (MMA) (Parente et al., 2004; Narciso et al., 2006) to lower one order of magnitude the boundaries definition of the morphotypes, thus allowing to observe microevolutionary patterns in coccolithophores and the use of coccoliths to trace short time palaeoenvironmental changes.

2.2 Methodology

The model-generated data used an EXCEL-based algorithm to stochastically generated placolith sizes within pre-established size ranges defined to the decimal of the micron. The theoretical matrixes reproduce the requirements necessary for morphometric data acquisition and size morphotype interpretation using MMA (Parente et al., 2004; Narciso et al. 2006).

Since MMA uses Principal Components Analysis (PCA) a minimum number of samples is required. There are several different approaches to this issue (see Shaukat et al., 2016), and MMA assumes that this number must be equal or higher than the number of 1μm size intervals (i.e. morphons) used for morphometric data tabulation (Parente et al, 2004; Narciso et al, 2006), although this isn't a mathematical obligation

for PCAs. In fact, according to Shaukat et al. (2016), the more important rule in PCA applied to palaeoenvironmental studies is to have a minimum of 40-50 samples.

For the present study sets of 45 theoretical samples were generated. In terms of cost-benefit between measurement efforts and statistical representativeness MMA considers, for each sample, data from a set of 100 specimens, randomly selected and measured in each slide. Thus, for our model-generated data matrix 100 measurements were computed for each of 45 (theoretical) samples. These measurements were stochastically selected from two theoretical morphotypes:

- A smaller (theoretical) morphotype (M_S) was defined in order to generate an hypothetical population of placoliths with sizes ranging randomly inside the interval [5.3, 9.6] μm through the equation (in Excel notation):

$$S_t\,(n) = 5.3+RAND()*4.3 \qquad n = 1 \text{ to } n1 \qquad (1)$$

- A larger (theoretical) morphotype (M_L) was computed to produce sets of hypothetical placoliths with sizes ranging randomly inside the interval [10.7, 13.2] μm through the equation (in Excel notation):

$$L_t\,(n) = 10.7+RAND()*2.5 \qquad n = 1 \text{ to } n2 \qquad (2)$$

n1 and n2 are the number of placoliths belonging to the smaller (MS) and to the larger (ML) morphotype, respectively, so that n1 + n2 = 100 (the maximum fixed number of specimens measured per sample).

Each of these morphotypes are activated according to an hypothetical palaeoecological scenario defined by the combination of two independent (linearly uncorrelated; r = 0.01) proxies (Var1 and Var2), which values were randomly generated for each one of the 45 samples/time slices. The morphometric data was generated in a way that Var1 directly influences the production of the smaller M_S morphotype while Var2 favours the occurrence of the larger M_L morphotype.

A simple percentage relationship was extracted to determine the relative influence of each of the two proxies in producing morphotypes for each time interval (samples). For example, if Var1 influences the palaeoecological scenario in 25% this is translated into the model-generated data set as: 25 coccolith sizes will be extracted from equation 1 while 75 coccolith sizes will derive from equation 2. This way the

relative abundance of these two proxies will be translated into coccolith sizes from the two predetermined size intervals so that they may be reconstructed through the application of the new methodology.

Since only two morphotypes where considered and the number of placoliths measured for each sample was fixed to 100 results will always reflect a spurious negative correlation between the two morphotypes. This anti-variation behaviour can be interpreted as migrations back and forth across the samples location of the boundary between the biogeographic areas or niches occupied by each of the morphotypes. The scores of the main component extracted will define which of the two morphotypes niche is active which, in turn, is interpreted as reflecting changes in palaeoenvironmental conditions.

To produce more realistic scenarios a degree of noise was also computed to generate M30%, meaning 30% of noise, i.e. 30 out of 100 sizes were randomly computed within the maximum size range possible (3 to 16μm) by the equation (in Excel notation):

$$N(n) = 3.0+RAND()*13.0 \qquad n = 1 \text{ to } 30 \qquad (3)$$

With MMA the Principal Component Analysis (PCA) is run once through a single matrix, and so morphotype limits are arbitrarily determined by the (generally) 1.0μm size limits of the data tabulation. Instead, the proposed new method, Integrated Multivariate Morphon Analysis (IMMA) runs PCA throughout a set of 10 distinct matrixes. These 10 matrixes are composed from the same initial data set. First matrix is the same as the one used for MMA, in which data is initially tabulated in 1.0 μm size intervals. The 9 additional matrixes are computed by shifting the morphon limits by 0.1 μm relative to the previous matrix.

M0 with tabulations for intervals: [3.0, 4.0[+ [4.0, 5.0[+ [5.0, 6.0[+ [6.0, 7.0[+ …

M1 with tabulations for intervals: [3.1, 4.1[+ [4.1, 5.1[+ [5.1, 6.1[+ [6.1, 7.1[+ …

M2 with tabulations for intervals: [3.2, 4.2[+ [4.2, 5.2[+ [5.2, 6.2[+ [6.2, 7.2[+ …

M3 with tabulations for intervals: [3.3, 4.3[+ [4.3, 5.3[+ [5.3, 6.3[+ [6.3, 7.3[+ …

(…)

M8 with tabulations for intervals: [3.8, 4.8[+ [4.8, 5.8[+ [5.8, 6.8[+ [6.8, 7.8[+ …

M9 with tabulations for intervals: [3.9, 4.9[+ [4.9, 5.9[+ [5.9, 6.9[+ [6.9, 7.9[+ …

This way IMMA uses a 1.0μm size window that shifts across the morphometric data in a similar way, for example, Wave Let Analysis perform relative to the Fourier analysis. With this procedure statistical significance is increased while obtaining the most significant combination of size limits to the morphotypes. In addition, morphotype size limits are determined independently of the size of the tabulation interval.

Initially MMA was performed using Factorial Analysis, i.e., PCA applied to a correlation matrix produced from the morphometric data. However, since the data is in only one scale, i.e., only coccolith length measurements, performing PCA upon a correlation matrix causes loss of information. Only when dealing with data sets composed of different types of data (for example, analysing morphometric data and other proxies such as stable isotopes or calcite coccolith weight) correlation matrix should be used in PCA to standardize the data. Since this is not the case, all data is in the same scale and PCA as a true component analysis using only a non-standardized covariance matrix.

Tests were carried out to observe if running 10 PCAs in the 10 matrixes or running one PCA in one matrix consisting on the 10 matrixes merged together gave different results. No simulation (both with theoretical and the real matrixes used in following chapters) produced different results between 10 PCAs or a PCA applied to an all data matrix (10 matrixes merged into one). Thus, instead of following the number of morphons rule of MMA, in IMMA all matrixes are merged together (generating a

matrix with more morphons than samples) to perform only one PCA. This makes it easier and less time consuming than needing to integrate 10 different PCAs.

The PCA multivariate statistical analysis was performed with IBM© SPSS© Statistics version 23.0 software package (see Field, 2009).

Summarizing, during the IMMA:

1. Morphon frequencies are determined for each sample;
2. A morphometric data matrix, with samples as rows and morphons as columns, is compiled from morphon frequencies;
3. The two previous steps are repeated, shifting the morphons by 0.1µm (in the end 10 morphometric matrixes are generated)
4. The 10 matrixes (M0 to M9) are combined creating one single morphometric matrix;
5. PCA is performed to the final matrix;
6. The PCA loadings are reordered according to consecutive morphons;
7. Analysis of the loadings of the most significant component(s) determines morphotypes and their morphometric limits;
8. Analysis of the scores of the most significant component(s) gives the morphotypes behaviour through the samples/time.

Main advantage of the new IMMA method is that it screens the morphometric measurements through a 1µm size window moving through the entire time series. Its usefulness is tested using the PCA loadings of the final integrated matrix (theoretical matrixes and results in table format are available in Annex-2).

2.3 Results

2.3.1 Theoretical Matrix without noise (M_0)

In this theoretical scenario two morphotypes were defined (Figure 2.1 presents the histogram of the global theoretical population) with an already expected opposite behaviour (Fig. 2.2).

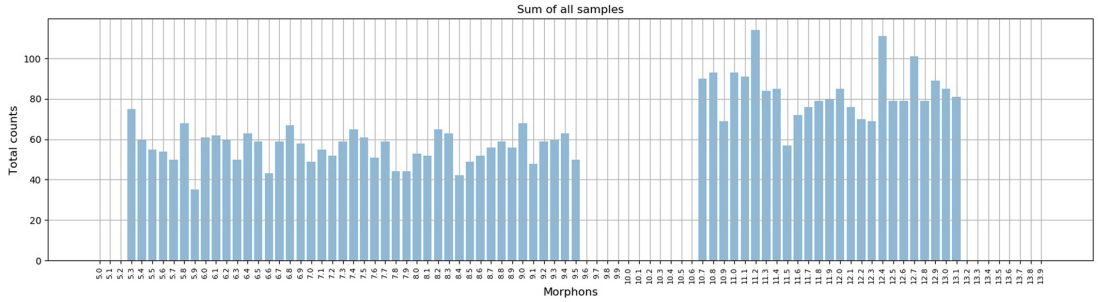

Figure 2.1 – Histogram of the entire theoretical population defined in M_0.

PCA loadings from IMMA (Figure 2.2) provide information regarding on how many morphotypes exist, their behaviour and their more precise boundaries.

The smaller morphotype (M_S) appears with positive loadings, while the large morphotype (M_L) presents negative values, reflecting the opposite behaviour between the morphotypes. What morphotype has positive and which one has negative values are artefacts of statistical internal PCA analysis. One being positive, and the other negative, is a result of the closer to 100 specimens and means that when placoliths of one morphotype abound the number of placoliths belonging to the other morphotype, they are less common in the sample and *vice versa*. Palaeoecological interpretation of the oscillations between two morphotypes depend on several factors, which can be a result of palaeobiogeographic distributions, nutrient availability variations, etc.

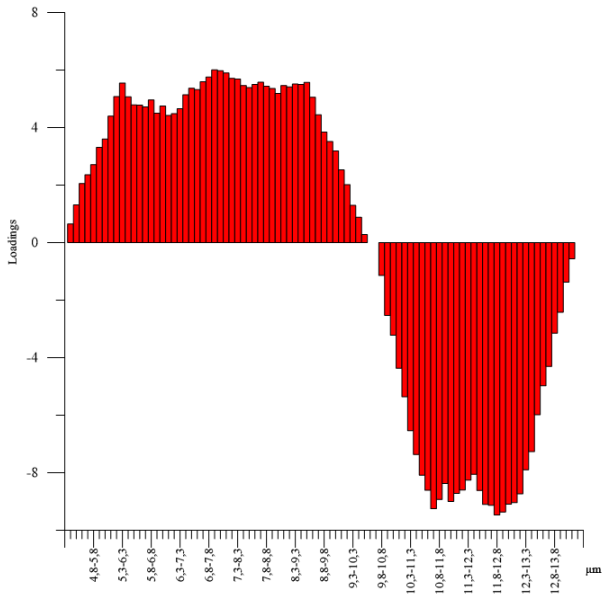

Figure 2.2 – PCA loadings for C1 in theoretical matrix M_0.

The size boundaries of each morphotype are rapidly disclosed from the loadings values in Figure 2.2 (Table A2-1 in Annex-2). Since in this case there is no noise, morphons [9.6 -10.6[µm and [9.7 -10.7[µm have no measurements. Loading values are analysed according to their signal and stability. Defining a morphotype consists on four basic steps (see table 2.1 and figure 2.3 for an example with random data):

1. Finding a set of consecutive morphons with strong loadings (e.g. > 2 or < -2);
2. Follow the loadings for the consecutive morphons below and above the pack of morphons identified in the previous step with the same signal;
3. Define the new set of morphons characterized by being consecutive and share the same signal;
4. The lower morphotype boundary is defined by the upper limit of the smallest morphon, while the upper morphotype boundary is defined by the lower limit of the largest morphon.

Table 2.1 – Example for the definition of a morphotype. Blue negative loadings; Orange positive loadings; Bold core of the morphotype. The boundaries of this morphotype would be 6.0µm to 6.6µm

Morphon	Loadings (C1)	Morphon	Loadings (C1)
4.5-5.5 µm	-0.104	*5.7-6.7 µm*	**-2.402**
4.6-5.6 µm	-0.203	*5.8-6.8 µm*	**-3.100**
4.7-5.7 µm	-0.158	*5.9-6.9 µm*	**-2.802**
4.8-5.8 µm	0.086	*6.0-7.0 µm*	**-2.304**
4.9-5.9 µm	0.105	*6.1-7.1 µm*	-1.081
5.0-**6.0 µm**	-0.110	*6.2-7.2 µm*	-0.770
5.1-6.1 µm	-0.128	*6.3-7.3 µm*	-0.357
5.2-6.2 µm	-0.113	*6.4-7.4 µm*	-0.132
5.3-6.3 µm	-0.233	*6.5-7.5 µm*	-0.211
5.4-6.4 µm	-0.944	**6.6**-7.6 µm	-0.083
5.5-6.5 µm	-1.579	6.7-7.7 µm	0.075
5.6-6.6 µm	**-2.089**	6.8-7.8 µm	-0.094

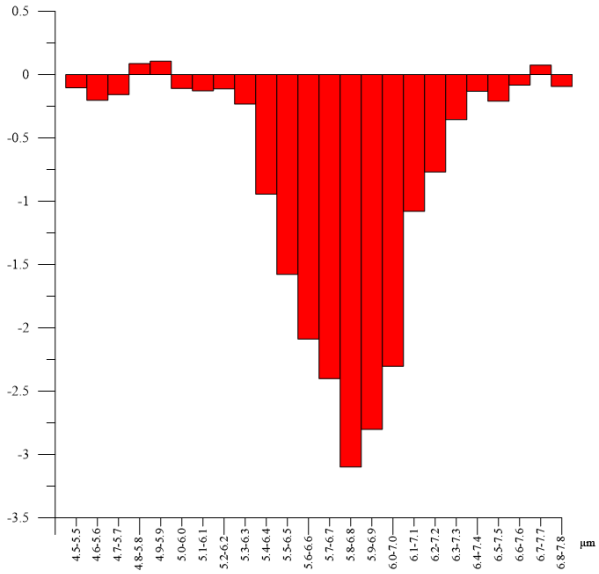

Figure 2.3 – Loadings of the example for the definition of a morphotype (table 1 data).

Through the factor loadings the morphotypes could be determined to the decimal of the micron with an error of 0.1µm error (Table 2.2).

After defining the boundary limits of the morphotypes IMMA components scores provide insight about morphotypes behaviour throughout the samples. Component 1 scores (C1) informs which morphotype is active and when. High negative scores indicate that M_S is dominant, while high positive values show the dominance of M_L. Scores values near zero, either positive or negative, indicate that there is no dominant morphotype.

Table 2.2 – Morphotypes limits defined at the matrix and determined by the PCA. M_S – smaller morphotype. M_L – large morphotype.

M_S (pre-determined)		**M_S (determined from IMMA)**	
5.3	9.6	5.4	9.5
M_L (pre-determined)		**M_L (determined from IMMA)**	
10.7	13.2	10.8	13.1

The relation between scores and morphotypes behaviour can be best seen in Figure 2.4 (Table A2-2 in Annex-2).

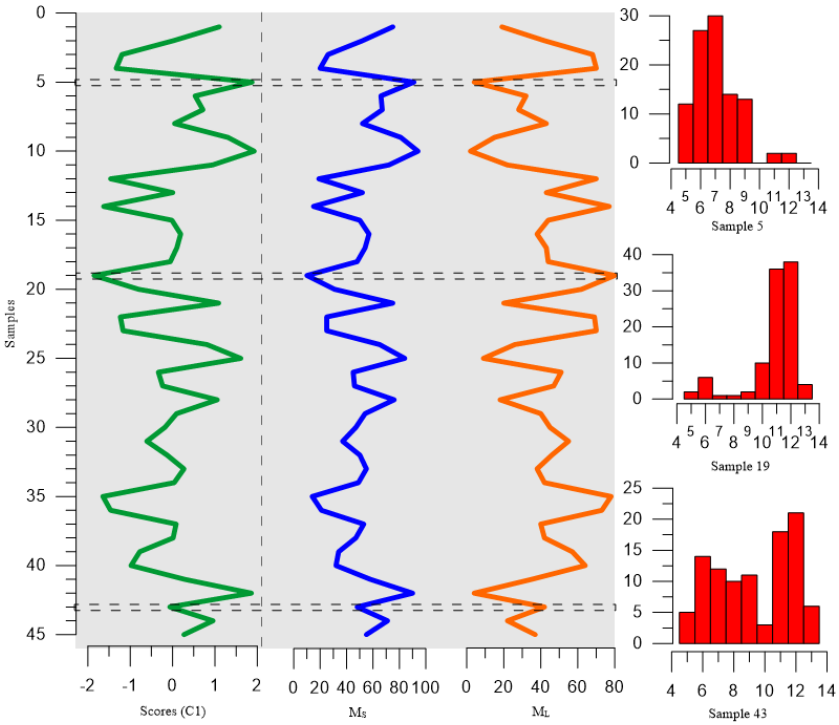

Figure 2.4 – PCA component 1 scores (green line) and morphotypes' counting's (M_S – blue line; M_L – red line) for M_0. Histograms of randomly selected samples (indicated by double traced lines) to enhance the relation between scores and sample morphometric histogram characteristics.

To better compare the improvement introduced by IMMA, the previous MMA was applied to M_0. Since it uses 1 μm arbitrary tabulation, MMA (Table 2.3 and Figure 2.5) with integer limits it can only define same morphotypes as having limits [5.0, 9.0[μm for the smallest and [10.0, 13.0[μm for the largest. MMA can extract the two morphotypes but with poor boundary resolution. With IMMA resolution increases ten fold.

Table 2.3 – PCA results using MMA. Orange for positive values; Blue for negative values.

Morphon	Loadings (C1)
5.0-6.0 μm	3,566
6.0-7.0 μm	4,776
7.0-8.0 μm	5,957
8.0-9.0 μm	5,196
9.0-10.0 μm	3,158
10.0-11.0 μm	-3,184
11.0-12.0 μm	-9,006
12.0-13.0 μm	-9,159
13.0-14.0 μm	-1,304

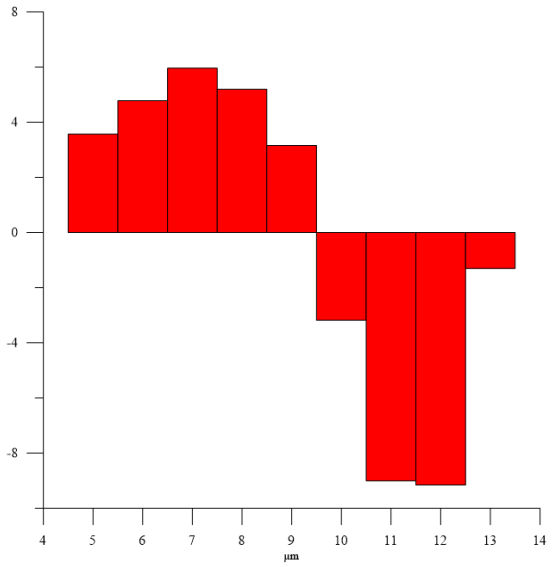

Figure 2.5 – PCA loadings for MMA applied to theoretical matrix M_0.

2.3.2 Theoretical Matrix with noise (M_{30})

This theoretical scenario used the same previous definition but with a 30% noise (M_{30}) added to the data, meaning that 30% of the data was randomly selected with no relation to the predetermined forcing parameters and allowing values to extend outside the intervals for the predefined morphotypes (Figure 2.6 presents the histogram of the global theoretical population).

PCA loadings for M_{30} (Fig. 2.7 – Table AII-3) allow the identification of the morphotypes limits. The increased noise in the theoretical matrixes does not affect the uncertainty in morphotype boundary determination, although there is some variability.

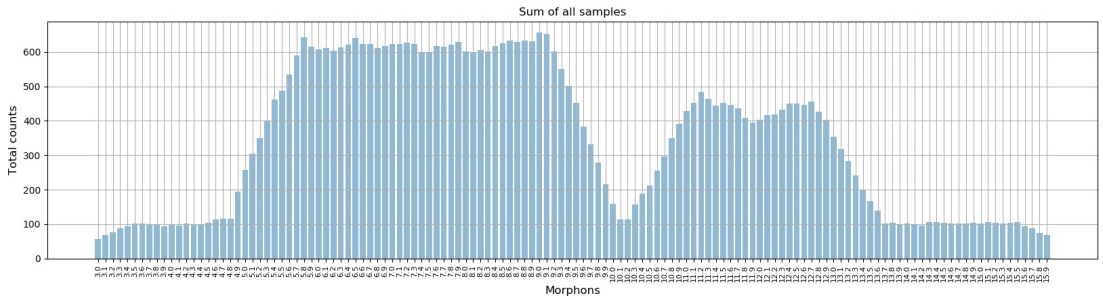

Figure 2.6 – Histogram of the entire theoretical population defined in M30.

The definition of each morphotype (Table 2.4) is easily disclosed by the component loadings in figure 2.7. The limits determination varies slightly when compared to the theoretical matrix without noise, with the uncertainty keeping constant to over 0.1µm.

Table 2.4 – Morphotypes limits defined at the matrix and determined by the PCA for matrix with 30% of error (M_{30}). M_S – smaller morphotype; M_L – large morphotype.

M_S (predetermined)		**M_S (M_{30})**	
5.3	9.6	5.4	9.7
M_L (predetermined)		**M_L (M_{30})**	
10.7	13.2	10.8	13.3

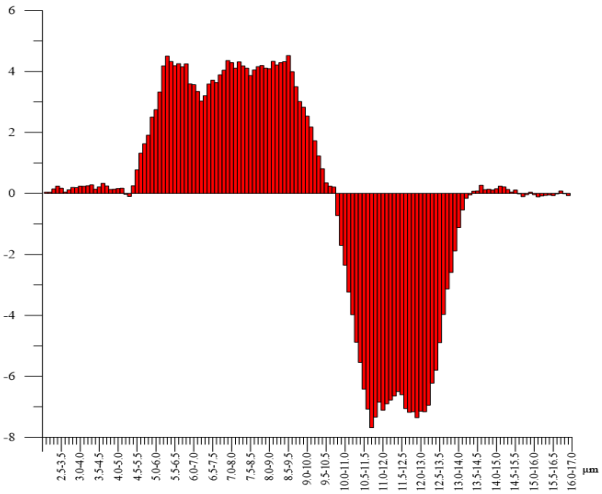

Figure 2.7 – PCA loadings C1 for theoretical matrix M_{30}.

The scores interpretation is the same as for the M_0. For M_{30} the correlation between counting's and scores are 0.992 for M_S and -0.997 for M_L, which can be best seen in Figure 2.8 (Table AII-4).

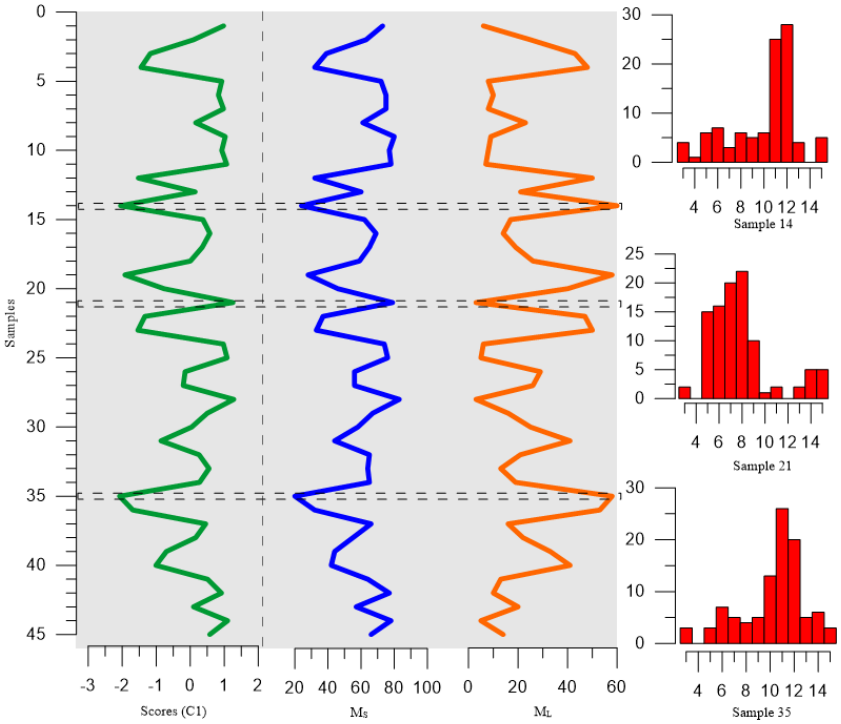

Figure 2.8 – PCA component 1 scores (green line) and morphotypes' counting's (MS – blue line; ML – red line) for M_{30}. Histograms of randomly selected samples (indicated by double traced lines) to enhance the relation between scores and samples morphometric histogram characteristics.

Summarizing, the definition of the lower and upper limits of a morphotype is based on the change and stability of the loadings. When a set of sequential morphons are determined to be a morphotype, the lower limit of a morphotype corresponds to the upper limit of the morphon, and the upper limit corresponds to the lower limit of the morphon (see Figure 2.9 for loadings of M_0 and M_{30}).

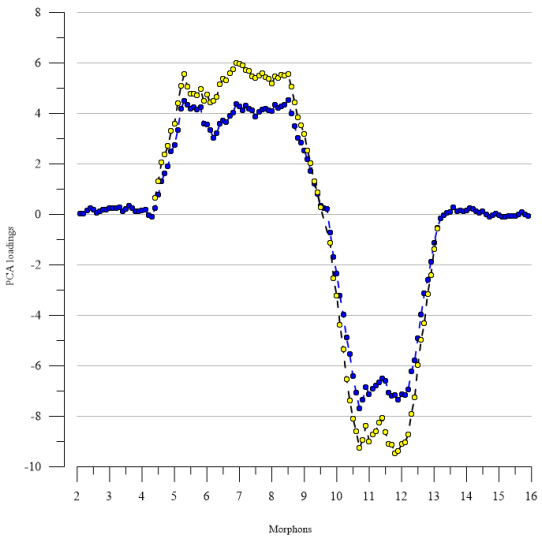

Figure 2.9 – PCA loadings for IMMA theoretical matrixes M_0 (yellow) and M_{30} (blue).

2.4 Discussion

IMMA increases precision and resolution on the determination of size boundaries of morphotypes from the integer to the decimal of the micron, thus opening new perspectives to study microevolution. It screens the entire morphometric matrix to look for patterns and relations between the measurements throughout the samples/time, in a similar way MMA already performed. However, it strengthens the morphometric analysis by performing the analysis on a combined matrix that reproduces ten times MMA analysis on a 1- (n × 0.1)µm (with n varying from 0 to 9) shifting-window across the morphometric data, thus increasing morphometric resolution (Figure 2.10).

Boundaries are particularly relevant for coccolithophore morphometric studies. When only one morphotype is present, the mean value gives enough information and histograms represent a simple method for the population morphometric parameters. However, when more than one morphotype is present, the mean is less descriptive, and does not separate information between different morphotypes. Frequency histograms don't present a normal distribution, with overlapping and/or complex, irregular, shapes, meaning that size boundaries matter.

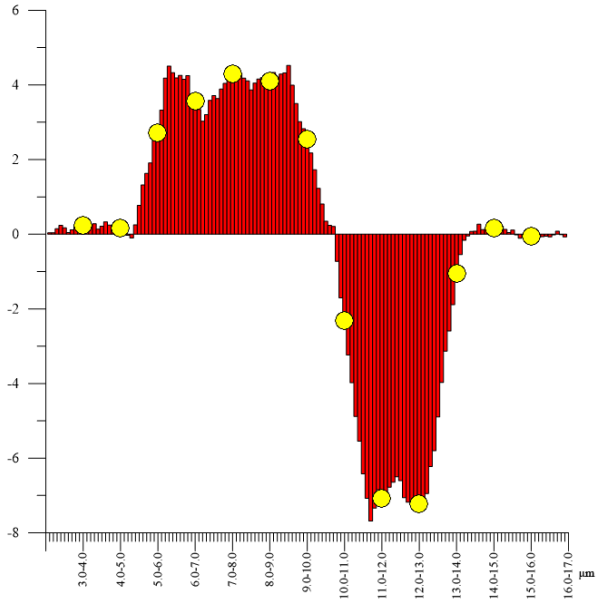

Figure 2.10 – Comparison between MMA (yellow dots) and IMMA (blue line) loadings applied to M_{30}.

Like MMA methodology, IMMA is based on 100 random coccolith measurements per sample. As referred, determining a predefined number of measurements raises the

probability of an automatic appearance of spurious negative correlation between the two main morphotypes present in the set of samples. This induced opposite behaviour that arises between the two main morphotypes are expressed by component 1 loadings that explains the larger amount of the matrix variance.

As a consequence, this spurious negative correlation between two morphotypes along the main component must always be further investigated with available additional data (e.g. abundances, community composition, current distribution for extant taxa).

To address this particular issue several tests were carried out. Increasing the number of coccoliths measured in each sample could slowly reduce these spurious results. If in fact there is no real opposition between two morphotypes, then increasing the number of measurements would reduce the spurious effects observed in the PCA but only over a significant number of measurements. However, morphometric analysis is a highly time demanding procedure. Morphometric methodologies and analysis usually do not count more than 100 specimens per sample (eg. Mattioli et al., 2004; Bornemann & Mutterlose, 2006; Hendericks & Törner, 2006; Thibault, 2010; Hermann et al., 2012; Baumann et al., 2016), although there are some studies that have performed 100 or more measurements (eg. Knapppertsbusch, 2000; Giraud et al., 2006; Linnert & Mutterlose, 2009). A cost-benefit relationship between measurement efforts and its statistical representativeness is highly limiting for research activities, thus IMMA method limitation may be better compensated by the use of additional data other than measuring many more specimens per sample.

A different methodology can also be tested to address this issue. Instead of measuring a fixed 100 coccoliths, the morphometric analysis could be performed by measuring all the coccoliths that appear in a predetermined sample area. For example, measuring all coccoliths of a certain species in three random rows of the sample would eliminate the spurious opposite behaviour between the morphotypes present in the sample and would potentially also introduce effects of abundance variations. This discussion will be addressed in Section IV.

2.5 Conclusions

IMMA improves over the traditional limitation of morphotypes boundaries to be defined only by integer values. With IMMA boundaries can be determined with a

resolution and precision up to 0.1µm. This opens new ways to explore microevolution and ecophenotipic plasticity patterns of coccolithophores, both fossil and extant.

Some caution is required though in the interpretation of morphotypes behaviour due to the closure problem of measuring a fixed number of specimens. This needs to use absolute abundances to complement the characterization of the community structure.

The use of rotation is showed to be at least potentially dangerous when analysing coccolithophore morphometric data using PCA. The data presented here discloses the loss of information on determining the limits of the morphotypes present in the samples, or at least lost in the extraction of information (see Annex-2).

References

Backman, J., Hermelin, J.O.R., 1986. Morphometry of the Eocene nannofossil *Reticulofenestra umbilicus* lineage and its biochronological consequences. Palaeogeogr. Palaeoclimatol. Palaeoecol. 57, 103–116. doi:10.1016/0031-0182(86)90009-X

Baumann, K.-H., Saavedra-Pellitero, M., Bockel, B., Ott, C., 2016. Morphometry, biogeography and ecology of *Calcidiscus* and *Umbilicosphaera* in the South Atlantic. Rev. Micropaleontol. 59, 239–251. doi:10.1016/j.revmic.2016.03.001

Baumann, K., 1995. Morphometry of Quaternary *Coccolithus pelagicus* coccoliths from Northern North Atlantic and its paleoceanographical significance. Proceedings 5th INA Conference. Salamanca, Spain, 11 – 21.

Bornemann, A., Mutterlose, J., 2006. Size analyses of the coccolith species *Biscutum constans* and *Watznaueria barnesiae* from the Late Albian "Niveau Breistroffer" (SE France): taxonomic and palaeoecological implications. Geobios 39, 599–615. doi:10.1016/j.geobios.2005.05.005

Cachão, M., Moita, M.T., 2000. *Coccolithus pelagicus*, a productivity proxy related to moderate fronts off Western Iberia. Mar. Micropaleontol. 39, 131–155.

Colmenero-Hidalgo, E., Flores, J.-A., Sierro, F.J., 2002. Biometry of *Emiliania huxleyi* and its biostratigraphic significance in the Eastern North Atlantic Ocean and Western Mediterranean Sea in the last 20 000 years. Mar. Micropaleontol. 46, 247–263. doi:10.1016/S0377-8398(02)00065-8

Daniels, C.J., Sheward, R.M., Poulton, A.J., 2014. Biogeochemical implications of comparative growth rates of *Emiliania huxleyi* and *Coccolithus* species. Biogeosciences 11, 6915–6925. doi:10.5194/bg-11-6915-2014

Faucher, G., Erba, E., Bottini, C., Gambacorta, G., 2017. Calcareous Nannoplankton Response To the Latest Cenomanian Oceanic Anoxic Event 2 Perturbation. Riv. It. Paleontol. Strat. Riv. Ital. di Paleontol. e Stratigr. (Research Paleontol. Stratigr. 123, 159–176. doi:10.13130/2039-4942/8092

Field, A., 2009. Discovering Statistics Using SPSS, 3rd ed. SAGE, London.

Gerecht, A.C., Šupraha, L., Edvardsen, B., Langer, G., Henderiks, J., 2015. Phosphorus availability modifies carbon production in *Coccolithus pelagicus* (Haptophyta). J. Exp. Mar. Bio. Ecol. 472, 24–31. doi:10.1016/j.jembe.2015.06.019

Gerecht, A.C., Šupraha, L., Edvardsen, B., Probert, I., Henderiks, J., 2014. High temperature decreases the PIC / POC ratio and increases phosphorus requirements in *Coccolithus pelagicus* (Haptophyta). Biogeosciences 11, 3531–3545. doi:10.5194/bg-11-3531-2014

Giraud, F., Pittet, B., Mattioli, E., Audouin, V., 2006. Paleoenvironmental controls on the morphology and abundance of the coccolith *Watznaueria britannica* (Late Jurassic, southern Germany). Mar. Micropaleontol. 60, 205–225. doi:10.1016/j.marmicro.2006.04.004

Guerreiro, C. 2013. (Paleo)ecology of Coccolithophores in the Submarine Canyons of the Central Portuguese Continental Margin: Environmental, Sedimentary and Oceanographic Implications. (PhD Dissertation), University of Lisbon, Portugal, 251 pp.

Guerreiro, C., Cachão, M., Drago, T., 2005. Calcareous nannoplankton as a tracer of the marine influence on the NW coast of Portugal over the last 14 000 years. J. Nannoplankt. Res. 27, 159–172.

Guerreiro, C., Cachão, M., Pawlowsky-Glahn, V., Oliveira, A., Rodrigues, A., 2015. Compositional Data Analysis (CoDA) as a tool to study the (paleo)ecology of coccolithophores from coastal-neritic settings off central Portugal. Sediment. Geol. 319, 134–146. doi:10.1016/j.sedgeo.2015.01.012

Henderiks, J., Törner, A., 2006. Reproducibility of coccolith morphometry: Evaluation of spraying and smear slide preparation techniques. Mar. Micropaleontol. 58, 207–218. doi:10.1016/j.marmicro.2005.11.002

Herrmann, S., Weller, A.F., Henderiks, J., Thierstein, H.R., 2012. Global coccolith size variability in Holocene deep-sea sediments. Mar. Micropaleontol. 82–83, 1–12. doi:10.1016/j.marmicro.2011.09.006

Jolliffe, I.T., 2002. Principal Components Analysis, 2nd ed, Springer Series in Statistics. Springer New York. doi:10.1007/b98835

Jordan, R.W., Green, J.C., 1994. A check-list of the extant hapto- phyta of the world. J. Mar. Biol. Assoc. U. K. 74, 149–174.

Knappertsbusch, M., 2000. Morphologic Evolution of the Coccolithophorid *Calcidiscus leptoporus* from the early Miocene to recent. J. Paleontol. 74, 712–730.

Linnert, C., Mutterlose, J., 2009. Biometry of the Late Cretaceous Arkhangelskiella group: ecophenotypes controlled by nutrient flux. Cretac. Res. 30, 1193–1204. doi:10.1016/j.cretres.2009.06.001

Mattioli, E., Pittet, B., Young, J.R., Bown, P.R., 2004. Biometric analysis of Pliensbachian-Toarcian (Lower Jurassic) coccoliths of the family Biscutaceae: intra- and interspecific variability versus palaeoenvironmental influence. Mar. Micropaleontol. 52, 5–27. doi:10.1016/j.marmicro.2004.04.004

Narciso, A., Cachão, M., Abreu, L. De, 2006. *Coccolithus pelagicus* subsp. *pelagicus* versus *Coccolithus pelagic*us subsp. *braarudii* (Coccolithophore, Haptophyta): A proxy for surface subarctic Atlantic waters off Iberia during the last 200 kyr. Mar. Micropaleontol. 59, 15–34. doi:10.1016/j.marmicro.2005.12.001

Parente, A., Cachão, M., Baumann, K., Abreu, L. De, Ferreira, J., 2004. Morphometry of *Coccolithus pelagicus s.l.* (Coccolithophore, Haptophyta) from offshore Portugal, during the last 200 kyr. Micropaleontology 50, 107–120.

Renaud, S., Klaas, C., 2001. Seasonal variations in the morphology of the coccolithophore *Calcidiscus leptoporus* off Bermuda (N . Atlantic). J. Plankton Res. 23, 779–795. doi:10.1093/plankt/23.8.779

Richman, M.B., 1986. Rotation of Principal Components. J. Climatol. 6, 293–335. doi:10.1007/BF00118735

Richman, M.B., 1987. Rotation of principal components: a reply. J. Climatol. 7, 511–520. doi:10.1002/joc.3370070507

Saez, A.G., Probert, I., Geisen, M., Quinn, P., Young, J.R., Medlin, L.K., 2003. Pseudo-cryptic speciation in coccolithophores. Proc. Natl. Acad. Sci. U. S. A. 100, 7163–7168. doi:10.1073/pnas.1132069100

Samtleben, C., 1980. Die Evolution der Coccolithophoriden-Gattung *Gephyrocapsa* nach Befunden im Atlantik. Paläont. Z.. 54, 91-127.

Shaukat, S., Rao, T.A., Khan, M.A., 2016. Impact of sample size on Principal Component Analysis ordination of an environmental data set: effects on eigenstructure. Ekológia (Bratislava) 35, 173-190. DOI:10.1515/eko-2016-0014

Sheward, R.M., Daniels, C.J., Gibbs, S.J., 2014. Growth rates and biometric measurements of coccolithophores (*Coccolithus pelagicus*, *Coccolithus braarudii*, *Emiliania huxleyi*) during experiments, PANGAEA, http://doi.pangaea.de/10.1594/ PANGAEA.836841.

Sheward, R.M., Poulton, A.J., Gibbs, S.J., Daniels, C.J., Bown, P.R., 2016. Physiology regulates the relationship between coccosphere geometry and growth phase in coccolithophores. Biogeosciences Discuss. 14, 1493–1509. doi:10.5194/bg-14-1493-2017

Silva, A., Palma, S., Moita, M.T., 2008. Coccolithophores in the upwelling waters of Portugal: Four years of weekly distribution in Lisbon bay. Cont. Shelf Res. 28, 2601–2613. doi:10.1016/j.csr.2008.07.009

Šupraha, L., Gerecht, A.C., Probert, I., Henderiks, J., 2015. Eco-physiological adaptation shapes the response of calcifying algae to nutrient limitation. Sci. Rep. 5, 16499. doi:10.1038/srep16499

Thibault, N., 2010. Biometric analysis of the Arkhangelskiella group in the upper Campanian-Maastrichtian of the Stevns-1 borehole, Denmark: Taxonomic implications and evolutionary trends. Geobios 43, 639–652. doi:10.1016/j.geobios.2010.06.002

Wei, W., 1992. Biometric study of Discoaster multiradiatus and its biochronological utility. Memorie Scienze Geologiche 43, 219–235.

Westbroek, P., de Jong, E.W., van der Wal, P., Borman, a. H., de Vrind, J.P.M., Kok, D., de Bruijn, W.C., Parker, S.B., 1984. Mechanism of Calcification in the Marine Alga *Emiliania huxleyi* [and Discussion]. Philos. Trans. R. Soc. B Biol. Sci. 304, 435–444. doi:10.1098/rstb.1984.0037

Young, J., 1990. Size variation of Neogene *Reticulofenestra* coccoliths from Indian Ocean DSDP Cores. J. Micropalaeontology 9, 71–86.

Young, J., Davis, S., Bown, P., Mann, S., 1999. Coccolith ultrastructure and biomineralisation. J. Struct. Biol. 126, 195–215. doi:10.1006/jsbi.1999.4132

Young, J.R., Geisen, M., Probert, I., 2005. A review of selected aspects of coccolithophore biology with implications for paleobiodiversity estimation. Micropaleontology 51, 267–288. doi:10.2113/gsmicropal.51.4.267

Young, J.R., Henriksen, K., 2003. Biomineralization Within Vesicles: The Calcite of Coccoliths. Rev. Mineral. Geochemistry 54, 189–215. doi:10.2113/0540189

Ziveri, P., Baumann, K, Bockel, B., Bollmann, J., Young, J.R., 2004. Biogeography of selected Holocene coccoliths in the Atlantic Ocean. Coccolithophores from Molecular Process to Global impact, 403-408.

Annex-2

Short note on Rotation with PCA

Another important aspect of PCA is the use of rotation techniques to simplify the data output. The most important step after performing a dimension reduction analysis, either with principal components or factor analysis, is to understand if rotation is increasing the information about the data, or simplifying the data interpretation, or if on the other hand is de-escalating data information and loosing information on dominant components.

Performing rotation on PCAs is common practice in many scientific fields, particularly in atmospheric sciences, where there has been extensive discussion of its advantages and disadvantages (see, for example Richman 1986, 1987). However, rotation in PCAs has several possible drawbacks. Jolliffe (2002) lists the potential problems starting with the choice of the type of rotation. There are several possibilities and the choosing criterion depends on a large number of choices. It is frequent this choice to be arbitrary (often varimax is selected), like by using the default criterion in a statistics software. Although the rotation chosen is important, one must enhance that when it comes to orthogonal rotation, often make little difference to the results.

PCA successively maximizes variance accounted for. This means that when rotation is done, the total variance within the rotated dimensional subspace remains unchanged; it is still the maximum that can be achieved, but it is redistributed amongst the rotated components more evenly than before rotation (Jolliffe, 2002). This means that information about the nature of any really dominant components may be lost.

To verify if the use of rotation on our theoretical matrixes would have an impact on the information extracted from the data, varimax rotation was applied, using IBM© SPSS© Statistics version 23.0. Just to remember that although the command is under Factor Analysis, choosing Principal Components means to perform a PCA (see Field, 2009).

For M_0, the comparison between unrotated and rotated PCA had to be performed with PCA with correlation matrix, since the rotation failed to perform with the

covariance matrix. Although correlation PCA is not the best choice to analyse our data, the comparison was made since the correlation matrix without rotation gives highly similar results to covariance matrix for M_0.

Varimax rotation in M_0 presents a major loss in the information extracted from the matrix (Fig. AII-1). In fact, varimax rotation completely failed in giving significant values for the morphotypes predefined in the data.

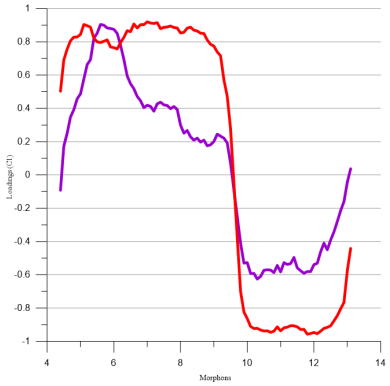

Figure A2-1 – Comparison between unrotated PCA (red line) and varimax rotation (purple line) for M_0 with correlation matrix.

For M_{30} varimax rotation was applied to a PCA with covariance matrix. In this case rotation shows results very similar to PCA with no rotation (Fig. AII-2), although it presents a loss in the covariance extraction for component one from 70.8% (unrotated) to 65.1% (varimax).

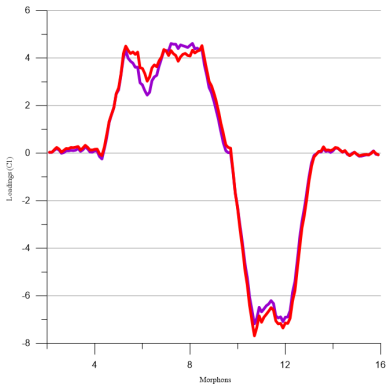

Figure A2-2 - Comparison between unrotated PCA (red line) and varimax rotation (purple line) for M_{30} with covariance matrix.

Looking at real data from samples of the west coast of Portugal (site MD95-2040), addressed in Section III, it is also possible to observe the loss of data when rotation is applied to PCA (in this case with covariance matrix). The analysis of the

coccolithophore morphometry is detailed in the next section, however for the purpose of the discussion undertaken in this section, it would be of great interest to present these results.

The correlation between the morphotypes counting's and the PCA scores for MD95-2040, where two morphotypes were identified, is 0.991 and -0.983 for morphotype one and morphotype two respectively in component one, and -0.875 and 0.823 in component two. When varimax rotation is applied the correlations drop to 0.934 (-5.8%) and -0.884 (-10.1%) in component one and -0.570 (-34.8%) and 0.807 (-1.9%) in component two. The covariance extraction also drops. Unrotated PCA presents 53.57% extraction for component one and 26.97% for component two, while varimax rotation shows 44.56% and 17.22% respectively.

Also important is to recognize why PCA is more adequate than Factor Analysis (FA) to extract information from coccoliths morphometry than factor analysis. Factor analysis assumes that there is a lower-dimensional structure underlying your data. PCA assumes no such structure – it simply looks for a lower-dimensional representation that displays the main features of the data (Jolliffe pers. comm., 2017). In other words, FA assumes a predetermined model while PCA does not. Since in morphometric data there is no previous assumption of a model, PCA is more adequate than FA to extract the morphometric information in the data.

Table A2-1 – Loadings for M_0. Orange for positive values; Blue for negative values.

Morphon	Loadings (C1)	Morphon	Loadings (C1)	Morphon	Loadings (C1)
4,4-5,4 µm	0,650	7,4-8,4 µm	5,461	10,3-11,3 µm	-6,539
4,5-5,5 µm	1,308	7,5-8,5 µm	5,392	10.4-11.4 µm	-7,370
4,6-5,6 µm	2,052	7,6-8,6 µm	5,498	10.5-11.5 µm	-8,087
4,7-5,7 µm	2,360	7,7-8,7 µm	5,576	10.6-11.6 µm	-8,613
4,8-5,8 µm	2,708	7,8-8,8 µm	5,436	10.7-11.7 µm	-9,254
4,9-5,9 µm	3,312	7,9-8,9 µm	5,358	10.8-11.8 µm	-8,934
5,0-6,0 µm	3,600	8,0-9,0 µm	5,187	10.9-11.9 µm	-8,380
5,1-6,1 µm	4,394	8,1-9,1 µm	5,458	11.0-12.0 µm	-8,999
5,2-6,2 µm	5,079	8,2-9,2 µm	5,411	11.1-12.1 µm	-8,719
5,3-6,3 µm	5,548	8,3-9,3 µm	5,511	11.2-12.2 µm	-8,600
5,4-6,4 µm	5,066	8,4-9,4 µm	5,495	11.3-12.3 µm	-8,259
5,5-6,5 µm	4,784	8,5-9,5 µm	5,570	11.4-12.4 µm	-8,057
5,6-6,6 µm	4,778	8,6-9,6 µm	5,052	11.5-12.5 µm	-8,622
5,7-6,7 µm	4,719	8,7-9,7 µm	4,445	11.6-12.6 µm	-9,103
5,8-6,8 µm	4,958	8,8-9,8 µm	3,841	11.7-12.7 µm	-9,133
5,9-6,9 µm	4,502	8,9-9,9 µm	3,518	11.8-12.8 µm	-9,470
6,0-7,0 µm	4,748	9,0-10,0 µm	3,188	11.9-12.9 µm	-9,365
6,1-7,1 µm	4,420	9,1-10,1 µm	2,526	12.0-13.0 µm	-9,099
6,2-7,2 µm	4,483	9,2-10,2 µm	2,017	12.1-13.1 µm	-9,044
6,3-7,3 µm	4,656	9,3-10,3 µm	1,293	12.2-13.2 µm	-8,735
6,4-7,4 µm	5,143	9,4-10,4 µm	0,880	12.3-13.3 µm	-7,898
6,5-7,5 µm	5,364	9,5-10,5 µm	0,277	12.4-13.4 µm	-7,269
6,6-7,6 µm	5,316	9,6-10,6 µm		12.5-13.5 µm	-5,987
6,7-7,7 µm	5,596	9,7-10,7 µm		12.6-13.6 µm	-4,981
6,8-7,8 µm	5,754	9,8-10,8 µm	-1,144	12.7-13.7 µm	-4,309
6,9-7,9 µm	6,006	9,9-10,9 µm	-2,531	12.8-13.8 µm	-3,148
7,0-8,0 µm	5,973	10,0-11,0 µm	-3,222	12.9-13.9 µm	-2,420
7,1-8,1 µm	5,898	10,1-11,1 µm	-4,370	13.0-14.0 µm	-1,376
7,2-8,2 µm	5,706	10,2-11,2 µm	-5,360	13.1-14.1 µm	-0,563
7,3-8,3 µm	5,688				

Table A2-2 – PCA scores and morphotypes counting's for each sample for M_0. Positive scores correspond to M_S and are presented in orange; Negative scores correspond to M_L and are presented in blue. (The correlation between the counting's and the scores is 0.997 for M_S and -0.998 for M_L).

Sample	C1 (scores)	M_S counts	M_L counts	Sample	C1 (scores)	M_S counts	M_L counts
sample 1	1,101	75	19	**sample 24**	0,810	65	26
sample 2	0,019	52	42	**sample 25**	1,610	84	9
sample 3	-1,196	26	68	**sample 26**	-0,336	45	51
sample 4	-1,330	20	70	**sample 27**	-0,235	46	47
sample 5	1,876	91	4	**sample 28**	1,054	76	18
sample 6	0,533	66	32	**sample 29**	0,094	54	40
sample 7	0,716	67	28	**sample 30**	-0,184	47	45
sample 8	0,046	52	43	**sample 31**	-0,608	37	55
sample 9	1,303	81	15	**sample 32**	-0,132	50	46
sample 10	1,925	94	2	**sample 33**	0,267	55	38
sample 11	0,940	72	22	**sample 34**	0,037	49	42
sample 12	-1,464	19	70	**sample 35**	-1,646	14	78

sample 13	0,004	52	43	**sample 36**	-1,464	21	73
sample 14	-1,629	15	77	**sample 37**	0,083	53	40
sample 15	-0,017	50	44	**sample 38**	0,013	47	42
sample 16	0,190	57	38	**sample 39**	-0,775	34	57
sample 17	0,099	54	43	**sample 40**	-0,981	32	64
sample 18	-0,055	48	44	**sample 41**	0,288	58	35
sample 19	-1,855	10	80	**sample 42**	1,860	90	4
sample 20	-0,802	31	62	**sample 43**	-0,066	48	42
sample 21	1,088	75	20	**sample 44**	0,953	71	22
sample 22	-1,233	25	69	**sample 45**	0,267	55	37
sample 23	-1,170	25	70				

Table A2-3 – Loadings for M_{30}. Orange for positive values; Blue for negative values.

Morphon	Loadings (C1)	Morphon	Loadings (C1)	Morphon	Loadings (C1)
2,1-3,1 µm	0,037	6,8-7,8 µm	4,040	11,4-12,4 µm	-6,502
2,2-3,2 µm	0,037	6,9-7,9 µm	4,361	11,5-12,5 µm	-6,603
2,3-3,3 µm	0,145	7,0-8,0 µm	4,291	11,6-12,6 µm	-7,058
2,4-3,4 µm	0,241	7,1-8,1 µm	4,109	11,7-12,7 µm	-7,183
2,5-3,5 µm	0,170	7,2-8,2 µm	4,315	11,8-12,8 µm	-7,163
2,6-3,6 µm	0,042	7,3-8,3 µm	4,184	11,9-12,9 µm	-7,357
2,7-3,7 µm	0,120	7,4-8,4 µm	4,107	12,0-13,0 µm	-7,144
2,8-3,8 µm	0,196	7,5-8,5 µm	3,866	12,1-13,1 µm	-7,165
2,9-3,9 µm	0,188	7,6-8,6 µm	4,051	12,2-13,2 µm	-6,947
3,0-4,0 µm	0,239	7,7-8,7 µm	4,160	12,3-13,3 µm	-6,224
3,1-4,1 µm	0,231	7,8-8,8 µm	4,195	12,4-13,4 µm	-5,799
3,2-4,2 µm	0,253	7,9-8,9 µm	4,110	12,5-13,5 µm	-4,899
3,3-4,3 µm	0,280	8,0-9,0 µm	4,088	12,6-13,6 µm	-3,970
3,4-4,4 µm	0,135	8,1-9,1 µm	4,331	12,7-13,7 µm	-3,131
3,5-4,5 µm	0,215	8,2-9,2 µm	4,214	12,8-13,8 µm	-2,596
3,6-4,6 µm	0,331	8,3-9,3 µm	4,290	12,9-13,9 µm	-1,889
3,7-4,7 µm	0,244	8,4-9,4 µm	4,324	13,0-14,0 µm	-1,122
3,8-4,8 µm	0,132	8,5-9,5 µm	4,523	13,1-14,1 µm	-0,547
3,9-4,9 µm	0,133	8,6-9,6 µm	3,992	13,2-14,2 µm	-0,164
4,0-5,0 µm	0,162	8,7-9,7 µm	3,499	13,3-14,3 µm	-0,048
4,1-5,1 µm	0,170	8,8-9,8 µm	3,016	13,4-14,4 µm	0,072
4,2-5,2 µm	-0,028	8,9-9,9 µm	2,830	13,5-14,5 µm	0,083
4,3-5,3 µm	-0,100	9,0-10,0 µm	2,533	13,6-14,6 µm	0,267
4,4-5,4 µm	0,252	9,1-10,1 µm	2,178	13,7-14,7 µm	0,123
4,5-5,5 µm	0,773	9,2-10,2 µm	1,725	13,8-14,8 µm	0,137
4,6-5,6 µm	1,320	9,3-10,3 µm	1,228	13,9-14,9 µm	0,110
4,7-5,7 µm	1,627	9,4-10,4 µm	0,810	14,0-15,0 µm	0,151
4,8-5,8 µm	1,910	9,5-10,5 µm	0,348	14,1-15,1 µm	0,240
4,9-5,9 µm	2,503	9,6-10,6 µm	0,241	14,2-15,2 µm	0,214
5,0-6,0 µm	2,746	9,7-10,7 µm	0,209	14,3-15,3 µm	0,128
5,1-6,1 µm	3,325	9,8-10,8 µm	-0,727	14,4-15,4 µm	0,046
5,2-6,2 µm	4,184	9,9-10,9 µm	-1,705	14,5-15,5 µm	0,112
5,3-6,3 µm	4,504	10,0-11,0 µm	-2,356	14,6-15,6 µm	-0,016
5,4-6,4 µm	4,325	10,1-11,1 µm	-3,239	14,7-15,7 µm	-0,105
5,5-6,5 µm	4,189	10,2-11,2 µm	-3,981	14,8-15,8 µm	-0,042
5,6-6,6 µm	4,257	10,3-11,3 µm	-4,883	14,9-15,9 µm	0,038
5,7-6,7 µm	4,154	10,4-11,4 µm	-5,545	15,0-16,0 µm	-0,039
5,8-6,8 µm	4,251	10,5-11,5 µm	-6,422	15,1-16,1 µm	-0,111
5,9-6,9 µm	3,594	10,6-11,6 µm	-7,075	15,2-16,2 µm	-0,085

6,0-7,0 µm	3,566	10,7-11,7 µm	-7,687	15,3-16,3 µm	-0,063
6,1-7,1 µm	3,345	10,8-11,8 µm	-7,338	15,4-16,4 µm	-0,055
6,2-7,2 µm	3,028	10,9-11,9 µm	-6,844	15,5-16,5 µm	-0,070
6,3-7,3 µm	3,206	11,0-12,0 µm	-7,115	15,6-16,6 µm	-0,016
6,4-7,4 µm	3,589	11,1-12,1 µm	-6,904	15,7-16,7 µm	0,082
6,5-7,5 µm	3,715	11,2-12,2 µm	-6,778	15,8-16,8 µm	-0,012
6,6-7,6 µm	3,637	11,3-12,3 µm	-6,647	15,9-16,9 µm	-0,071
6,7-7,7 µm	3,889				

Table A2-4 - PCA scores and morphotypes counting's for each sample for M_{30}. Positive scores correspond to M_S and are presented in orange; Negative scores correspond to M_L and are presented in blue. (The correlation between the counting's and the scores is 0.992 for M_S and -0.997 for M_L).

Sample	C1 (scores)	M_S counts	M_L counts	Sample	C1 (scores)	M_S counts	M_L counts
sample 1	0,980	73	6	**sample 24**	0,974	74	6
sample 2	0,095	63	25	**sample 25**	1,082	76	5
sample 3	-1,174	39	43	**sample 26**	-0,151	56	29
sample 4	-1,449	32	48	**sample 27**	-0,207	56	26
sample 5	0,927	72	8	**sample 28**	1,280	83	3
sample 6	0,827	75	10	**sample 29**	0,501	67	16
sample 7	0,977	75	8	**sample 30**	0,043	58	25
sample 8	0,160	61	23	**sample 31**	-0,861	44	41
sample 9	1,029	80	9	**sample 32**	0,260	65	21
sample 10	0,926	77	8	**sample 33**	0,552	64	13
sample 11	1,070	78	7	**sample 34**	0,273	65	19
sample 12	-1,527	32	50	**sample 35**	-2,079	20	58
sample 13	0,144	60	21	**sample 36**	-1,689	32	53
sample 14	-2,051	24	60	**sample 37**	0,453	66	16
sample 15	0,371	62	17	**sample 38**	0,158	55	22
sample 16	0,577	69	14	**sample 39**	-0,702	44	33
sample 17	0,353	65	19	**sample 40**	-1,009	42	41
sample 18	0,004	59	26	**sample 41**	0,507	64	13
sample 19	-1,921	28	58	**sample 42**	0,917	77	10
sample 20	-0,767	46	40	**sample 43**	0,095	57	20
sample 21	1,256	79	3	**sample 44**	1,098	78	5
sample 22	-1,332	37	47	**sample 45**	0,572	66	14
sample 23	-1,539	33	50				

III. IMMA APPLIED TO CENOZOIC

CHAPTER 3

Reassessing Coccolithus pelagicus *s.l. data*

Abstract

Taxonomy in fossil coccolithophores is based mainly on the heterococcolith life cycle stage morphology and, at species level, on fine variations in size and shape. Coccolith size is relevant on routine identification of certain calcareous nannofossil species. But morphometry can also be a tool to study their morphological plasticity. Here we used a new morphometry statistical method to reassess *Coccolithus pelagicus* s. l. data from two Holocene sites and one covering from the Upper Miocene to the Holocene. Our results suggest that both *C. pelagicus* subsp. *braarudii* and *C. pelagicus* subsp. *pelagicus* present morphological plasticity in response to (palaeo)environmental changes, mainly variations in the upwelling regime in the west coast of Portugal and (palaeo)oceanographic conditions in the North Atlantic linked to glacial periods of the Holocene.

Keywords: *C. pelagicus pelagi*cus; *C. pelagicus braarudii*; Placolith morphometry; IMMA; Quaternary.

3.1 Introduction

Taxonomy of both living and fossil coccolithophores is mainly based on the heterococcolith life cycle stage (hereafter simply referred as coccolith) crystallographic orientation (V and R crystal sets) and morphology, and at species level on fine variations in size and shape (Jordan & Green, 1994) (see Section I of this work). This has been successfully applied to the fossil record and compares well with findings from other research disciplines such as cell physiology and molecular genetics (Sáez et al., 2003; Young et al., 2005). Research indicates that many broad taxa are in fact composed of several discrete species with distinct holococcolith life cycles (see Balch 2018) and/or that morphologic differences within certain morphotypes (e.g., Baumann & Sprengel, 2000; Baumann et al., 2000; Geisen et al., 2002) are indeed genetically distinct species (Sáez et al., 2003).

The morphometry of coccolith morphological parameters is based on the fact that these exoskeleton structures are produced intracellularly, and so their final proportions, prior being extruded to the coccosphere around the cell (Westbroek et al., 1984; Young et al., 1999; Young & Henriksen, 2003; Raven & Giordano, 2009; Taylor et al., 2017) may be constrained species-wise. Hence coccolith size may be considered an intrinsic property of a particular species or ecophenotype and was already used to address questions such as taxonomy, biostratigraphy and palaeoecology of several calcareous nannoplankton (e.g. Samtleben, 1980; Backman & Hermelin, 1986; Young, 1990; Wei, 1992; Baumann, 1995; Knappertsbusch, 2000; Colmenero-Hidalgo et al., 2002; Parente et al., 2004; Narciso et al., 2006).

Several morphometrical studies on extant coccolithophores have been carried out namely on *Emiliania huxleyi* (e.g., Colmenero-Hidalgo et al., 2002; Bollmann et al., 2009; Young et al., 2014), *Calcidiscus leptoporus* (e.g., Knappertsbusch et al., 1997; Baumann & Sprengel, 2000; Renaud & Klaas, 2001; Renaud et al., 2002; Quinn et al., 2004), or *Coccolithus pelagicus* (e.g., Geisen et al., 2002; Parente et al., 2004; Narciso et al., 2006, Cubillos et al., 2012). The last taxon has been documented as two distinct entities in the modern nannoflora, with culture studies and molecular genetics showing that these are genotypically discrete but very closely related. They are variably distinguished as sub-species (Geisen et al., 2003, Young et al., 2003: *C. pelagicus* subsp. *pelagicus* and *C. pelagicus* subsp. *braarudii*) or species (Saez et al., 2003: *C. pelagicus* and *C. braarudii*), being the length of the coccolith and the oceanographic

regime the main differential characteristics. More recently, a third morphotype was described having larger coccoliths and present on surface sediments off the Azores archipelago, (*C. pelagicus* subsp. *azorinus* in Parente et al., 2004).

Beyond routine identification morphometry can also be a tool to study coccolith morphological plasticity, i.e. changes in morphology that are ecological significant. This may occur under two conditions: 1) must have an impact in fitness to that (palaeo)environment; 2) must differ across environmental conditions for some ecological reason (Travis, 1994). This means that a particular taxon such as *C. pelagicus* s.l. may have different morphotypes in response to different environmental conditions. Morphotypes may be recognized simply through coccoliths size. For example, Parente et al. (2004) and Narciso et al. (2006) confirmed the assumption of Cachão & Moita (2000) that a distinct morphotype for *Coccolithus pelagicus* should occur off Iberia, adapted to distinct environmental conditions than the subpolar species. Being a long aspiration for micropalaeontologists, that phenotypic variations have genotypic counterparts, genetic studies have been able to distinguish the two established morphotypes of *C. pelagicus* s.l. into two different taxa (Sáez et al., 2003), which more likely have evolved due to the physical separation: *C. pelagicus* subspecies *pelagicus*, the smaller in subpolar waters; *C. pelagicus* subspecies *braarudii*, the larger morphotype from upwelling regions.

In this work it will be used the new statistical approach Integrated Multivariate Morphon Analysis (IMMA) (Section II) to study *C. pelagicus* s.l. morphometry. As the name implies IMMA directly derives from the Multivariate Morphon Analysis (MMA) (Parente et al., 2004; Narciso et al., 2006) which scope is enlarged and improved for higher resolutions. IMMA enables to observe small variations in size with a resolution of 0.1µm in response to environmental conditions. The goal of the present work is to demonstrate that by using the IMMA new aspects of the morphologic plasticity of *C. pelagicus s.l.* can be addressed. These will be re-interpreted allowing new (palaeo)oceanographic interpretations.

3.2 Materials and Methodology

Three already known *C. pelagicus* s.l. data sets from three different sites (Parente et al., 2004; Narciso et al., 2006) were reassessed to apply Integrated Multivariate Morphon Analysis (IMMA). The three sites are all in the North Atlantic: MD95-2040

from the West coast of Iberia, GeoB5559-2 from the Canary Islands, and DSDP 608 located north of the Azores (Fig. 3.1).

The main differences between previous MMA methodology and new IMMA are:

i) MMA computes a morphometric matrix from tabulating sizes along arbitrary 1.0μm intervals, the morphons. This morphometric matrix is subsequently analysed through Factorial Analysis (FA) with Varimax optimization;

ii) IMMA computes 10 morphometric matrixes by shifting the 1.0 μm morphon tabulations by 0.1 micron. The 10 matrixes are combined in one. The combined morphometric matrix is subsequently analysed through Principal Component Analysis (PCA).

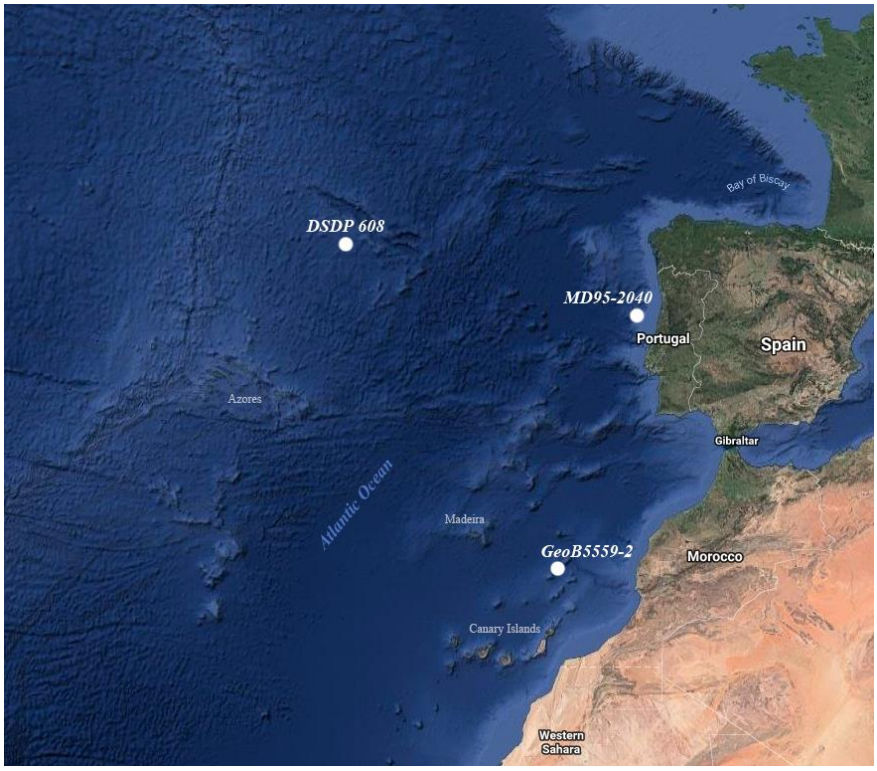

Figure 3.1 – Location of the three sites studied: DSDP 608; MD95-2040; GeoB5559-2.

IMMA was applied to the total samples of the original work and to a subset of it by removing a series of "anomalous samples", i.e., samples with significantly low abundance of *C. pelagicus* s.l., having less than 100 measurements. For sites MD95-2040 and DSDP 608 IMMA performed better with the subset of samples compared to the entire data, meaning that anomalous samples were interfering with the analysis of

the data. For site GeoB5559-2 IMMA performed highly similar with all samples or without anomalous. Anomalous samples represented 12.2% in MD95-2040, 10.0% in DSDP 608 and only 5.9% in GeoB5559-2. Moreover GeoB5559-2 was the site with the largest set of samples (discussion on the importance of the total number of samples in section IV). Since the results were close but more accurate with the subset analysis for sites MD95-2040 and DSDP 608, only IMMA applied to no anomalous samples set will be detailed and discussed. All samples IMMA is present at the annexes of this chapter, with the exception of a brief comment at the beginning and a comparison between morphotypes determined at the end on each site results description. Regarding GeoB5559-2 the results for all samples and for the subset were virtually the same, however both are presented and discussed. The multivariate statistical analysis (PCA) was carried out using IBM© SPSS© version 23.0 software.

3.2.1 MD95-2040

Samples from MD95-2040 core collected during the IMAGES MD101 cruise aboard the R/V Marion Dufresne, were reassessed using morphometric data from Narciso et al. (2006). A total of 98 smear slides from 2cm to 2606cm were analysed, with a mean resolution of 2.3ka, covering isotope stages 1 to 7. Samples were screened under an optical polarizing microscope (Olympus BX40) and measurements of the larger coccolith axis (L) were obtained using a Olympus DP11 camera and Scion-Image software.

The age model of MD95-2040 core was established from a combination of oxygen isotope stratigraphy, ^{14}C dating and synchronisation of the sea-surface temperature (SST) records and the GISP2 $\delta^{18}O$ data (de Abreu et al., 2003). Isotopic stages are recognised and ages assigned in accordance with the standard curve SPECMAP of Martinson et al. (1987). The detailed stratigraphy for the last deglaciation and the Holocene is consistent with the planktonic $\delta^{18}O$ record from the nearby core SU81-18 (37º46'N, 10º11'W) described in Bard et al. (1989) (de Abreu 2000; de Abreu et al. 2003).

The palaeotemperature estimates for MD95-2040 are from de Abreu (2000) and were obtained with both the CLIMAP transfer function equation FA20 (Imbrie & Kipp, 1971) and with a modern analogue technique SIMMAX28 (Pflaumann et al., 1996).

3.2.2 GeoB5559-2

The survey was realized in 1998 on the ship Meteor as part of the European project CANIGO16 in the submarine mountain slope of Agadir, 31° 38,7'N and 13° 11,2'W (Wefer et al., 1998). The hole was performed at a depth of 3178m, with a recovery of 5.85m of sediment, from isotopic stages 1 to 8. Due to the proximity of this site to the upwelling regime of Cape Ghir, climate-induced variations on the palaeoproductivity are reflected in the sediment core (Moreno et al., 2002).

A total of 117 samples were selected from this survey with 5cm spacing between samples. Age model was obtained from the correlation between $\delta^{18}O$ data from the sediment and the SPECMAP $\delta^{18}O$ chronological curve (Martinson et al., 1987 *in* Moreno et al., 2002). Samples were dated through a linear interpolation of the corresponding dating to the control points used, which in this case were associated to isotopic events. The final correlation between SPECMAP curve and GeoB5559-2 survey is 0.807, resulting in a mean resolution of 2.4ka between samples (Moreno et al., 2001).

3.2.3 DSDP608

The survey was carried out in 1983 as part of the Deep Sea Drilling Project in the south flank of the King's Trough tectonic complex, 700km north of the Azores Archipelago (42° 50,21'N and 23° 05,25'W). The hole was performed at a depth of 3533.6m, down to 530.9m into the sediment (Ruddiman et al., 1987).

The age model was built using the temporal scale of Shackleton et al. (1994), calibrated accordingly to the orbital model based on Milankovitch, which is regarded with high precision for the Neogene. Nearly all magnetochronological data from this survey were used as age control points, together with biochronological (FAD and LAD) data obtained from calcareous nannofossils. A linear interpolation of these data was used to date the samples selected (Su, 1996). A total of 70 samples were selected, covering from the Upper Miocene to the Holocene.

3.3 Results

3.3.1 MD95-2040

Applied to the entire set of samples (98 samples) IMMA extracted two main components representing a total of 78.1% of variance, distributed as 58.3% for component 1 (C1) and 19.8% for component 2 (C2). For the restricted subset of samples (86 samples) IMMA increased the total extracted variance to 80.5%, lowering C1 importance to 53.6% but increasing C2 relative importance to 26.9%.

Relative to morphotype boundaries both analyses led to similar results, however removing the anomalous samples improved morphotype definition and characterization.

3.3.1.2 No anomalous IMMA analysis

After removing samples with less than 100 coccoliths measured ("no anomalous" sample set or NA), the morphotypes limits were for the smaller morphotype [3.9; 10.2[µm ($_{S}C1_{NA}$) and for the larger form [11.3; 15.7[µm ($_{L}C1_{NA}$) (extracted by C1). C2 also extracted a second smaller morphotype $_{S}C2_{NA}$ ranging between [9.5; 12.5[µm and a second larger $_{L}C2_{NA}$ ranging between [13.6; 17.2[µm (Fig. 3.2).

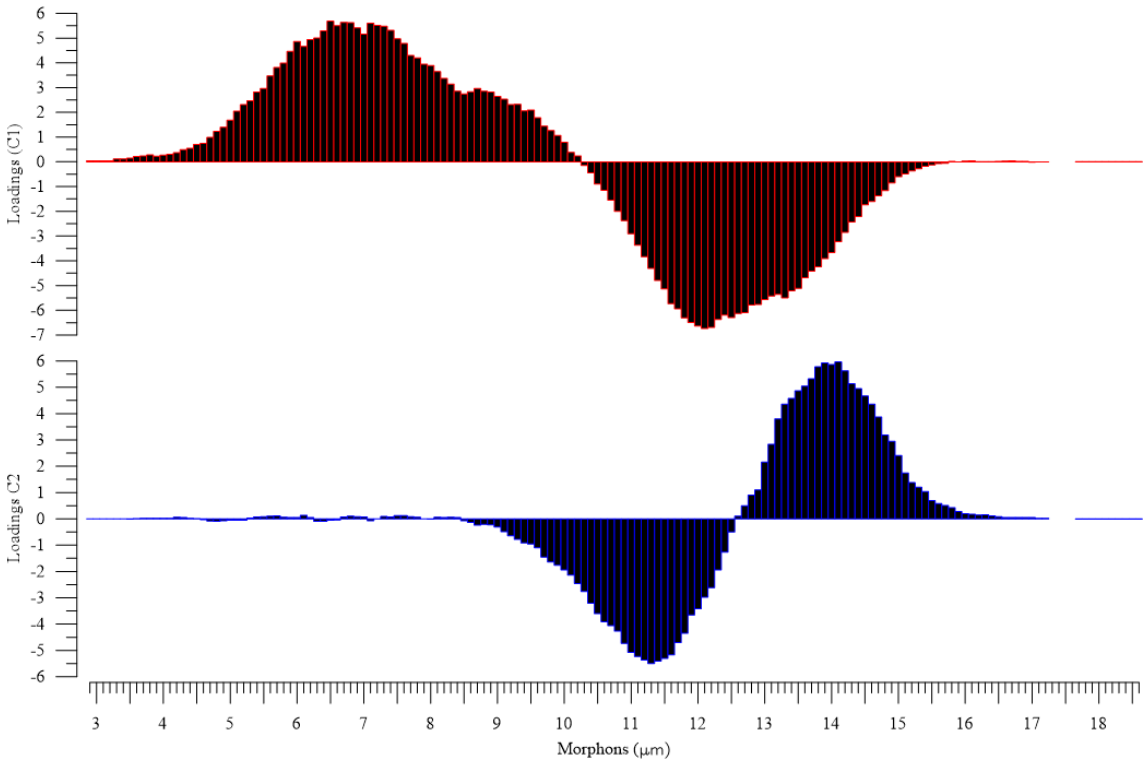

Figure 3.2 – Loadings of component one (red bars) and component two (blue bars) of IMMA applied to the subset of samples after removing "anomalous" samples in MD95-2040.

Scores show the dominance of $_{L}C1_{NA}$ in C1, with 69.8% of the samples, while along C2 there is a slight dominance of $_{S}C2_{NA}$ with 52.3% of the samples (Fig. 3.4).

Correlation between counting's and scores show nearly perfect correlations in C1, and very strong correlations in C2 (Table 3.1).

Table 3.1 – Correlation between morphotypes counting's and PCA scores for C1 and C2 with MD95-2040 NA matrix (values found for AD present in *italic*).

Interval (µm)	Morphotype	Correlation with counting's
3.9 – 10.2	$_{S}C1_{NA}$	0.99 *(0.84)*
11.3 – 15.7	$_{L}C1_{NA}$	-0.98 *(-0.98)*
9.5 – 12.5	$_{S}C2_{NA}$	-0.87 *(-0.65)*
13.6 – 17.2	$_{L}C2_{NA}$	0.82 *(0.72)*

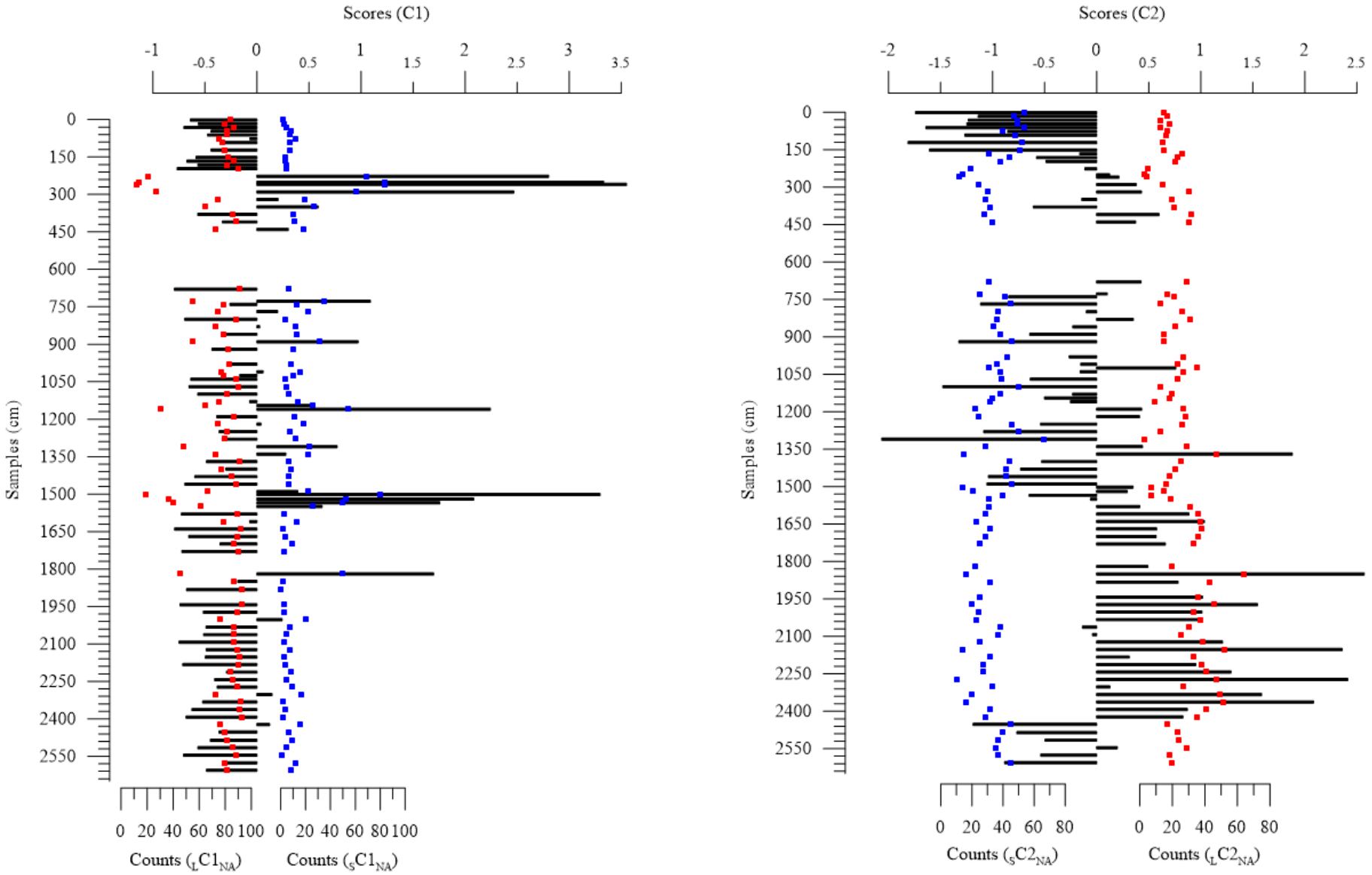

Figure 3.3 – C1 and C2 scores (black bars) and morphotypes counting's (red dots for larger morphotype and blue dots for smaller morphotype) in MD95-2040 NA.

3.3.2 GeoB5559-2

Applied to the entire set of samples (117 samples) IMMA extracted two main components representing a total of 73.5% of variance, distributed as 50.7% for C1 and 22.8% for C2. For the restricted subset of samples (110 samples) extraction was very similar, with total extracted variance of 73.7%, distributed as 59.3% for C1 and 14.4% for C2.

Relative to morphotype boundaries both analyses were equal regarding C1, but slight different in C2.

3.3.2.1 All samples and No anomalous IMMA analysis

IMMA analysis applied to the entire set of samples (all dataset – AD) determined three sets of significant morphons, two for C1 and one for C2. According to C1 the limits were determined as [6.9; 12.9[µm for the smaller ($_{S}C1_{AD}$) and [14.0; 17.2[µm for the larger ($_{L}C1_{AD}$). C2 defined a third (median) morphotype with size ranges as [11.5; 15.2[µm ($_{M}C2_{AD}$).

After removing anomalous samples (NA) IMMA also extracted three sets of significant morphons, two for C1 and one for C2 (see Fig. 3.4). The limits were exactly the same for C1, but different for component two: [12.2; 14.5[µm ($_{M}C2_{NA}$).

Scores show a small dominance of the smaller morphotype in C1, with 53% (AD) and 52% (NA) of the samples, while along C2 the morphotype is active in 68% (AD) and 60% (NA) of the samples (Fig. 3.5).

Correlation between counting's and scores improves with the elimination of the anomalous samples for C1. However for C2 occurs the opposite (Table 3.2). Since the PCA applied to AD managed to extract more information from C1 than the PCA applied to NA, it is more likely for the morphotype boundaries defined with C2 in PCA with AD to better represent the real limits. Moreover, since the two morphotypes observed in C1 are exactly the same in both PCAs, the increase in correlation from PCA in AD to PCA in NA seems linked only to the remove of anomalous data (Fig. 3.4).

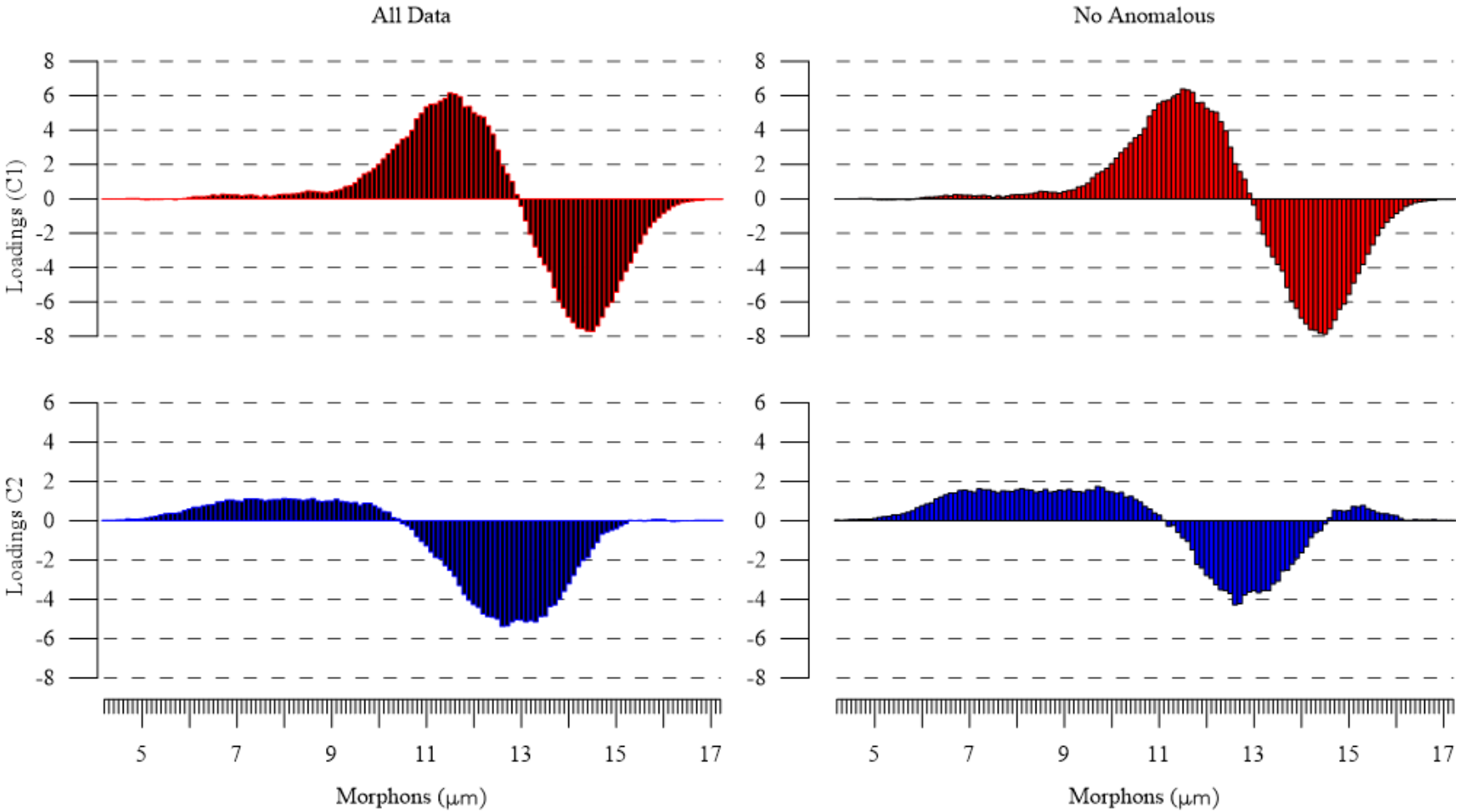

Figure 3.4 – Loadings of component one (red bars) and component two (blue bars) of IMMA applied to GeoB5559-2 AD (left side) and GeoB5559-2 NA (right side).

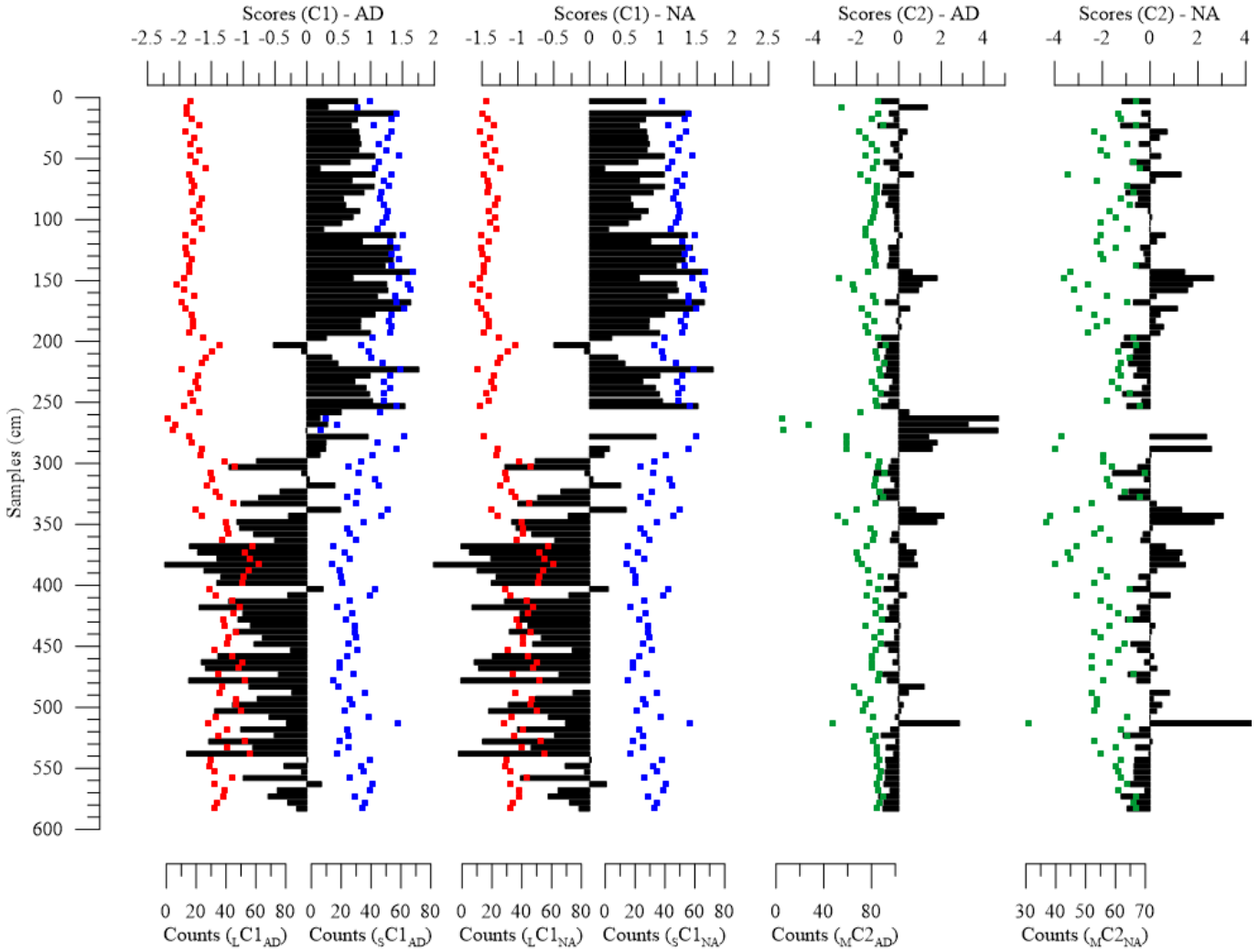

Figure 3.5 – Scores and counting's for GeoB5559-2. From left to right: C1 scores in AD; C1 scores in NA; C2 scores in AD; C2 scores in NA (black bars). Blue dots correspond to smaller moprhotype; red dots to larger morphotype; green dots to C2 morphotype.

Table 3.2 – Correlation between morphotype counting's and PCA scores for C1 and C2 with Geob5559-2 AD and NA matrixes

Interval (µm)	Morphotype	Correlation with counting's	
		AD	NA
6.9 – 12.9	$_{S}C1$	0.88	0.94
14.0 – 17.2	$_{L}C1$	-0.93	-0.97

Interval (µm)	Morphotype	Correlation with counting's
11.5 – 15.2	$_{M}C2_{AD}$	-0.98
12.2 – 14.5	$_{M}C2_{NA}$	-0.93

3.3.3 DSDP608

Applied to the entire set of samples (70 samples) IMMA extracted two main components representing a total of 79.3% of variance, distributed as 46.9% for C1 and 32.4% for C2 (see Annex-3 for DSDP608 AD analysis). For the restricted subset of samples (63 samples) extraction was similar, with total extracted variance of 82.2%, distributed as 47.1% for C1 and 35.1% for C2.

3.3.3.2 No anomalous IMMA analysis

After removing anomalous samples, the smaller morphotype extracted by C1 was determined between [5.0; 9.1[µm ($_{S}C1_{NA}$) whereas the larger form ranged between [10.2; 16.3[µm ($_{L}C1_{NA}$). In C2 the small morphotype identified was [5.0; 7.2[µm ($_{S}C2_{NA}$) and $_{L}C2_{NA}$ [8.3; 10.8[µm. Component three (C3) also brought results worth being considered, defining a smaller morphotype ($_{S}C3_{NA}$) [9.6; 11.1[µm and a larger one ($_{L}C3_{NA}$)[12.2; 16.3[µm (see Fig. 3.6).

Scores show the dominance of $_{S}C1_{NA}$ in C1, with 69.8% of the samples, $_{L}C2_{NA}$ in C2 with 57.1% of the samples, and of $_{S}C1_{NA}$ in C3 with 52.4% of samples (Fig. 3.7).

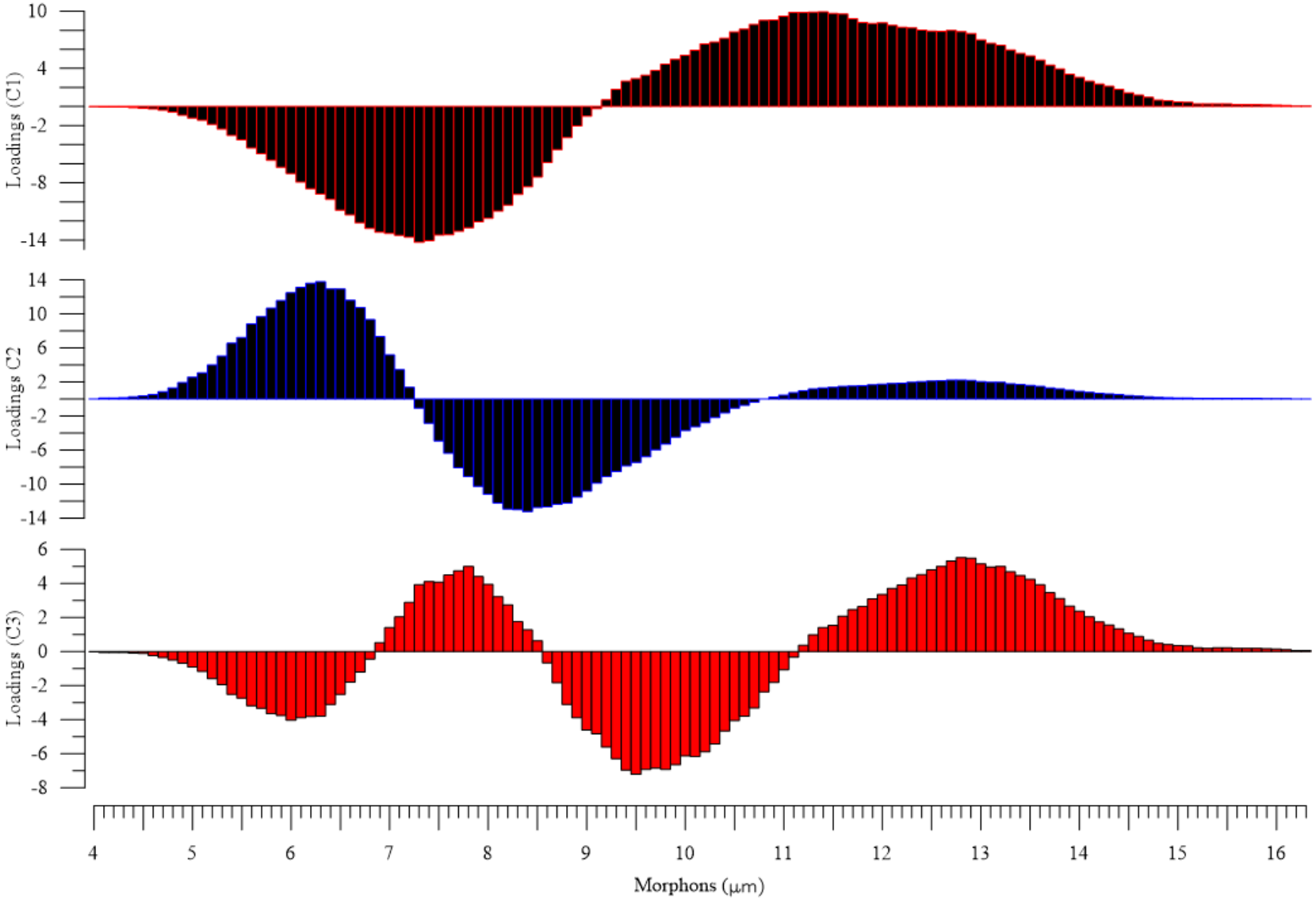

Figure 2.6 – Loadings of C1 (black bars+red line), C2 (black bars+blue line) and C3 (red bars) of IMMA applied to the subset of samples in DSDP608 NA.

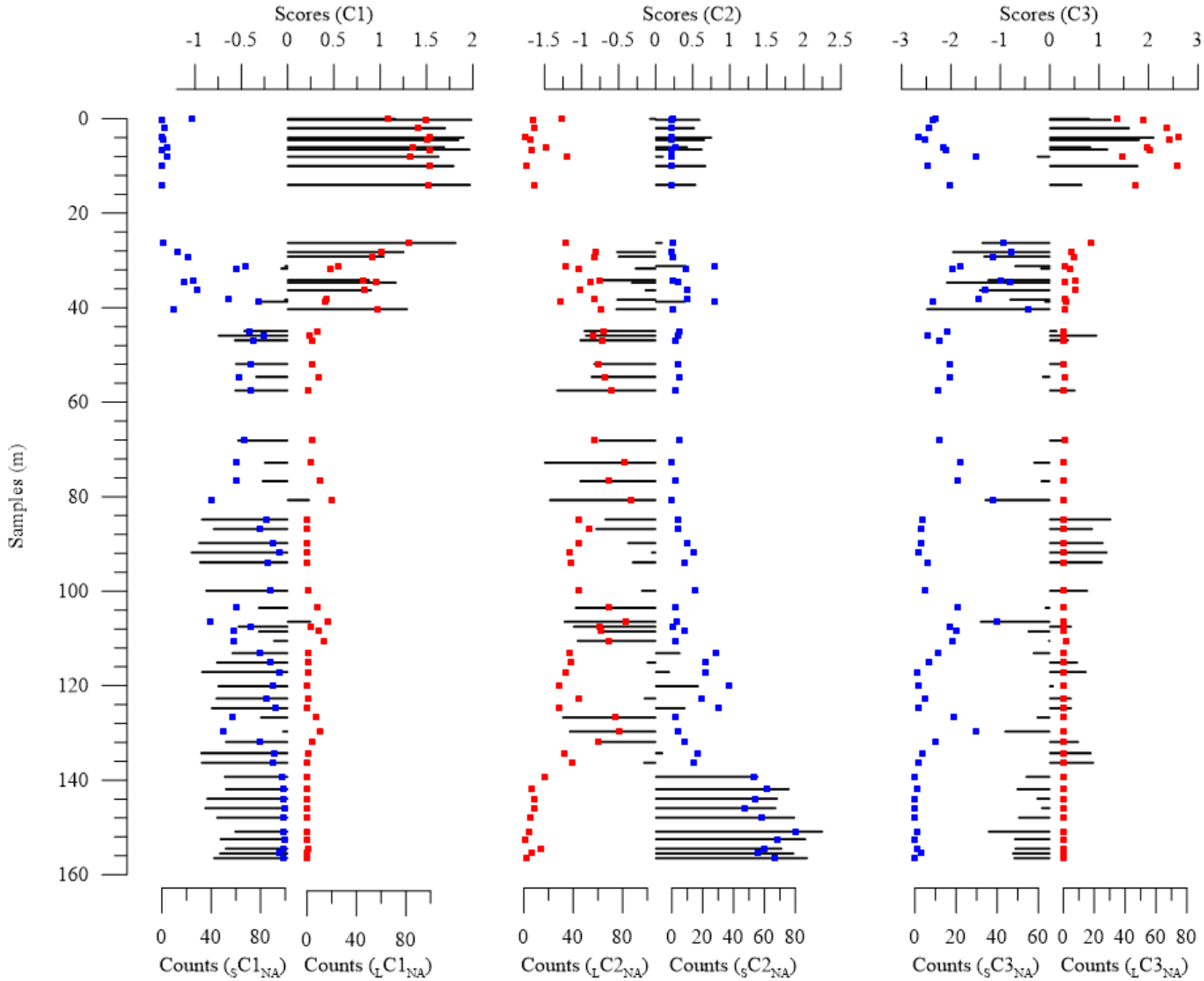

Figure 3.7 – Scores and counting's for DSDP 608 NA. From left to right: C1 scores; C2 scores and C3 scores (black bars). Blue dots correspond to smaller morphotype and red dots to larger morphotype counting's.

Correlation between counting's and scores present nearly perfect correlations in C1 and very strong values in C2. C3 has fair correlations between scores and counting's, however these were taking into account for the discussion of the data (Table 3.3).

Table 3.3 – Correlation between morphotype counting's and PCA scores for C1, C2 and C3 with DSDP608 NA matrix (values found for AD present in *italic*).

Interval (µm)	Morphotype	Correlation with counting's
5.0 – 9.1	$_{S}C1_{NA}$	-0.97 *(-0.96)*
10.2 – 16.3	$_{L}C1_{NA}$	0.98 *(0.91)*
5.0 – 7.2	$_{S}C2_{NA}$	0.82 *(0.82)*
8.3 – 10.8	$_{L}C2_{NA}$	-0.93 *(0.87)*
9.6 – 11.1	$_{S}C3_{NA}$	-0.67
12.2 – 16.3	$_{L}C3_{NA}$	0.51

3.4 Discussion

Before starting the discussion of the results it should be pointed that the separation, either as species or subspecies, between *C. pelagicus* and *C. braarudii* is an accepted fact, based on genetic and culture studies, and biogeographic distribution (see Geisen et al., 2004). *C. pelagicus* is described under 10µm length coccoliths and occurring in subpolar waters of the North Atlantic, while *C. braarudii* is described as over 10µm length coccoliths and present in coastal upwelling regions, mainly in the East Atlantic (Young et al., 2018). For these reasons, hereafter the small morphotype will be referred to as *C. pelagicus* and the larger morphotype as *C. braarudii*, although this is merely to simplify the text and does not reflect a taxonomic preference. The taxonomical implications of considering a division in species or subspecies is not the object of this work.

3.4.1 MD95-2040

Site MD95-2040 is located in the West coast of Iberia, a region where currently *C. braarudii* is present, and covers the last 225ka. The IMMA results show the presence of two morphotypes, a smaller under 10µm, *C. pelagicus*, and a larger one over 10µm, *C. braarudii*. The separation of the two is clear on C1. The smaller, *C. pelagicus*, is associated to subpolar waters and the intermediate, *C. braarudii*, is associated to coastal

upwelling, which is in line with previous interpretations from Cachão & Moita (2000), Parente et al. (2004) and Narciso et al. (2006).

IMMA C1 provides information about the overall palaeoceanographic scenario during the glacial-interglacial intervals (MIS 6 to 1) by expressing the opposite behaviour between: i) the smaller morphotype, *C. pelagicus*, indicative of the occasional presence of cold subpolar waters off north Iberia during terminations II and I; ii) the intermediate morphotype, *C. braarudii*, indicative of the establishment of a coastal upwelling regime during interglacials till present day.

IMMA C2 gives information on the morphological plasticity of *C. braarudii*, which is the dominant form in Iberian waters. Instead of characterizing another morphotype, C2 scores evidence the existence of a coccolith size variability associated to the intermediate morphotype, i.e. *C. braarudii* morphological plasticity, in response to smaller palaeoenvironmental changes. Analysing both scores at the same time shows shifts on *C. braarudii* size from smaller to larger placoliths (Fig. 3.8).

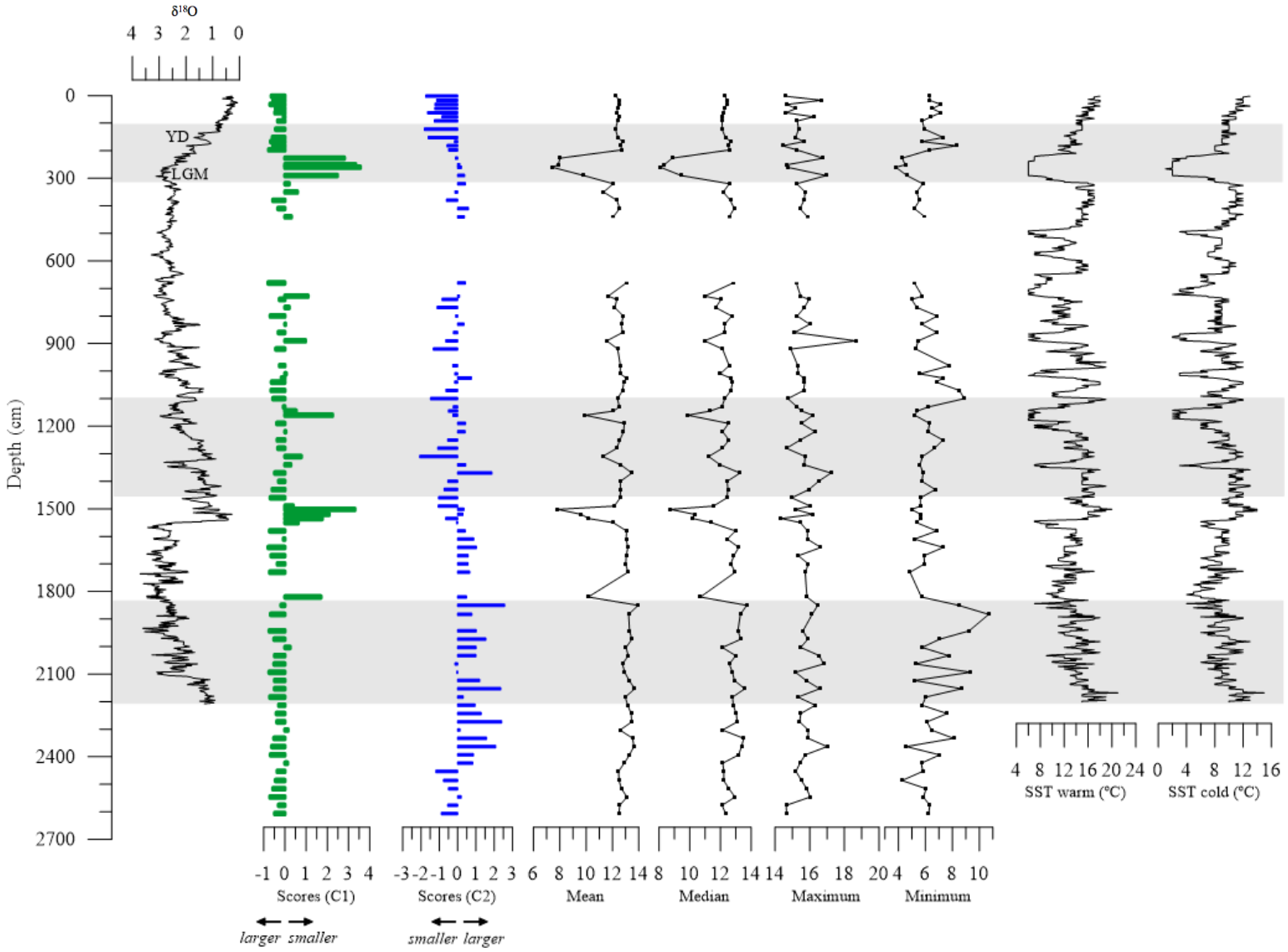

Figure 3.8 – Variation of *C. pelagicus* s.l. size in the samples subset MD95-2040 NA. Green bars for C1 scores from IMMA; Blue bars for C2 scores from IMMA. Grey bands represent sections detailed in figures 3.9, 3.10 and 3.11.

When C1 presents positive scores, *C. pelagicus* is the dominant morphotype and C2 scores loose their relation to *C. braarudii* size variability. In figures 3.9, 3.10 and 3.11 it is shown in more detail the relation between scores, median and histograms.

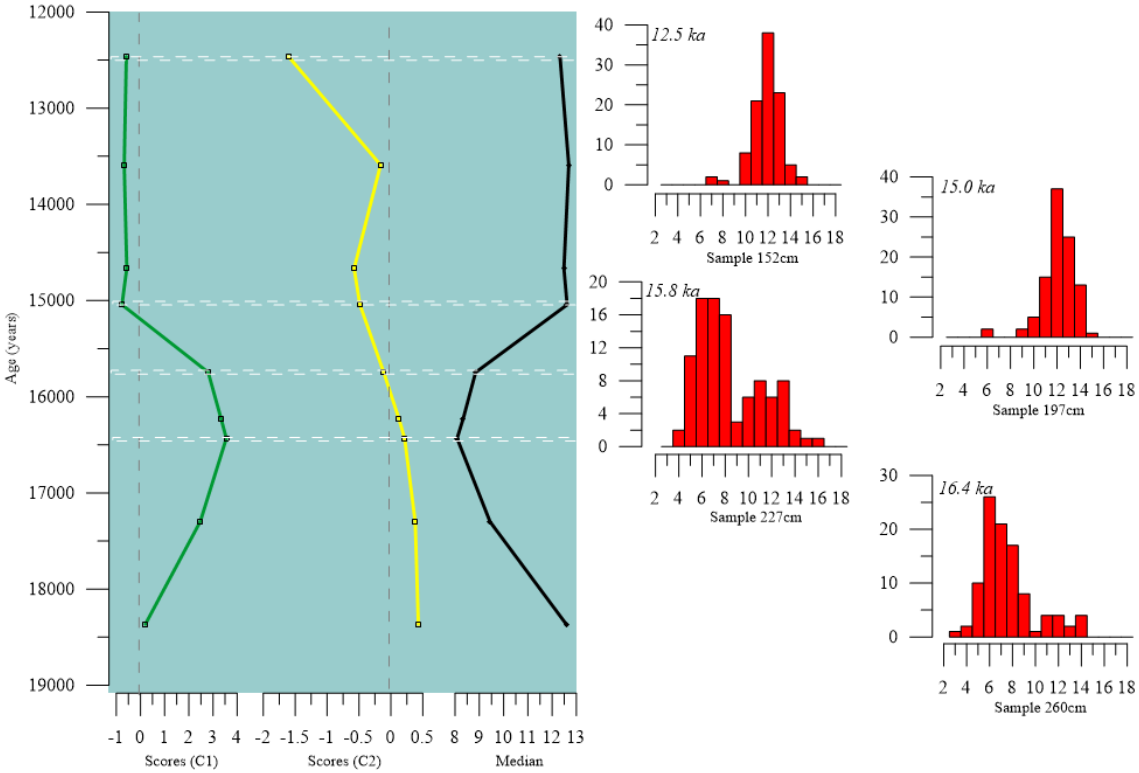

Figure 3.9 – C1 scores (green line), C2 scores (yellow line) and median (black line) in section 152-320 cm. Histograms for randomly selected samples (double traced lines): 152cm, 197cm, 227cm and 260cm**.**

The dominance by *C. pelagicus* between ~17.5ka and ~15.5ka is visible both in PCA scores and the histograms, with C1 scores showing high positive values and the histograms clearly dominated by small morphons. *C. pelagicus* was expected to be dominant during this interval since it corresponds to the Last Glacial Maximum. The change observed in the scores around 15ka is also seen in the histograms. *C. pelagicus* virtually disappears and *C. braarudii* becomes the dominant morphotype. Moreover, C2 scores indicate that *C. braarudii* is characterized by smaller sizes, which is also supported by the decrease in samples median (12.73µm to 12.40µm) and mean (12.62µm to 12.32µm) from 197cm to 152cm.

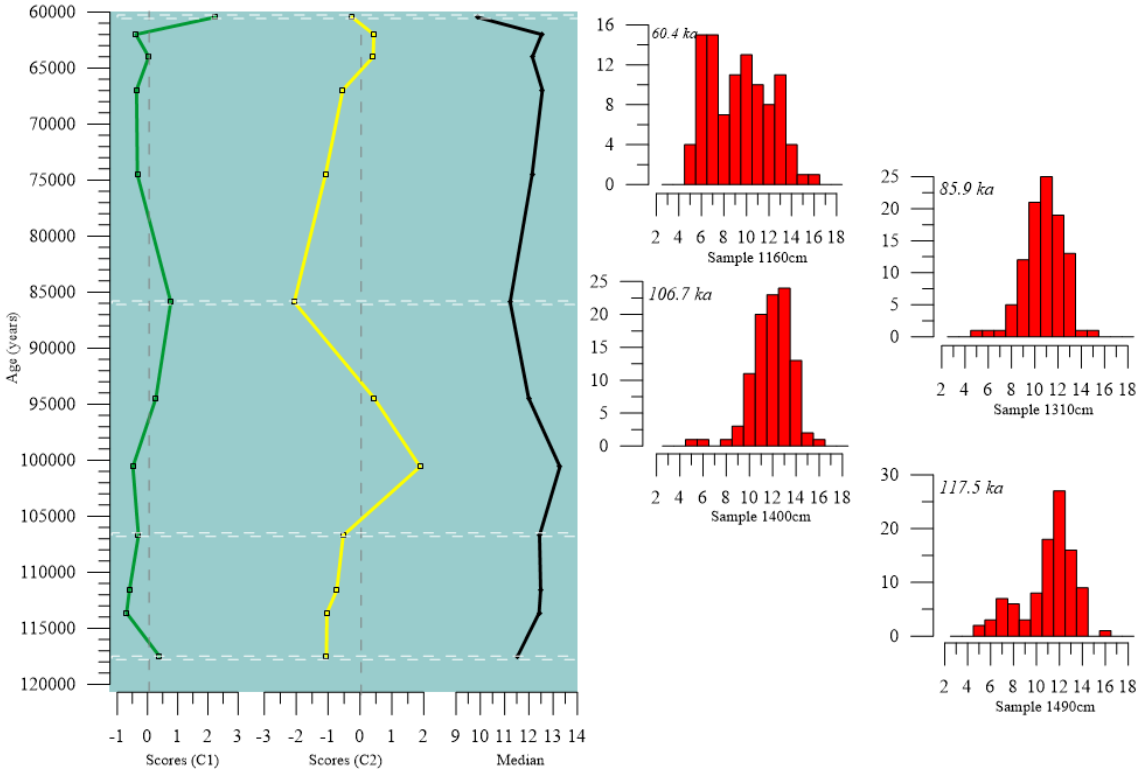

Figure 3.10 – C1 scores (green line), C2 scores (yellow line) and median (black line) in section 1160-1490 cm. Histograms for samples 1160cm, 1310cm, 1400cm and 1490cm.

The histogram of sample 1160cm corroborates the scores of C1, with the dominance of smaller morphons 6µm and 7µm, and measurements of C. braarudii present in the sample dominated by morphon 10, in line with C2 negative scores. In sample 1310cm morphons 10µm and 11µm dominate the histogram, with C1 scores being slightly positive (meaning that C. pelagicus has a significant presence – which is corroborated by few measurements in morphons 5, 6 and 7) and C2 scores indicating dominance of sizes between the morphon 9µm and morphon 12µm.

PCA results give a slight dominance to the intermediate morphotype, *C. braarudii*, in its smallest sizes, in sample 1400cm. The histogram for this sample shows dominance of morphons 12µm and 13µm and a few counting's in small morphons that are attributed to *C. pelagicus*, which is in line with the C1 score being close to zero.

Regarding the last histogram, sample 1490cm, PCA results and sample histogram are again in good agreement. Through PCA results it was expected the dominance of *C. braarudii* with lower sizes, C1 score slightly positive (close to zero) with negative C2 score, and the presence of *C. pelagicus*, which is what is observed in the sample histogram.

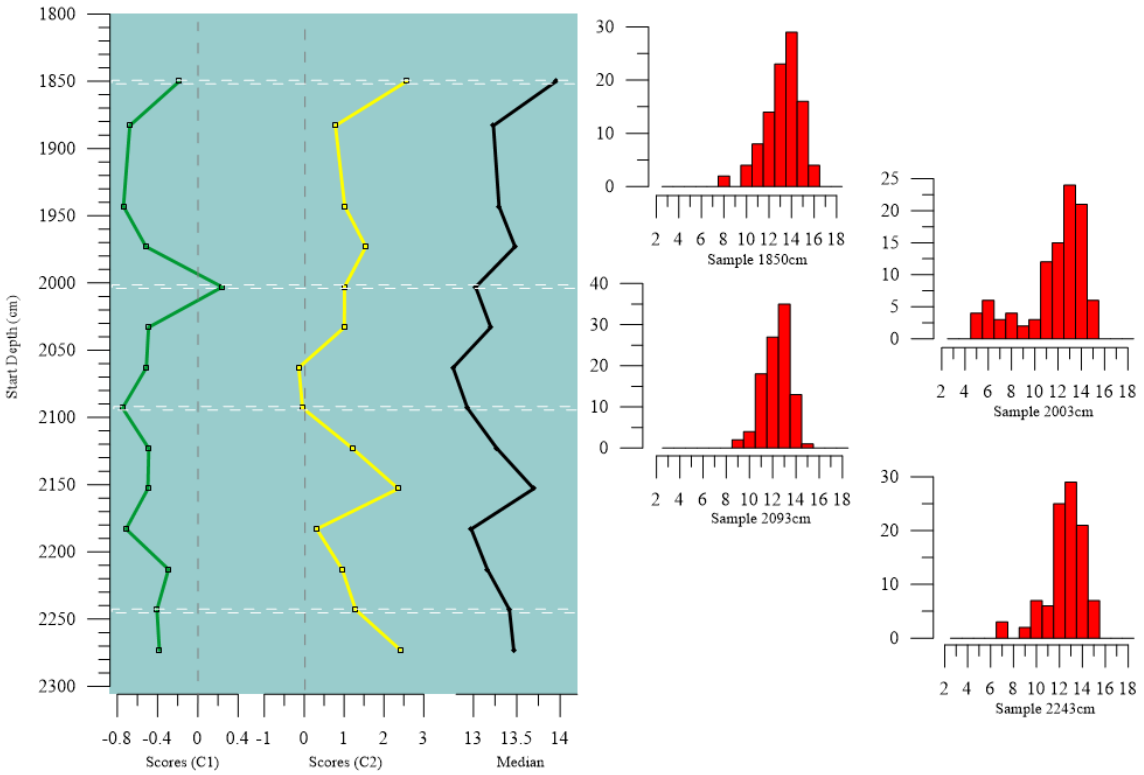

Figure 3.11 – C1 scores (green line), C2 scores (yellow line) and median (black line) in section 1850-2273 cm. Histograms for samples 1850cm, 2003cm, 2093cm and 2243cm.

The last selected section continues to support the findings of the PCA. Samples 1850cm, 2093cm and 2243cm were expected to be dominated by *C. braarudii* due to the negative C1 scores. The histograms confirm this dominance and also agree with C2 scores, deflecting to larger sizes when C2 is positive (1850cm and 2243cm) and to smaller sizes when it is negative (2093cm). Sample 2003cm would be expected to show presence of *C. pelagicus* by C1 and larger sizes in *C. braarudii* by C2. Its histogram depicts exactly that reality, with *C. pelagicus* present and *C. braarudii* centred in morphons 13µm and 14µm.

It is also worth it to look at the global histogram of NA matrix morphometry (Fig. 3.12). It should not be used to characterize the entire population, since this histogram contains data from different moments in time, but it is useful to have a global idea of the morphometric boundaries and distributions through time in a certain region.

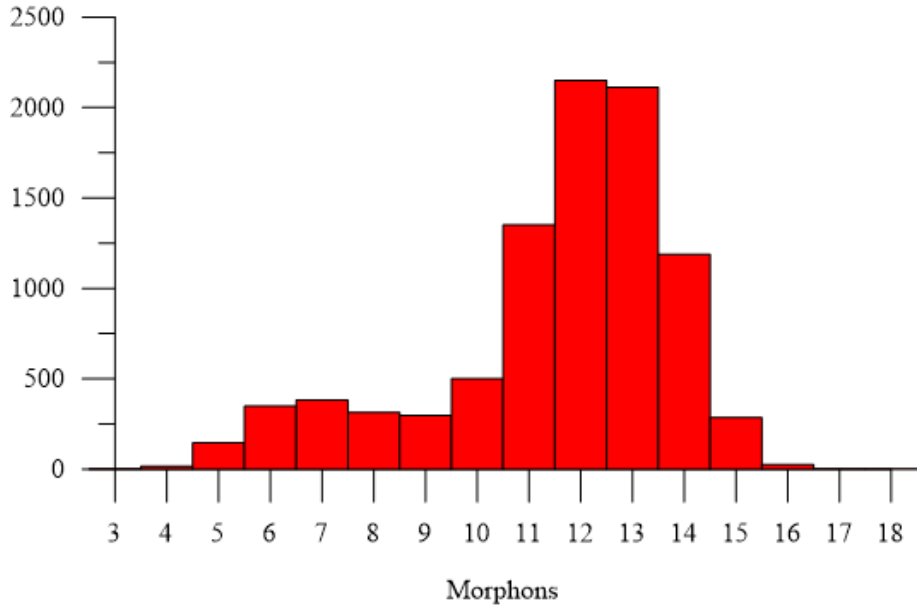

Figure 3.12 – Global histogram of MD95-2040.

The global histogram suggests the dominance of *C. braarudii* during this ~225ka interval, with occasional appearances of *C. pelagicus*. However it does not allow the identification of the limits of each morphotype, only their most likely core size.

3.4.1.1 Evidences of C. braarudii *morphological plasticity in West Iberia*

Assuming that the morphometric interval defined with C1 is the core size of the *C. braarudii* morphotype and that the two morphotypes defined by C2 represent its lower and upper limit variation, thus *C. braarudii* size varies between 9.5µm and 17.2µm with a core size between ~[11.3; 15.7]µm, limits that fit well with recent culture measurements between 7.87µm and 17.32µm, with 12.21µm mean (see Sheward et al., 2016).

The first analysis on the data strongly suggested that C2 was giving information on *C. braarudii* size variation, an expected morphological response to palaeoenvironmental variations (see Daniels et al., 2014; Gerecht et al., 2014; Gerecht et al., 2015; Šupraha et al., 2015; Sheward et al., 2014, 2016). To investigate further this interpretation, each morphotype was analysed in more detail.

In each sample the limits of *C. pelagicus* and *C. braarudii* were determined following C1 scores. From the initial analysis there is a morphometric interval where both morphotypes overlap, 9.5µm to 10.2µm. In order to establish the limits of each morphotype in each sample C1 scores were used. Positive scores mean that *C. pelagicus*

is dominant and thus the overlap region would belong to this (sub)species. Negative scores would place the overlap region has belonging to *C. braarudii*. When scores presented values close to zero (-0.1 < 0.1) measurements in the overlapping region were ignored. An error of 0.05µm was defined for the attribution of the measurement, meaning that a measurement of 10.24µm with C1 positive scores over 0.1 would be attributed to *C. pelagicus*.

The analysis was performed only with NA matrix, to avoid samples with very few measurements, which give a poor representation of the data and reduce the outcome reliability (as shown in table 3.4 regarding the correlations between scores and morphotypes limits, mean and median for AD and NA matrixes) (see this chapter annexes for data in table A3-16).

Table 3.4 – Correlations between morphotypes (*C. braarudii* and *C. pelagicus*) minimum, maximum, mean and median in AD and NA matrixes.

CORRELATIONS	**AD Matrix**		**NA Matrix**	
C. braarudii				
	C1	C2	C1	C2
Minimum	0,61	0,05	0,48	0,04
Maximum	-0,19	0,32	0,05	0,39
Mean	-0,08	0,85	-0,13	0,94
Median	-0,03	0,86	-0,12	0,96
C. pelagicus				
	C1	C2	C1	C2
Minimum	-0,53	0,11	-0,50	0,09
Maximum	0,62	-0,08	0,61	-0,10
Mean	0,01	0,01	0,10	-0,01
Median	-0,03	0,02	0,09	0,02

The correlation between C2 scores and mean and median of *C. braarudii* is very good in AD matrix however it presents stronger values in NA matrix. In fact the variation of C2 scores and mean and median values are nearly identical (Fig. 3.13)

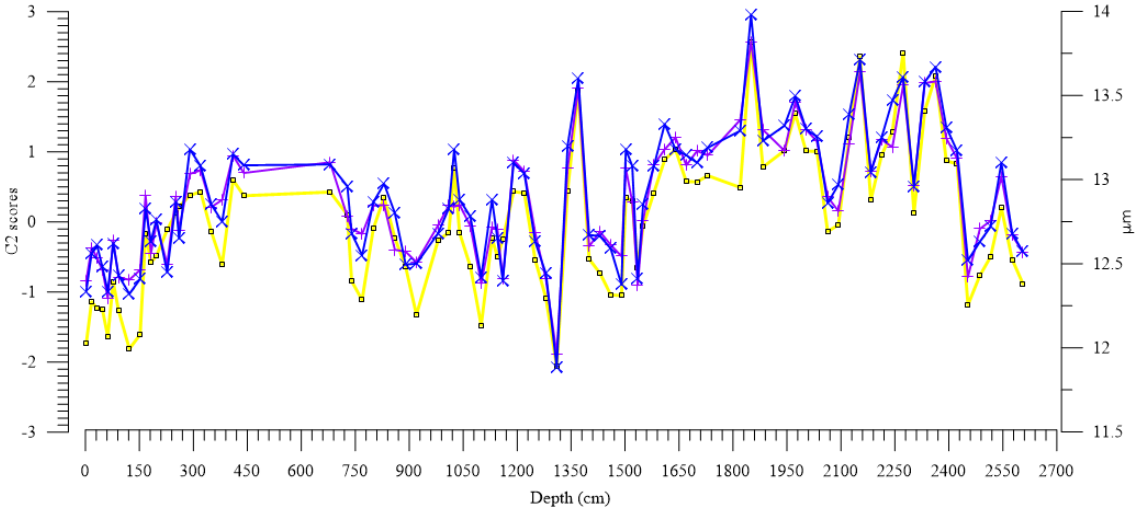

Figure 3.13 – Variation of C2 scores (yellow line) and mean (purple line) and median (blue line) in NA matrix for *C. braarudii*.

The variation of the mean and median is closely connected with C2 variability (see Fig. 3.14), and the histograms clearly show how the core size of *C. braarudii* shifts according to C2 and how C1 reflects the presence of *C. pelagicus* (Figs. 3.15 and 3.16). When C2 is positive, the histograms are displaced to the right, while when the scores of C2 are negative the opposite occurs.

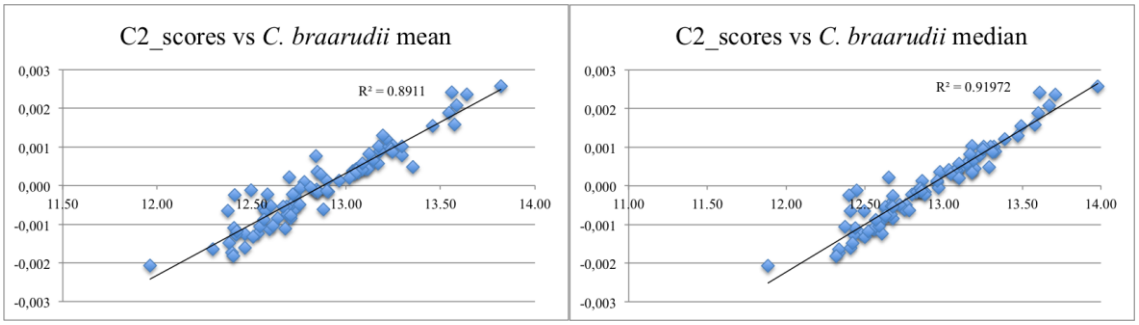

Figure 3.14 – Scatter plot of the relation between C2 scores with *C. braarudii* mean and median in MD95-2040 NA matrix.

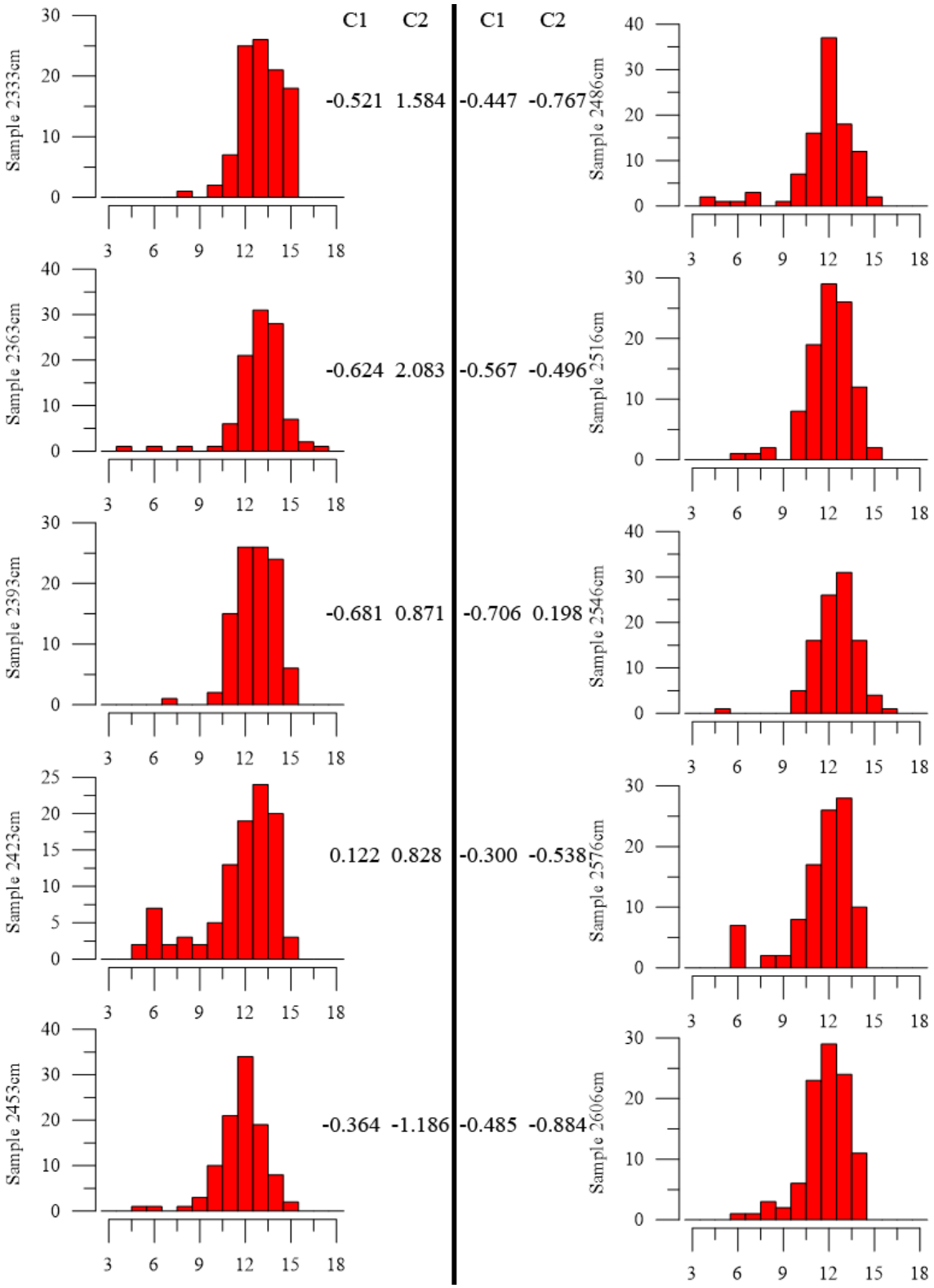

Figure 3.15 – Histograms from sample 2333cm to sample 2606cm and the respective C1 and C2 scores in NA matrix.

From figure 3.15 it is easily observed that when C2 is positive, the dominant morphons are centred in morphon 13µm, while when it is negative larger morphons

show less counting's and the centre moves to morphon 12µm. When C1 is negative the presence of *C. pelagicus* is residual or it is absent.

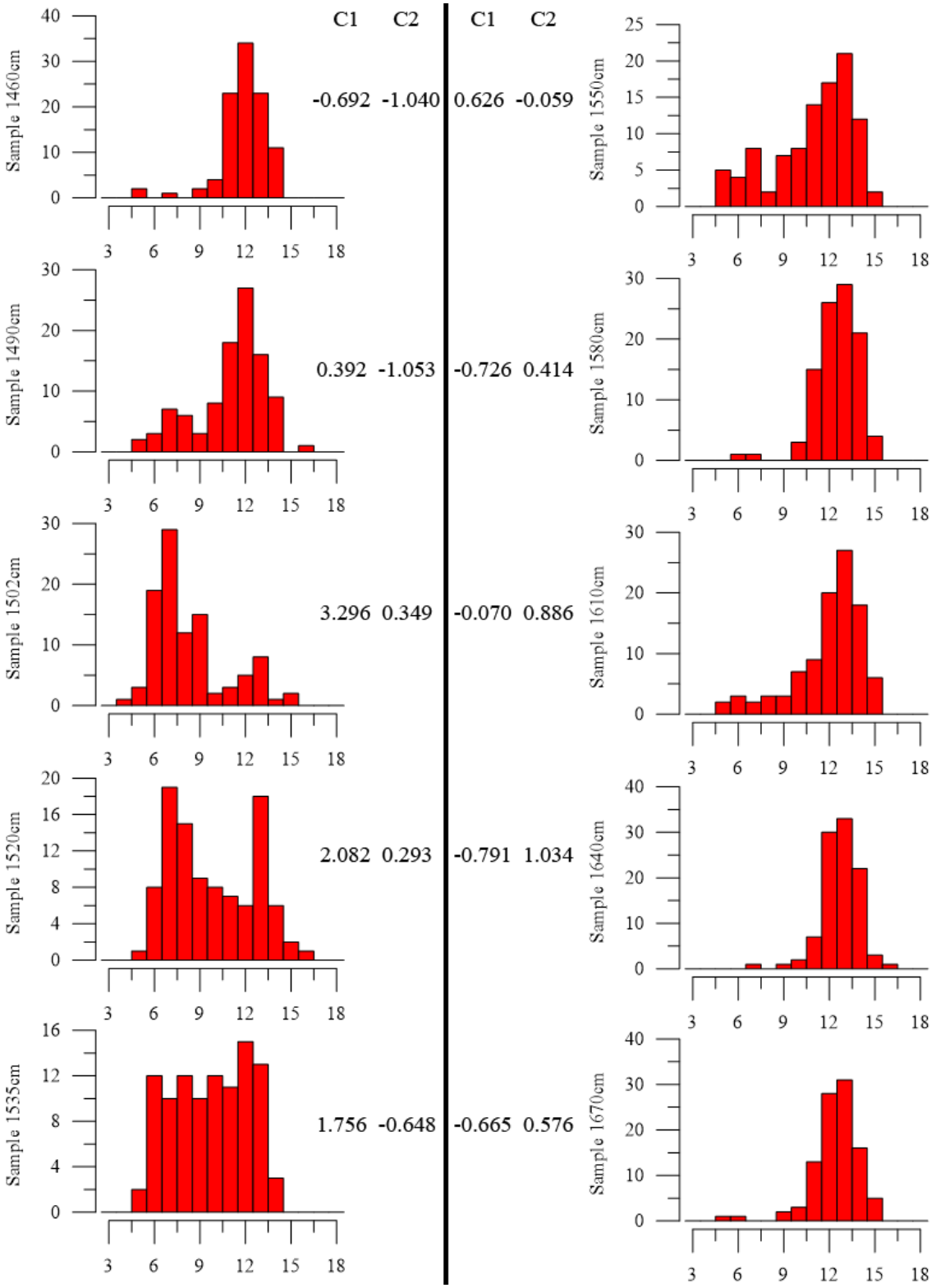

Figure 3.16 – Histograms from sample 1460cm to sample 1670cm and the respective C1 and C2 scores in NA matrix.

In this set of histograms (Fig. 3.16) the effect of C1 is more visible. When it has positive values *C. pelagicus* is present and higher values have higher *C. pelagicus* counting's. Again C2 scores show the same pattern as in the previous histograms. Negative values place the counting's centred on morphon 12µm, while positive values follow the centre displacement to morphon 13µm, together with an increase in larger morphons counting's.

There is a strong focus on the median since this is a very good indicator on how the morphotype is behaving regarding its size. The mean value is easily influenced by a few measurements far from the average size within a certain sample, while the median is less affected by these "abnormal" values. It is interesting to observe how the median has been getting smaller over the period studied (last ~225 ka) (Fig. 3.17). This could be interpreted as a strengthening/intensification of the upwelling regime in the West coast of Iberia.

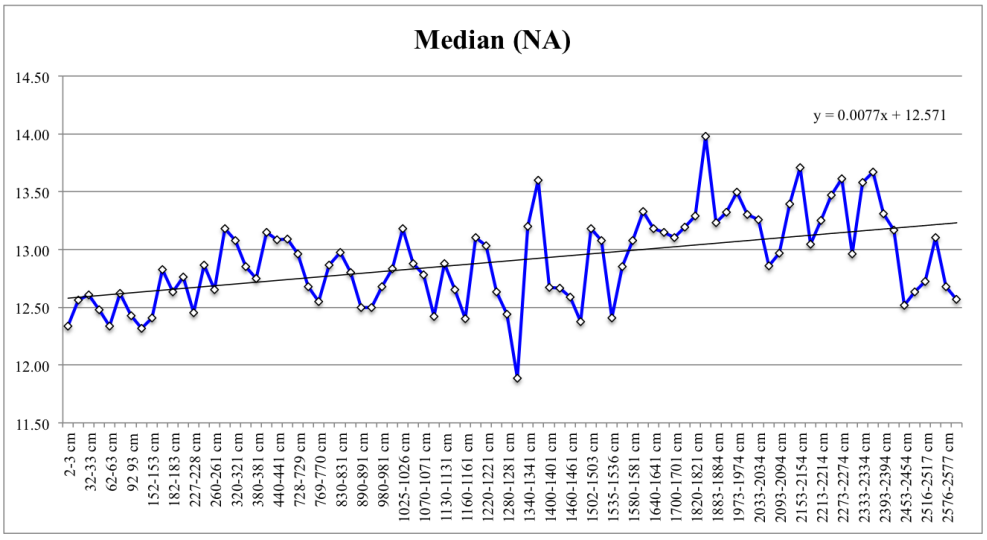

Figure 3.17 – Median value of *C. braarudii* in NA MD95-2040 matrix and tendency line.

According to Salgueiro et al. (2014) there is an increase tendency in productivity for site MD95-2040 over the past 35ka, although in Salgueiro et al. (2010) the same site in a 150ka record presents a slight general tendency to decrease. The same study however shows increased productivity in site SU92-03, which is located off coast West Galicia.

Studying site MD95-2039 in the West coast of Portugal, Thomson et al. (2000) noticed ~130-125ka and ~17-15ka were the highest productivity periods in the region over the past 350ka. In our samples these periods are dominated by *C. pelagicus*,

corresponding to colder glacial time intervals. The same authors determined the Holocene productivity lower than older periods, however diatom abundance is higher which means that for some reason primary productivity is enhanced.

In another study, Incarbona et al. (2010) show an increase in late spring-summer productivity, with a slight decrease in summer-autumn over the past 70ka in site MD01-2444 (located in Southwest coast of Portugal). Despite these results, they show an overall decrease in surface productivity for the entire time interval studied. However they also noted an increase in small placoliths during this period, and an increase in deep-ocean ventilation with North Atlantic Deep Water (NADW) formation starting during the Last Glacial Maximum and being highly active since.

Ocean water masses names, particularly in the Atlantic Ocean, are very confusing. Different authors and papers use different terms to name the same water mass and vice-versa (Morozov et al., 2010). For this reason it is hard to understand the NADW reference from Incarbona et al. (2010). Moreover, being a complex issue in current times studies, it is even more complicated in palaeoceanography to precisely identify specific water masses formation. However it is clear that deep and intermediate waters from and in the North Atlantic are highly important for the West Iberia Upwelling System (WIUS) (e.g. Fiúza, 1983; Fiúza et al., 1998; Peliz et al., 2002; Cordeiro et al., 2018). Thus it is important to notice that an increase in NADW formation since the Last Glacial Maximum should have a positive impact in WIUS productivity, which would be in line with the decrease in placoliths size found in Incarbona et al. (2010) and the median drop found in our study.

The absence of extractable information about *C. pelagicus* besides its presence or not in this set of samples is most likely the result of its very low presence. Only in four samples (either in AD or NA matrix) it represents more than 50% of the coccoliths measured. Thus, the smaller morphotype presents a low number of coccoliths in MD95-2040, which explains why there seems to be no major information extracted from PCA besides its presence and opposition to *C. braarudii*.

Regarding $\delta^{18}O$ and *C. pelagicus s.l.* relative abundance, no kind of relation was found between morphometric data and these parameters. However fair correlations were found between SSTs and C1 scores. Warm SST shows a -0.42 correlation while cold SST present -0.51. This means that when C1 is positive (*C. pelagicus* active) temperatures tend to be colder than when C1 is negative (*C. braarudii* active). This is an

expected result since *C. pelagicus* is indicative of cold North Atlantic subpolar waters, while *C. braarudii* is a proxy for coastal upwelling conditions. The main reason why this correlation isn't stronger is probably due to the fact that upwelling regions also present colder temperatures due to the surfacing of deep nutrient rich waters.

Thus according to this model, the size of *C. braarudii* can be used as a proxy for the upwelling conditions, being relatively smaller during stronger upwelling episodes and larger during weaker upwelling periods.

In light of this new interpretation model, the seasonal upwelling regime that characterizes the west coast of Portugal has been progressively becoming relatively stronger particularly after the Last Glacial Maximum.

This interpretation is also supported by several other recent, and not so recent, studies. Renaud & Klaas (2001) found morphological plasticity in *Calcidiscus leptoporus* as a response to environmental conditions over a three-year period. Daniels et al. (2014) and Sheward et al. (2014, 2016) found that coccosphere size in all species studied (*Helicosphaera carteri*, *Calcidiscus leptoporus*, *Calcidiscus quadriperforatus*, *Coccolithus pelagicus*, and *Coccolithus braarudii*) is statistically smaller during the exponential-phase growth than during days of slowed, nutrient-depleted, early stationary-phase growth. An increase in cell size has also previously been observed in response to nutrient limitation in *Coccolithus* and *Helicosphaera* (Gerecht et al., 2014; Gerecht et al., 2015; Šupraha et al., 2015). Since larger coccoliths tend to occur in larger cells (see Renaud & Klaas, 2001; Sheward et al., 2016), the shift to larger coccoliths in the intermediate morphotype may be a sign of stationary growth during non-upwelling periods.

Thus, when C1 scores related to *C. braarudii* are active (negative values) C2 gives information about the palaeoceanographic upwelling conditions off Iberia. When C2 scores are negative *C. braarudii* has smaller sizes, indicating a sequence of more intense upwelling regimes. If on the other hand the scores are positive, then its size increases and points to weaken upwelling regimes.

This model works as a proxy for different information: 1) it can be used as a proxy for palaeoceanographic regimes, showing the changes between subpolar cold waters and temperate coastal upwelling (C1 scores information); 2) it is also a proxy for morphological plasticity of *C. braarudii* and upwelling regime variations (C2 scores information).

After removing this linear trend there is a noticeable cyclicity in the data which have already been tackled but it will be proper addressed in the future.

3.4.2 GeoB5559-2

Site GeoB5559-2 is located near Canary Islands, a region where only *C. braarudii* is expected to be found. The results suggest the presence of *C. braarudii*, with its core size defined by C2, while C1 shows its variability in size due to palaeoceanographic changes. Since only one morphotype is present, PCA C1 is expected to show its variability. Instead of two or more morphotypes defining the major variance in the data, with only one morphotype it is its variability where most of the data variance is found.

The very similar results between AD and NA matrixes, together with the better results in C2 of AD matrix, determined the use of AD matrix in this site to discuss the results. There was no point in analysing the results after removing anomalous samples since these were not negatively affecting the PCA results.

The region of the Canary Islands is an area of the ocean characterized by the presence of both coastal upwelling and eolian input from the Sahara/Sahel regions (Nave et al., 2001 and references within). Cape Ghir filament is a quasi-permanent feature and its origin is thought to be on the cyclonic relative vorticity injection by the wind-stress curl (Troupin et al., 2012; Sangrà et al., 2015). Filaments at Cape Jubi and between Cape Jubi and Cape Bojador are smaller, show intermittency and are variable in their location due to their interaction with the eddy field induced by the Canary Islands (Barton et al., 1998, 2004). It has been proposed that their origin is in the entrainment of upwelled water by such offshore eddy field. Cape Blanc filament is also a permanent feature, as the Cape Ghir filament (see Fig. 3.18).

This means that the Canary Islands region is, to some extent, similar to the West coast of Iberia, with an upwelling regime, which in the Spanish archipelago goes from nearly permanent to intermittent, while in West Iberia has a more seasonal character. In fact, these two upwelling regions are often considered part of the same system, the Portuguese-Canary eastern boundary upwelling system (Peliz et al. 2005).

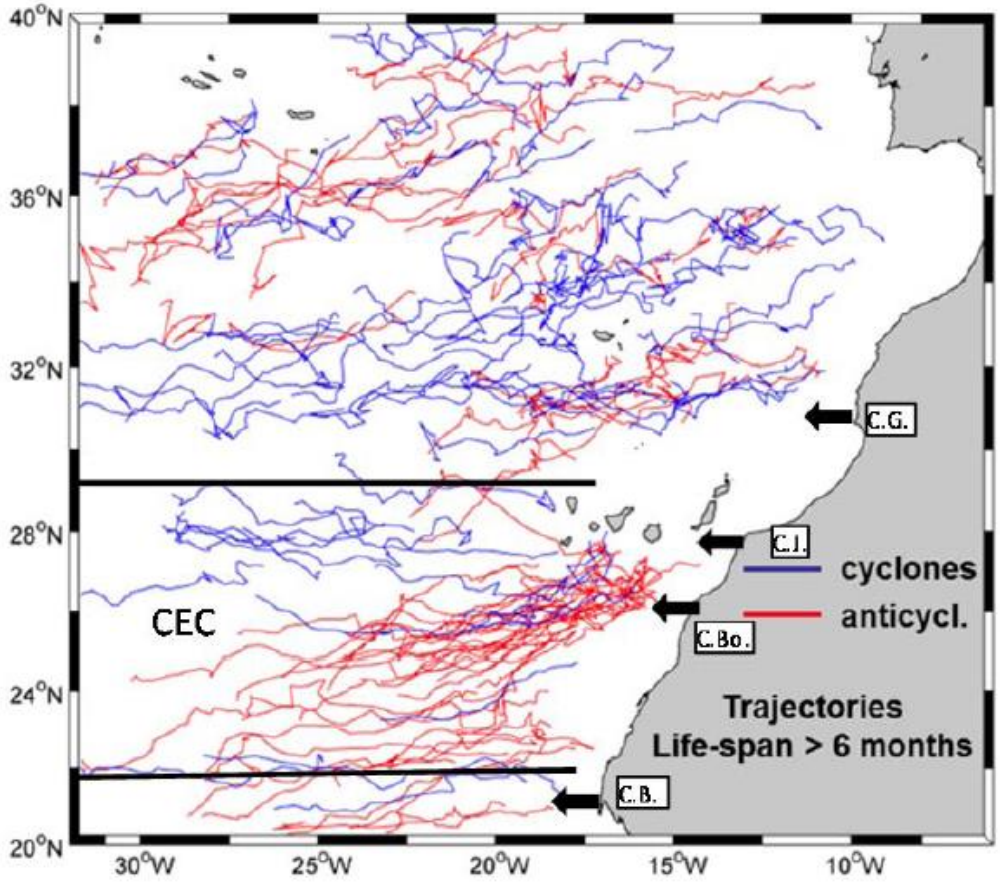

Figure 3.18 – Westward-propagating eddy trajectories lasting over 6 months, as obtained from 14 years (1992–2006) of merged altimeter data, showing the Canary Eddy Corridor (CEC) extending from 22°N to 29°N. Black arrows indicate the sites of recurrently observed upwelling filaments. They are located in the region near Cape Ghir (C.G.), near and between Cape Jubi (CJ) and Cape Bojador (C.bo.), and near Cape Blanc (C.B.). Adapted from Sangrà et al. (2009).

However in the Canary Islands *C. pelagicus* is not found during Ice Age periods like it happens off shore West Iberia. The main reason is the latitude. The cooling and ice extent of the glacial periods often pushed the polar front as far south as North of Iberia (Eynaud et al., 2009), which would mean pushing *C. pelagicus* and its oceanographic realm down to the West coast of the Iberian Peninsula. In the Canary Islands region increased winds during glacial periods should be expected (see Grousset et al., 1998 for the Last Glacial Maximum), which would in turn increase upwelling events/strength in the region. If so, this would be observed in the size variability of *C. braarudii*, with smaller coccoliths dominating during periods of stronger upwelling.

The results of the PCA show in C1 two morphotypes, which are in fact the size variability of *C. braarudii* in the region. C2 gives the core size of the morphotype, between 11.5µm and 15.2µm, values that completely agree with current *C. braarudii*

characterization. Since the main information in the data is in fact *C. braarudii* size variability, has it is the only morphotype present, the morphological plasticity information is expected to be in the first component, the component that extracts the most significant variability.

The variability described by C1 gives *C. braarudii* a variation between 6.9µm and 17.2µm in the region, which is also in agreement with culture studies (minimum 7.87µm and maximum 17.32µm, with 12.21µm mean (see Sheward et al., 2016)).

3.4.2.1 Evidences of C. braarudii *morphological plasticity in Canary Islands*

The data analysis extracted only one morphotype, which was the expected result from this region. The upwelling regime of the Canary Islands represents a typical oceanographic regime inhabited by *C. braarudii* and the lower latitude of this site would make it unreachable by the smaller *C. pelagicus*, even in glacial periods.

Looking at the global histogram of this site (Fig. 3.19) it is interesting to note that it suggests the presence of *C. braarudii*, however with a residual tail towards small morphons which is, apparently, out of this morphotype spectrum. Moreover, the histogram, although in a one morphotype set of data can roughly determine its limits, is unable to extract size variations and morphotype behaviour through time.

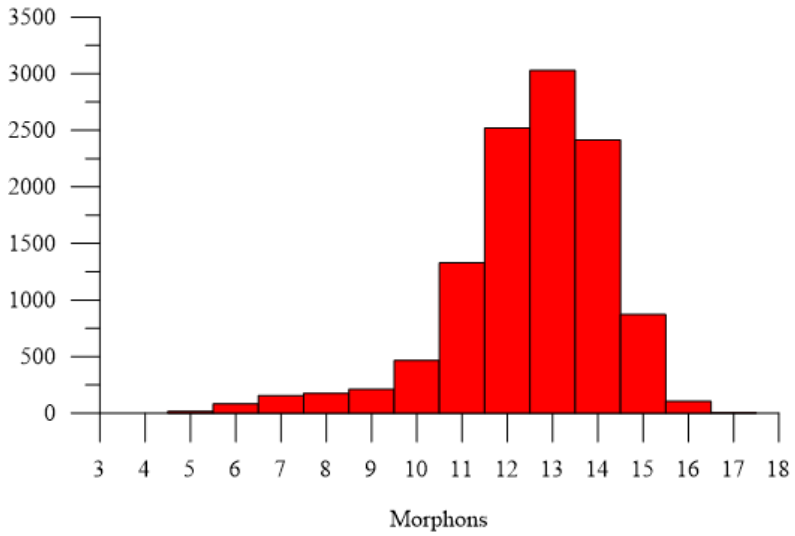

Figure 3.19 – Global histogram of GeoB5559-2.

PCA results gave the presence of *C. braarudii*, with a core size between 11.5µm and 15.2µm. However, it is very interesting to observe the size evolution. The oldest

samples, up to 155ka, are dominated by larger sizes, with an average size above 13µm. Between 151ka and 129ka a transition period is identified, and onwards, with only six exceptions with an average around 13µm, the mean size of *C. braarudii* drops to morphon 12µm or 11µm (Fig. 3.20).

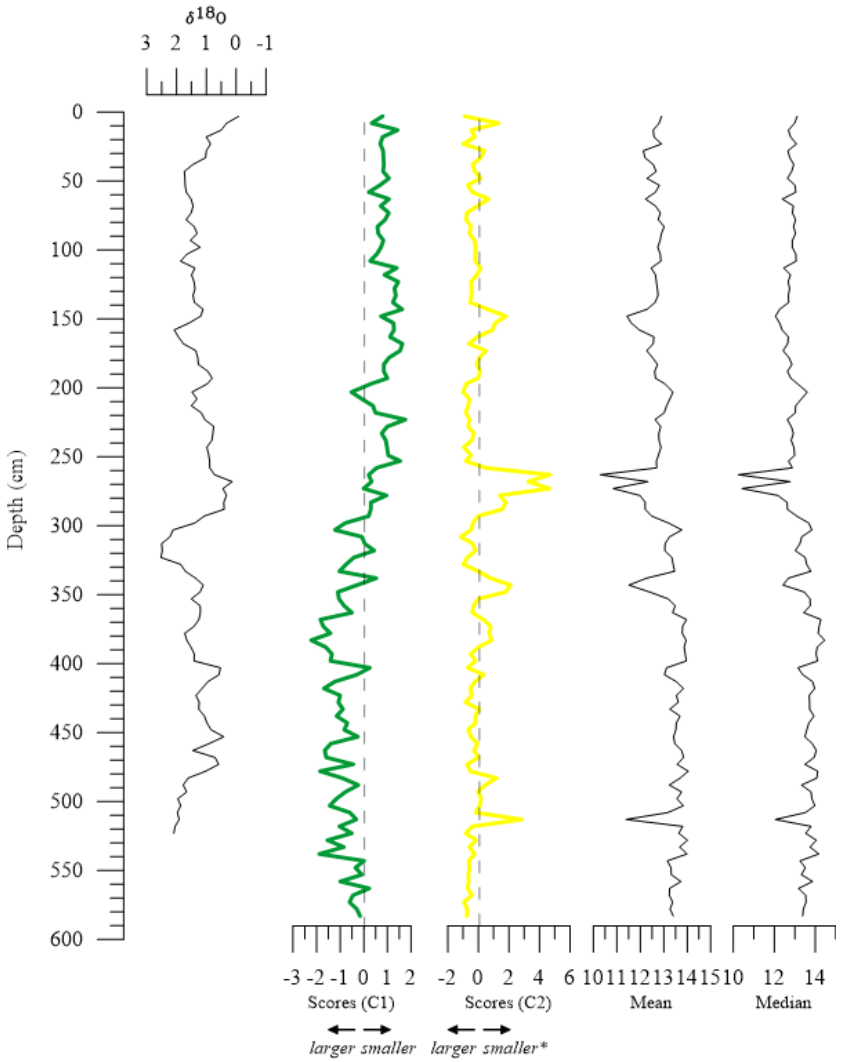

Figure 3.20 – C1 scores (green), C2 scores (yellow), mean and median of *C. braarudii* in site GeoB5559-2. *when C2 scores are positive, although PCA loadings did not give strong values, are linked to smaller morphons.

Moreno et al. (2002) describe higher primary productivity in GeoB5559-2 between 240ka and 150ka when compared to 120ka to 60ka. The results of the authors conflict with the interpretation of lower sizes in *C. braarudii* being indicative of stronger upwelling, thus higher primary productivity. However they discuss the higher dissolution rate of carbonate in this site, which could, theoretically, affect more small placoliths than larger ones. If this would be the case, then the shift in *C. braarudii* size observed in this site would be merely a consequence of organic carbon dissolution.

However there were no signs of dissolution in the samples prepared for calcareous nannoplankton morphometry, meaning that other parameters could be influencing the shift in *C. braarudii* size over the last 250ka in GeoB5559-2.

In fact there is a strong tendency towards smaller sizes in the mean size and median of the measurements obtained in this site, which in turn correlate very well with C2 scores that determine the morphotype core size (Fig. 3.21).

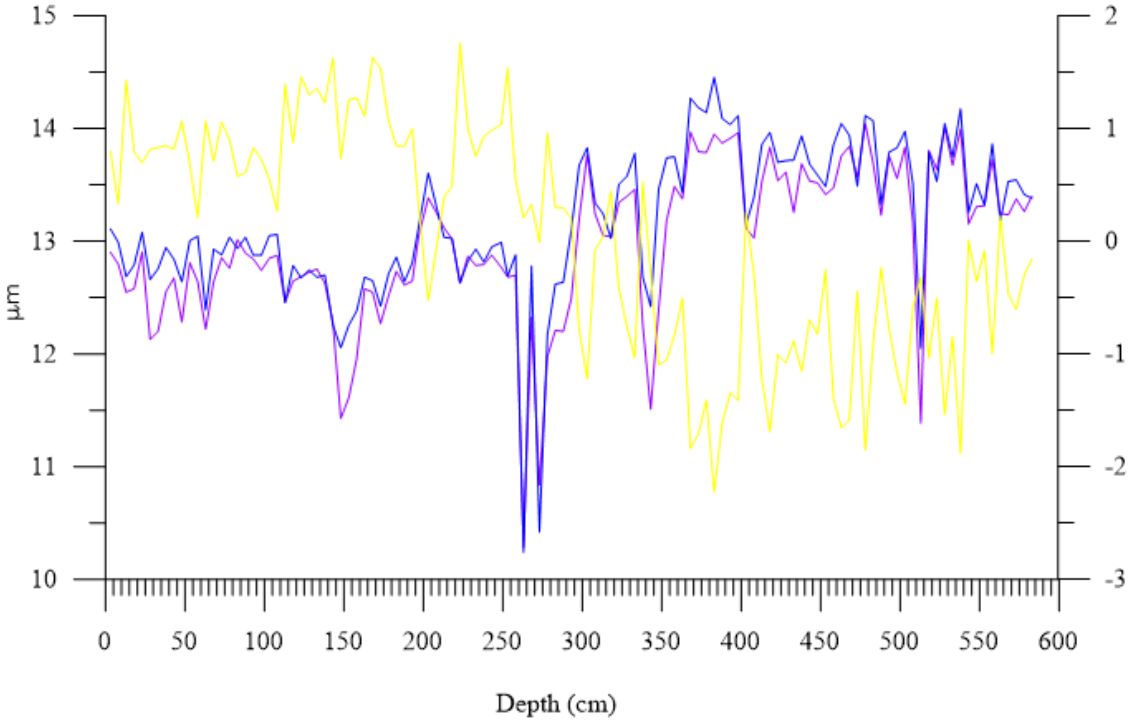

Figure 3.21– Mean (purple), median (blue) and C2 scores (yellow) of *C. braarudii* in site GeoB5559-2.

Histograms also show how scores predict size variability and how positive C2 scores reflect the presence of small coccoliths (Fig. 3.22). Sample 23cm has presence of small coccoliths, as predicted by C1 positive scores. The negative C2 scores define the morphometric data in this sample as characteristic of *C. braarudii*, which is supported by the histogram centred in morphons 12 and 13.

Sample 123cm has a high positive C1 score and morphon 12 is dominant, while C2 reflects a *C. braarudii* morphometric characterization. In samples 148cm and 343cm the information given by a positive C2 score is well visible in the histograms. When C2 is positive lower sizes are more prevalent, and C1 should indicate the dominant morphon of the sample. In the first case C1 score is positive and morphon 8 appears with significant relevance. In the second case C1 score is negative and morphons 13 and 14

dominate, with small morphons presenting relevant counting's but with none standing out.

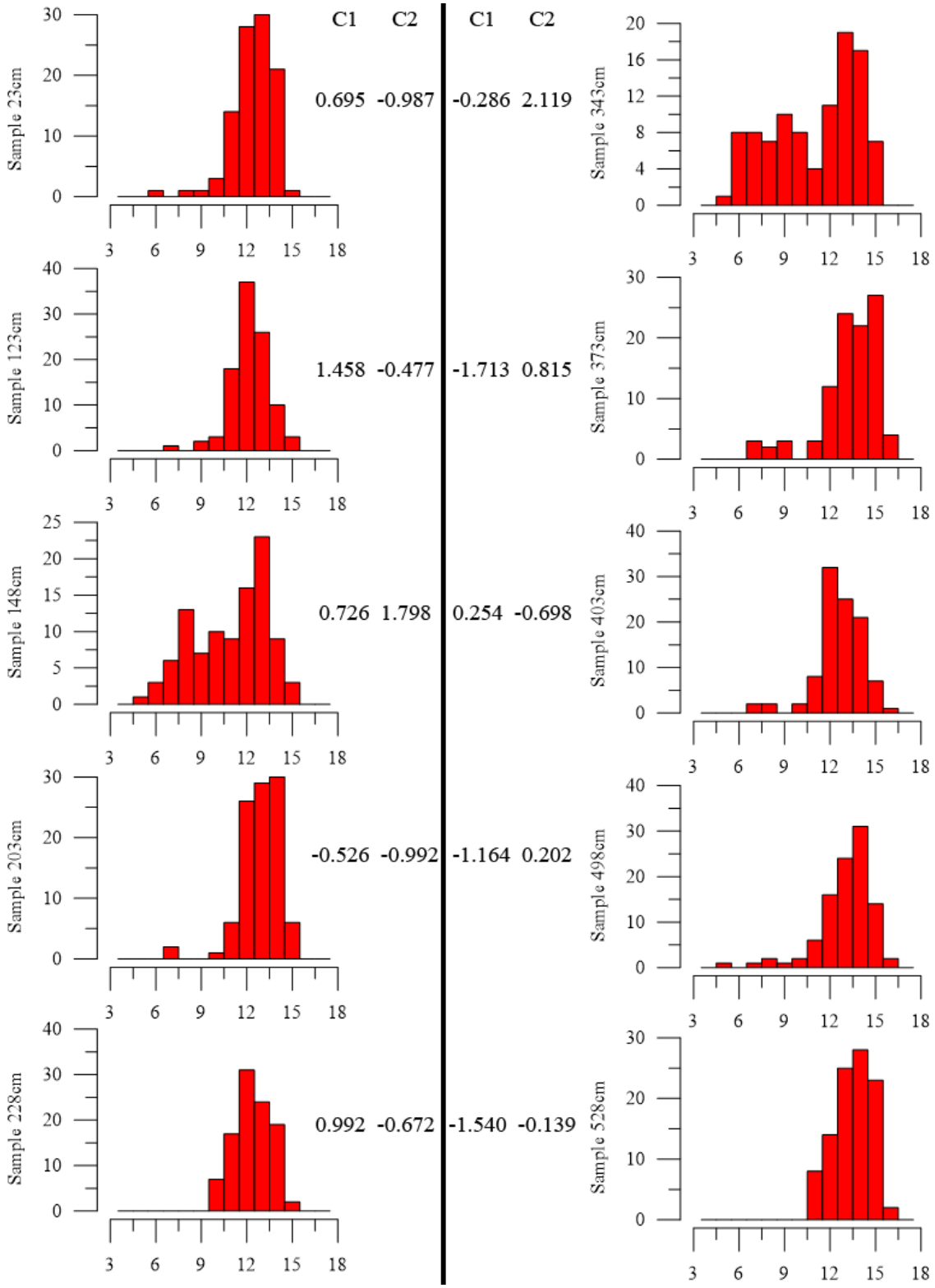

Figure 3.22 – Histograms and scores of selected samples from GeoB5559-2.

Samples 203cm, 228cm, 373cm, 403cm, 498cm and 528cm represent the common pattern of these site histograms, which are characteristic of *C. braarudii* populations. C1 scores clearly depict the size variation of the population, with negative scores in samples dominated by morphon 14, morphon 15 in one case, and positive scores in samples dominated by morphon 12.

3.4.3 DSDP608

Site DSDP608 covers a much larger time interval, from the Upper Miocene to the Holocene, meaning that its 70 samples present a much lower resolution when compared to the previous two sites. Since this work looks for microevolution and size variability as response to climate evolution, low time resolution samples present a major challenge. Coccolithophores have short generation time, which mean that size variability, or morphological plasticity, can be observed in very short time scales. A low-resolution set of samples misses a lot of information. However the analysis of DSDP608 managed to highlight some aspects of *C. pelagicus s.l.* (referred here to the broad definition of *C. pelagicus* due to the fact that this site covers from the Upper Miocene, making it uncomfortable to use Quaternary definition of *C. pelagicus* and *C. braarudii*).

C1 of the PCA shows *C. pelagicus s.l.* divided into two distinct periods. A first period dominated by a smaller morphotype, ranging from 5.0µm to 9.1µm, and a second period dominated by a larger morphotype, ranging from 10.2µm to 16.3µm.

The smaller morphotype dominates up to nearly 2.0Ma, and a transitional period is observed between this moment up to 1.5Ma. From that moment until present the larger morphotype becomes dominant (see Table 3.5).

According to the PCA C2, the smaller morphotype would vary between 5.0µm and 10.8µm. However, observing the maximum and minimum values it is possible to observe values up to morphon 11µm, with exceptional cases of morphon 13µm. This is likely a consequence of the low resolution of these samples, which generate major gaps in the temporal evolution of *C. pelagicus s.l.*, preventing the PCA to extract more accurate information.

Table 3.5 – Coccoliths size parameters variation in DSDP608 samples (color scale blue – lowest to red – highest).

Samples	MIN	MAX	AVERAGE	MEDIAN
0.03 m	7,04	15,13	11,24	11,55
0.25 m	9,42	14,64	12,32	12,26
02.00 m	8,25	16,39	12,82	13,06
04.03 m	10,76	16,38	13,03	12,97
04.51 m	8,79	15,15	12,86	12,91
06.04 m	6,88	15,57	12,06	12,35
06.54 m	9,71	16,12	12,47	12,39
08.02 m	8,61	15,45	11,76	11,70
10.02 m	9,30	15,57	13,08	13,29
14.02 m	9,49	15,85	12,20	12,07
26.29 m	6,59	13,74	11,15	11,15
28.22 m	7,42	12,45	10,40	10,35
29.22 m	6,67	13,13	10,25	10,32
31.22 m	5,68	12,69	8,55	8,26
31.72 m	5,70	13,29	8,93	8,73
34.21 m	6,81	12,95	10,11	10,00
34.72 m	5,50	12,27	10,15	10,46
36.32 m	5,92	12,83	9,86	9,96
38.32 m	6,11	12,30	8,93	8,86
38.72 m	5,37	12,52	8,23	8,11
40.33 m	6,94	12,51	10,34	10,33
44.98 m	6,18	10,63	8,65	8,75
45.92 m	6,55	11,66	8,47	8,46
46.92 m	7,00	10,67	8,63	8,68
51.92 m	6,04	10,52	8,57	8,57
54.66 m	6,11	12,22	8,74	8,71
57.52 m	7,04	10,44	8,69	8,66
68.11 m	5,92	13,70	8,59	8,53
72.81 m	7,48	10,40	8,97	8,98
76.71 m	6,77	11,72	8,89	8,86
80.72 m	7,59	11,30	9,38	9,24
84.84 m	6,93	10,06	8,29	8,24

Samples	MIN	MAX	AVERAGE	MEDIAN
86.82 m	6,79	10,05	8,39	8,37
89.82 m	6,86	9,85	8,16	8,19
91.83 m	6,12	9,69	7,98	8,05
93.92 m	6,43	10,19	8,17	8,17
99.92 m	6,43	10,48	8,12	8,18
103.53 m	6,31	10,97	8,85	8,79
106.48 m	6,71	11,79	9,35	9,39
107.52 m	7,14	10,86	8,71	8,66
108.53 m	6,49	11,04	8,73	8,78
110.52 m	6,85	13,05	9,08	8,89
113.13 m	5,51	10,35	7,99	7,74
115.12 m	5,47	10,57	8,01	8,05
117.12 m	5,91	11,33	7,92	7,87
120.12 m	5,45	9,90	7,65	7,64
122.73 m	5,89	10,31	8,13	8,14
124.76 m	5,19	10,14	7,71	7,76
126.72 m	6,83	10,54	8,89	8,96
129.72 m	6,44	10,61	9,04	9,11
131.91 m	6,03	10,48	8,46	8,52
134.29 m	5,83	10,74	7,97	7,95
136.32 m	6,39	10,06	8,07	8,09
139.32 m	5,20	9,31	7,18	7,01
141.92 m	4,98	9,65	6,95	6,83
143.93 m	5,60	9,15	7,18	7,10
145.92 m	5,76	9,04	7,19	7,23
147.92 m	5,65	9,32	7,03	6,95
150.89 m	5,07	9,74	6,75	6,75
152.52 m	5,05	8,50	6,90	6,95
154.52 m	5,42	10,40	7,07	6,97
155.52 m	5,55	10,15	7,12	7,10
156.51 m	5,33	9,29	7,02	6,95

The global histogram (Fig. 3.21), in this case, is highly misleading in giving a general idea of *C. pelagicus s.l.* in DSDP608. Looking at it one would easily conclude that a morphotype with the morphometric characteristics of *C. pelagicus* dominates the entire sample, not being able to explain the larger sizes tail.

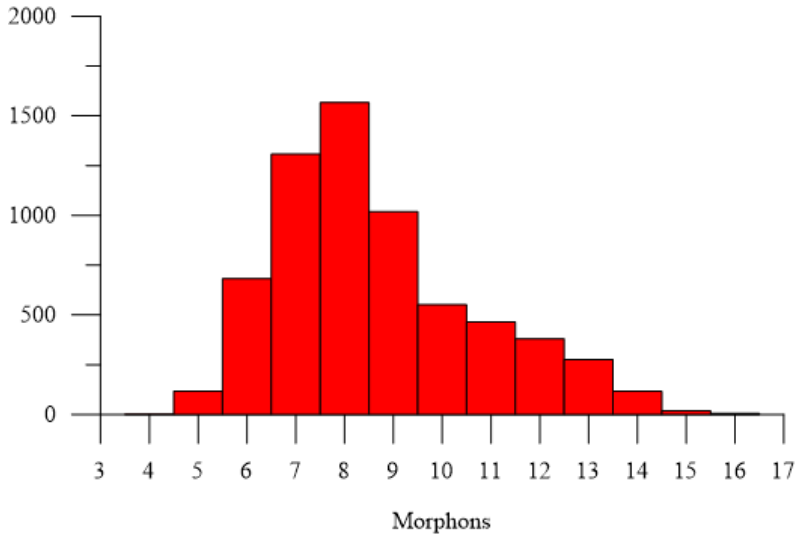

Figure 3.21 – Global histogram of DSDP608.

However, as Table 3.5 shows, size increased over time in DSDP608, and samples were progressively dominated by larger sizes more compatible to *C. braarudii* morphometry.

3.4.3.1 Evidences of C. pelagicus *s.l. morphological plasticity in DSDP608*

Thoroughly analysing the data, it seems that C2 should be looked at only when C1 is negative. If counting's and scores are removed from C2 when C1 is positive, correlation between counting's and scores increases for 0.98 for morphotype [5.0; 7.2[µm and for -0.97 for morphotype [8.3; 10.8[µm. If the same is performed to C3, but looking at it only when C1 positive, a major increase in the correlations also occurs, becoming -0.99 for morphotype [9.6; 11.1[µm and 0.97 for morphotype [12.2; 16.3[µm, pointing for a size variability of the larger morphotype between 9.6µm and 16.3µm. (see table 3.6).

Again, values in lower morphons, up to morphon 7µm, are observed in samples largely dominated by the larger morphotype. This can be an effect of the lower resolution of these samples, since there is a mean interval between samples of 74ka, decreasing the precision on the determination of the morphotypes limits by the PCA.

Table 3.6 – Morphotypes correlation between counting's and scores considering C1 scores: when C1 negative only C2 is taken into account; when C1 positive, only C3 is used.

Interval (µm)	Morphotype	Correlation with counting's
5.0 – 9.1	$_{S}C1_{NA}$	-0.97
10.2 – 16.3	$_{L}C1_{NA}$	0.98
5.0 – 7.2	$_{S}C2_{NA}$	**0.98**
8.3 – 10.8	$_{L}C2_{NA}$	**-0.97**
9.6 – 11.1	$_{S}C3_{NA}$	**-0.99**
12.2 – 16.3	$_{L}C3_{NA}$	**0.97**

This would mean that C2 gives information on the plasticity of the small morphotype defined by C1, with positive scores indicating lower sizes, and negative scores indicative of a shift towards larger sizes. C3 gives information on the plasticity of the large morphotype defined by C1, with positive scores indicating larger sizes, and negative scores indicative of a shift towards smaller sizes (see Fig. 3.22).

When C1 scores are positive [10.2; 16.3[µm (samples 10.02m, 34.21m and 40.33m) C3 scores indicate if the coccoliths size is dislocated towards smaller or larger sizes. In sample 10.02m the positive values of C3 scores are indicative of larger sizes (C3 positive scores [12.2; 16.3[µm), which is observable in the histogram that goes from morphon 9 to 16, centred in morphon 13. Samples 34.21m and 40.33m have C3 negative scores [9.6; 11.1[µm and the histogram is centred in morphon 9 in the first one and morphon 10 in the second.

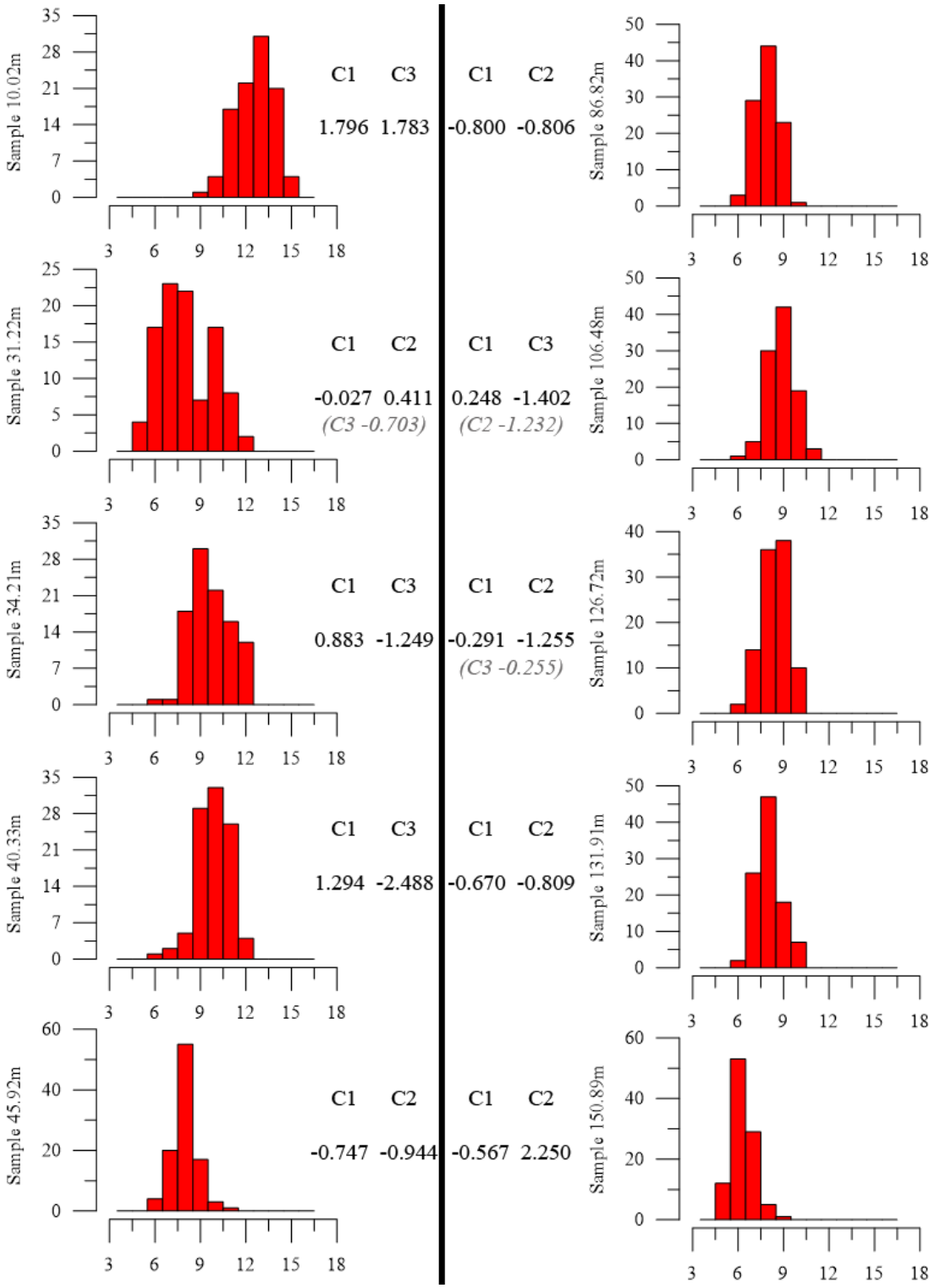

Figure 3.22 – Histograms and scores of selected samples from DSDP608.

Negative C1 scores [5.0; 9.1[µm (samples 45.92m, 86.82m, 131.91m and 150.89m) are compared with C2 scores to predict the behaviour of the sample morphometric patterns. In samples 45.92m, 86.82m and 131.91m C2 scores are negative [8.3; 10.8[µm, with all three samples showing histograms centred in morphon 8, and

displaying counting's from morphon 6 to morphon 10 (except 45.92m which has residual counting's for morphon 11). Sample 150.89m has C2 positive scores [5.0: 7.2[µm and the histogram is dislocated to the left, with counting's from morphon 5 to 9, centred in morphon 6.

Three samples were placed to illustrate how to analyse when C1 scores are low, either positive or negative. In sample 31.22m C1 is very close to zero, which means that non of the morphotypes identified by this component is dominating the sample. C2 scores are positive and C3 scores are negative. This would mean that the sample would be characterized by the dominance of sizes from 5.0µm to 7.2µm (positive C2) and 9.6µm to 11.1µm (negative C3). In fact the sample morphometry shows a distribution from morphon 5 to morphon 11 with two different peaks, one in morphon 7 and the other in morphon 10, which fits very well with the three components scores.

The other two samples show low scores values for C1. In one case C1 is positive (sample 106.48m) and in the other negative (sample 126.72m). Both the histograms corroborate the PCA scores analysis.

In sample 106.48m C1 scores indicate morphotype [10.2; 16.3[µm, C2 morphotype [8.3; 10.8[µm, and C3 morphotype [9.6; 11.1[µm. The histogram presents morphometric analysis strongly distributed between morphon 8 and 10, with few counting's in morphons 7 and 11 and residual in morphon 6. Sample 126.72m has the same information in C2 and C3 scores, but C1 indicate morphotype [5.0; 9.1[µm. When compared to sample 106.48m, the histogram shows an increase in morphons 6 and 7 counting's, the disappearance of morphon 11, a drop in morphon 10 and a shared dominance by morphons 8 and 9.

This stack of samples from DSDP608 presents a very clear pattern of domination, with the small morphotype dominating samples from 156.51m to 44.98m (exception of two samples in this total of 42), a transition period with alternate dominance, three samples each, from 40.33m to 31.22m, and a final period from 29.22m to 0.03m (total of 13 samples) completely dominated by the larger morphotype (see Fig. 3.23).

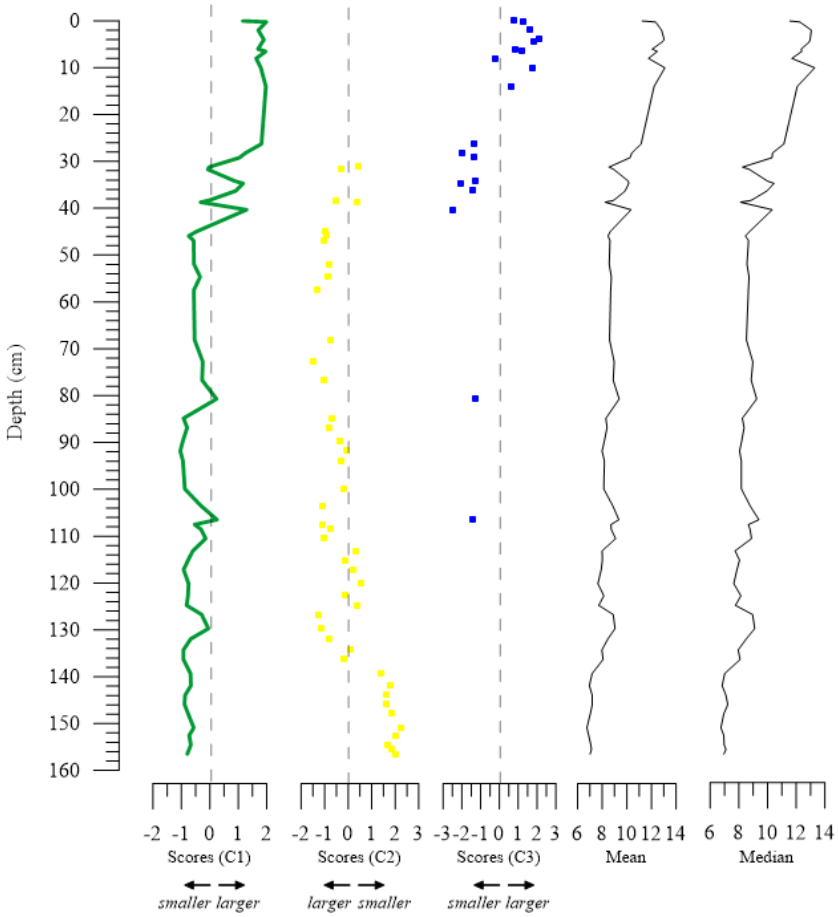

Figure 3.23 – Scores (C1 – green; C2 – yellow; C3 – blue), mean and median for site DSDP608. C2 and C3 scores plotted accordingly to C1 scores (C2 plotted when C1 negative; C3 plotted when C1 positive).

The morphotypes sizes and variability are in accordance with present description for *C. pelagicus* and *C. braarudii* (see Fig. 3.24), raising the question if this North Atlantic region could have been inhabited by *C. pelagicus* up to the Pleistocene, period when it would have been gradually replaced by *C. braarudii*. This could be indicative of a transition in the palaeoceanographic conditions, from higher nutrient availability to seasonal nutrient availability. Temperature is not an issue here since *C. pelagicus* s.l. evolved from warm-temperate waters to cold-temperate waters throughout the Cenozoic, something that still needs to be better understood.

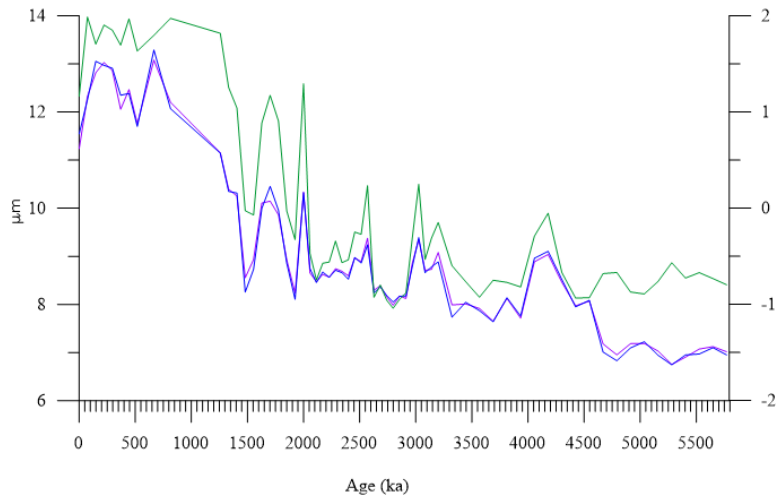

Figure 3.24 – Size variability of *C. pelagicus* s.l. in DSDP608 from Upper Miocene to the Holocene. Median (blue line); Average (purple line) and C1 scores (green line).

It is, however, important to notice that this site may show a different process, one that could only be addressed with morphometric data of high resolution. Can this site allow to observe *C. pelagicus* evolution to *C. braarudii*? The genetic differences of the sequenced strains are relatively low, and coccolith sizes overlap between both *Coccolithus* (sub)species (e.g. culture studies from Daniels et al., 2014; Sheward et al., 2014, 2016). Since presently this region is inhabited by *C. braarudii*, but was clearly dominated from Upper Miocene to the Pleistocene by a smaller morphotype (*C. pelagicus*?), could this be a place to look for the probable divergent evolution of these two *Coccolithus* forms?

Since this model can be tested by studying the morphometry of *C. braarudii* off the west coast of Portugal, where a seasonal upwelling regime is present together with *C. braarudii*, it would be useful a study on the variation of the mean size of *C. braarudii* from the water column compared with the upwelling index (intensity) at the time. The degree of correlation would be a measure of the pertinence of the proposed model and the equation that will express it may be used as a new transfer function for palaeoproductivity.

3.5 Conclusions

The application of IMMA methodology opens the possibility of studying morphological plasticity in fossil coccolithophores. The interpretation model presented here shows the morphological/morphometric response of *C. braarudii* to environmental variability, particularly to upwelling variations.

With the use of IMMA, morphotypes are more accurately defined and can be used as proxies for palaeoenvironmental changes. A shift to lower sizes in *C. braarudii* indicates that upwelling was stronger or, in same cases, maybe permanent. While the opposite, a shift towards larger sizes, would show a weak or even absent upwelling, leading to nutrient depletion and increase in cell size, with low levels of replication.

The new IMMA methodology brings new insights into fossil coccolithophores, allowing the observation of morphological plasticity of morphotypes, which can be used both as a proxy for genetic plasticity and palaeoenvironmental variability.

References

Backman, J., Hermelin, J.O.R., 1986. Morphometry of the Eocene nannofossil *Reticulofenestra umbilicus* lineage and its biochronological consequences. Palaeogeogr. Palaeoclimatol. Palaeoecol. 57, 103–116. doi:10.1016/0031-0182(86)90009-X

Balch, W.M., 2018. The ecology, biogeochemistry, and optical properties of coccolithophores. Ann. Rev. Mar. Sci. 10, 71–98. doi:10.1146/annurev-marine-121916-063319

Barcelos e Ramos, J., Schulz, K.G., Voss, M., Narciso, Á., Müller, M.N., Reis, F.V., Cachão, M., Azevedo, E.B. (in press). Nutrient-specific responses of a phytoplankton community: a case study of the North Atlantic Gyre, Azores. J. Plankton Res. (2017). doi:10.1093/plankt/fbx025.

Bard, E., Fairbanks, R., Arnold, M., Maurice, P., Duprat, J., Moyes, J., Duplessy, J.C., 1989. Sea-level estimates during the last deglaciation based on δ18O and accelerator mass spectrometry14C ages measured in *Globigerina bulloides*. Quat. Res. 31, 381–391. doi:10.1016/0033-5894(89)90045-8

Barton, E.D., Aristegui, J., Tett, P., Canton, M., García-Braun, J., Hernández-León, S., Nykjaer, L., Almeida, C., Almunia, J., Ballesteros, S., Basterretxea, G., Escanez, J., García-Weill, L., Hernández-Guerra, A., López-Laatzen, F., Molina, R., Montero, M.F., Navarro-Peréz, E., Rodríguez, J.M., Van Lenning, K., Vélez, H., Wild, K., 1998. The transition zone of the Canary Current upwelling region. Prog. Oceanogr. 41, 455–504. doi:10.1016/S0079-6611(98)00023-8

Barton, E.D., Arístegui, J., Tett, P., Navarro-Pérez, E., 2004. Variability in the Canary Islands area of filament-eddy exchanges. Prog. Oceanogr. 62, 71–94. doi:10.1016/j.pocean.2004.07.003

Baumann, K.-H., Sprengel, C., 2000. Morphological variations of selected coccolith species in a sediment trap north of the Canary Islands. J. Nannoplankt. Res. 22, 185-193.

Baumann, K., 1995. Morphometry of Quaternary *Coccolithus pelagicus* coccoliths from Northern North Atlantic and its paleoceanographical significance. Proceedings 5th INA Conference. Salamanca, Spain, 11 – 21.

Baumann, K.H., Andruleit, H., Samtleben, C., 2000. Coccolithophores in the Nordic Seas: Comparison of living communities with surface sediment assemblages. Deep. Res. Part II Top. Stud. Oceanogr. 47, 1743–1772. doi:10.1016/S0967-0645(00)00005-9

Bollmann, J., Herrle, J.O., Cortés, M.Y., Fielding, S.R., 2009. The effect of sea water salinity on the morphology of *Emiliania huxleyi* in plankton and sediment samples. Earth Planet. Sci. Lett. 284, 320–328. doi:10.1016/j.epsl.2009.05.003

Cachão, M., Moita, M.T., 2000. *Coccolithus pelagicus*, a productivity proxy related to moderate fronts off Western Iberia. Mar. Micropaleontol. 39, 131–155.

Colmenero-Hidalgo, E., Flores, J.-A., Sierro, F.J., 2002. Biometry of *Emiliania huxleyi* and its biostratigraphic significance in the Eastern North Atlantic Ocean and Western Mediterranean Sea in the last 20 000 years. Mar. Micropaleontol. 46, 247–263. doi:10.1016/S0377-8398(02)00065-8

Cordeiro, N.G.F., Dubert, J., Nolasco, R., Barton, E.D., 2018. Transient response of the Northwestern Iberian upwelling regime. PLoS One 13, 1–19. doi:10.1371/journal.pone.0197627

Cravo, A., Relvas, P., Cardeira, S., Rita, F., Madureira, M., Sánchez, R., 2010. An upwelling filament off southwest Iberia: effect on the chlorophyll a and nutrient export. Continental Shelf Research 30, 1601-1613. doi:10.1016/j.csr.2010.06.007

Cubillos, J.C., Henderiks, J., Beaufort, L., Howard, W.R., Hallegraeff, G.M., 2012. Reconstructing calcification in ancient coccolithophores: Individual coccolith weight and morphology of *Coccolithus pelagicus* (sensu lato). Mar. Micropaleontol. 92–93, 29–39. doi:10.1016/j.marmicro.2012.04.005

Daniels, C.J., Sheward, R.M., Poulton, A.J., 2014. Biogeochemical implications of comparative growth rates of *Emiliania huxleyi* and *Coccolithus* species. Biogeosciences 11, 6915–6925. doi:10.5194/bg-11-6915-2014

de Abreu, L., 2000. High resolution Palaeoceanography off Portugal during the last two Glacial Cycles. Dissertation PhD, University of Cambridge, U. K. 365 pp.

de Abreu, L., Shackleton, N.J., Schönfeld, J., Hall, M., Chapman, M., 2003. Millennial-scale oceanic climate variability off the Western Iberian margin during the last two glacial periods. Mar. Geol. 196, 1–20. doi:10.1016/S0025-3227(03)00046-X

Eynaud, F., De Abreu, L., Voelker, A., Schönfeld, J., Salgueiro, E., Turon, J.L., Penaud, A., Toucanne, S., Naughton, F., Sánchez Goñi, M.F., Malaizé, B., Cacho, I., 2009. Position of the Polar Front along the western Iberian margin during key cold episodes of the last 45 ka. Geochemistry, Geophys. Geosystems 10. doi:10.1029/2009GC002398

Ferreira, J., Cachão, M., González, R., 2008. Reworked calcareous nannofossils as ocean dynamic tracers: The Guadiana shelf case study (SW Iberia). Estuar. Coast. Shelf Sci. 79, 59–70. doi:10.1016/j.ecss.2008.03.012

Fiúza A.F.G., 1983. Upwelling Patterns off Portugal. In: Suess E., Thiede J. (eds) Coastal Upwelling Its Sediment Record. NATO Conference Series (IV Marine Sciences), 10B. Springer, Boston, MA. https://doi.org/10.1007/978-1-4615-6651-9_5

Fiúza, A.F.G., Hamann, M., Ambar, I., Díaz Del Río, G., González, N., Cabanas, J.M., 1998. Water masses and their circulation off western Iberia during May 1993. Deep. Res. Part I Oceanogr. Res. Pap. 45, 1127–1160. doi:10.1016/S0967-0637(98)00008-9

Geisen, M., Billard, C., Broerse, A.T.C., Cros, L., Probert, I., Young, J.R., 2002. Life-cycle associations involving pairs of holococcolithophorid species: intraspecific variation or cryptic speciation? Eur. J. Phycol. 37, 531–550.

Geisen, M., Young, J.R., Probert, I., Saez, A.G., Baumann, K.-H., Sprengel, C., Bollmann, J., Cros, L., De Vargas, C., Medlin, L.K., 2004. Species level variation in coccolithophores. Coccolithophores From Mol. Process. to Glob. Impact 327–366.

Gerecht, A.C., Šupraha, L., Edvardsen, B., Langer, G., Henderiks, J., 2015. Phosphorus availability modifies carbon production in *Coccolithus pelagicus* (Haptophyta). J. Exp. Mar. Bio. Ecol. 472, 24–31. doi:10.1016/j.jembe.2015.06.019

Gerecht, A.C., Šupraha, L., Edvardsen, B., Probert, I., Henderiks, J., 2014. High temperature decreases the PIC / POC ratio and increases phosphorus requirements in *Coccolithus pelagicus* (Haptophyta). Biogeosciences 11, 3531–3545. doi:10.5194/bg-11-3531-2014

Grousset, F.E., Parra, M., Bory, A., Martinez, P., Bertrand, P., Shimmield, G., Ellam, R.M., 1998. Saharan wind regimes traced by the Sr-Nd isotopic composition of subtropical Atlantic sediments: Last Glacial Maximum vs today. Quat. Sci. Rev. 17, 395–409. doi:10.1016/S0277-3791(97)00048-6

Guerreiro, C. 2013. (Paleo)ecology of Coccolithophores in the Submarine Canyons of the Central Portuguese Continental Margin: Environmental, Sedimentary and Oceanographic Implications. (PhD Dissertation), University of Lisbon, Portugal, 251 pp.

Guerreiro, C., Cachão, M., Drago, T., 2005. Calcareous nannoplankton as a tracer of the marine influence on the NW coast of Portugal over the last 14 000 years. J. Nannoplankt. Res. 27, 159–172.

Guerreiro, C., Cachão, M., Pawlowsky-Glahn, V., Oliveira, A., Rodrigues, A., 2015. Compositional Data Analysis (CoDA) as a tool to study the (paleo)ecology of coccolithophores from coastal-neritic settings off central Portugal. Sediment. Geol. 319, 134–146. doi:10.1016/j.sedgeo.2015.01.012

Imbrie, J., Kipp, N.G., 1971. A new micropaleontological method for quantitative paleoclimatology. Application to a late Pleistocene core. In: Terekian, J. (Ed.), The Late Cenozoic Glacial Age. Yale University Press, pp. 71– 181.

Incarbona, A., Martrat, B., Stefano, E. Di, Grimalt, J.O., Pelosi, N., Patti, B., Tranchida, G., 2010. Primary productivity variability on the Atlantic Iberian Margin over the last 70,000 years: Evidence from coccolithophores and fossil organic compounds. Paleoceanography 25, 1–15. doi:10.1029/2008PA001709

Jordan, R.W., Green, J.C., 1994. A check-list of the extant hapto- phyta of the world. J. Mar. Biol. Assoc. U. K. 74, 149–174.

Knappertsbusch, M., 2000. Morphologic Evolution of the Coccolithophorid *Calcidiscus leptoporus* from the early Miocene to recent. J. Paleontol. 74, 712–730.

Knappertsbusch, M., Cortes, M.Y., Thierstein, H.R., 1997. Morphologic variability of the coccolithophorid *Calcidiscus leptoporus* in the plankton, surface sediments and from the Early Pleistocene. Mar. Micropaleontol. 30, 293–317. doi:10.1016/S0377-8398(96)00053-9

Martinson, D.G., Pisias, N.G., Hays, J.D., Imbrie, J., Moore, T.C., Shackleton, N.J., 1987. Age dating and the orbital theory of the ice ages: Development of a high resolution 0 to 300 000 year chronostratigraphy. Quat. Res. 27, 1–29. doi:10.1016/0033-5894(87)90046-9

Meunier, T., Rossi, V., Morel, Y., Carton, X., 2010. Influence of bottom topography on an upwelling current: Generation of long trapped filaments. Ocean Modelling 35, 277-303. doi:10.1016/j.ocemod.2010.08.004

Moreno, A., Nave, S., Kuhlmann, H., Canals, M., Targarona, J., Freudenthal, T., Abrantes, F., 2002. Productivity response in the North Canary Basin to climate changes during the last 250 000 yr: A multi-proxy approach. Earth Planet. Sci. Lett. 196, 147–159. doi:10.1016/S0012-821X(01)00605-7

Morozov, E.G., Demidov, A.N., Tarakanov, R.Y., Zenk, W., 2010. Abyssal Channels in the Atlantic Ocean. Water Structure and Flows. Springer Netherlands. doi:10.1007/978-90-481-9358-5

Narciso, A., Cachão, M., Abreu, L. De, 2006. *Coccolithus pelagicus* subsp. *pelagicus* versus *Coccolithus pelagicus* subsp. *braarudii* (Coccolithophore, Haptophyta): A proxy for surface subarctic Atlantic waters off Iberia during the last 200 kyr. Mar. Micropaleontol. 59, 15–34. doi:10.1016/j.marmicro.2005.12.001

Narciso, Á., Gallo, F., Valente, A., Cachão, M., Cros, L., Azevedo, E.B., e Ramos, J.B., 2016. Seasonal and interannual variations in coccolithophore abundance off Terceira Island, Azores (Central North Atlantic). Cont. Shelf Res. 117, 43–56. doi:10.1016/j.csr.2016.01.019

Nave, S., Freitas, P., Abrantes, F., 2001. Coastal upwelling in the Canary Island region: Spatial variability reflected by the surface sediment diatom record. Mar. Micropaleontol. 42, 1–23. doi:10.1016/S0377-8398(01)00008-1

Parente, A., Cachão, M., Baumann, K., Abreu, L. De, Ferreira, J., 2004. Morphometry of *Coccolithus pelagicus* s.l. (Coccolithophore, Haptophyta) from offshore Portugal, during the last 200 kyr. Micropaleontology 50, 107–120.

Peliz, Á., Dubert, J., Santos, A.M.P., Oliveira, P.B., Le Cann, B., 2005. Winter upper ocean circulation in the Western Iberian Basin - Fronts, Eddies and Poleward Flows: An overview. Deep. Res. Part I Oceanogr. Res. Pap. 52, 621–646. doi:10.1016/j.dsr.2004.11.005

Peliz, Á., Rosa, T.L., Santos, A.M.P., Pissarra, J.L., 2002. Fronts, jets, and counter-flows in the Western Iberian upwelling system. J. Mar. Syst. 35, 61–77. doi:10.1016/S0924-7963(02)00076-3

Pflaumann, U., Duprat, J., Pujol, C., Labeyrie, L.D., 1996. SIMMAX: A modern analog technique to deduce Atlantic sea surface temperatures from planktonic foraminifera in deep-sea sediments. Paleoceanography 11, 15–35.

Quinn, P.S., Sáez, A.G., Baumann, K.-H., Steel, B.A., Sprengel, C., Medlin, L.K., 2004. Coccolithophorid biodiversity: evidence from the cosmopolitan species *Calcidiscus leptoporus*, in: Thierstein, H.R., Young, J.R. (Eds.), Coccolithophores: From Molecular Processes to Global Impact. Springer Berlin Heidelberg, Berlin, Heidelberg, pp. 299–326. doi:10.1007/978-3-662-06278-4_12

Raven, J.A., Giordano, M., 2009. Biomineralization by photosynthetic organisms: Evidence of coevolution of the organisms and their environment? Geobiology 7, 140–154. doi:10.1111/j.1472-4669.2008.00181.x

Renaud, S., Klaas, C., 2001. Seasonal variations in the morphology of the coccolithophore *Calcidiscus leptoporus* off Bermuda (N . Atlantic). J. Plankton Res. 23, 779–795. doi:10.1093/plankt/23.8.779

Renaud, S., Ziveri, P., Broerse, A.T.C., 2002. Geographical and seasonal differences in morphology and dynamics of the coccolithophore *Calcidiscus leptoporus*. Mar. Micropaleontol. 46, 363–385. doi:10.1016/S0377-8398(02)00081-6

Saez, A.G., Probert, I., Geisen, M., Quinn, P., Young, J.R., Medlin, L.K., 2003. Pseudo-cryptic speciation in coccolithophores. Proc. Natl. Acad. Sci. U. S. A. 100, 7163–7168. doi:10.1073/pnas.1132069100

Salgueiro, E., Naughton, F., Voelker, A.H.L., de Abreu, L., Alberto, A., Rossignol, L., Duprat, J., Magalhães, V.H., Vaqueiro, S., Turon, J.L., Abrantes, F., 2014. Past circulation along the western Iberian margin: A time slice vision from the Last Glacial to the Holocene. Quat. Sci. Rev. 106, 316–329. doi:10.1016/j.quascirev.2014.09.001

Salgueiro, E., Voelker, A.H.L., de Abreu, L., Abrantes, F., Meggers, H., Wefer, G., 2010. Temperature and productivity changes off the western Iberian margin during the last 150 ky. Quat. Sci. Rev. 29, 680–695. doi:10.1016/j.quascirev.2009.11.013

Samtleben, C., 1980. Die Evolution der Coccolithophoriden-Gattung *Gephyrocapsa* nach Befunden im Atlantik. Paläont. Z.. 54, 91-127.

Sangrà, P., Pascual, A., Rodríguez-Santana, Á., Machín, F., Mason, E., McWilliams, J.C., Pelegrí, J.L., Dong, C., Rubio, A., Arístegui, J., Marrero-Díaz, Á., Hernández-Guerra, A., Martínez-Marrero, A., Auladell, M., 2009. The Canary Eddy Corridor: A major pathway for long-lived eddies in the subtropical North Atlantic. Deep. Res. Part I Oceanogr. Res. Pap. 56, 2100–2114. doi:10.1016/j.dsr.2009.08.008

Sangrà, P., Troupin, C., Barreiro-González, B., Desmond Barton, E., Orbi, A., Arístegui, J., 2015. The Cape Ghir filament system in August 2009 (NW Africa). J. Geophys. Res. C Ocean. 120, 4516–4533. doi:10.1002/2014JC010514

Sheward, R.M., Daniels, C.J., Gibbs, S.J., 2014. Growth rates and biometric measurements of coccolithophores (*Coccolithus pelagicus*, *Coccolithus braarudii*, *Emiliania huxleyi*) during experiments, PANGAEA, http://doi.pangaea.de/10.1594/ PANGAEA.836841.

Sheward, R.M., Poulton, A.J., Gibbs, S.J., Daniels, C.J., Bown, P.R., 2016. Physiology regulates the relationship between coccosphere geometry and growth phase in coccolithophores. Biogeosciences Discuss. 14, 1493–1509. doi:10.5194/bg-14-1493-2017

Silva, A., Brotas, V., Valente, A., Sá, C., Diniz, T., Patarra, R.F., Álvaro, N. V., Neto, A.I., 2013. Coccolithophore species as indicators of surface oceanographic conditions in the vicinity of Azores islands. Estuar. Coast. Shelf Sci. 118, 50–59. doi:10.1016/j.ecss.2012.12.010

Silva, A., Palma, S., Moita, M.T., 2008. Coccolithophores in the upwelling waters of Portugal: Four years of weekly distribution in Lisbon bay. Cont. Shelf Res. 28, 2601–2613. doi:10.1016/j.csr.2008.07.009

Šupraha, L., Gerecht, A.C., Probert, I., Henderiks, J., 2015. Eco-physiological adaptation shapes the response of calcifying algae to nutrient limitation. Sci. Rep. 5, 16499. doi:10.1038/srep16499

Taylor, A.R., Brownlee, C., Wheeler, G., 2017. Coccolithophore Cell Biology: Chalking Up Progress. Ann. Rev. Mar. Sci. 9, 283–310. doi:10.1146/annurev-marine-122414-034032

Thomson, J., Nixon, S., Summerhayes, C.P., Rohling, E.J., Schonfeld, J., Zahn, R., Grootes, P., Abrantes, F., Gaspar, L., Vaqueiro, S., 2000. Enhanced productivity on the Iberian margin during glacial/interglacial transitions revealed by barium and diatoms. J. Geol. Soc. London. 157, 667–677. doi:10.1144/jgs.157.3.667

Travis, J., 1994. Evaluating the Adaptative Role of Morphological Plasticity, in: Wainwright, P.C., Reilly, S.M. (Eds.), Ecological Morphology: Integrative Organismal Biology. University of Chicago Press, Chicago, p. 367.

Troupin, C., Mason, E., Beckers, J.M., Sangrà, P., 2012. Generation of the Cape Ghir upwelling filament: A numerical study. Ocean Model. 41, 1–15. doi:10.1016/j.ocemod.2011.09.001

Wei, W., 1992. Biometric study of *Discoaster multiradiatus* and its biochronological utility. Memorie Scienze Geologiche 43, 219-235.

Westbroek, P., de Jong, E.W., van der Wal, P., Borman, a. H., de Vrind, J.P.M., Kok, D., de Bruijn, W.C., Parker, S.B., 1984. Mechanism of Calcification in the Marine Alga *Emiliania huxleyi* [and Discussion]. Philos. Trans. R. Soc. B Biol. Sci. 304, 435–444. doi:10.1098/rstb.1984.0037

Young, J., 1990. Size variation of Neogene *Reticulofenestra* coccoliths from Indian Ocean DSDP Cores. J. Micropalaeontology 9, 71–86.

Young, J., Davis, S., Bown, P., Mann, S., 1999. Coccolith ultrastructure and biomineralisation. J. Struct. Biol. 126, 195–215. doi:10.1006/jsbi.1999.4132

Young, J.R., Bown, P.R., Lees, J.A., 2018. *Coccolithus pelagic*us sp. *braarudi* Nannotax3 website. 28th Novembre 2018. http://archive.is/boun0

Young, J.R., Geisen, M., Probert, I., 2005. A review of selected aspects of coccolithophore biology with implications for paleobiodiversity estimation. Micropaleontology 51, 267–288. doi:10.2113/gsmicropal.51.4.267

Young, J.R., Geisen, M., Probert, I., 2005. A review of selected aspects of coccolithophore biology with implications for paleobiodiversity estimation. Micropaleontology 51, 267–288. doi:10.2113/gsmicropal.51.4.267

Young, J.R., Henriksen, K., 2003. Biomineralization Within Vesicles: The Calcite of Coccoliths. Rev. Mineral. Geochemistry 54, 189–215. doi:10.2113/0540189

Young, J.R., Poulton, A.J., Tyrrell, T., 2014. Morphology of *Emiliania huxleyi* coccoliths on the North West European shelf – is there an influence of carbonate chemistry? Biogeosciences Discuss. 11, 4531–4561. doi:10.5194/bgd-11-4531-2014

Ziveri, P., Baumann, K, Bockel, B., Bollmann, J., Young, J.R., 2004. Biogeography of selected Holocene coccoliths in the Atlantic Ocean. Coccolithophores from Molecular Process to Global impact, 403-408.

Annex-3

MD95-2040 – All samples IMMA analysis

IMMA analysis applied to the entire set of samples (all data or AD) determined four sets of significant morphons, two for C1 and two others for C2. The limits were determined as [3.9; 9.9[µm (the first smaller: $_{S}C1_{AD}$) and [11.0; 16.5[µm (the first larger: $_{L}C1_{AD}$) according to C1, and as [5.4; 12.5[µm (the second smaller: $_{S}C2_{AD}$) and [13.6; 17.2[µm (the second larger: $_{L}C2_{AD}$) determined by C2.

PCA scores show when each one is active or not, with $_{L}C1_{AD}$ dominating within C1 (68.4% of the samples), while for C2 an alternate dominance occurs between $_{S}C2_{AD}$ and $_{L}C2_{AD}$ (49% and 51% respectively) (Tables A3-1 and A3-2).

Table A3-1 – IMMA component 1 (C1) scores (negative scores in blue and positive scores in orange) and morphotype counts for all samples in MD95-2040.

Samples	$_{S}C1_{AD}$	$_{L}C1_{AD}$	Scores (C1)	Samples	$_{S}C1_{AD}$	$_{L}C1_{AD}$	Scores (C1)
2-3 cm	2	89	-0.801	**1220-1221 cm**	16	76	-0.199
17-18 cm	3	87	-0.726	**1250-1251 cm**	4	86	-0.518
32-33 cm	3	92	-0.859	**1280-1281 cm**	9	83	-0.550
47-48 cm	7	89	-0.619	**1310-1311 cm**	20	59	0.418
62-63 cm	5	87	-0.667	**1340-1341 cm**	22	74	0.023
77-78 cm	10	80	-0.304	**1370-1371 cm**	6	93	-0.570
92 93 cm	6	84	-0.536	**1400-1401 cm**	5	82	-0.468
122-123 cm	6	88	-0.627	**1430-1431 cm**	5	89	-0.754
152-153 cm	3	89	-0.756	**1460-1461 cm**	4	91	-0.834
167-168 cm	4	94	-0.801	**1490-1491 cm**	20	71	0.093
182-183 cm	3	88	-0.729	**1502-1503 cm**	77	19	2.531
197-198 cm	4	91	-0.897	**1520-1521 cm**	51	40	1.530
227-228 cm	68	25	2.160	**1535-1536 cm**	45	42	1.241
251-152 cm	80	14	2.596	**1550-1551 cm**	26	66	0.317
260-261 cm	84	14	2.773	**1580-1581 cm**	2	95	-0.826
290-291 cm	57	30	1.892	**1610-1611 cm**	13	80	-0.240
320-321 cm	19	78	-0.033	**1640-1641 cm**	2	95	-0.870
350 351 cm	26	67	0.278	**1670-1671 cm**	4	93	-0.759
380-381 cm	10	90	-0.730	**1700-1701 cm**	9	89	-0.491
410-411 cm	11	89	-0.485	**1730-1731 cm**	3	95	-0.821
440-441 cm	18	77	0.071	**1760-1761 cm**	45	12	2.316
470-471 cm	16	37	0.935	**1790-1791 cm**	24	5	2.090
500-501 cm	10	4	1.929	**1820-1821 cm**	45	48	1.229

530-531 cm	18	17	1.654	**1850-1851 cm**	2	94	-0.225
560-561 cm	14	22	1.502	**1883-1884 cm**	0	96	-0.734
590-591 cm	14	4	1.975	**1913-1914 cm**	28	30	1.492
620-621 cm	24	33	1.303	**1943-1944 cm**	1	94	-0.831
650-651 cm	11	58	0.343	**1973-1974 cm**	2	95	-0.587
680-681 cm	5	93	-0.904	**2003-2004 cm**	19	78	0.028
710-711 cm	17	11	1.862	**2033-2034 cm**	6	90	-0.608
728-729 cm	34	58	0.690	**2063-2064 cm**	5	90	-0.637
740-741 cm	13	83	-0.443	**2093-2094 cm**	2	94	-0.875
769-770 cm	18	76	-0.081	**2123-2124 cm**	7	90	-0.604
800-801 cm	4	91	-0.818	**2153-2154 cm**	2	94	-0.542
830-831 cm	11	79	-0.177	**2183-2184 cm**	4	94	-0.825
860-861 cm	10	82	-0.524	**2213-2214 cm**	8	89	-0.413
890-891 cm	30	59	0.603	**2243-2244 cm**	5	88	-0.526
920-921 cm	7	85	-0.615	**2273-2274 cm**	9	90	-0.486
950-951 cm	15	29	1.272	**2303-2304 cm**	17	77	-0.102
980-981 cm	7	89	-0.415	**2333-2334 cm**	1	97	-0.577
1010-1011 cm	16	79	-0.172	**2363-2364 cm**	3	95	-0.678
1025-1026 cm	6	81	-0.341	**2393-2394 cm**	1	97	-0.754
1040-1041 cm	2	94	-0.751	**2423-2424 cm**	16	79	-0.082
1070-1071 cm	1	93	-0.786	**2453-2454 cm**	6	84	-0.545
1100-1101 cm	5	84	-0.747	**2486-2487 cm**	8	85	-0.604
1130-1131 cm	12	79	-0.303	**2516-2517 cm**	4	88	-0.717
1145-1146 cm	25	68	0.222	**2546-2547 cm**	1	94	-0.807
1160-1161 cm	49	35	1.664	**2576-2577 cm**	11	81	-0.512
1190-1191 cm	11	88	-0.560	**2606-2607 cm**	6	87	-0.655

Table A3-2 – IMMA component 2 (C2) scores (negative scores in blue and positive scores in orange) and morphotype counts for all samples in MD95-2040.

Samples	$_{S}C2_{AD}$	$_{L}C2_{AD}$	Scores (C2)	Samples	$_{S}C2_{AD}$	$_{L}C2_{AD}$	Scores (C2)
2-3 cm	56	15	-1.804	**1220-1221 cm**	39	28	0.395
17-18 cm	50	17	-1.177	**1250-1251 cm**	49	26	-0.558
32-33 cm	51	13	-1.267	**1280-1281 cm**	56	13	-1.148
47-48 cm	53	18	-1.302	**1310-1311 cm**	79	3	-2.269
62-63 cm	56	13	-1.716	**1340-1341 cm**	46	29	0.407
77-78 cm	48	17	-0.926	**1370-1371 cm**	19	47	2.002
92 93 cm	54	16	-1.332	**1400-1401 cm**	47	25	-0.553
122-123 cm	58	14	-1.896	**1430-1431 cm**	46	22	-0.747
152-153 cm	54	15	-1.668	**1460-1461 cm**	46	18	-1.060
167-168 cm	35	26	-0.139	**1490-1491 cm**	64	16	-1.176
182-183 cm	46	23	-0.590	**1502-1503 cm**	85	7	0.007
197-198 cm	40	22	-0.474	**1520-1521 cm**	70	15	0.073
227-228 cm	81	5	-0.411	**1535-1536 cm**	78	7	-0.884
251-152 cm	83	3	-0.217	**1550-1551 cm**	52	19	-0.148
260-261 cm	88	4	-0.150	**1580-1581 cm**	33	31	0.475

290-291 cm	73	14	0.141	**1610-1611 cm**	39	36	0.916
320-321 cm	46	30	0.404	**1640-1641 cm**	25	37	1.135
350 351 cm	54	20	-0.234	**1670-1671 cm**	36	38	0.640
380-381 cm	42	21	-0.619	**1700-1701 cm**	37	36	0.610
410-411 cm	37	32	0.634	**1730-1731 cm**	27	33	0.734
440-441 cm	49	30	0.342	**1760-1761 cm**	45	7	0.293
470-471 cm	29	11	0.242	**1790-1791 cm**	25	2	0.340
500-501 cm	12	3	0.430	**1820-1821 cm**	62	20	0.328
530-531 cm	30	2	-0.295	**1850-1851 cm**	18	64	2.722
560-561 cm	20	8	0.590	**1883-1884 cm**	32	43	0.871
590-591 cm	20	1	0.124	**1913-1914 cm**	42	10	0.136
620-621 cm	41	10	0.067	**1943-1944 cm**	26	36	1.111
650-651 cm	21	22	0.612	**1973-1974 cm**	22	46	1.657
680-681 cm	35	29	0.491	**2003-2004 cm**	42	33	1.018
710-711 cm	22	2	0.090	**2033-2034 cm**	28	37	1.079
728-729 cm	59	17	-0.033	**2063-2064 cm**	42	30	-0.122
740-741 cm	50	21	-0.890	**2093-2094 cm**	38	25	-0.008
769-770 cm	59	13	-1.226	**2123-2124 cm**	29	39	1.291
800-801 cm	39	26	-0.072	**2153-2154 cm**	15	52	2.516
830-831 cm	46	31	0.339	**2183-2184 cm**	36	33	0.363
860-861 cm	42	22	-0.251	**2213-2214 cm**	34	38	1.010
890-891 cm	66	15	-0.796	**2243-2244 cm**	30	41	1.371
920-921 cm	52	15	-1.383	**2273-2274 cm**	18	47	2.547
950-951 cm	29	6	-0.120	**2303-2304 cm**	47	27	0.087
980-981 cm	47	27	-0.277	**2333-2334 cm**	21	49	1.705
1010-1011 cm	49	23	-0.197	**2363-2364 cm**	18	51	2.232
1025-1026 cm	36	35	0.788	**2393-2394 cm**	33	41	0.958
1040-1041 cm	40	27	-0.135	**2423-2424 cm**	44	35	0.834
1070-1071 cm	40	23	-0.638	**2453-2454 cm**	51	17	-1.242
1100-1101 cm	53	13	-1.535	**2486-2487 cm**	46	23	-0.792
1130-1131 cm	49	20	-0.273	**2516-2517 cm**	41	24	-0.500
1145-1146 cm	57	18	-0.606	**2546-2547 cm**	36	29	0.249
1160-1161 cm	77	9	-0.514	**2576-2577 cm**	48	18	-0.576
1190-1191 cm	33	27	0.456	**2606-2607 cm**	50	20	-0.918

The correlation between the scores and the counting's of the morphotypes defined by IMMA are strong, although in component two the correlation found drops to weaker values (Table A3-3).

Table A3-3 – Correlation between morphotype counting's and PCA scores for C1 and C2 with MD95-2040 AD matrix.

Interval (µm)	Morphotype	Correlation with counting's
3.9 – 9.9	$_{S}C1_{AD}$	0.84
11.0 – 16.5	$_{L}C1_{AD}$	-0.98
5.4 – 12.5	$_{S}C2_{AD}$	-0.65
13.6 – 17.2	$_{L}C2_{AD}$	0.72

DSDP 608 – All samples IMMA analysis

IMMA analysis applied to the entire set of samples (AD) determined four sets of significant morphons, two for C1 and two for C2 (see Fig. A3-1). The limits were determined as [5.0; 9.3[µm (the smaller: $_{S}C1_{AD}$) and [10.4; 16.3[µm (the larger: $_{L}C1_{AD}$) according to C1, and as [5.0; 7.2[µm ($_{S}C2_{AD}$) and [8.3; 11.3[µm ($_{L}C2_{AD}$) in C2.

Scores show the dominance of $_{S}C1_{NA}$ in C1, with 64% of the samples, while along C2 the morphotype $_{L}C2_{AD}$ is slightly more dominant with 53% of the samples (Tables A3-4 and A3-5).

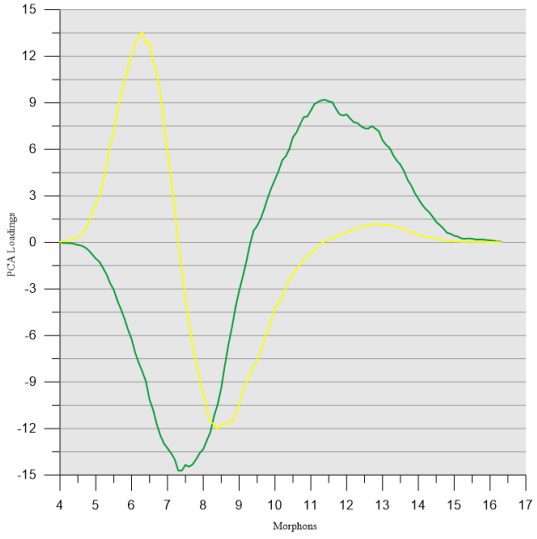

Figure A3-3 – Loadings for DSDP608 AD (green line C1; yellow line C2)

Table A2-4 – IMMA component 1 (C1) scores (negative scores in blue and positive scores in orange) and morphotype counts for all samples in DSDP608.

Samples	$_{S}C1_{AD}$	$_{L}C1_{AD}$	Scores (C1)	Samples	$_{S}C1_{AD}$	$_{L}C1_{AD}$	Scores (C1)
0.03 m	25	65	1,058	**72.81 m**	68	1	-0,482
0.25 m	0	96	1,938	**76.71 m**	70	8	-0,464
02.00 m	2	90	1,666	**80.72 m**	53	12	-0,002

04.03 m	0	99	1,884	**84.84 m**	93	0	-1,079
04.51 m	1	97	1,821	**86.82 m**	87	0	-0,966
06.04 m	6	84	1,633	**89.82 m**	95	0	-1,086
06.54 m	0	99	1,924	**91.83 m**	97	0	-1,141
08.02 m	5	77	1,539	**93.92 m**	92	0	-1,071
09.52 m	20	32	0,842	**99.92 m**	92	1	-0,997
10.02 m	0	98	1,774	**103.53 m**	68	7	-0,507
11.52 m	4	43	1,211	**106.48 m**	44	12	0,028
14.02 m	0	96	1,917	**107.52 m**	78	2	-0,727
16.02 m	15	54	1,123	**108.53 m**	70	7	-0,481
17.62 m	0	0	0,799	**110.52 m**	63	12	-0,344
19.62 m	1	0	0,768	**113.13 m**	83	0	-0,675
21.12m	2	6	0,809	**115.12 m**	90	1	-0,868
23.12 m	3	9	0,841	**117.12 m**	97	1	-1,008
26.29 m	2	76	1,705	**120.12 m**	93	0	-0,797
28.22 m	14	47	1,088	**122.73 m**	90	0	-0,884
29.22 m	25	48	0,880	**124.76 m**	95	0	-0,880
31.22 m	68	21	-0,096	**126.72 m**	70	4	-0,503
31.72 m	64	18	-0,199	**129.72 m**	60	6	-0,262
34.21 m	30	39	0,708	**131.91 m**	83	1	-0,837
34.72 m	20	51	1,024	**134.29 m**	93	1	-1,024
36.32 m	31	39	0,777	**136.32 m**	93	0	-1,041
38.32 m	58	14	-0,183	**139.32 m**	99	0	-0,658
38.72 m	80	15	-0,392	**141.92 m**	98	0	-0,610
40.33 m	11	46	1,122	**143.93 m**	100	0	-0,833
44.98 m	80	3	-0,654	**145.92 m**	100	0	-0,854
45.92 m	87	1	-0,923	**147.92 m**	99	0	-0,702
46.92 m	81	1	-0,760	**150.89 m**	99	0	-0,473
51.92 m	77	2	-0,734	**152.52 m**	100	0	-0,652
54.66 m	71	6	-0,521	**154.52 m**	98	1	-0,623
57.52 m	80	1	-0,780	**155.52 m**	96	0	-0,675
68.11 m	76	2	-0,704	**156.51 m**	100	0	-0,726

Table A3-5 – IMMA component 2 (C2) scores (negative scores in blue and positive scores in orange) and morphotype counts for all samples in DSDP608.

Samples	$_{S}C2_{AD}$	$_{L}C2_{AD}$	Scores (C2)	Samples	$_{S}C2_{AD}$	$_{L}C2_{AD}$	Scores (C2)
0.03 m	1	36	-0,264	**72.81 m**	0	82	-1,563
0.25 m	0	12	0,330	**76.71 m**	2	72	-1,064
02.00 m	0	13	0,301	**80.72 m**	0	91	-1,557
04.03 m	0	3	0,514	**84.84 m**	4	44	-0,623
04.51 m	0	7	0,423	**86.82 m**	4	53	-0,770
06.04 m	2	24	0,195	**89.82 m**	10	44	-0,303
06.54 m	0	17	0,366	**91.83 m**	14	37	0,042
08.02 m	0	44	-0,138	**93.92 m**	8	38	-0,237
09.52 m	6	11	0,362	**99.92 m**	15	44	-0,118

10.02 m	0	10	0,449	**103.53 m**	2	72	-1,122
11.52 m	0	12	0,268	**106.48 m**	3	86	-1,352
14.02 m	0	25	0,274	**107.52 m**	1	62	-1,117
16.02 m	2	16	0,210	**108.53 m**	8	64	-0,750
17.62 m	0	1	0,380	**110.52 m**	2	73	-1,116
19.62 m	0	1	0,357	**113.13 m**	29	37	0,381
21.12m	0	6	0,296	**115.12 m**	22	38	-0,055
23.12 m	1	7	0,336	**117.12 m**	22	34	0,278
26.29 m	1	51	-0,187	**120.12 m**	37	29	0,662
28.22 m	0	74	-0,748	**122.73 m**	19	44	-0,095
29.22 m	1	65	-0,698	**124.76 m**	30	29	0,483
31.22 m	28	40	0,395	**126.72 m**	2	74	-1,304
31.72 m	9	48	-0,312	**129.72 m**	4	77	-1,240
34.21 m	1	73	-0,893	**131.91 m**	8	60	-0,790
34.72 m	4	74	-0,531	**134.29 m**	17	33	0,181
36.32 m	10	60	-0,302	**136.32 m**	14	39	-0,084
38.32 m	10	62	-0,575	**139.32 m**	53	17	1,489
38.72 m	28	33	0,421	**141.92 m**	62	6	1,924
40.33 m	1	80	-0,764	**143.93 m**	54	8	1,783
44.98 m	5	65	-0,976	**145.92 m**	47	8	1,764
45.92 m	4	56	-0,919	**147.92 m**	58	5	2,011
46.92 m	2	64	-1,022	**150.89 m**	80	4	2,379
51.92 m	4	60	-0,830	**152.52 m**	68	1	2,162
54.66 m	5	67	-0,896	**154.52 m**	60	14	1,821
57.52 m	2	71	-1,347	**155.52 m**	56	6	1,995
68.11 m	5	57	-0,761	**156.51 m**	67	2	2,191

Correlation between counting's and scores present very strong values for C1 and very good correlations in C2 (Table A3-6)

Table A3-6 – Correlation between morphotype counting's and PCA scores for C1 and C2 with AD DSDP608

Interval (µm)	Morphotype	Correlation with counting's
5.0 – 9.3	$_{S}C1_{AD}$	-0.96
10.4 – 16.3	$_{L}C1_{AD}$	0.91
5.0 – 7.2	$_{S}C2_{AD}$	0.82
8.3 – 11.3	$_{L}C2_{AD}$	-0.87

Table A3-7 – IMMA component 1 (C1) scores (negative scores in blue and positive scores in orange) and morphotype counts for MD95-2040 NA matrix.

Samples	$_{s}C1_{NA}$	$_{L}C1_{NA}$	Scores (C1)	Samples	$_{s}C1_{NA}$	$_{L}C1_{NA}$	Scores (C1)
2-3 cm	2	84	-0,640	**1310-1311 cm**	23	48	0,770
17-18 cm	3	80	-0,562	**1340-1341 cm**	22	73	0,278
32-33 cm	5	87	-0,702	**1370-1371 cm**	6	91	-0,484
47-48 cm	8	81	-0,441	**1400-1401 cm**	8	77	-0,299
62-63 cm	7	81	-0,474	**1430-1431 cm**	6	85	-0,597
77-78 cm	12	75	-0,067	**1460-1461 cm**	6	88	-0,692
92 93 cm	7	78	-0,338	**1490-1491 cm**	22	66	0,392
122-123 cm	7	80	-0,440	**1502-1503 cm**	80	19	3,296
152-153 cm	4	82	-0,585	**1520-1521 cm**	52	37	2,082
167-168 cm	4	87	-0,672	**1535-1536 cm**	50	40	1,756
182-183 cm	5	81	-0,567	**1550-1551 cm**	26	61	0,626
197-198 cm	5	90	-0,766	**1580-1581 cm**	3	89	-0,726
227-228 cm	69	21	2,802	**1610-1611 cm**	13	79	-0,070
251-152 cm	84	14	3,331	**1640-1641 cm**	2	92	-0,791
260-261 cm	84	12	3,550	**1670-1671 cm**	4	89	-0,655
290-291 cm	61	27	2,468	**1700-1701 cm**	9	87	-0,354
320-321 cm	19	74	0,203	**1730-1731 cm**	3	90	-0,721
350 351 cm	27	65	0,587	**1820-1821 cm**	50	45	1,697
380-381 cm	10	86	-0,568	**1850-1851 cm**	2	87	-0,184
410-411 cm	11	88	-0,331	**1883-1884 cm**	0	93	-0,676
440-441 cm	18	73	0,301	**1943-1944 cm**	3	93	-0,739
680-681 cm	6	91	-0,793	**1973-1974 cm**	3	89	-0,515
728-729 cm	35	55	1,090	**2003-2004 cm**	20	76	0,242
740-741 cm	13	79	-0,260	**2033-2034 cm**	7	87	-0,489
769-770 cm	22	74	0,199	**2063-2064 cm**	5	87	-0,512
800-801 cm	4	88	-0,693	**2093-2094 cm**	3	87	-0,748
830-831 cm	12	73	0,026	**2123-2124 cm**	7	89	-0,488
860-861 cm	13	79	-0,312	**2153-2154 cm**	3	91	-0,496
890-891 cm	31	55	0,972	**2183-2184 cm**	4	90	-0,713
920-921 cm	10	82	-0,432	**2213-2214 cm**	8	84	-0,292
980-981 cm	8	83	-0,255	**2243-2244 cm**	5	86	-0,406
1010-1011 cm	16	77	0,059	**2273-2274 cm**	9	89	-0,382
1025-1026 cm	10	79	-0,165	**2303-2304 cm**	17	73	0,145
1040-1041 cm	4	88	-0,636	**2333-2334 cm**	2	92	-0,521
1070-1071 cm	5	90	-0,652	**2363-2364 cm**	4	91	-0,624
1100-1101 cm	6	81	-0,569	**2393-2394 cm**	2	93	-0,681
1130-1131 cm	14	75	-0,070	**2423-2424 cm**	16	76	0,122
1145-1146 cm	26	65	0,529	**2453-2454 cm**	6	80	-0,364

1160-1161 cm	54	30	2,242	**2486-2487 cm**	9	81	-0,447
1190-1191 cm	11	87	-0,386	**2516-2517 cm**	5	86	-0,567
1220-1221 cm	18	74	0,039	**2546-2547 cm**	1	88	-0,706
1250-1251 cm	7	81	-0,363	**2576-2577 cm**	12	80	-0,300
1280-1281 cm	12	80	-0,334	**2606-2607 cm**	8	81	-0,485

Table A3-8 – IMMA component 2 (C2) scores (negative scores in blue and positive scores in orange) and morphotype counts for MD95-2040 NA matrix.

Samples	$_{s}C2_{NA}$	$_{L}C2_{NA}$	Scores (C2)	Samples	$_{s}C2_{NA}$	$_{L}C2_{NA}$	Scores (C2)
2-3 cm	54	15	-1,740	**1310-1311 cm**	66	3	-2,064
17-18 cm	47	17	-1,138	**1340-1341 cm**	29	29	0,440
32-33 cm	49	13	-1,233	**1370-1371 cm**	15	47	1,879
47-48 cm	49	18	-1,247	**1400-1401 cm**	44	25	-0,528
62-63 cm	54	13	-1,641	**1430-1431 cm**	42	22	-0,731
77-78 cm	40	17	-0,854	**1460-1461 cm**	42	18	-1,040
92 93 cm	48	16	-1,266	**1490-1491 cm**	46	16	-1,053
122-123 cm	52	14	-1,812	**1502-1503 cm**	14	7	0,349
152-153 cm	51	15	-1,605	**1520-1521 cm**	21	15	0,293
167-168 cm	31	26	-0,163	**1535-1536 cm**	40	7	-0,648
182-183 cm	44	23	-0,577	**1550-1551 cm**	31	19	-0,059
197-198 cm	38	22	-0,486	**1580-1581 cm**	31	31	0,414
227-228 cm	19	5	-0,113	**1610-1611 cm**	29	36	0,886
251-152 cm	14	3	0,124	**1640-1641 cm**	23	37	1,034
260-261 cm	12	4	0,214	**1670-1671 cm**	32	38	0,576
290-291 cm	24	14	0,380	**1700-1701 cm**	29	36	0,571
320-321 cm	30	30	0,430	**1730-1731 cm**	25	33	0,660
350 351 cm	29	20	-0,143	**1820-1821 cm**	22	20	0,492
380-381 cm	32	21	-0,609	**1850-1851 cm**	16	64	2,570
410-411 cm	28	32	0,599	**1883-1884 cm**	32	43	0,782
440-441 cm	33	30	0,374	**1943-1944 cm**	25	36	1,017
680-681 cm	31	29	0,426	**1973-1974 cm**	20	46	1,545
728-729 cm	25	17	0,101	**2003-2004 cm**	24	33	1,011
740-741 cm	41	21	-0,846	**2033-2034 cm**	23	37	1,006
769-770 cm	45	13	-1,115	**2063-2064 cm**	38	30	-0,137
800-801 cm	37	26	-0,099	**2093-2094 cm**	37	25	-0,041
830-831 cm	36	31	0,352	**2123-2124 cm**	25	39	1,209
860-861 cm	34	22	-0,230	**2153-2154 cm**	14	52	2,358
890-891 cm	38	15	-0,643	**2183-2184 cm**	32	33	0,312
920-921 cm	46	15	-1,324	**2213-2214 cm**	27	38	0,952
980-981 cm	43	27	-0,264	**2243-2244 cm**	27	41	1,290
1010-1011 cm	36	23	-0,153	**2273-2274 cm**	10	47	2,412
1025-1026 cm	31	35	0,760	**2303-2304 cm**	33	27	0,127
1040-1041 cm	38	27	-0,159	**2333-2334 cm**	20	49	1,584
1070-1071 cm	39	23	-0,637	**2363-2364 cm**	16	51	2,083
1100-1101 cm	50	13	-1,478	**2393-2394 cm**	32	41	0,871

1130-1131 cm	38	20	-0,231	**2423-2424 cm**	29	35	0,828
1145-1146 cm	33	18	-0,501	**2453-2454 cm**	45	17	-1,186
1160-1161 cm	32	9	-0,252	**2486-2487 cm**	40	23	-0,767
1190-1191 cm	22	27	0,432	**2516-2517 cm**	37	24	-0,496
1220-1221 cm	24	28	0,412	**2546-2547 cm**	35	29	0,198
1250-1251 cm	46	26	-0,539	**2576-2577 cm**	37	18	-0,538
1280-1281 cm	50	13	-1,085	**2606-2607 cm**	45	20	-0,884

Table A3-9 – IMMA component 1 (C1) scores (negative scores in blue and positive scores in orange) and morphotype counts for GeoB5559-2 AD.

Samples	$_{s}C1_{AD}$	$_{L}C1_{AD}$	Scores (C1)	Samples	$_{s}C1_{AD}$	$_{L}C1_{AD}$	Scores (C1)
3 cm	39	16	0,795	**298 cm**	33	39	-0,788
8 cm	31	14	0,329	**303 cm**	25	46	-1,223
13 cm	57	14	1,428	**308 cm**	32	30	-0,079
18 cm	54	17	0,791	**313 cm**	43	31	0,038
23 cm	42	22	0,695	**318 cm**	45	27	0,440
28 cm	54	13	0,815	**323 cm**	31	33	-0,422
33 cm	51	19	0,829	**328 cm**	24	36	-0,756
38 cm	45	16	0,847	**333 cm**	30	45	-1,034
43 cm	50	22	0,814	**338 cm**	51	20	0,526
48 cm	59	16	1,065	**343 cm**	47	24	-0,286
53 cm	45	20	0,679	**348 cm**	35	40	-1,098
58 cm	43	26	0,207	**353 cm**	24	41	-1,055
63 cm	54	15	1,069	**358 cm**	26	42	-0,836
68 cm	49	17	0,708	**363 cm**	30	37	-0,504
73 cm	52	19	1,056	**368 cm**	15	58	-1,842
78 cm	47	17	0,897	**373 cm**	22	53	-1,713
83 cm	46	24	0,575	**378 cm**	26	56	-1,411
88 cm	49	22	0,608	**383 cm**	14	62	-2,229
93 cm	51	18	0,829	**388 cm**	19	55	-1,615
98 cm	50	22	0,725	**393 cm**	20	52	-1,348
103 cm	48	19	0,547	**398 cm**	21	51	-1,414
108 cm	44	24	0,263	**403 cm**	43	29	0,254
113 cm	61	13	1,394	**408 cm**	39	33	-0,297
118 cm	53	18	0,872	**413 cm**	26	44	-1,224
123 cm	57	13	1,458	**418 cm**	17	49	-1,691
128 cm	54	14	1,297	**423 cm**	27	45	-1,005
133 cm	59	17	1,356	**428 cm**	23	38	-1,080
138 cm	54	15	1,227	**433 cm**	29	39	-0,885
143 cm	68	15	1,622	**438 cm**	29	47	-1,156
148 cm	59	12	0,726	**443 cm**	30	42	-0,699
153 cm	65	7	1,253	**448 cm**	25	41	-0,827
158 cm	66	12	1,272	**453 cm**	31	32	-0,254
163 cm	56	19	1,105	**458 cm**	24	44	-1,397
168 cm	57	10	1,631	**463 cm**	19	51	-1,657

173 cm	62	13	1,532	**468 cm**	19	48	-1,592
178 cm	54	17	1,069	**473 cm**	28	35	-0,446
183 cm	52	18	0,844	**478 cm**	15	53	-1,854
188 cm	54	18	0,843	**483 cm**	18	37	-0,908
193 cm	53	15	0,998	**488 cm**	36	36	-0,236
197 cm	41	25	0,305	**493 cm**	26	47	-0,778
203 cm	33	36	-0,526	**498 cm**	27	47	-1,164
208 cm	38	31	-0,081	**503 cm**	22	50	-1,446
213 cm	40	26	0,388	**508 cm**	38	33	-0,593
218 cm	48	24	0,488	**513 cm**	58	28	-0,318
223 cm	60	10	1,758	**518 cm**	24	41	-1,038
228 cm	53	21	0,992	**523 cm**	25	35	-0,509
233 cm	49	20	0,752	**528 cm**	19	53	-1,540
238 cm	53	21	0,929	**533 cm**	25	41	-0,847
243 cm	49	16	0,983	**538 cm**	17	56	-1,886
249 cm	49	18	1,034	**543 cm**	39	30	0,010
253 cm	57	12	1,539	**548 cm**	33	29	-0,358
258 cm	46	22	0,540	**553 cm**	35	32	-0,084
263 cm	10	1	0,206	**558 cm**	26	44	-0,999
268 cm	17	6	0,326	**563 cm**	41	32	0,228
273 cm	6	4	-0,011	**568 cm**	39	39	-0,464
278 cm	62	15	0,960	**573 cm**	29	38	-0,607
283 cm	44	17	0,300	**578 cm**	36	34	-0,299
288 cm	57	24	0,294	**583 cm**	34	32	-0,159
293 cm	41	23	0,206				

Table A3-10 – IMMA component 2 (C2) scores (negative scores in blue and positive scores in orange) and morphotype counts for GeoB5559-2 AD.

Samples	MC2AD	Scores (C2)	Samples	MC2AD	Scores (C2)
3 cm	86	-0,901	**298 cm**	87	-0,351
8 cm	55	1,340	**303 cm**	86	-0,473
13 cm	86	-0,445	**308 cm**	91	-1,159
18 cm	80	-0,222	**313 cm**	83	-0,366
23 cm	90	-0,987	**318 cm**	82	-0,182
28 cm	70	0,381	**323 cm**	87	-0,718
33 cm	75	0,155	**328 cm**	90	-0,982
38 cm	80	-0,368	**333 cm**	83	-0,015
43 cm	85	-0,231	**338 cm**	68	0,795
48 cm	75	0,149	**343 cm**	52	2,119
53 cm	85	-0,700	**348 cm**	58	1,792
58 cm	81	-0,399	**353 cm**	79	0,003
63 cm	71	0,678	**358 cm**	82	-0,318
68 cm	77	-0,048	**363 cm**	81	-0,394
73 cm	85	-0,743	**368 cm**	76	0,332
78 cm	85	-0,797	**373 cm**	68	0,815

83 cm	82	-0,480	**378 cm**	69	0,708
88 cm	83	-0,597	**383 cm**	72	0,871
93 cm	82	-0,255	**388 cm**	77	0,013
98 cm	81	-0,179	**393 cm**	88	-0,499
103 cm	79	-0,193	**398 cm**	78	-0,189
108 cm	75	-0,196	**403 cm**	86	-0,698
113 cm	75	0,148	**408 cm**	76	0,358
118 cm	81	-0,087	**413 cm**	83	-0,217
123 cm	82	-0,477	**418 cm**	88	-0,528
128 cm	84	-0,427	**423 cm**	84	-0,425
133 cm	82	-0,447	**428 cm**	89	-0,850
138 cm	83	-0,531	**433 cm**	75	0,059
143 cm	77	0,630	**438 cm**	88	-0,197
148 cm	53	1,798	**443 cm**	82	-0,186
153 cm	64	1,094	**448 cm**	88	-0,665
158 cm	66	0,923	**453 cm**	83	-0,474
163 cm	81	-0,066	**458 cm**	80	-0,053
168 cm	84	-0,638	**463 cm**	80	-0,279
173 cm	72	0,505	**468 cm**	80	0,014
178 cm	77	0,075	**473 cm**	87	-0,733
183 cm	82	-0,105	**478 cm**	86	-0,534
188 cm	75	0,108	**483 cm**	65	1,191
193 cm	77	-0,017	**488 cm**	70	0,445
197 cm	86	-0,801	**493 cm**	79	-0,036
203 cm	92	-0,992	**498 cm**	75	0,202
208 cm	84	-0,587	**503 cm**	73	0,084
213 cm	85	-0,659	**508 cm**	81	-0,165
218 cm	91	-0,816	**513 cm**	47	2,854
223 cm	87	-0,571	**518 cm**	78	-0,378
228 cm	88	-0,672	**523 cm**	84	-0,829
233 cm	80	-0,284	**528 cm**	81	-0,139
238 cm	83	-0,429	**533 cm**	85	-0,594
243 cm	88	-0,957	**538 cm**	85	-0,243
249 cm	83	-0,478	**543 cm**	87	-0,627
253 cm	85	-0,835	**548 cm**	85	-0,590
258 cm	71	0,477	**553 cm**	88	-0,653
263 cm	5	4,698	**558 cm**	87	-0,635
268 cm	27	3,267	**563 cm**	85	-0,698
273 cm	6	4,670	**568 cm**	86	-0,410
278 cm	59	1,395	**573 cm**	90	-0,947
283 cm	59	1,802	**578 cm**	87	-0,708
288 cm	59	1,573	**583 cm**	85	-0,752
293 cm	77	-0,012			

Table A3-11 – IMMA component 1 (C1) scores (negative scores in blue and positive scores in orange) and morphotype counts in GeoB5559-2 NA matrix.

Samples	$_{s}C1_{NA}$	$_{L}C1_{NA}$	Scores (C1)	Samples	$_{s}C1_{NA}$	$_{L}C1_{NA}$	Scores (C1)
3 cm	38	16	0,786	**308 cm**	32	29	-0,061
13 cm	56	14	1,404	**313 cm**	43	30	0,047
18 cm	53	17	0,779	**318 cm**	45	26	0,436
23 cm	42	21	0,694	**323 cm**	31	33	-0,400
28 cm	54	12	0,795	**328 cm**	24	36	-0,723
33 cm	50	19	0,812	**333 cm**	29	45	-1,001
38 cm	45	15	0,833	**338 cm**	50	20	0,509
43 cm	49	22	0,804	**343 cm**	46	24	-0,298
48 cm	58	16	1,043	**348 cm**	35	40	-1,084
53 cm	45	20	0,674	**353 cm**	24	41	-1,025
58 cm	42	26	0,211	**358 cm**	26	41	-0,806
63 cm	53	15	1,041	**363 cm**	30	37	-0,483
68 cm	48	17	0,695	**368 cm**	15	58	-1,794
73 cm	52	18	1,044	**373 cm**	22	52	-1,675
78 cm	47	17	0,886	**378 cm**	26	55	-1,378
83 cm	46	24	0,572	**383 cm**	14	61	-2,176
88 cm	49	22	0,604	**388 cm**	19	54	-1,569
93 cm	50	18	0,817	**393 cm**	20	52	-1,303
98 cm	49	22	0,714	**398 cm**	20	51	-1,372
103 cm	47	19	0,540	**403 cm**	42	29	0,260
108 cm	44	23	0,264	**408 cm**	39	32	-0,287
113 cm	60	13	1,365	**413 cm**	26	43	-1,185
118 cm	52	18	0,857	**418 cm**	17	48	-1,639
123 cm	56	13	1,433	**423 cm**	27	44	-0,970
128 cm	53	14	1,276	**428 cm**	23	37	-1,041
133 cm	58	17	1,335	**433 cm**	29	38	-0,860
138 cm	53	15	1,208	**438 cm**	29	46	-1,117
143 cm	67	15	1,584	**443 cm**	30	41	-0,673
148 cm	58	12	0,692	**448 cm**	25	41	-0,794
153 cm	65	7	1,216	**453 cm**	31	31	-0,240
158 cm	66	12	1,236	**458 cm**	23	44	-1,356
163 cm	56	18	1,086	**463 cm**	19	50	-1,609
168 cm	56	10	1,602	**468 cm**	19	48	-1,548
173 cm	61	13	1,497	**473 cm**	28	34	-0,424
178 cm	54	16	1,047	**478 cm**	15	52	-1,797
183 cm	51	18	0,831	**488 cm**	35	36	-0,230
188 cm	53	18	0,828	**493 cm**	25	47	-0,753
193 cm	52	15	0,978	**498 cm**	27	46	-1,132
197 cm	40	25	0,309	**503 cm**	21	50	-1,408
203 cm	33	36	-0,497	**508 cm**	37	33	-0,572
208 cm	38	31	-0,069	**513 cm**	57	28	-0,334
213 cm	39	26	0,390	**518 cm**	23	41	-1,006
218 cm	47	24	0,492	**523 cm**	25	35	-0,486

223 cm	59	10	1,725	**528 cm**	19	53	-1,494
228 cm	52	21	0,981	**533 cm**	25	40	-0,815
233 cm	48	20	0,742	**538 cm**	17	55	-1,830
238 cm	52	21	0,917	**543 cm**	38	30	0,022
243 cm	49	16	0,974	**548 cm**	32	29	-0,339
249 cm	49	18	1,018	**553 cm**	35	32	-0,069
253 cm	57	12	1,514	**558 cm**	26	43	-0,962
278 cm	61	15	0,927	**563 cm**	41	32	0,235
288 cm	56	24	0,277	**568 cm**	39	38	-0,439
293 cm	41	23	0,204	**573 cm**	29	38	-0,578
298 cm	33	38	-0,757	**578 cm**	35	34	-0,279
303 cm	24	46	-1,182	**583 cm**	33	32	-0,144

Table A3-12 – IMMA component 2 (C2) scores (negative scores in blue and positive scores in orange) and morphotype counts in GeoB5559-2 NA matrix.

Samples	mC1NA	Scores (C2)	Samples	mC1NA	Scores (C2)
3 cm	67	-1,169	**308 cm**	70	-1,568
13 cm	61	-0,348	**313 cm**	57	-0,239
18 cm	62	-0,057	**318 cm**	58	-0,008
23 cm	67	-1,232	**323 cm**	63	-0,888
28 cm	53	0,711	**328 cm**	68	-1,322
33 cm	56	0,383	**333 cm**	52	0,259
38 cm	64	-0,455	**338 cm**	47	1,319
43 cm	55	0,018	**343 cm**	38	3,062
48 cm	57	0,439	**348 cm**	37	2,677
53 cm	66	-0,831	**353 cm**	55	0,081
58 cm	68	-0,516	**358 cm**	53	-0,295
63 cm	44	1,293	**363 cm**	58	-0,388
68 cm	54	0,218	**368 cm**	47	0,638
73 cm	64	-0,806	**373 cm**	44	1,335
78 cm	66	-1,008	**378 cm**	45	1,210
83 cm	62	-0,486	**383 cm**	40	1,473
88 cm	65	-0,608	**388 cm**	55	0,277
93 cm	58	-0,078	**393 cm**	57	-0,468
98 cm	60	0,061	**398 cm**	53	-0,142
103 cm	55	-0,006	**403 cm**	65	-0,847
108 cm	64	-0,016	**408 cm**	47	0,837
113 cm	55	0,636	**413 cm**	55	-0,034
118 cm	54	0,268	**418 cm**	58	-0,546
123 cm	60	-0,399	**423 cm**	61	-0,403
128 cm	55	-0,254	**428 cm**	65	-1,027
133 cm	56	-0,192	**433 cm**	58	0,195
138 cm	67	-0,526	**438 cm**	53	0,060
143 cm	45	1,444	**443 cm**	55	0,001
148 cm	43	2,660	**448 cm**	63	-0,799

153 cm	51	1,775	**453 cm**	61	-0,528
158 cm	46	1,566	**458 cm**	52	0,142
163 cm	57	0,250	**463 cm**	58	-0,231
168 cm	64	-0,697	**468 cm**	52	0,282
173 cm	48	1,145	**473 cm**	66	-0,922
178 cm	53	0,424	**478 cm**	56	-0,561
183 cm	57	0,214	**488 cm**	52	0,812
188 cm	54	0,562	**493 cm**	54	0,131
193 cm	51	0,402	**498 cm**	54	0,490
197 cm	66	-1,080	**503 cm**	53	0,270
203 cm	67	-1,212	**508 cm**	64	-0,012
208 cm	61	-0,679	**513 cm**	31	4,241
213 cm	65	-0,820	**518 cm**	62	-0,441
218 cm	62	-0,897	**523 cm**	64	-1,128
223 cm	61	-0,526	**528 cm**	53	0,076
228 cm	62	-0,678	**533 cm**	60	-0,611
233 cm	59	-0,109	**538 cm**	55	-0,039
238 cm	61	-0,314	**543 cm**	62	-0,638
243 cm	65	-1,145	**548 cm**	60	-0,670
249 cm	57	-0,347	**553 cm**	61	-0,680
253 cm	68	-0,973	**558 cm**	62	-0,667
278 cm	42	2,360	**563 cm**	64	-0,845
288 cm	40	2,566	**568 cm**	61	-0,216
293 cm	56	0,028	**573 cm**	67	-1,210
298 cm	56	-0,163	**578 cm**	66	-0,805
303 cm	59	-0,512	**583 cm**	67	-0,971

Table A3-13 – IMMA component 1 (C1) scores (negative scores in blue and positive scores in orange) and morphotype counts in DSDP608 NA matrix.

Samples	$sC1_{NA}$	$lC1_{NA}$	Scores (C1)	Samples	$sC1_{NA}$	$lC1_{NA}$	Scores (C1)
0.03 m	24	66	1,163	**86.82 m**	80	0	-0,800
0.25 m	0	96	1,987	**89.82 m**	90	0	-0,958
02.00 m	2	90	1,704	**91.83 m**	95	0	-1,041
04.03 m	0	99	1,904	**93.92 m**	86	0	-0,948
04.51 m	1	97	1,849	**99.92 m**	88	1	-0,882
06.04 m	4	86	1,694	**103.53 m**	60	8	-0,312
06.54 m	0	99	1,967	**106.48 m**	39	17	0,248
08.02 m	4	84	1,633	**107.52 m**	72	3	-0,533
10.02 m	0	99	1,796	**108.53 m**	58	10	-0,312
14.02 m	0	98	1,973	**110.52 m**	58	14	-0,149
26.29 m	1	82	1,817	**113.13 m**	80	1	-0,599
28.22 m	13	60	1,255	**115.12 m**	88	1	-0,765
29.22 m	21	53	1,040	**117.12 m**	95	1	-0,927
31.22 m	68	25	-0,027	**120.12 m**	90	0	-0,750
31.72 m	60	19	-0,071	**122.73 m**	85	1	-0,772

34.21 m	25	45	0,883	**124.76 m**	92	0	-0,820
34.72 m	18	56	1,172	**126.72 m**	57	7	-0,291
36.32 m	29	46	0,905	**129.72 m**	50	11	-0,053
38.32 m	54	16	-0,029	**131.91 m**	80	4	-0,670
38.72 m	78	15	-0,327	**134.29 m**	91	1	-0,935
40.33 m	10	57	1,294	**136.32 m**	90	0	-0,930
44.98 m	71	8	-0,470	**139.32 m**	97	0	-0,681
45.92 m	83	2	-0,747	**141.92 m**	98	0	-0,669
46.92 m	74	4	-0,573	**143.93 m**	98	0	-0,872
51.92 m	72	4	-0,561	**145.92 m**	100	0	-0,892
54.66 m	63	10	-0,342	**147.92 m**	99	0	-0,763
57.52 m	72	1	-0,567	**150.89 m**	99	0	-0,567
68.11 m	67	4	-0,537	**152.52 m**	100	0	-0,727
72.81 m	60	3	-0,249	**154.52 m**	98	1	-0,671
76.71 m	60	11	-0,272	**155.52 m**	95	0	-0,732
80.72 m	40	20	0,234	**156.51 m**	98	0	-0,797
84.84 m	85	0	-0,927				

Table A3-14 – IMMA component 2 (C2) scores (negative scores in blue and positive scores in orange) and morphotype counts in DSDP608 NA matrix.

Samples	$_{S}C2_{NA}$	$_{L}C2_{NA}$	Scores (C2)	Samples	$_{S}C2_{NA}$	$_{L}C2_{NA}$	Scores (C2)
0.03 m	1	31	-0,080	**86.82 m**	4	53	-0,806
0.25 m	0	7	0,595	**89.82 m**	10	44	-0,376
02.00 m	0	8	0,522	**91.83 m**	14	37	-0,055
04.03 m	0	1	0,753	**93.92 m**	8	38	-0,312
04.51 m	0	5	0,659	**99.92 m**	15	44	-0,188
06.04 m	2	18	0,427	**103.53 m**	2	69	-1,083
06.54 m	0	6	0,625	**106.48 m**	3	83	-1,232
08.02 m	0	35	0,102	**107.52 m**	1	61	-1,107
10.02 m	0	2	0,674	**108.53 m**	8	63	-0,723
14.02 m	0	9	0,540	**110.52 m**	2	69	-1,057
26.29 m	1	34	0,085	**113.13 m**	29	37	0,328
28.22 m	0	58	-0,524	**115.12 m**	22	38	-0,116
29.22 m	1	57	-0,504	**117.12 m**	22	34	0,187
31.22 m	28	34	0,411	**120.12 m**	37	29	0,576
31.72 m	9	44	-0,273	**122.73 m**	19	44	-0,153
34.21 m	1	61	-0,712	**124.76 m**	30	29	0,395
34.72 m	4	54	-0,325	**126.72 m**	2	74	-1,255
36.32 m	10	46	-0,140	**129.72 m**	4	77	-1,162
38.32 m	10	57	-0,520	**131.91 m**	8	60	-0,809
38.72 m	28	30	0,398	**134.29 m**	17	33	0,093
40.33 m	1	63	-0,533	**136.32 m**	14	39	-0,162
44.98 m	5	65	-0,963	**139.32 m**	53	17	1,379
45.92 m	4	56	-0,944	**141.92 m**	62	6	1,798
46.92 m	2	64	-1,020	**143.93 m**	54	8	1,642

51.92 m	4	60	-0,833	**145.92 m**	47	8	1,621
54.66 m	5	66	-0,869	**147.92 m**	58	5	1,874
57.52 m	2	71	-1,333	**150.89 m**	80	4	2,250
68.11 m	5	57	-0,764	**152.52 m**	68	1	2,023
72.81 m	0	82	-1,499	**154.52 m**	60	14	1,701
76.71 m	2	69	-1,021	**155.52 m**	56	6	1,864
80.72 m	0	87	-1,432	**156.51 m**	67	2	2,045
84.84 m	4	44	-0,681				

Table A3-15 – IMMA component 3 (C3) scores (negative scores in blue and positive scores in orange) and morphotype counts in DSDP608 NA matrix.

Samples	$_{S}C3_{NA}$	$_{L}C3_{NA}$	Scores (C3)	Samples	$_{S}C3_{NA}$	$_{L}C3_{NA}$	Scores (C3)
0.03 m	10	35	0,802	**86.82 m**	3	0	0,864
0.25 m	9	52	1,238	**89.82 m**	3	0	1,079
02.00 m	7	67	1,611	**91.83 m**	2	0	1,158
04.03 m	2	75	2,109	**93.92 m**	6	0	1,061
04.51 m	5	69	1,812	**99.92 m**	5	0	0,764
06.04 m	14	54	0,825	**103.53 m**	21	0	-0,088
06.54 m	15	56	1,171	**106.48 m**	40	0	-1,402
08.02 m	30	38	-0,252	**107.52 m**	17	0	0,434
10.02 m	6	74	1,783	**108.53 m**	20	0	-0,435
14.02 m	17	47	0,649	**110.52 m**	18	2	-0,023
26.29 m	43	18	-1,369	**113.13 m**	11	0	-0,334
28.22 m	47	5	-1,962	**115.12 m**	7	0	0,561
29.22 m	38	7	-1,333	**117.12 m**	1	0	0,737
31.22 m	22	1	-0,703	**120.12 m**	2	0	0,072
31.72 m	18	4	-0,181	**122.73 m**	5	0	0,430
34.21 m	42	8	-1,249	**124.76 m**	2	0	0,435
34.72 m	46	1	-2,089	**126.72 m**	19	0	-0,255
36.32 m	34	8	-1,422	**129.72 m**	30	0	-0,906
38.32 m	31	1	-0,803	**131.91 m**	10	0	0,582
38.72 m	9	2	-0,097	**134.29 m**	4	0	0,836
40.33 m	55	1	-2,488	**136.32 m**	2	0	0,885
44.98 m	16	0	0,145	**139.32 m**	0	0	-0,477
45.92 m	6	0	0,949	**141.92 m**	1	0	-0,660
46.92 m	12	0	0,376	**143.93 m**	0	0	-0,257
51.92 m	17	0	0,272	**145.92 m**	0	0	-0,161
54.66 m	17	1	-0,143	**147.92 m**	0	0	-0,630
57.52 m	11	0	0,509	**150.89 m**	1	0	-1,240
68.11 m	12	1	0,251	**152.52 m**	0	0	-0,710
72.81 m	22	0	-0,320	**154.52 m**	1	0	-0,699
76.71 m	21	0	-0,172	**155.52 m**	3	0	-0,748
80.72 m	38	0	-1,304	**156.51 m**	0	0	-0,723
84.84 m	4	0	1,234				

Table A4-16 – Examples for the morphotypes limits in MD95-2040 exercise related to table 3.4. Blue – smaller morphotype; Green – larger morphotype; White – overlapping region)

	Samples						
Measurements	1520-1521 cm	1535-1536 cm	1550-1551 cm	1580-1581 cm	1610-1611 cm	1640-1641 cm	1670-1671 cm
1	5,65	5,63	5,34	6,83	5,18	7,32	5,89
2	6,11	5,84	5,38	7,86	5,66	9,46	6,71
3	6,16	6,00	5,85	10,17	6,11	10,27	9,05
4	6,41	6,06	5,86	10,64	6,30	10,91	9,11
5	6,45	6,13	5,88	10,78	6,85	11,10	10,38
6	6,49	6,17	6,09	11,01	7,06	11,18	10,88
7	6,67	6,31	6,15	11,08	7,26	11,27	10,91
8	6,68	6,54	6,48	11,19	8,36	11,42	11,12
9	6,69	6,55	6,97	11,29	8,46	11,81	11,13
10	7,14	6,57	7,02	11,29	8,53	11,83	11,15
11	7,14	6,58	7,23	11,67	9,44	11,90	11,21
12	7,30	6,76	7,26	11,76	9,70	12,01	11,53
13	7,32	6,77	7,29	11,77	9,82	12,02	11,56
14	7,36	6,89	7,41	11,88	10,34	12,06	11,61
15	7,38	7,04	7,64	11,88	10,47	12,15	11,64
16	7,44	7,20	7,79	11,90	10,66	12,15	11,71
17	7,50	7,22	7,91	11,94	10,69	12,18	11,76
18	7,52	7,22	8,50	11,97	10,71	12,18	11,78
19	7,53	7,28	8,52	11,97	10,81	12,19	11,84
20	7,57	7,46	9,06	11,98	10,88	12,21	11,94
21	7,63	7,76	9,18	12,01	11,48	12,30	12,00
22	7,67	7,82	9,23	12,07	11,58	12,36	12,04
23	7,70	7,90	9,35	12,12	11,67	12,36	12,05
24	7,71	7,99	9,55	12,12	11,68	12,41	12,06
25	7,71	8,00	9,60	12,15	11,79	12,41	12,09
26	7,78	8,02	9,76	12,18	11,85	12,52	12,10
27	7,81	8,12	10,30	12,20	11,92	12,54	12,14
28	7,85	8,19	10,48	12,24	11,92	12,56	12,14
29	8,05	8,34	10,53	12,26	11,98	12,61	12,14
30	8,13	8,36	10,57	12,31	12,04	12,66	12,24
31	8,13	8,37	10,60	12,35	12,05	12,75	12,25
32	8,24	8,71	10,63	12,47	12,21	12,75	12,33
33	8,24	8,79	10,80	12,48	12,22	12,81	12,33
34	8,30	8,89	10,85	12,52	12,32	12,82	12,35
35	8,39	8,90	11,07	12,56	12,36	12,83	12,38
36	8,44	8,91	11,15	12,63	12,38	12,87	12,44
37	8,61	9,38	11,15	12,67	12,41	12,87	12,50
38	8,67	9,42	11,18	12,69	12,42	12,88	12,51
39	8,70	9,57	11,27	12,76	12,44	12,89	12,55

40	8,72	9,62	11,31	12,78	12,46	12,95	12,67
41	8,78	9,63	11,40	12,84	12,51	12,99	12,80
42	8,97	9,67	11,78	12,90	12,56	13,00	12,85
43	8,99	9,70	11,80	12,92	12,58	13,00	12,86
44	9,02	9,73	11,82	12,93	12,59	13,06	12,88
45	9,15	9,81	11,84	12,95	12,68	13,09	12,88
46	9,21	9,97	11,85	12,97	12,76	13,10	12,91
47	9,26	10,01	11,94	13,00	12,80	13,11	12,95
48	9,37	10,02	11,98	13,02	12,83	13,12	12,97
49	9,49	10,03	12,02	13,03	12,95	13,12	13,02
50	9,54	10,08	12,03	13,07	13,02	13,15	13,03
51	9,70	10,28	12,07	13,07	13,07	13,18	13,07
52	9,91	10,44	12,12	13,09	13,09	13,18	13,10
53	10,62	10,48	12,21	13,09	13,14	13,22	13,19
54	10,69	10,56	12,38	13,09	13,23	13,23	13,21
55	10,74	10,66	12,51	13,09	13,29	13,23	13,27
56	10,74	10,69	12,62	13,10	13,32	13,27	13,28
57	10,89	10,84	12,63	13,10	13,33	13,30	13,29
58	10,92	10,89	12,64	13,16	13,35	13,35	13,32
59	10,96	11,13	12,64	13,19	13,41	13,46	13,38
60	10,97	11,24	12,80	13,24	13,43	13,51	13,47
61	11,04	11,39	12,82	13,28	13,45	13,54	13,54
62	11,05	11,43	12,82	13,29	13,48	13,55	13,57
63	11,46	11,55	12,84	13,32	13,51	13,58	13,60
64	11,54	11,59	12,86	13,34	13,59	13,62	13,65
65	11,68	11,59	12,87	13,42	13,60	13,62	13,69
66	11,76	11,65	13,04	13,50	13,60	13,75	13,71
67	11,95	11,77	13,09	13,53	13,62	13,80	13,78
68	12,06	11,87	13,09	13,55	13,64	13,87	13,79
69	12,15	11,94	13,12	13,58	13,69	13,89	13,79
70	12,25	12,01	13,13	13,70	13,70	13,91	13,81
71	12,61	12,06	13,14	13,80	13,70	13,92	13,83
72	12,90	12,09	13,15	13,81	13,75	13,93	13,88
73	12,94	12,13	13,17	13,94	13,77	13,97	13,92
74	13,02	12,16	13,18	13,99	13,84	13,99	13,94
75	13,04	12,39	13,27	13,99	13,90	14,02	13,94
76	13,07	12,41	13,28	14,09	13,97	14,05	13,95
77	13,09	12,41	13,35	14,11	14,09	14,21	13,97
78	13,14	12,45	13,43	14,16	14,10	14,22	13,99
79	13,17	12,59	13,44	14,17	14,14	14,28	13,99
80	13,18	12,65	13,49	14,18	14,14	14,31	14,02
81	13,26	12,76	13,49	14,18	14,16	14,34	14,05
82	13,35	12,80	13,62	14,20	14,26	14,42	14,08
83	13,38	12,96	13,68	14,22	14,27	14,43	14,08
84	13,46	12,96	13,83	14,26	14,35	14,43	14,10
85	13,50	13,07	13,89	14,34	14,35	14,44	14,12

86	13,71	13,16	13,90	14,35	14,49	14,45	14,18
87	13,75	13,21	14,00	14,44	14,62	14,47	14,20
88	13,75	13,23	14,04	14,44	14,64	14,64	14,25
89	13,85	13,27	14,12	14,47	14,66	14,71	14,32
90	13,98	13,35	14,14	14,51	14,76	14,72	14,33
91	13,99	13,44	14,22	14,53	14,77	14,74	14,41
92	14,19	13,46	14,31	14,54	14,77	14,79	14,42
93	14,26	13,56	14,59	14,67	14,79	14,79	14,44
94	14,53	13,68	14,66	14,75	14,82	14,79	14,86
95	14,63	13,74	14,72	14,76	15,07	14,93	14,97
96	14,67	13,84	14,75	14,81	15,09	14,94	15,02
97	14,87	13,91	14,84	15,00	15,14	15,20	15,08
98	15,21	14,18	14,98	15,33	15,32	15,28	15,12
99	15,43	14,31	15,17	15,60	15,45	15,48	15,25
100	16,18	14,35	15,46	15,87	15,86	16,64	15,34
Scores							
C1	2,082	1,756	0,626	-0,726	-0,070	-0,791	-0,655
C2	0,293	-0,648	-0,059	0,414	0,886	1,034	0,576
C. pelagicus							
Min	5,65	5,63	5,34	6,83	5,18	7,32	5,89
Max	9,91	10,08	9,76	7,86	8,53	7,32	9,11
Mean	*8,03*	*8,13*	*7,74*	*9,02*	*7,40*	*9,46*	*8,81*
Median	*7,83*	*8,07*	*7,53*	*9,02*	*7,16*	*9,46*	*9,08*
C. braarudii							
Min	10,62	10,44	10,30	10,17	10,34	9,46	10,38
Max	16,18	14,35	15,46	15,87	15,86	16,64	15,34
Mean	*12,87*	*12,37*	*12,76*	*13,09*	*13,18*	*13,25*	*13,09*
Median	*13,08*	*12,41*	*12,85*	*13,08*	*13,33*	*13,18*	*13,15*

CHAPTER 4

EOT and Miocene – effects of reducing number of samples, reducing time resolution, and focusing only on disturbed periods

Abstract

IMMA was applied to two sets of samples covering the Eocene-Oligocene Transition (EOT) and Miocene Climatic Optimum and its transition, searching for answers to the questions surrounding *C. pelagicus* s.l. adaptations and responses to Cenozoic climate evolution. The method was able to produce morphometric data that is coherent with current knowledge on *C. pelagicus* s.l. morphometry. However due to low-resolution and short number of samples no morphological plasticity was observed in the two sets of samples, besides the general variations that are obtained by simple arithmetic data, like average, minimum, maximum and median. In the case of EOT the time interval prevented to extract more information from PCA since this was entirely within the climatic event and related deterioration. To look for answers regarding *C. pelagicus* s.l. morphological plasticity and morphometric response to the climate variations of these (or other) time intervals, it is necessary to obtain more samples in order to increase time resolution.

Keywords: Eocene-Oligocene Transition; Miocene; *C. pelagicus* s.l.; Morphometry; IMMA; Morphological plasticity

4.1 Introduction

In the path to uncover answers regarding *C. pelagicus* s.l. evolution and plasticity throughout the Cenozoic, two extremely important time intervals were selected for samples: 1) the Eocene-Oligocene transition (EOT), which represents a period of major global environmental and biotic changes, both in the oceanic and continental records (Zachos et al., 2001; Héran et al., 2010; Cotton e Pearson, 2011), marking the beginning of the continental glaciations in Antarctica; 2) the Miocene, particularly the Miocene Optimum Climate and its transition during the Middle Miocene, period of global warming followed by global cooling, which culminated with the beginning of seasonal Arctic ice sheets formation (see Prista et al., 2015).

Around 40Ma the Middle Eocene Optimum Climate occurred, with subtropical diatoms expanding towards higher latitudes and eutrophization phenomena occurring in Antarctic waters (Witkowski et al., 2012). After this climatic event, a cooling trend took place, with an increase of 3.0‰ in $\delta^{18}O$ from the Middle Eocene until the Lower Oligocene. The increase of 1.8‰ in $\delta^{18}O$ until the Late Eocene reflects a cooling of the deep ocean water in ~7ºC, which means a drop from 12.5ºC to 4.5ºC. Later, the continuous change in $\delta^{18}O$ reflects a combined effect of ice volume increase and temperature cooling, particularly in the short event of 1.0‰ increase in $\delta^{18}O$ at 34Ma (Zachos et al., 2001, 2008).

The EOT represents a very important period since a marked global cooling, with major eustatic variations, was felt globally. The oceans suffered a global temperature drop of 2.5°C (Héran et al., 2010), followed by an increase in marine productivity (Roth-Nebelsick et al., 2004), and sea level dropped nearly 20m (Houben et al., 2012).

A high abundance of *C. pelagicus* s.l. has often been considered as indicative for warm-to-temperate temperatures (e.g. Wei & Wise, 1990; Persico & Villa, 2004; Villa et al., 2008). In the modern oceans, *C. pelagicus* s.l. seems to be restricted to cool-temperate waters and high-nutrient conditions (e.g. Cachão & Moita, 2000; Boeckel et al., 2006), but during the Palaeogene it was cosmopolitan (Haq & Lohmann, 1976). This apparent contradiction in the interpretation of *C. pelagicus* s.l. comes from the fact that this species occurred from tropical to higher latitudes since the Palaeogene.

Over the Cenozoic, *C. pelagicus* s.l. evolved and adapted to a cooling world, changing from dominant at low-mid latitudes up until the Oligocene, to dominant in high northern latitudes from the Miocene onwards (Haq et al., 1977; Haq, 1980).

Looking at the EOT should give clues about the adaptation strategy taken by *C. pelagicus* s.l. as a response to the global cooling trend.

To bring the puzzle together, the Miocene should give insights into why *C. pelagicus* s.l. didn't return to its dominance in low-mid latitudes, despite the global warming felt during the Early and Middle Miocene, which, to some extent, brought the world back to its Late Eocene patterns (see Prista et al., 2015). Was the evolution of *C. pelagicus* s.l. to cooler environments a consequence of adaptation to climate change, or from pressure of new and better adapted phytoplankton species, more effective in competing for resources? Or could it be that the main oceanographic pattern that characterizes *C. pelagicus* s.l. is the nutrient content rather than temperature? If so, could there have been a change in the palaeoceanographic conditions, with low-mid latitude oceans becoming more oligotrophic, forcing *C. pelagicus* s.l. towards higher latitudes and richer waters?

IMMA was applied to EOT and Miocene samples searching for answers to the questions surrounding *C. pelagicus* s.l. adaptations and responses to Cenozoic climate evolution. Three main goals were defined for this work: 1) see if the IMMA method developed for Quaternary samples is applicable to other Cenozoic larger time intervals, namely the EOT and the Miocene; 2) test its usefullness on low resolution samples, since high resolution in older sediments is seldom possible; 3) look for *C. pelagicus* s.l. plasticity across the EOT and the Miocene.

4.2 Materials and Methodology

EOT samples were prepared from the ODP site 1263, leg 208, located at Walvis Ridge, Atlantic Southeast (Fig. 4.1), with a mean resolution of approximately 16.88ka (see age model in Annex-4), from 34.4Ma to 33.5Ma, courtesy of Professor Jorjintje Henderiks from Uppsala University. A total of 40 samples were prepared following the "drop" technique method described in Bordiga et al. (2015).

Figure 4.1 - Location of site ODP1263 (map from Google Earth©).

Miocene samples were prepared from DSDP site 369A, located at the Canary Islands archipelago, Atlantic Northeast (Fig. 4.2), with a mean resolution of 120ka, although most samples have a resolution of 90ka, covering from NN4 to NN7 (see age model and biostratigraphy notes in Annex-4), courtesy of Professor Giuliana Villa from Parma University. A total of 38 samples were prepared using the smear slide technique described in Backman & Shackleton (1983).

Figure 4.2 – Location of site DSDP369A (map from Google Earth©).

The total of 78 samples were studied for *C. pelagicus* s.l. morphometry using a petrographic microscope Zeiss Ortholux II Pol-BK with polarizing light and magnification × 1250. For morphometry, 100 placoliths were randomly selected throughout the slide of each sample, and their maximum diameters (length) measured. An incorporated camera Olympus DP21 was used to perform the measurements.

The morphometric data analysis was performed using Integrated Multivariate Morphon Analysis (IMMA) as detailed in Section II – Chapter 2.

4.3 Results

4.3.1 – EOT

PCA results from IMMA applied to EOT data extracted a total of 62.1% of the variance in the first two components, with 50.2% in C1 and 11.9% in C2. PCA loadings gave two morphotypes in each of the first two components: C1 with a small [5.5; 8.3[µm ($_{S}C1_{EOT}$) and a large [9.4; 19.8[µm ($_{L}C1_{EOT}$); C2 with [8.1; 9.3[µm ($_{S}C2_{EOT}$) and [10.4; 12.8[µm ($_{L}C2_{EOT}$) (Fig. 4.3).

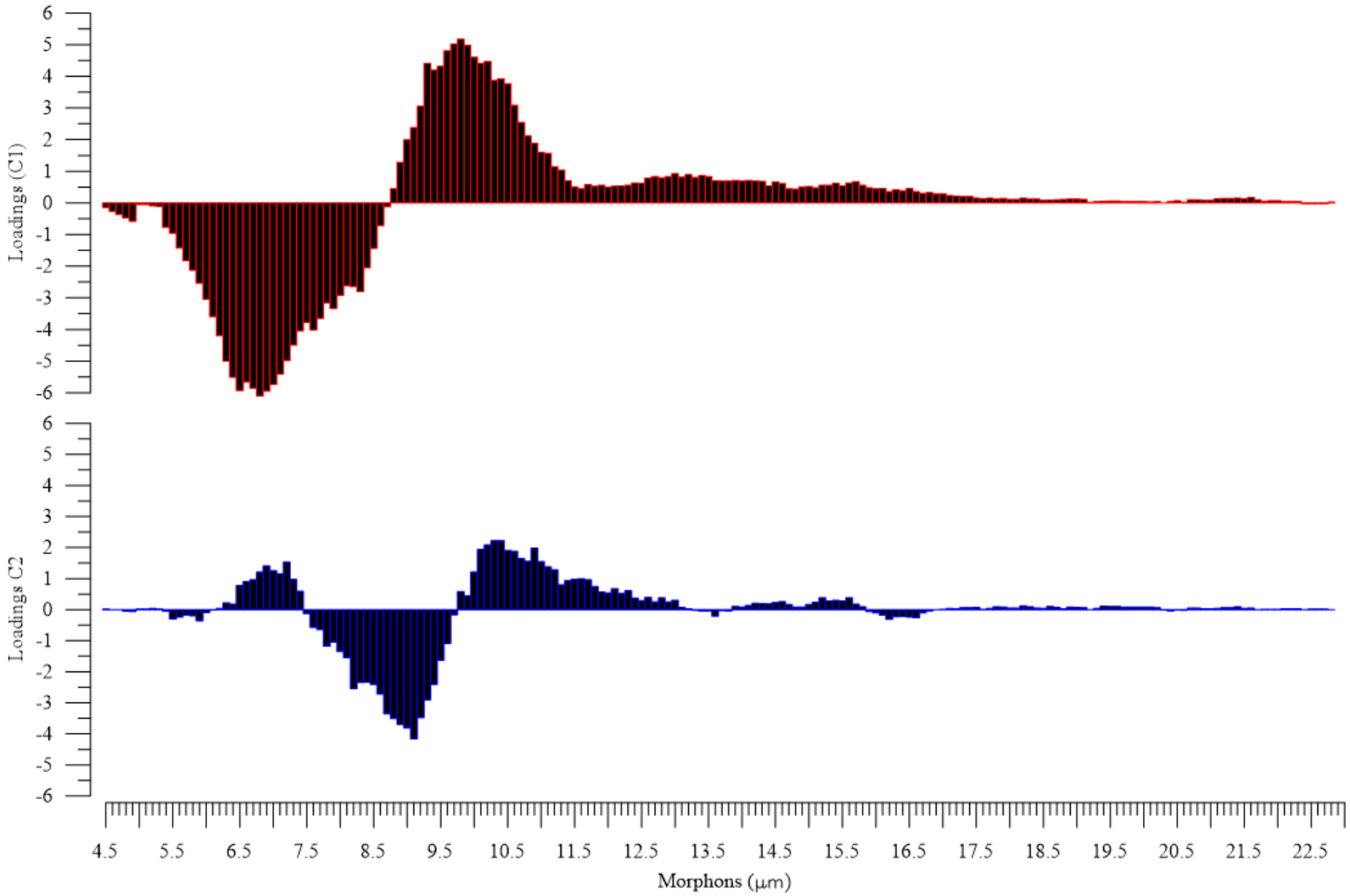

Figure 4.3 – PCA loadings for component one (red bars) and component two (blue bars) in EOT ODP1263.

Morphotypes counting's and C1 scores show a very good correlation, -0.96 for $_{S}C1_{EOT}$ and 0.93 for $_{L}C1_{EOT}$. The smaller morphotype is dominant is the first 22 samples, with only three exceptions where the large morphotype as a slight dominance. Then for 15 samples the larger morphotype dominates, and finally in the last three samples the small one is dominant again. Regarding C2 the small morphotype identified presents a good correlation with C2 scores (-0.80). However the larger morphotype has a week correlation with the C2 scores, only 0.48. A clear alternation between morphotypes is observed throughout the samples (Fig. 4.4 – Tables A4-1 and A4-2 in Annex-4).

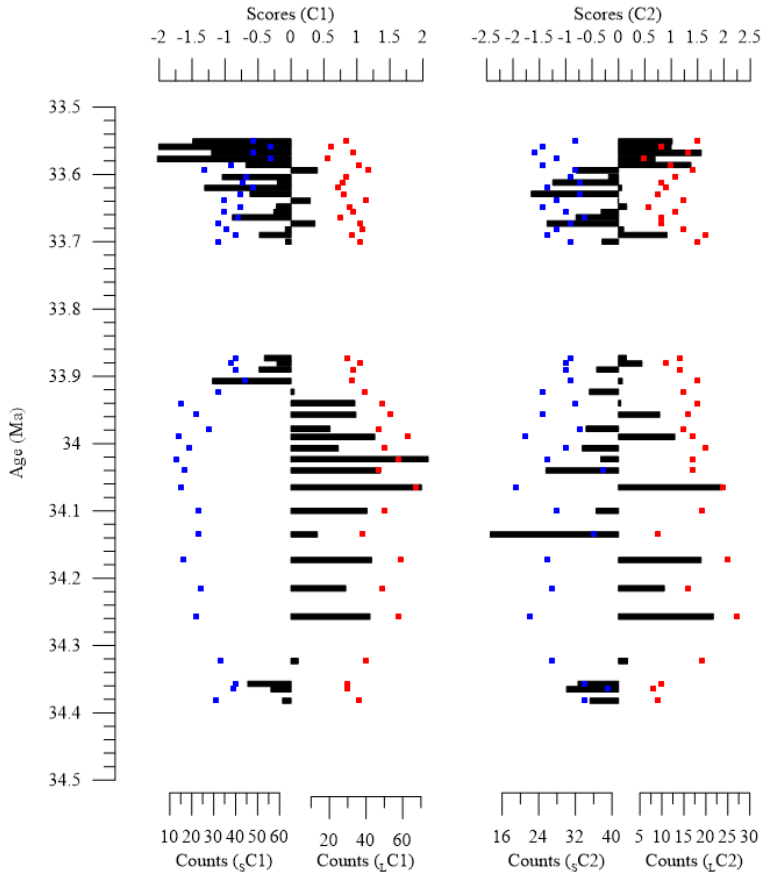

Figure 4.4 – C1 and C2 scores (black bars) and morphotypes counting's (red dots for larger morphotype and blue dots for smaller morphotype) in EOT ODP 1263.

4.3.2 – Miocene

PCA results from IMMA applied to Miocene data extracted a total of 69.9% of the variance in the first two components, with 49.9% in C1 and 20.0% in C2. C1 shows two morphotypes, a small [5.1; 6.9[µm ($_{S}C1_{MIO}$) and a large [8.0; 14.5[µm ($_{L}C1_{MIO}$), while C2 defines [6.9; 8.5[µm ($_{S}C2_{MIO}$) and [9.6; 14.5[µm ($_{L}C2_{MIO}$) (Fig. 4.5).

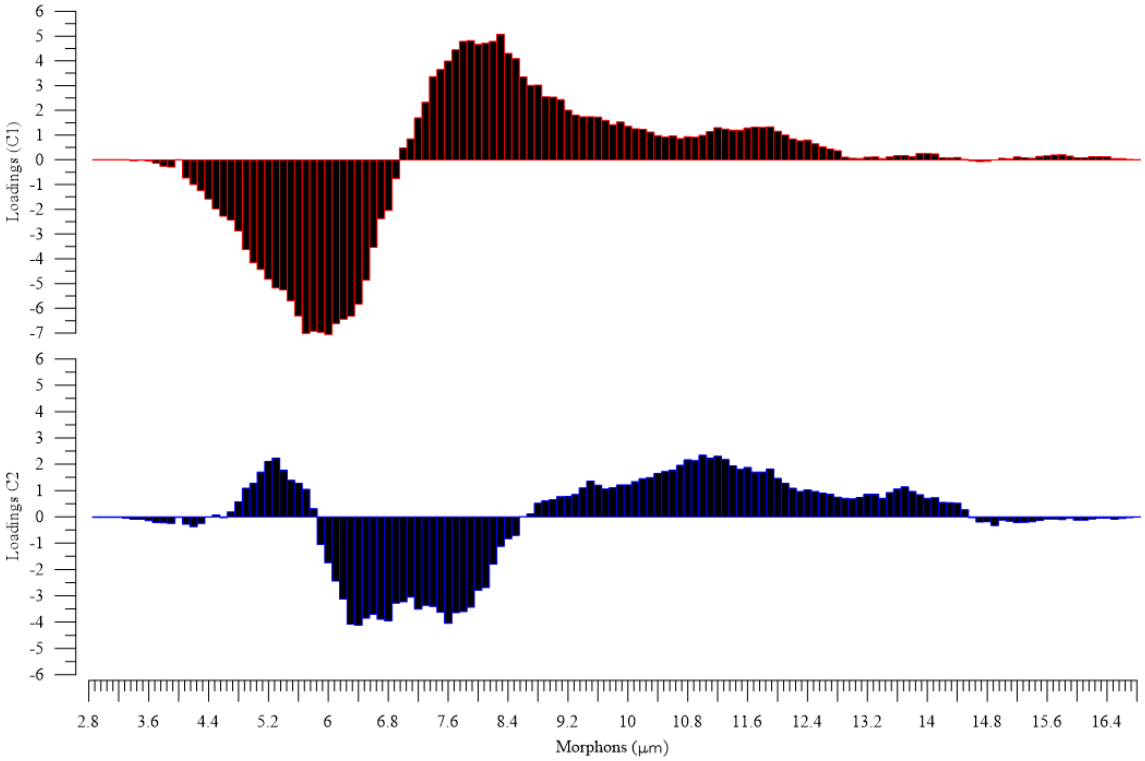

Figure 4.5 – PCA loadings for component one (red bars) and component two (blue bars) in Miocene DSDP369A.

Morphotypes counting's and C1 scores show a very good correlation, -0.98 for $_{S}C1_{MIO}$ and 0.90 for $_{L}C1_{MIO}$. No morphotype clearly dominates the set of samples, with 47.4% (18) of the samples dominated by the small and 52.6% (20) dominated by the large morphotype. Regarding C2, morphotypes counting's and scores show a good correlation of -0.84 for $_{S}C2_{MIO}$ and 0.76 for $_{L}C2_{MIO}$. Here the smaller form has a slight dominance, with 57.9% (22) of the samples (Fig. 4.6 – Tables A4-3 and A4-4 in Annex-4).

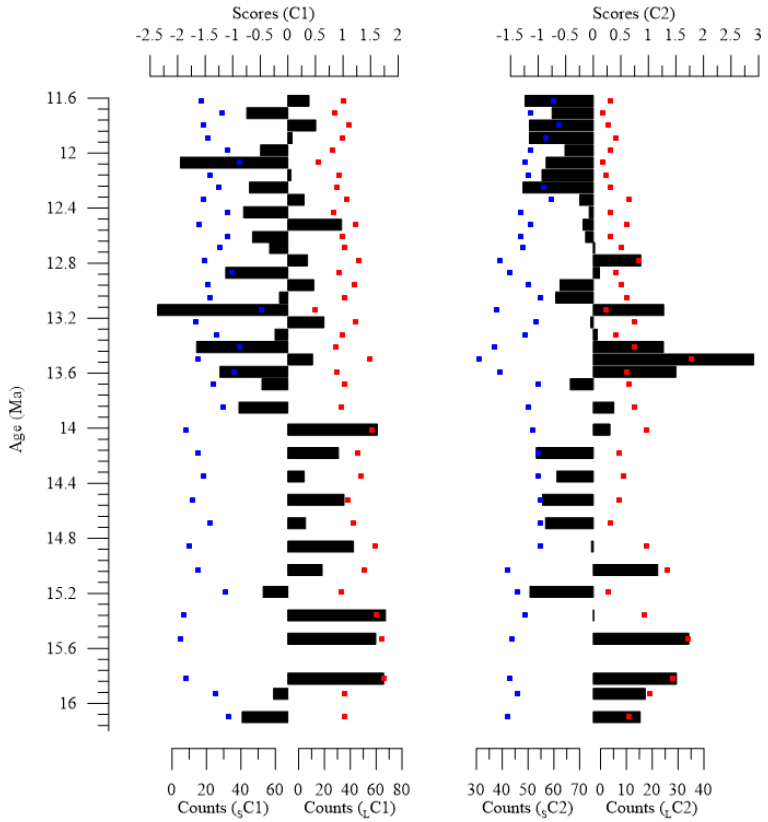

Figure 4.6 – C1 and C2 scores (black bars) and morphotypes counting's (red dots for larger morphotype and blue dots for smaller morphotype) in Miocene DSDP 369A.

4.4 Discussion

4.4.1 – EOT morphometry

IMMA applied to EOT data describes the presence of two morphotypes, a small up to 8.3µm and a larger one from 9.4µm to 19.8µm. Although the correlations with scores are high, it seems that information is being lost by the low number of samples and lower resolution, when compared to the Quaternary data.

Analysing the samples characteristics, minimum, maximum, average and median, higher values in the four parameters tend to occur with C1 positive (Table 4.1), i.e., when the large morphotype is active. However it is hard to extract the information in C2. The smaller morphotype defined by C2, [8.1; 9,3[µm, has a good correlation and it could signify plasticity of the small morphotype defined in C1, but it shows no apparent relation with the morphometric data and has zero relation with samples parameters (see Table 4.2).

Table 4.1 – Samples parameters (minimum, maximum, average and median) and C1 scores for EOT ODP1263 (color scale: blue – lower to red highest values).

Samples	Min	Max	Mean	Median	C1 scores
B-5H-1 55-56	5,22	13,30	8,60	8,35	-1,490
A-10H-7 10-11	6,10	14,80	8,29	8,01	-2,005
A-10H-6 140-141	5,78	14,60	8,76	8,39	-1,203
A-10H-6 100-101	5,10	22,30	8,57	8,00	-2,026
A-10H-6 75-76	5,86	21,90	9,17	8,60	-0,683
A-10H-6 50-51	6,06	22,00	9,63	9,11	0,401
A-10H-6 27-28	5,64	19,80	8,81	8,49	-1,042
A-10H-6 6-7	5,90	16,40	8,71	8,68	-0,207
A-10H-5 131-132	5,60	20,60	8,78	8,48	-1,308
A-10H-5 120-121	5,55	12,70	8,57	8,74	-0,621
A-10H-5 110-11	5,46	13,30	8,87	8,94	0,293
A-10H-5 100101	5,41	11,70	8,39	8,57	-0,219
A-10H-5 95-96	5,80	20,20	8,89	8,84	-0,260
A-10H-5 80-81	6,01	16,30	8,66	8,58	-0,888
A-10H-5 70-71	5,72	16,60	9,04	9,09	0,362
A-10H-5 60-61	5,38	14,40	8,88	8,85	-0,086
A-10H-5 50-51	5,57	12,40	8,66	8,84	-0,478
A-10H-5 40-41	5,69	21,00	9,32	8,99	-0,080
A-10H-5 30-31	5,34	21,10	9,04	8,88	-0,402
A-10H-5 20-21	5,96	19,00	9,13	8,95	-0,211
A-10H-5 11-12	5,63	13,60	8,77	8,75	-0,483
A-10H-5 0-1	5,52	21,10	9,16	8,45	-1,189
A-10H-4 141-142	5,50	20,20	9,60	9,15	0,047
A-10H-4 130-131	5,76	22,40	10,15	9,60	0,970
A-10H-4 120-121	6,42	20,40	10,03	9,65	0,984
A-10H-4 110-111	5,76	20,60	9,69	9,23	0,591
A-10H-4 100-101	5,73	21,20	10,71	9,98	1,272
A-10H-4 90-91	6,49	18,40	9,83	9,40	0,718
A-10H-4 81-82	7,38	21,90	10,37	9,71	2,081
A-10H-4 71-72	6,66	15,30	9,54	9,29	1,351
A-10H-4 60-61	6,97	21,20	10,32	9,89	1,979
A-10H-4 49-50	6,93	21,60	9,90	9,45	1,155
A-10H-4 40-41	6,99	18,10	9,82	9,14	0,399
A-10H-4 31-32	6,38	21,00	10,40	9,96	1,223
A-10H-4 2021	6,38	19,90	10,03	9,50	0,831
A-10H-4 10-11	5,88	15,70	9,76	9,69	1,199
A-10H-4 0-1	5,56	18,50	9,31	9,02	0,108
A-10H-3 140-141	5,48	20,70	8,80	8,66	-0,654
A-10H-3 130-131	5,36	21,20	9,03	8,66	-0,303
A-10H-3 120-121	5,86	21,10	9,25	8,83	-0,127

Table 4.2 – Correlations between samples parameters and PCA components scores in EOT ODP1263.

	C1	**C2**
Minimum	0,67	-0,07
Maximum	0,26	0,04
Average	**0,86**	0,16
Median	**0,95**	0,13

Moreover, looking at the histograms of selected samples (Fig. 4.7) it is possible to observe size variation for the dominant morphon along the samples, varying from morphon 7 to morphon 9, suggesting a size variation as a response to environmental variations. It is also clear that the very large coccoliths present very low abundance and that are little related to the lower sized and more abundant ones.

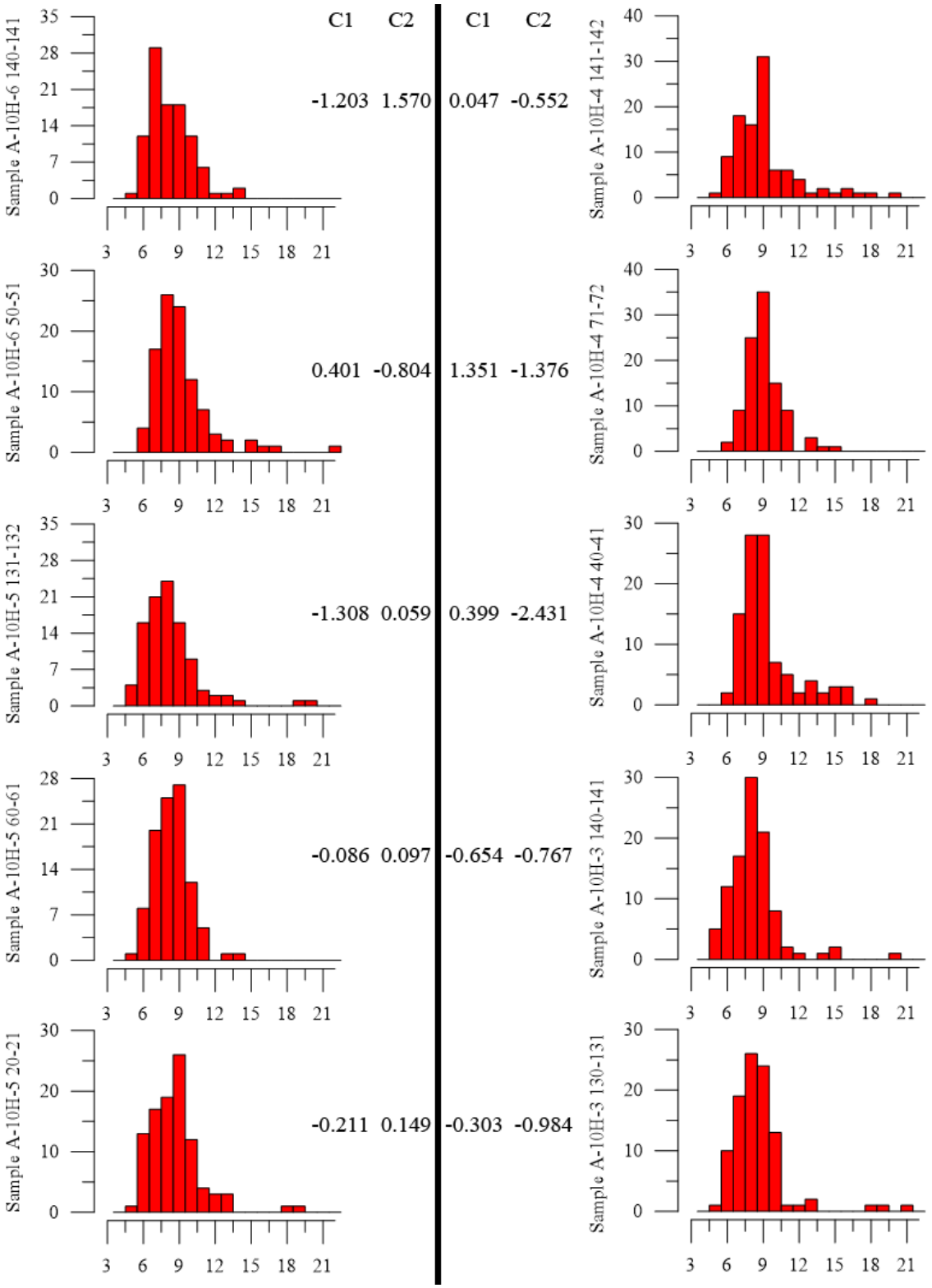

Figure 4.7 – Histograms and components one and two scores for selected samples from EOT ODP1263.

Despite the strong correlations between components scores and counting's, it is easily perceived from the histograms that PCA scores are not so easy to use to predict the morphometric characteristics of a sample. In fact, the histogram with all samples (Fig.

4.8) suggests a normal distribution with a long tale towards very large coccoliths, centred in morphons 8 and 9.

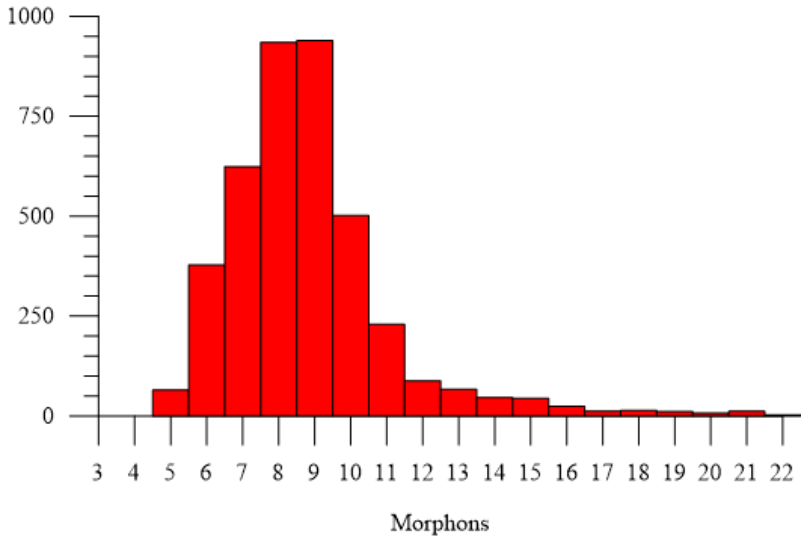

Figure 4.8 – All samples from EOT ODP1263 histogram.

The data analysis strengthens the idea that there is just not enough data on this 40 samples to better separate the morphotypes and observe size variations. The samples number and resolution is one possible reason for these results, but the fact that this set comprises from 34.38Ma to 33.55Ma should also be considered, since it means that the set of samples is entirely within a highly disturbed interval. Several perturbations and, consequently responses/variations in *C. pelagicus* s.l., occurred during this interval, meaning that it is highly likely that rapid and numerous variations may have occurred during this period.

IMMA has proven to work with theoretical samples and with high-resolution samples of the Quaternary, thus pointing to some type of deficiency with the morphometric data. Three aspects raise attention: 1) number of samples; 2) time resolution; 3) interval covered.

The number of samples is significantly lower than the ones studied for the Quaternary sites. For the EOT a total of 40 samples were analysed, while in the Quaternary 117 in GeoB5559-2 and 98 in MD95-2040. So it is possible that this number of samples, although meeting the standards needed for a PCA (number of samples superior to number of morphons), may not be sufficient to reveal and extract the information on *C. pelagicus* s.l. during this agitated period.

The time resolution, although good for Palaeogene studies, is very low when trying to observe morphological changes/responses to climate variation in a species with such a short generation time. Quaternary samples had a resolution near 2ka. EOT samples have a mean resolution of ~17ka, with a set of 21 samples with ~8ka resolution. So at best the resolution is four times lower when compared to Quaternary samples.

Finally the interval covered. Climate deterioration begun by the end of the Eocene, with progressive cooling and major drop in the ocean deep waters temperature (Zachos et al., 2001, 2008). The transition from Eocene to Oligocene intensified the climatic deterioration, with impacts on marine productivity (Roth-Nebelsick et al., 2004) and sea level (Houben et al., 2012). The first continental glaciation of Antarctica (Oi1) finally took place at 33.55Ma (Miller et al., 2009). The 40 EOT samples cover from 34.38Ma to 33.55Ma, which means they cover around 800ka within the period of climatic deterioration and oscillations.

Morphometric responses were probably frequent during this period, which means that 8ka between samples is a huge interval to account for the morphometric variations. Moreover, since the samples start after the beginning of the event, and end at the culmination of the continental glaciation, there is no information on *C. pelagicus* s.l. before the EOT or after the Oi1. This results in the absence of information about from and to what *C. pelagicus* s.l. evolved morphometrically.

The causes for the difficulties with EOT interpretation are, most likely, all three issues mentioned: short number of samples, low resolution and all samples within the climatic event. When they are all put together, it explains the lack of sufficient morphometric information to characterize *C. pelagicus* s.l. behaviour and adaptations during this crucial time interval of the Cenozoic.

Since it was not possible to increase the number of samples, either by expanding the time period covered or by increasing the resolution, it was tested if increasing the number of measurements per sample would increase morphometric information extraction with the PCA. Another 100 measurements were performed in each slide by an independent researcher. The results (see Annex-4 in the end of this chapter) show that in this case increasing the number of measurements does not improve the PCA extraction. Correlations between counting's and scores, although high in two morphotypes defined, were lower than the ones obtained with only 100 measurements. This analysis suggests that, besides the minimum number of measurements per sample

to have analysable data, there is a maximum number of measurements from which there is no information increment.

Although IMMA failed to retrieve information regarding morphological plasticity, it seems that in C1 two morphotypes were roughly defined, according to the strong correlation found between C1 and morphotypes counting's, as well as the strong relation between C1 scores and median and average of the samples (see Fig. 4.9). Thus, two morphotypes could have been present at this site during the EOT, a smaller morphotype under 10µm and a larger one over 10µm. An overlapping region would be possible in morphon 9.

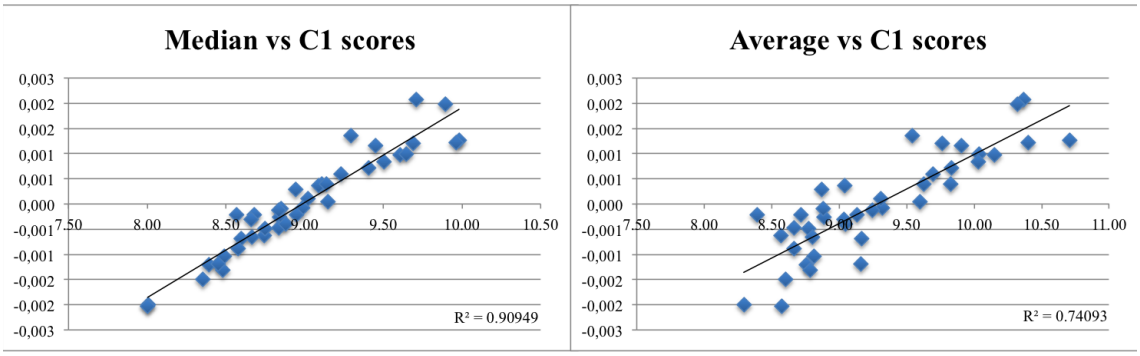

Figure 4.9 – Median and average *vs* C1 scores in EOT ODP1263. r^2 is the squared correlation coeficient.

However this simplification of IMMA information does not fit well with all data. First of all it either neglects very large placoliths or puts them into the larger morphotype, which would give to this morphotype a very wide morphometric spectrum, from 9µm to more than 20µm. Secondly, the low resolution and low number of samples preclude any attempt to extract information from size variability, generating significant leaps in morphometric information. This makes the opposition between these two morphotypes look like the *C. pelagicus* – *C. braarudii* opposition. However there is no data to support any interpretation of that kind. Finally, the global histogram of the samples does suggest that there are some large coccoliths that should belong to a specific morphotype or, less probable, represent a morphometric response from the larger morphotype. Also, looking at individual samples histograms, size variability is observable. For these reasons it seems that IMMA failed in extracting reliable information from this EOT site set of samples.

This IMMA underachievement opened a very interesting opportunity to test if IMMA can actually detect morphotype limits variations over time, while trying to generate a

clearer picture of this EOT time interval. IMMA was applied together with MMA to stacks of 20 samples of the EOT. Stack 1 from 34.38 to 33.89 Ma (B-5H-1 55-56 to A-10H-5 20-21); Stack 2 from 34.04 to 33.64 (A-10H5 110-111 to A-10H-4 71-72); Stack 3 from 33.88 to 33.55 Ma (A-10H-5 11-12 to A-10H-3 120-121) (Fig. 4.10)

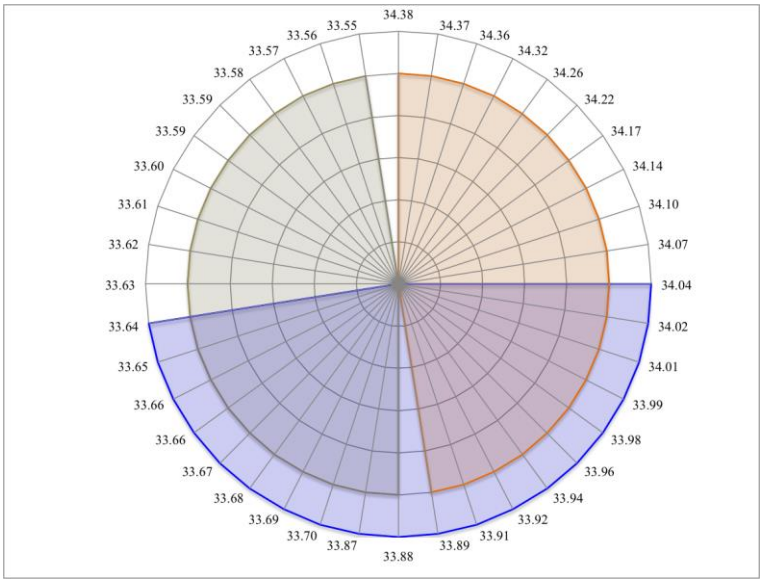

Figure 4.10 – Sample stacks distribution. Stack 1 orange (34.38 to 33.89 Ma); Stack 2 blue (33.64 to 33.04 Ma) and Stack 3 brown (33.88 to 33.55Ma)

The IMMA analysis of Stack 1 showed the presence of two morphotypes, a smaller [6.6; 7.9[µm and a larger [8.2; 10.7[µm, while MMA shows significance of a smaller morphotype [6.0; 7.0[µm and a larger [9.0; 10.0[µm (Fig. 4.11). For Stack 2 IMMA defined two morphotypes, a smaller [5.5; 8.1[µm and a larger [9.2; 10.9[µm, and gave a possible third morphotype with weaker significance, [13.0; 18.9[µm. MMA also expanded the smaller morphotype to [6.0; 8.0[µm but kept the larger morphotype [9.0; 10.0[µm (Fig. 4.12). Applied to Stack 3 IMMA continues to expand the interval of the smaller morphotype to [5.4; 8.5[µm and defines the larger morphotype as [9.6; 18.0[µm, although PCA loadings suggest a possible separation of the larger morphotype around morphon 12 µm. With MMA the morphotypes where kept as 5 to 8 µm and 9 to 10 µm (Fig. 4.13).

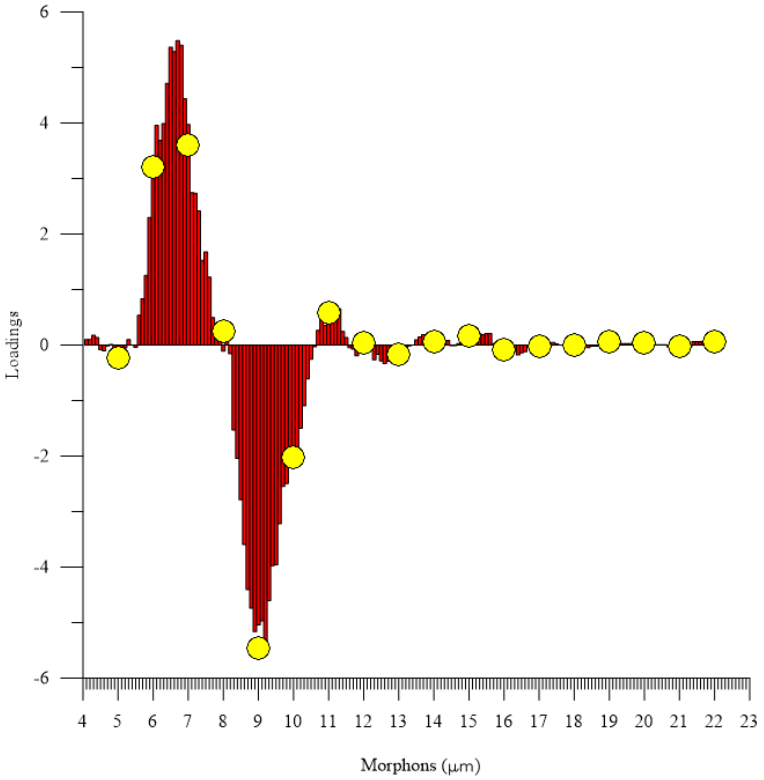

Figure 4.11 – IMMA loadings (red bars) and MMA loadings (yellow circles) for Stack 1 of EOT ODP1263.

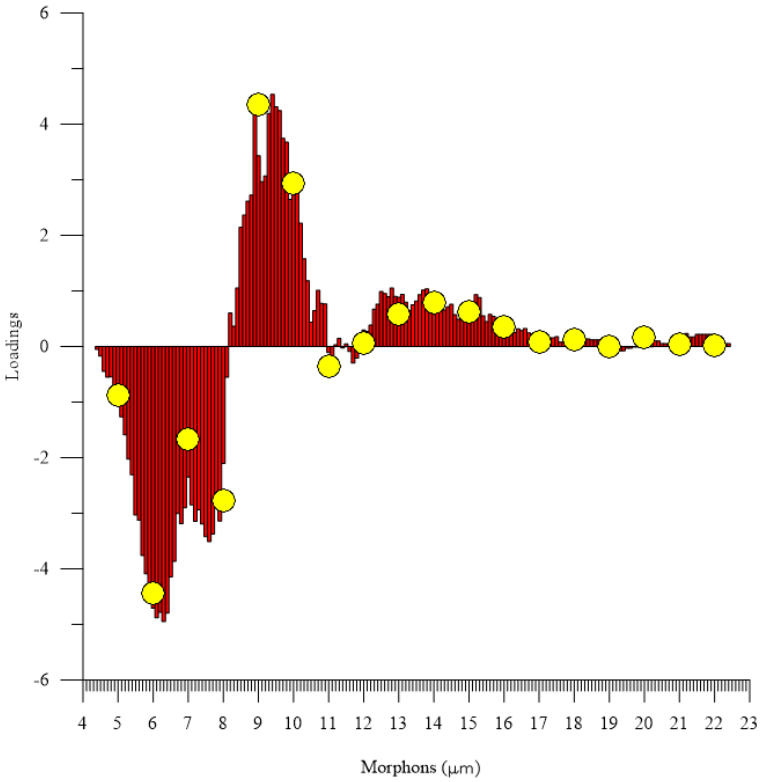

Figure 4.12 – IMMA loadings (red bars) and MMA loadings (yellow circles) for Stack 2 of EOT ODP1263.

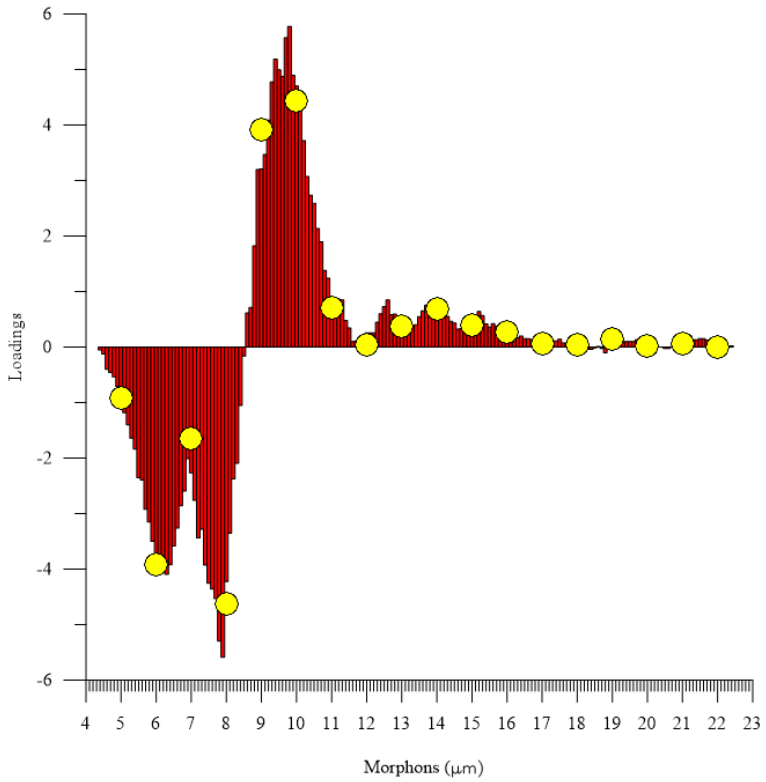

Figure 4.13 – IMMA loadings (red bars) and MMA loadings (yellow circles) for Stack 3 of EOT ODP1263.

The results obtained by slicing the dataset into three (in this case equal sized) overlapping sets show on one side that IMMA can track morphotype changes over time, something that MMA can't, but also strengthen the previous hypothesis that the high perturbations of this time interval, together with the resolution of these samples, are preventing IMMA from extracting more accurate morphometric information.

The stack analysis shows that the larger sizes tend to gain significance towards the first continental glaciation event on Antarctica (33.55 Ma – Oi1), however this observation is an illusion created by the time series analysed. There is a gap in the dataset from 33.87 Ma to 33.70 Ma (170ka), marking two apparent very distinct periods. From 34.38 Ma to 33.87 Ma samples have a mean resolution of ~24ka and the average size of the coccoliths are mostly in morphon 8 with a few samples in morphon 9, showing an increasing trend. The size peak between 34.3 and 34.2 Ma suggests that changes in the palaeoceanographic conditions may have occurred during this interval (Fig. 4.14). From 33.70 Ma to 33.55 Ma (mean resolution of 8.78ka) average jumps to morphons 9 and 10, with steady oscillations in size until near the Oi1 (Fig. 4.15).

Neither IMMA or MMA can be applied to these two distinct sets of the EOT since the second set, 33.70 – 33.55 Ma, has only 18 samples, which equals the number of morphons.

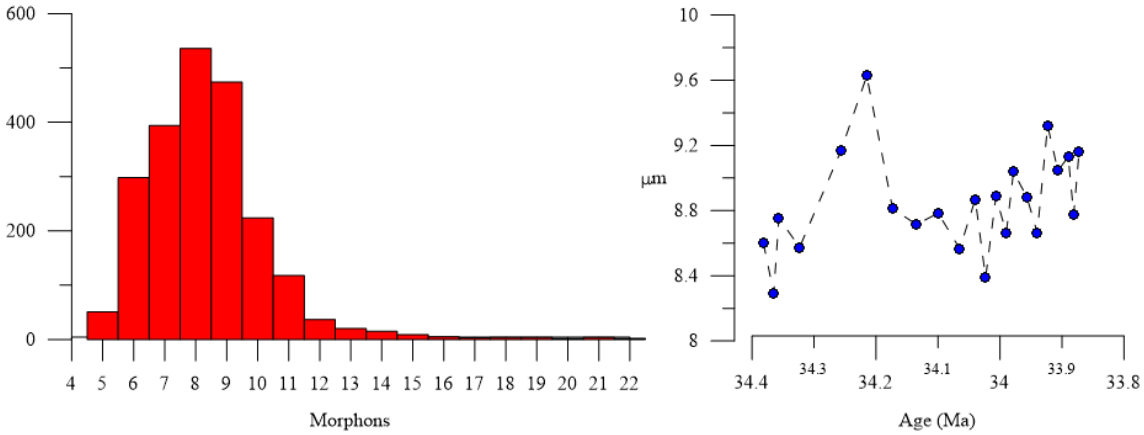

Figure 4.14 – Histogram and coccolith size average for the first EOT set 34.38-33.87 Ma.

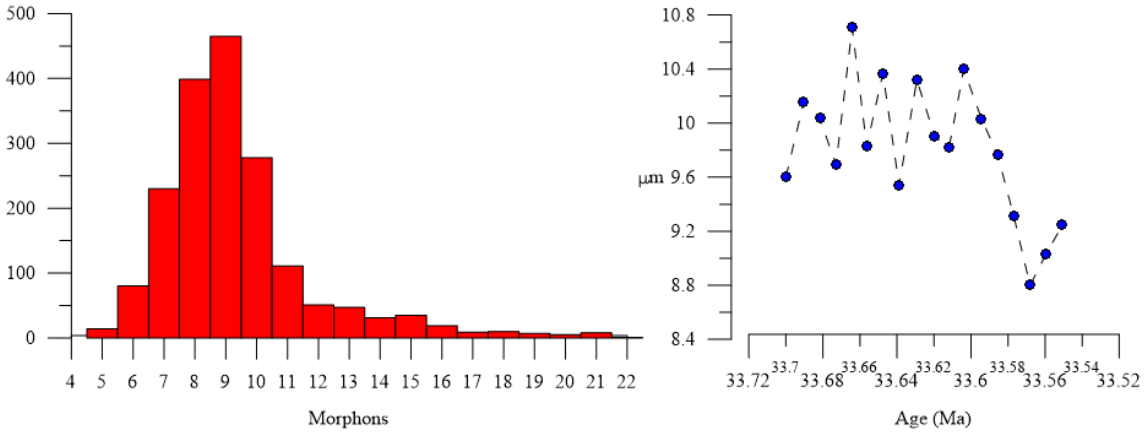

Figure 4.15 – Histogram and coccolith size average for the second EOT set 33.70-33.55 Ma.

4.4.2 – Miocene morphometry

Morphometry on this set of samples presents an even bigger challenge because of its low time resolution. With a mean time resolution of ~120ka, and with the best set of samples with 90ka resolution, the leap between samples makes it nearly impossible to look for microevolution in *C. pelagicus* s.l.. However, despite this significant limitation, morphotypes identified show a very good correlation with PCA scores.

IMMA clearly identifies the presence of two morphotypes: a small one, dominant in more recent samples, and a larger one that dominates oldest samples. This agrees well

with samples parameters (see Table 4.3) and the relation found between C1 scores and median, and to some extent, average of the samples (Fig. 4.16).

Table 4.3 – Samples parameters (minimum, maximum, average and median) and C1 scores for Miocene DSDP369A

Age (Ma)	Samples	C1	Min	Max	Average	Median
11,62	A-2_1-48-49	0,383	4,55	15,80	7,76	7,66
11,71	A-2_2-48-49	-0,744	4,30	16,10	7,53	7,30
11,80	A-2_3-48-49	0,506	5,14	12,70	7,76	7,63
11,89	A-2_4-48-49	0,077	5,10	15,60	8,10	7,79
11,98	A-2_5-48-49	-0,495	4,52	14,40	7,43	7,53
12,07	A-2_6-48-49	-1,947	4,68	15,50	7,23	7,10
12,16	A-3_1-48-49	0,053	3,87	16,50	7,63	7,56
12,25	A-3_2-48-49	-0,695	4,90	14,90	7,64	7,37
12,34	A-3_3-48-49	0,294	5,07	16,80	8,12	7,71
12,43	A-3_4-48-49	-0,801	4,32	16,70	7,43	7,30
12,52	A-3_5-48-49	0,975	4,89	16,40	8,51	8,00
12,61	A-3_6-48-49	-0,642	4,98	14,70	7,66	7,44
12,69	A-4_1-48-49	-0,330	4,74	14,60	7,80	7,67
12,78	A-4_2-48-49	0,356	5,60	14,60	8,66	8,01
12,87	A-4_3-48-49	-1,126	5,35	15,00	7,77	7,37
12,96	A-4_4-48-49	0,470	5,48	15,60	8,04	7,81
13,05	A-4_5-48-49	-0,153	5,79	15,40	8,15	7,71
13,14	A-5_1-48-49	-2,362	4,75	15,10	6,90	6,69
13,23	A-5_2-48-49	0,653	4,43	14,50	8,21	7,82
13,32	A-5_3-48-49	-0,232	5,06	15,70	7,97	7,62
13,41	A-5_4-48-49	-1,655	5,24	15,60	7,79	7,16
13,50	A-5_5-48-49	0,448	5,21	15,93	9,63	8,81
13,59	A-5_6-48-49	-1,231	5,03	13,70	7,60	7,29
13,68	A-6_1-48-49	-0,469	5,20	14,10	7,96	7,49
13,85	A-6_3-48-49	-0,886	5,19	13,50	7,84	7,43
14,01	A-6_5-48-49	1,623	5,94	14,40	8,58	8,28
14,18	A-7_1-48-49	0,917	5,56	14,90	8,19	7,85
14,35	A-7_3-48-49	0,296	5,53	14,20	8,08	7,79
14,52	A-7_5-48-49	1,019	5,85	16,70	8,55	7,86
14,69	A-8_1-48-49	0,318	5,90	15,50	8,01	7,78
14,86	A-8_3-48-49	1,190	5,68	13,50	8,47	8,19
15,03	A-8_5-48-49	0,623	6,11	13,80	8,73	8,01
15,19	A-9_1-48-49	-0,447	5,53	13,20	7,65	7,46
15,36	A-9_3-48-49	1,771	5,43	14,20	8,70	8,33
15,53	A-9_5-48-49	1,594	6,04	14,10	9,03	8,61
15,82	A-10_1-70-71	1,739	5,68	16,40	9,07	8,46
15,93	A-10_3-48-49	-0,260	5,64	14,10	8,21	7,67
16,10	A-10_5-48-49	-0,829	5,08	15,00	7,91	7,52

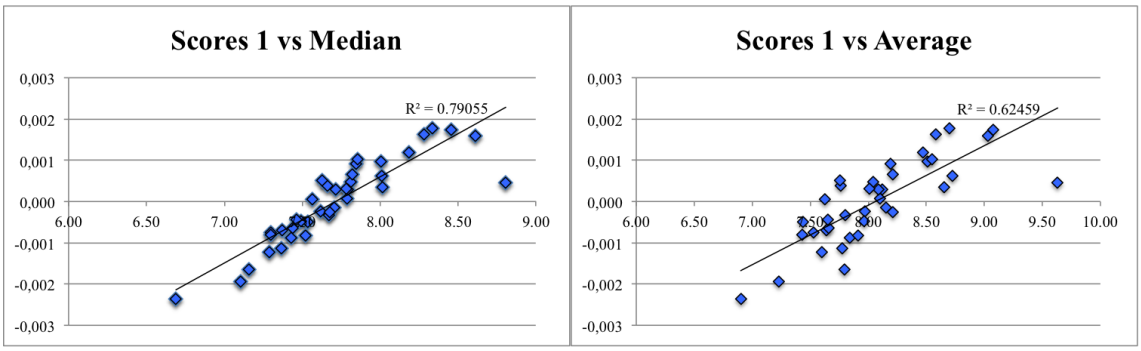

Figure 4.16 – Sactter plot of the relation between C1 scores and median and average of *C. pelagicus* s.l. coccolith lenght in Miocene DSDP 369A.

But looking at the previous table and observing the samples histograms (Fig. 4.17), it is clear that a lot of information is missing for an accurate PCA extraction. Histograms suggest a possible morphometric characterization similar to the Quaternary, with a smaller morphotype up to ~10µm and a larger morphotype over ~11µm, but largely dominated in this case by the smaller form. The counting's of the morphotypes found by IMMA also point to holes in morphometric information. C1 defines two morphotypes, however neither is clearly dominant in any sample (exception of four samples – A-10_1-70-71; A-9_5-48-49; A-9_3-48-49; A-6_5-48-49 – in which the large morphotype clearly dominates) regardless of the C1 score.

When counting's of C1 and C2 are compared (Fig. 4.6 and Table A4.5) we see a permanent dominance of the lower morphotype in C2, [6.9; 8.5[µm (except for sample A-5_5 48-49), which is totally independent of which morphotype is active in C1. This means that the dominant morphon should be morphon 7, which is confirmed by the histograms.

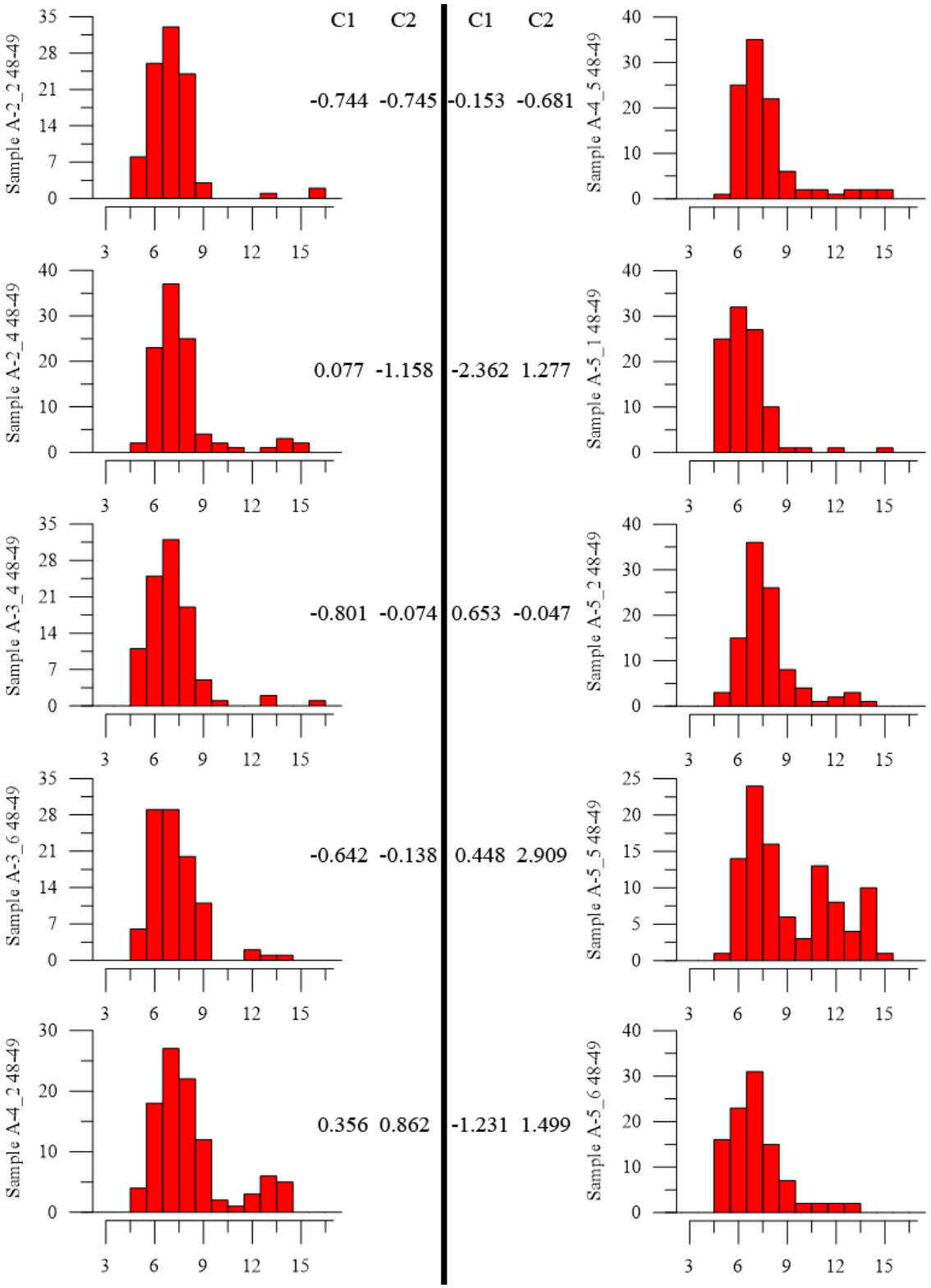

Figure 4.17 – Histograms and components one and two scores for selected samples from Miocene DSDP369A.

Size variability, or morphological plasticity, is not possible to observe in this set of samples most likely due to a very low time resolution. Leaps of 100ka between samples only allow a general characterization of *C. pelagicus* s.l. during this time interval. Thus,

the observation of microvariations in *C. pelagicus* s.l. morphometric parameter for this set of Miocene samples is, sadly, not possible. *C. pelagicus* s.l. presents sizes between 4μm and 16μm (Fig. 4.18), showing a progressive reduction in size, from the oldest samples with a median around morphon 8, to a median in morphon 7 in the more recent samples.

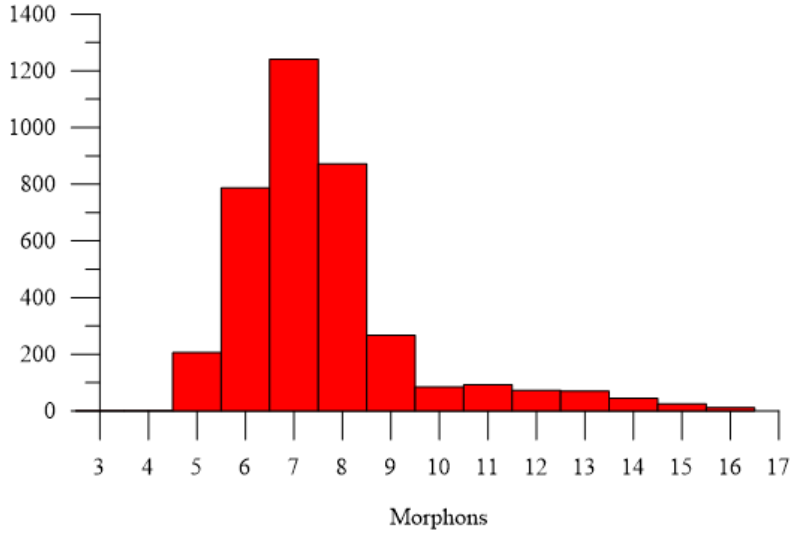

Figure 4.18 – Global histogram of DSDP 369A.

The global histogram of this set of samples confirms the dominance of morphon 7 (and 8), although it does not show how it evolved from the former to the first. It is also useful to support the idea that information is being lost with the presence of coccoliths up to morphon 16. Together with individual samples histograms, it is possible to observe that there is size variability and probably two morphotypes in this site during this period, although neither PCA or histograms are able to extract it.

The size of *C. pelagicus* s.l. in this site is consistent with high primary productivity waters, possibly with a progressive increase in the nutrient content and availability during the Miocene Climatic Optimum transition, which started at 14.8Ma (see Prista et al., 2015), and being concomitant with the drop in *C. pelagicus* s.l. median from morphon 8 to morphon 7. This hypothesis is supported by Lancelot et al. (1977), where the Middle Miocene is classified as one of the highest primary productivity periods, together with Middle Oligocene and Pleistocene, at this site.

4.5 Conclusions

Three main goals were set for this work: 1) see if the method developed for Quaternary samples was applicable to other Cenozoic larger time intervals, namely the EOT and the Miocene; 2) to see the impact of low resolution samples; 3) look for *C. pelagicus* s.l. plasticity across the EOT and the Miocene.

Respecting the first goal it is clear that IMMA can be applied to other periods of the Cenozoic. The method was able to produce morphometric data that is coherent with current knowledge on *C. pelagicus* s.l. morphometry. Moreover IMMA demonstrated to be able to detect microvariations in coccolith size through the samples set by slicing it in to smaller stacks of samples, as shown with EOT samples.

As for the impact of low-resolution samples, the findings are evident. Since the aim of IMMA is to extract morphological plasticity, i.e., morphometric variations as a response to environmental patterns, and because coccolithophores have short generation time, temporal resolution of the samples plays a major role for this methodology. For IMMA to be able to extract this type of information it is fundamental that the set of samples have high temporal resolution. However, when morphometric responses are gradual or have a cyclic behaviour, even with short generation time species, IMMA can detect these microvariations and even morphological plasticity, as seen with DSDP608, MD90-2040 and GeoB5559-2 (Chapter 3).

Also the number of samples and the time interval they cover is important. Increasing the number of samples is useful, most of all because it can increase resolution. But it is also very important, since it is impossible to obtain samples with a resolution compatible with coccolithophores life cycle/generation time, for the set of samples to cover a period before climate deterioration and another period after the climatic event. This enables the morphometric characterization of the species before it was forced to respond/adapt and to what it has evolved to.

For the reasons above, no morphological plasticity was observed in the two sets of samples, besides the general variations that are obtained by simple arithmetic data, like average, minimum, maximum and median. To look for answers regarding *C. pelagicus* s.l. morphological plasticity and morphometric response to the climate variations of these (or others) time intervals, it is necessary to obtain more samples in order to increase temporal resolution. By the experience with Quaternary samples, it seems that

resolution up to 2.5-3.0ka could be the maximum value for IMMA to produce valuable results regarding morphological plasticity.

References

Backman, J., Shackleton, N.J., 1983. Quantitative biochronology of Pliocene and early Pleistocene calcareous nannofossils from the Atlantic, Indian and Pacific oceans. Mar. Micropaleontol. 8, 141–170. doi:10.1016/0377-8398(83)90009-9

Backman, J., Raffi, I., Rio, D., Fornaciari, E., Pälike, H., 2012. Biozonation and biochronology of Miocene through Pleistocene calcareous nannofossils from low and middle latitudes. Newsletters Stratigr. 45, 221–244. doi:10.1127/0078-0421/2012/0022

Boeckel, B., Baumann, K.-H., Henrich, R., Kinkel, H., 2006. Coccolith distribution patterns in South Atlantic and Southern Ocean surface sediments in relation to environmental gradients. Deep Sea Res. Part I Oceanogr. Res. Pap. 53, 1073–1099. doi:10.1016/j.dsr.2005.11.006

Bordiga, M., Bartol, M., Henderiks, J., 2015. Absolute nannofossil abundance estimates: Quantifying the pros and cons of different techniques. Rev. Micropaleontol. 58, 155–165. doi:10.1016/j.revmic.2015.05.002

Cachão, M., Moita, M.T., 2000. Coccolithus pelagicus, a productivity proxy related to moderate fronts off Western Iberia. Mar. Micropaleontol. 39, 131–155.

Cotton, L.J., Pearson, P.N., 2011. Extinction of larger benthic foraminifera at the Eocene/Oligocene boundary. Palaeogeogr. Palaeoclimatol. Palaeoecol. 311, 281–296. doi:10.1016/j.palaeo.2011.09.008

Haq, B.U., 1980. Biogeographic history of Miocene calcareous nannoplankton and paleoceanography of the Atlantic Ocean. Micropaleontology 26, 414–443.

Haq, B.U., Lohmann, G.P., 1976. Early Cenozoic calcareous nannoplankton biogeography of the Atlantic Ocean. Mar. Micropaleontol. 1, 119–194. doi:10.1016/0377-8398(76)90008-6

Haq, B.U., Lohmann, G.P., Wise, S.W., 1977. Calcareous nannoplankton biogeography and its paleoclimatic implications: Cenozoic of the Falkland Plateau (DSDP Leg 36) and Miocene of the Atlantic Ocean. Mar. Micropaleontol. 1, 119–194. doi:10.2973/dsdp.proc.36.114.1977

Héran, M.-A., Lécuyer, C., Legendre, S., 2010. Cenozoic long-term terrestrial climatic evolution in Germany tracked by δ18O of rodent tooth phosphate. Palaeogeogr. Palaeoclimatol. Palaeoecol. 285, 331–342. doi:10.1016/j.palaeo.2009.11.030

Houben, A.J.P., van Mourik, C. a., Montanari, A., Coccioni, R., Brinkhuis, H., 2012. The Eocene–Oligocene transition: Changes in sea level, temperature or both? Palaeogeogr. Palaeoclimatol. Palaeoecol. 335–336, 75–83. doi:10.1016/j.palaeo.2011.04.008

Lancelot, Y., Seibold, E., Cepek, P., Dean, W.E., Eremeev, V., Gardner, J., Jansa, L.F., Johnson, D., Krasheninnikov, V., Pflaumann, U., Rankig, J.G., Trabant, P., Bukry, D., Herring, J. (1977). Site 369; continental slope off Cape Bojador, Spanish Sahara. Initial Reports of the Deep Sea Drilling Project, Vol. 41, p.327-420. doi:10.2973/dsdp.proc.41.105.1978

Miller, K.G., Wright, J.D., Katz, M.E., Wade, B.S., Browning, J. V, Cramer, B.S., Rosenthal, Y., 2009. Climate threshold at the Eocene-Oligocene transition: Antarctic ice sheet influence on ocean circulation, in: Koeberl, C., Montanari, A. (Eds.), The Late Eocene Earth - Hothouse, Icehouse, and Impacts. Geological Society of America Special Paper 452, pp. 169–178. doi:10.1130/2009.2452(11).

Persico, D., Villa, G., 2004. Eocene–Oligocene calcareous nannofossils from Maud Rise and Kerguelen Plateau (Antarctica): paleoecological and paleoceanographic implications. Mar. Micropaleontol. 52, 153–179. doi:10.1016/j.marmicro.2004.05.002

Prista, G.A., Agostinho, R.J., Cachão, M.A., 2015. Observing the past to better understand the future: a synthesis of the Neogene climate in Europe and its perspectives on present climate change. Open Geosci. 7, 65–83. doi:10.1515/geo-2015-0007

Roth-nebelsick, A., Utescher, T., Mosbrugger, V., Diester-Haass, L., Walther, H., 2004. Changes in atmospheric CO_2 concentrations and climate from the Late Eocene to Early Miocene : palaeobotanical reconstruction based on fossil floras from Saxony , Germany. Palaeogeogr. Palaeoclimatol. Palaeoecol. 205, 43–67. doi:10.1016/j.palaeo.2003.11.014

Villa, G., Fioroni, C., Pea, L., Bohaty, S., Persico, D., 2008. Middle Eocene–late Oligocene climate variability: Calcareous nannofossil response at Kerguelen Plateau, Site 748. Mar. Micropaleontol. 69, 173–192. doi:10.1016/j.marmicro.2008.07.006

Wei, W., Wise, S.W., 1990. Biogeographic gradients of middle Eocene-Oligocene calcareous nannoplankton in the South Atlantic Ocean. Palaeogeogr. Palaeoclimatol. Palaeoecol. 79, 29–61.

Witkowski, J., Bohaty, S.M., Mccartney, K., Harwood, D.M., 2012. Enhanced siliceous plankton productivity in response to middle Eocene warming at Southern Ocean ODP Sites 748 and 749. Palaeogeogr. Palaeoclimatol. Palaeoecol. 326–328, 78–94. doi:10.1016/j.palaeo.2012.02.006

Zachos, J., Pagani, M., Sloan, L., Thomas, E., Billups, K., 2001. Trends, rhythms, and aberrations in global climate 65 Ma to present. Science 292, 686–93. doi:10.1126/science.1059412

Zachos, J.C., Dickens, G.R., Zeebe, R.E., 2008. An early Cenozoic perspective on greenhouse warming and carbon-cycle dynamics. Nature 451, 279–83. doi:10.1038/nature06588

Annex-4

Data for figures 4.3 and 4.5

Table A4-1 – IMMA component 1 (C1) scores (negative scores in blue and positive scores in orange) and morphotype counts for all samples in ODP1263 for EOT.

Samples	$sC1_{EOT}$	$lC1_{EOT}$	C1	Samples	$sC1_{EOT}$	$lC1_{EOT}$	C1
B-5H-1 55-56	48	29	-1.490	A-10H-5 11-12	40	33	-0.483
A-10H-7 10-11	56	21	-2.005	A-10H-5 0-1	44	32	-1.189
A-10H-6 140-141	48	33	-1.203	A-10H-4 141-142	32	39	0.047
A-10H-6 100-101	56	19	-2.026	A-10H-4 130-131	15	49	0.970
A-10H-6 75-76	38	36	-0.683	A-10H-4 120-121	22	53	0.984
A-10H-6 50-51	26	41	0.401	A-10H-4 110-111	28	47	0.591
A-10H-6 27-28	45	29	-1.042	A-10H-4 100-101	14	63	1.272
A-10H-6 6-7	43	27	-0.207	A-10H-4 90-91	19	50	0.718
A-10H-5 131-132	48	25	-1.308	A-10H-4 81-82	13	58	2.081
A-10H-5 120-121	42	28	-0.621	A-10H-4 71-72	17	47	1.351
A-10H-5 110-11	35	40	0.293	A-10H-4 60-61	15	67	1.979
A-10H-5 100-101	42	31	-0.219	A-10H-4 49-50	23	50	1.155
A-10H-5 95-96	35	33	-0.260	A-10H-4 40-41	23	38	0.399
A-10H-5 80-81	41	26	-0.888	A-10H-4 31-32	16	59	1.223
A-10H-5 70-71	32	37	0.362	A-10H-4 20-21	24	49	0.831
A-10H-5 60-61	36	38	-0.086	A-10H-4 10-11	22	58	1.199
A-10H-5 50-51	40	32	-0.478	A-10H-4 0-1	33	40	0.108
A-10H-5 40-41	32	37	-0.080	A-10H-3 140-141	40	30	-0.654
A-10H-5 30-31	40	30	-0.402	A-10H-3 130-131	39	30	-0.303
A-10H-5 20-21	38	37	-0.211	A-10H-3 120-121	31	36	-0.127

Table A4-2 – IMMA component 2 (C2) scores (negative scores in blue and positive scores in orange) and morphotype counts for all samples in ODP1263 for EOT.

Samples	$sC2_{EOT}$	$lC2_{EOT}$	C2	Samples	$sC2_{EOT}$	$lC2_{EOT}$	C2
B-5H-1 55-56	32	18	1.018	A-10H-5 11-12	30	14	-0.412
A-10H-7 10-11	25	10	0.999	A-10H-5 0-1	31	18	0.072
A-10H-6 140-141	23	16	1.570	A-10H-4 141-142	25	15	-0.552
A-10H-6 100-101	28	6	0.693	A-10H-4 130-131	32	18	0.043
A-10H-6 75-76	25	12	1.372	A-10H-4 120-121	25	16	0.781
A-10H-6 50-51	32	17	-0.804	A-10H-4 110-111	33	15	-0.615
A-10H-6 27-28	31	13	-0.188	A-10H-4 100-101	21	17	1.067
A-10H-6 6-7	33	10	-1.245	A-10H-4 90-91	30	20	-0.687
A-10H-5 131-132	26	11	0.059	A-10H-4 81-82	26	17	-0.336
A-10H-5 120-121	33	9	-1.653	A-10H-4 71-72	38	17	-1.376
A-10H-5 110-11	28	15	-0.008	A-10H-4 60-61	19	24	1.975

A-10H-5 100-101	25	7	0.154	**A-10H-4 49-50**	28	19	-0.424
A-10H-5 95-96	30	13	-0.327	**A-10H-4 40-41**	36	9	-2.431
A-10H-5 80-81	34	10	-0.805	**A-10H-4 31-32**	26	25	1.567
A-10H-5 70-71	31	10	-1.352	**A-10H-4 20-21**	27	16	0.868
A-10H-5 60-61	28	15	0.097	**A-10H-4 10-11**	22	27	1.798
A-10H-5 50-51	26	20	0.919	**A-10H-4 0-1**	27	19	0.171
A-10H-5 40-41	31	18	-0.310	**A-10H-3 140-141**	34	10	-0.767
A-10H-5 30-31	31	14	0.149	**A-10H-3 130-131**	39	8	-0.984
A-10H-5 20-21	30	11	0.444	**A-10H-3 120-121**	34	9	-0.539

Table A4-3 – IMMA component 1 (C1) scores (negative scores in blue and positive scores in orange) and morphotype counts for all samples in DSDP369A for Miocene.

Samples	sC1MIO	lC1MIO	C1	Samples	sC1MIO	lC1MIO	C1
A-2_1-48-49	17	35	0.383	A-5_3-48-49	26	34	-0.232
A-2_2-48-49	29	28	-0.744	A-5_4-48-49	39	29	-1.655
A-2_3-48-49	18	39	0.506	A-5_5-48-49	15	55	0.448
A-2_4-48-49	21	34	0.077	A-5_6-48-49	36	30	-1.231
A-2_5-48-49	32	26	-0.495	A-6_1-48-49	24	36	-0.469
A-2_6-48-49	39	15	-1.947	A-6_3-48-49	30	33	-0.886
A-3_1-48-49	22	31	0.053	A-6_5-48-49	8	57	1.623
A-3_2-48-49	27	30	-0.695	A-7_1-48-49	15	46	0.917
A-3_3-48-49	18	37	0.294	A-7_3-48-49	18	48	0.296
A-3_4-48-49	32	27	-0.801	A-7_5-48-49	12	38	1.019
A-3_5-48-49	16	44	0.975	A-8_1-48-49	22	42	0.318
A-3_6-48-49	32	34	-0.642	A-8_3-48-49	10	59	1.190
A-4_1-48-49	28	36	-0.330	A-8_5-48-49	15	51	0.623
A-4_2-48-49	19	47	0.356	A-9_1-48-49	31	33	-0.447
A-4_3-48-49	35	31	-1.126	A-9_3-48-49	7	60	1.771
A-4_4-48-49	21	43	0.470	A-9_5-48-49	5	64	1.594
A-4_5-48-49	22	36	-0.153	A-10_1-70-71	8	66	1.739
A-5_1-48-49	52	13	-2.362	A-10_3-48-49	25	36	-0.260
A-5_2-48-49	14	44	0.653	A-10_5-48-49	33	36	-0.829

Table A4-4 – IMMA component 2 (C2) scores (negative scores in blue and positive scores in orange) and morphotype counts for all samples in DSDP369A for Miocene.

Samples	sC2MIO	lC2MIO	C2	Samples	sC2MIO	lC2MIO	C2
A-2_1-48-49	60	4	-1.237	A-5_3-48-49	49	6	0.072
A-2_2-48-49	51	1	-0.745	A-5_4-48-49	37	13	1.272
A-2_3-48-49	62	3	-1.158	A-5_5-48-49	31	35	2.909
A-2_4-48-49	57	6	-1.158	A-5_6-48-49	39	10	1.499
A-2_5-48-49	51	4	-0.512	A-6_1-48-49	54	11	-0.416
A-2_6-48-49	49	1	-0.856	A-6_3-48-49	50	13	0.373
A-3_1-48-49	50	2	-0.930	A-6_5-48-49	52	18	0.302
A-3_2-48-49	56	4	-1.275	A-7_1-48-49	54	7	-1.033

A-3_3-48-49	59	11	-0.246	A-7_3-48-49	54	9	-0.660
A-3_4-48-49	47	4	-0.074	A-7_5-48-49	55	7	-0.921
A-3_5-48-49	51	10	-0.186	A-8_1-48-49	55	4	-0.865
A-3_6-48-49	47	4	-0.138	A-8_3-48-49	55	18	-0.031
A-4_1-48-49	48	8	0.025	A-8_5-48-49	42	26	1.168
A-4_2-48-49	39	15	0.862	A-9_1-48-49	46	3	-1.149
A-4_3-48-49	43	6	0.113	A-9_3-48-49	49	17	0.011
A-4_4-48-49	50	8	-0.602	A-9_5-48-49	44	34	1.734
A-4_5-48-49	55	10	-0.681	A-10_1-70-71	43	28	1.508
A-5_1-48-49	38	2	1.277	A-10_3-48-49	46	19	0.944
A-5_2-48-49	53	13	-0.047	A-10_5-48-49	42	11	0.851

Table A4.5 – Counting's and scores of both components and respective morphotypes in Miocene DSDP369A.

$_{s}C1_{MIO}$	$_{L}C1_{MIO}$	C1	$_{s}C2_{MIO}$	$_{L}C2_{MIO}$	C2
5,1 - 6,9	**8 - 14,5**	**scores**	**6,9 - 8,5**	**9,6 - 14,5**	**scores**
17	35	0,383	60	4	-1,237
29	28	-0,744	51	1	-0,745
18	39	0,506	62	3	-1,158
21	34	0,077	57	6	-1,158
32	26	-0,495	51	4	-0,512
39	15	-1,947	49	1	-0,856
22	31	0,053	50	2	-0,930
27	30	-0,695	56	4	-1,275
18	37	0,294	59	11	-0,246
32	27	-0,801	47	4	-0,074
16	44	0,975	51	10	-0,186
32	34	-0,642	47	4	-0,138
28	36	-0,330	48	8	0,025
19	47	0,356	39	15	0,862
35	31	-1,126	43	6	0,113
21	43	0,470	50	8	-0,602
22	36	-0,153	55	10	-0,681
52	13	-2,362	38	2	1,277
14	44	0,653	53	13	-0,047
26	34	-0,232	49	6	0,072
39	29	-1,655	37	13	1,272
15	55	0,448	31	35	2,909
36	30	-1,231	39	10	1,499
24	36	-0,469	54	11	-0,416
30	33	-0,886	50	13	0,373
8	57	1,623	52	18	0,302
15	46	0,917	54	7	-1,033
18	48	0,296	54	9	-0,660
12	38	1,019	55	7	-0,921

22	42	0,318	55	4	-0,865
10	59	1,190	55	18	-0,031
15	51	0,623	42	26	1,168
31	33	-0,447	46	3	-1,149
7	60	1,771	49	17	0,011
5	64	1,594	44	34	1,734
8	66	1,739	43	28	1,508
25	36	-0,260	46	19	0,944
33	36	-0,829	42	11	0,851

Biostratigraphy and Age Model of Miocene site DSDP369A

Following Backman et al. (2012)

SAMPLE 10-5 48-49

Species	Observations	Nanno Zone
Sphenolithus heteromorphus	Common	NN4-NN5
Sphenolithus moriformis	A few specimens	Lower Eocene-NN10
Cyclacargolithus floridanus	Common	Palaeogene-NN7
Coccolithus pelagicus	Common. The common larger forms are below 14µm	Cenozoic
Calcidiscus premacintyrei	A few specimens	NN4-NN6
Discoaster petaliformis	Probably not abundant but present	NN4-NN5
Discoaster deflandrei	More or less common	Palaeogene-NN7
Helicosphaera intermedia	Both common, together with other *Helicosphaera* forms	NP21-NN12
Helicosphaera ampliaperta		NN2-NN4

Sample 10-5 is within NN4 zone. *S. heteromorphus* marks the base of NN4 (17.75Ma) and *H. ampliaperta* marks the top of NN4 (14.86Ma). The present of both species limits the sediments to NN4. The other species found are in agreement with the placing of this sample in NN4.

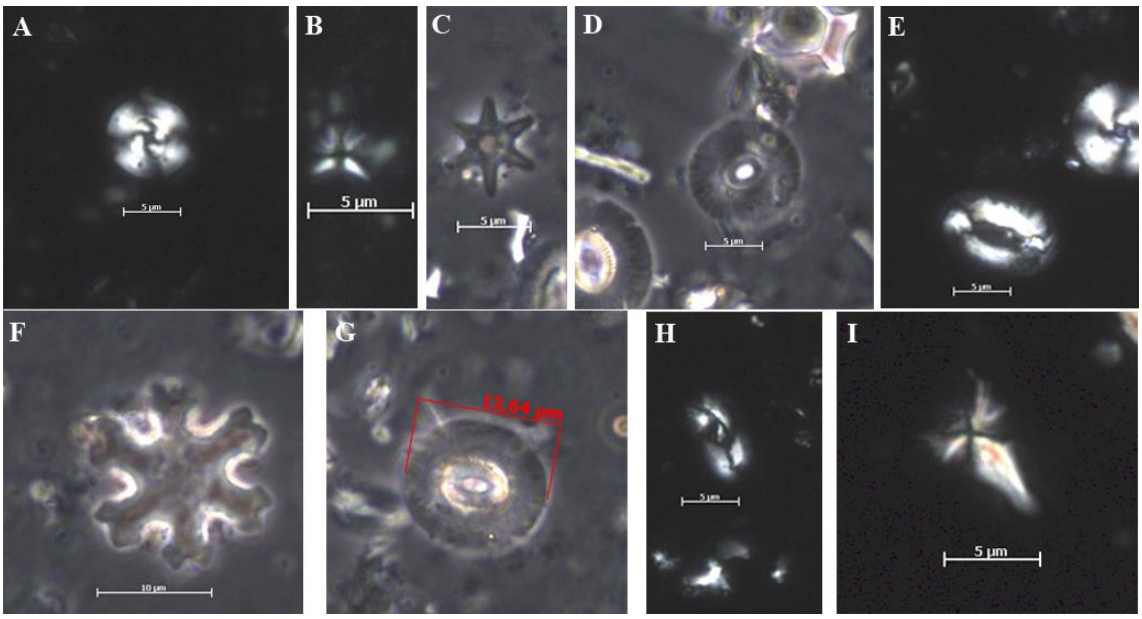

Figure A4-1 – A) *Cyclacargolithus floridanus*; B) *Sphenolithus moriformis*; C) *Discoaster petaliformis*; D) *Calcidiscus premacintyrei*; E) *Helicosphaera ampliaperta*; F) *Discoaster deflandrei*; G) *Cocclithus pelagicus*; H) *Helicosphaera intermedia*; I) *Sphenolithus heteromorphus*

SAMPLE 9-3 48-49

Species	Observations	Nanno Zone
Sphenolithus heteromorphus	Common	NN4-NN5
Helicosphaera ampliaperta	Common	NN2-NN4
Discoaster signus	Relatively common	NN4-NN5

Sample 9-3 is within NN4 zone. *S. heteromorphus* marks the base of NN4 (17.75Ma) and *H. ampliaperta* marks the top of NN4 (14.86Ma). The present of both species limits the sediments to NN4. *D. signus* appears at 15.73Ma, in the upper part of NN4.

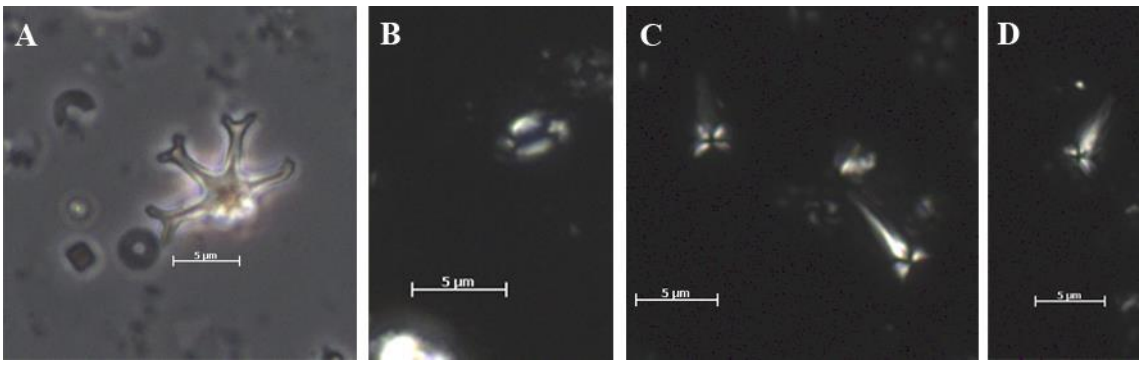

Figure A4-2 – A) *Discoaster signus*; B) *Helicosphaera ampliaperta*; C and D) *Sphenolithus heteromorphus*.

SAMPLE 5-5 48-49

Species	Observations	Nanno Zone
Sphenolithus heteromorphus	Common	NN4-NN5
Discoaster exilis	Common	NN4-NN9

Sample 5-5 is within NN5 zone. *S. heteromorphus* marks the base of NN4 (17.75Ma) and has its last occurrence in the end of NN5 (13.53Ma). *D. exilis* appears in the base of NN4. H. ampliaperta has its top at the top of NN4 (14.86Ma) and is no longer present.

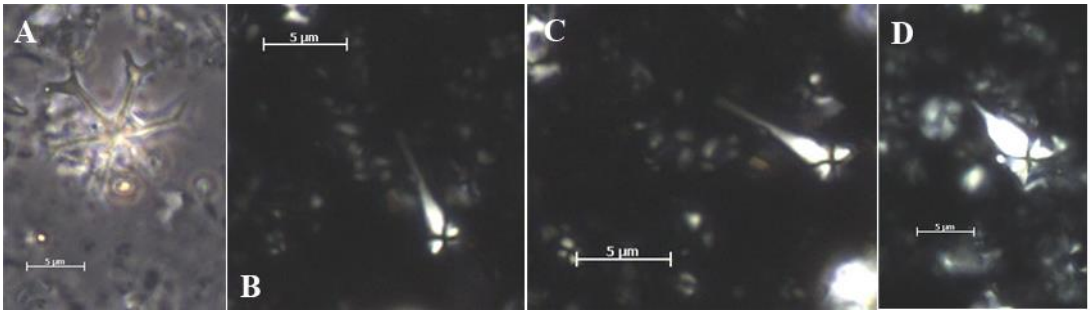

Figure A4-3 – A) *Discoaster exilis*; B, C and D) *Sphenolithus heteromorphus*.

SAMPLE 2-4 48-49

Species	Observations	Nanno Zone
Calcidiscus tropicus	Common	NN4-NN9
Calcidiscus macintyrei	Common	NN6-MIS 58
Coccolithus miopleagicus	Relatively common	NN5-NN8
Discoaster deflandrei	Relatively common	NP10-NN7
Discoaster exilis	Common	NN4-NN9

Sample 2-4 is within NN6 zone. The presence of *D. decorus* and *C. macintyrei* places this sample within NN6.

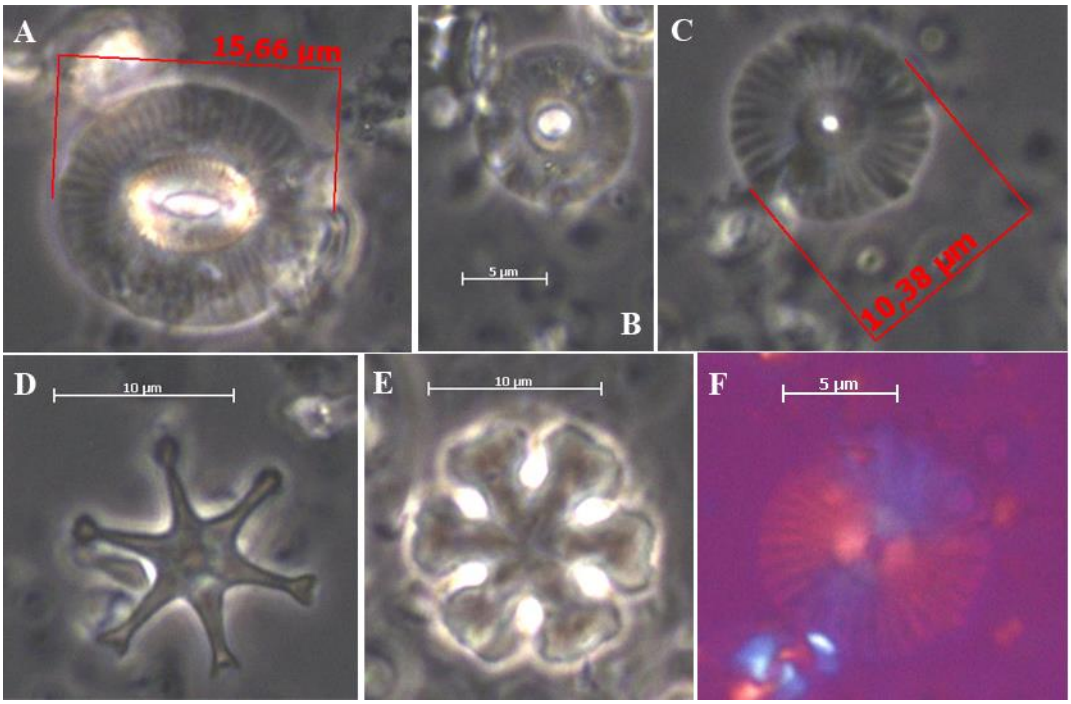

Figure A4-4 – A) *Coccolithus miopelagicus*; B) *Calcidiscus tropicus*; C and F) *Calcidiscus macintyrei*; D) *Discoaster exilis*; E) *Discoaster deflandrei*.

SAMPLE 2-2 48-49

Species	Observations	Nanno Zone
Discoaster kugleri	Common	Base of NN7 (CNM10)
Orthorhabdus rugosus	Common	NN6-NN12
Calcidiscus macintyrei	Common	NN6-MIS 58
Coccolithus miopleagicus	Relatively common	NN5-NN8
Discoaster deflandrei	Relatively common	NP10-NN7
Discoaster exilis	Common	NN4-NN9

Sample 2-2 is within NN7 zone. The presence of *D. kugleri* places this sample between 11.88Ma and 11.60Ma. The other species found do not represent any conflict with this zone.

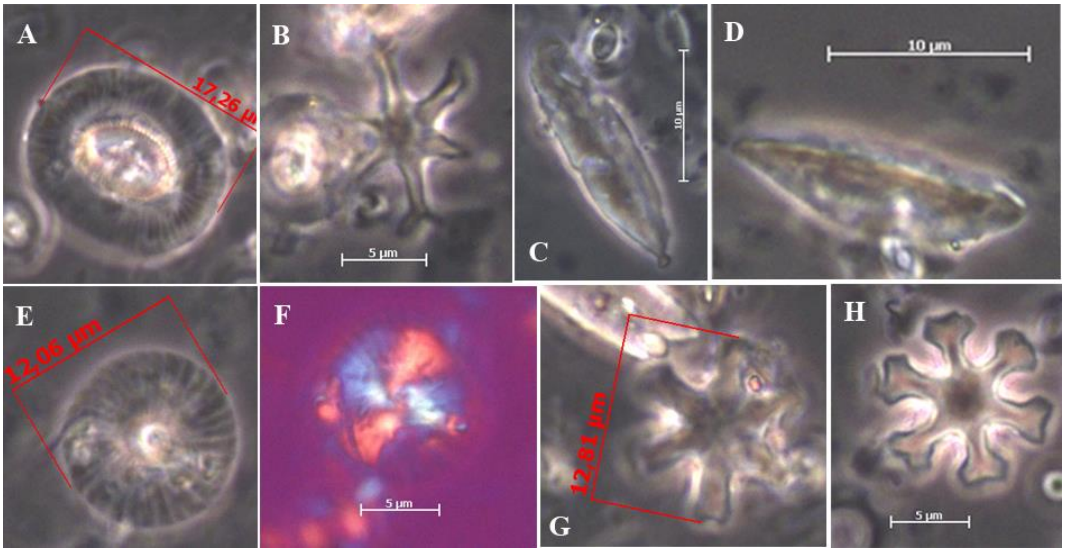

Figure A4-5 – A) *Coccolithus miopelagicus*; B) *Discoaster exilis*; C and D) *Orthorhabdus rugosus*; E and F) *Calcidiscus macintyrei*; G) *Discoaster kugleri*; H) *Discoaster deflandrei*.

Table A4-6 – Samples age attributed and samples resolution. Samples age was attributed crossing the biostratigraphy data with sedimentation rate from Lancelot et al. (1977).

Age (Ma)	Resolution (Ma)	Samples	Observations
11.62	0.09	A-2_1-48-49	
11.71	0.09	A-2_2-48-49	NN7
11.80	0.09	A-2_3-48-49	
11.89	0.09	A-2_4-48-49	NN6
11.98	0.09	A-2_5-48-49	
12.07	0.09	A-2_6-48-49	
12.16	0.09	A-3_1-48-49	
12.25	0.09	A-3_2-48-49	
12.34	0.09	A-3_3-48-49	
12.43	0.09	A-3_4-48-49	
12.52	0.09	A-3_5-48-49	
12.61	0.09	A-3_6-48-49	
12.69	0.09	A-4_1-48-49	
12.78	0.09	A-4_2-48-49	
12.87	0.09	A-4_3-48-49	
12.96	0.09	A-4_4-48-49	
13.05	0.09	A-4_5-48-49	
13.14	0.09	A-5_1-48-49	
13.23	0.09	A-5_2-48-49	
13.32	0.09	A-5_3-48-49	
13.41	0.09	A-5_4-48-49	
13.50	0.09	A-5_5-48-49	NN5
13.59	0.08	A-5_6-48-49	
13.68	0.17	A-6_1-48-49	
13.85	0.17	A-6_3-48-49	
14.01	0.17	A-6_5-48-49	
14.18	0.17	A-7_1-48-49	
14.35	0.17	A-7_3-48-49	
14.52	0.17	A-7_5-48-49	
14.69	0.17	A-8_1-48-49	
14.86	0.17	A-8_3-48-49	
15.03	0.17	A-8_5-48-49	
15.19	0.17	A-9_1-48-49	
15.36	0.17	A-9_3-48-49	NN4
15.53	0.29	A-9_5-48-49	
15.82	0.11	A-10_1-70-71	Has *Discoaster signus* – NN4
15.93	0.17	A-10_3-48-49	
16.10		A-10_5-48-49	NN4

Age Model of EOT site ODP1263

Table A4-7 – Age model and samples information for EOT site ODP1263.

Site	Core/Section	Interval	MBSF_TOP	MCD_TOP	Resolution (ka)	Resolution (Ma)	Age (Ma)
1263A	10H-3	120-121	82.5	94.29	8.73	0.008731	33.551
1263A	10H-3	130-131	82.6	94.39	8.73	0.008731	33.559
1263A	10H-3	140-141	82.7	94.49	8.73	0.008731	33.568
1263A	10H-4	0-1	82.8	94.59	8.73	0.008731	33.577
1263A	10H-4	10--11	82.9	94.69	8.73	0.008731	33.586
1263A	10H-4	20-21	83	94.79	9.60	0.009604	33.594
1263A	10H-4	31-32	83.11	94.9	7.86	0.007858	33.604
1263A	10H-4	40-41	83.2	94.99	7.86	0.007858	33.612
1263A	10H-4	49-50	83.29	95.08	9.60	0.009604	33.620
1263A	10H-4	60-61	83.4	95.19	9.60	0.009604	33.629
1263A	10H-4	71-72	83.51	95.3	8.73	0.008731	33.639
1263A	10H-4	81-82	83.61	95.4	8.73	0.008731	33.648
1263A	10H-4	90-91	83.71	95.5	7.86	0.007858	33.656
1263A	10H-4	100-101	83.8	95.59	8.73	0.008731	33.664
1263A	10H-4	110-111	83.9	95.69	8.73	0.008731	33.673
1263A	10H-4	120-121	84	95.79	8.73	0.008731	33.682
1263A	10H-4	130-131	84.1	95.89	9.60	0.009604	33.690
1263A	10H-4	141-142	84.21	96	7.86	0.007858	33.700
1263A	10H-5	0-1	84.3	96.09	8.73	0.008731	33.873
1263A	10H-5	11--12	84.4	96.19	8.73	0.008731	33.881
1263A	10H-5	20-21	84.5	96.29	8.73	0.008731	33.890
1263A	10H-5	30-31	84.6	96.39	16.67	0.016667	33.907

1263A	10H-5	40-41	84.7	96.49	16.67	0.016667	33.923
1263A	10H-5	50-51	84.8	96.59	16.67	0.016667	33.940
1263A	10H-5	60-61	84.9	96.69	16.67	0.016667	33.957
1263A	10H-5	70-71	85	96.79	21.67	0.021667	33.978
1263A	10H-5	80-81	85.13	96.92	11.67	0.011667	33.990
1263A	10H-5	95-96	85.2	96.99	16.67	0.016667	34.007
1263A	10H-5	100-101	85.3	97.09	16.67	0.016667	34.023
1263A	10H-5	110-111	85.4	97.19	16.67	0.016667	34.040
1263A	10H-5	120-121	85.5	97.29	25.00	0.025000	34.065
1263A	10H-5	131-132	85.65	97.44	35.00	0.035000	34.100
1263A	10H-6	6--7	85.86	97.65	35.00	0.035000	34.135
1263A	10H-6	27-28	86.07	97.86	38.33	0.038333	34.173
1263A	10H-6	50-51	86.3	98.09	41.67	0.041667	34.215
1263A	10H-6	75-76	86.55	98.34	41.67	0.041667	34.257
1263A	10H-6	100-101	86.8	98.59	66.67	0.066667	34.323
1263A	10H-6	140-141	87.2	98.99	33.33	0.033333	34.357
1263A	10H-7	10--11	87.4	99.19	8.33	0.008333	34.365
1263B	5H-1	55-56	84.55	99.24	16.67	0.016667	34.382

Results of increasing measurements to 200 per sample in Eocene ODP 1263

Table A4-8 – Morphotypes defined with 200 measurements for the Eocene ODP1263

Morphotypes C1					
4.0	5.1	6.2	8.5	9.6	10.5
Morphotypes C2					
4.0	8.1	9.2	17.7		
Morphotypes C3					
5.7	6.2	7.3	8.2	9.6	10.2

Table A4-9 – Variance extraction of the PCA applied to 200 measurements in Eocene ODP 1263.

Total Variance Explained						
Component	**Initial Eigenvalues**			**Extraction Sums of Squared Loadings**		
	Total	*% of Variance*	*Cumulative %*	*Total*	*% of Variance*	*Cumulative %*
1	1695.538	39.177	39.177	1695.538	39.177	39.177
2	1047.495	24.204	63.381	1047.495	24.204	63.381
3	441.114	10.192	73.573	441.114	10.192	73.573

Table A4-10 – Correlation between morphotype's counting's and PCA scores for Eocene ODP1263 with 200 measurements. In italic the values obtained with 100 measurements.

Interval (µm)	**Morphotype Component**	**Correlation with counting's**
4.0 – 5.1 ***(5.5 – 8.3)***	C1	0.78 *(-0.96)*
6.2 – 8.5 ***(9.4 – 19.8)***	C1	-0.85 *(0.93)*
9.6 – 10.5	C1	0.35
4.0 – 8.1 ***(8.1 – 9.3)***	C2	-0.93 *(-0.80)*
9.2 – 17.7 ***(10.4 – 12.8)***	C2	0.89 *(0.48)*
5.7 – 6.2	C3	-0.56
7.3 – 8.2	C3	0.67
9.6 – 10.2	C3	-0.50

IV. IMMA FUTURE DEVELOPMENTS

CHAPTER 5

Considerations on IMMA future development and microevolutionary studies on coccolithophores

Abstract

Applied to coccolithophore morphometry IMMA have a great potential for microevolutionary studies but there are still issues to be solved. For IMMA to properly work is important to answer: Is there a minimum number of samples needed? Which is the lowest resolution necessary? How many coccoliths must be measured in each sample? Should there be a fixed number of measurements or should these be performed in a defined area of the slides? To look for answers, new theoretical scenarios were designed and tested and the process automatized in an open source mathematical language software. Not all questions were answered, but new steps into the design of future work to develop IMMA were identified and will be targeted in the near future.

Keywords: IMMA; morphometry; coccolithophores; microevolution; future prospects

5.1 Introduction

Using *C. pelagicus* s.l. as the targeted species, IMMA results have shown a great potential for microevolutionary studies applied to coccolithophore morphometry. However the application of this new methodology to different Cenozoic periods highlighted some key issues in morphometric studies, and specifically regarding microevolution in calcareous nannoplankton.

Due to the short life cycle of coccolithophores, samples resolution plays a major role in evolutionary studies. Coccolithophores are able to produce morphometric responses to environmental conditions variations in very short time scales, more precisely at annual level, as shown in several recent works (Renaud & Klaas, 2001; Daniels et al., 2014; Gerecht et al., 2014, 2015; Šupraha et al., 2015; Sheward et al., 2014, 2016; Tsutsui et al., 2016). This presents an incredible challenge for palaeontological studies, since recovering samples with such high resolution grows towards impossibility as we go further back in time.

Quaternary data, which is easily obtained with resolution on the centennial or millennial time scale, provided the best results with IMMA, with the plasticity of *C. pelagicus* s.l. being easily extracted and observed from the data. Moreover, the results from IMMA applied to Quaternary samples from different regions of the North Atlantic are in close agreement with current knowledge on *C. p. pelagicus* and *C. p. braarudii*, proving that this methodology, when applied to high resolution samples, is able to produce reliable results. But, as demonstrated with the Eocene-Oligocene Transition (EOT) data, resolution is not all that matters.

The sample set of the EOT didn't have a resolution as high as the one from Quaternary samples, although it should be enough to provide some information on the size variability of *C. pelagicus* s.l. during that period. The fact that IMMA wasn't capable of extracting more information raised questions regarding the number of samples, the number of measurements, the (palaeo)conditions of the time interval covered and, of course, the minimum resolution needed.

The only possible test to be performed was to increase the number of measurements, since no more samples, either by increasing the time period covered or by increasing the resolution, when available. However, doubling the number of measurements per sample did not improve the information extracted by IMMA. In fact it made it even more confusing, strengthening the idea that there was simply too much going on during that

period, and that increasing the morphometric information was just increasing information on the data turmoil.

In a strange way, it was the Miocene that provided a possible explanation for what happened during the EOT interval. From the beginning it was known that the sample set of the Miocene had a resolution not compatible with microevolutionary studies. Looking into the Miocene samples was purely an exercise to improve knowledge of IMMA and help to better develop its skills. It was surprising when the Miocene results weren't even close to the EOT mess! Although no morphometric plasticity was observed in the Miocene set (as expected), the results were stable, with IMMA providing reliable information on the morphotypes present and their size evolution throughout the set of samples. How could a set of samples with a resolution near 100ka give better results than a set with a resolution more than 10 times lower?

More frequently than we usually recognize, we found our answers where we least expect. Both the EOT and the Miocene data sets are composed of 40 samples, so the number of samples is not influencing the outcome. The main difference between the two sets was the palaeoenvironmental conditions of the intervals covered. The Miocene was a set of samples covering the Miocene Climatic Optimum and part of its transition, located in the Canary Islands. So the Miocene set was characterized by a relatively stable period during an high temperature interval, followed by its transition and deterioration, which was more pronounced in mid and high latitudes, and more mild and progressive in lower latitudes (see Prista et al., 2015). This means that a relatively stable morphometric population of *C. pelagicus* s.l. most likely to be represented within this sample set, with primary productivity variability being the major source of morphometric responses, as discussed in Chapter 4.

The EOT set registers most probably the exact opposite. The time covered by the 40 samples is within the abrupt climate changes of this interval, from 33.55 to 34.38Ma, covering exclusively the high climatically disturbed interval (see Lear et al., 2008). This suggests that more than the resolution, the main reason why the data appears chaotic with the PCA, even increasing its chaos when the number of coccoliths measured is increased, is because the data is truly chaotic, although with some kind of structure that was roughly identified (see Chapter 4). It is highly probable that *C. pelagicus* s.l. underwent several distinct microevolutions and adaptations in several and even contradictory directions during this period, with global sea surface and deep temperature

rising and dropping several times (see e.g. Coxall et al., 2005; Miller et al., 2009; Houben et al., 2012), dramatic changes in palaeoproductivity (Diester-Haass & Zahn, 1996, 2001), eustatic variations (Miller et al., 2009), ocean circulation changes (Goldner et al., 2014), and a global climate change (Zachos et al., 2001, 2008; Katz et al., 2008; Liu et al., 2009). Thus, morphometric responses from coccolithophores must have been also multiple. With a short life cycle and a fast morphometric response, as seen with extant species, the samples resolution for this period not only would need to be much higher, but would probably be also highly dependent of two sets of samples: 1) a set previous but close to the EOT, to characterize *C. pelagicus* s.l. before the event; 2) a set immediately after the EOT, to define the *C. pelagicus* s.l. after the event. This would give information on from what to whom it had evolved and would isolate the more chaotic set of samples, while providing to the PCA with crucial information to untangle the morphometric data.

Despite all these reflections supported by the data and by the interpretation of this series of both theoretical and practical knowledge and experiences, the raised questions need to be further explored.

i) For IMMA to properly work is there a minimum number of samples needed?
ii) What kind of temporal resolution is necessary?
iii) How many coccoliths must be measured in each sample?
iv) Should there be a fixed number of measurements or should these be performed in a defined area of the slides?

To look for answers, new theoretical scenarios were designed and tested and the process of automatizing IMMA in open source mathematical language software was started.

5.2 Theoretical scenarios designed

Coccolithophores are usually described as having a normal distribution of its morphometric parameters (e.g. Bornemann & Mutterlose, 2006; Henderiks, 2008; Tsutsui & Takahashi, 2011). For that reason a theoretical population with two morphotypes was defined with a normal truncated distribution, written with Python language using Spyder – The Scientific Python Development Environment, and

assuming an abundant presence of the species (equivalent to 36.000 coccoliths per slide).

From this theoretical population several scenarios were drawn (IMMA was run with SPSS method – Chapter 2):

- 100 measurements on a total of 25 and 150 samples with exclusive presence of the morphotypes (25S_100m_NE; 150S_100m_NE);
- 100 measurements on a total of 25 and 150 samples with 10% error on the population (10% of the coccoliths out of the morphotypes boundaries predefined in the population) (25S_100m_10%; 150S_100m_10%);
- 100 measurements on a total of 25 and 150 samples with 40% error on the population (40% of the coccoliths out of the morphotypes boundaries predefined in the population) (25S_100m_40%; 150S_100m_40%);
- Variable number of measurements per slide on a total of 150 samples with 10% error on the population (10% of the coccoliths out of the morphotypes boundaries predefined in the population), creating a simulation of measuring in a certain area instead of a fixed number of coccoliths (150S_VARm_10%);

5.3 Results

5.3.1 25S_100m_NE and 150S_100m_NE

The results for both distributions with no error were similar to what was demonstrated in Chapter 2. (see Table 5.1).

Table 5.1 – Results for PCA on theoretical matrixes 25S_100m_NE and 150S_100m_NE

	25 Samples		**100 measurements**		**150 Samples**		**100 measurements**	
	REAL				**REAL**			
Predefined	4.3	8.7	10.5	13.6	4.3	8.7	10.5	13.6
	SPSS				**SPSS**			
	4.5	8.6	10.6	13.5	4.4	8.6	10.6	13.5
Difference for real	*0.2*	*-0.1*	*0.1*	*-0.1*	*0.1*	*-0.1*	*0.1*	*-0.1*
Error %	*4.65*	*1.15*	*0.95*	*0.74*	*2.33*	*1.15*	*0.95*	*0.74*

5.3.2 25S_100m_10% and 150S_100m_10%

Comparing 25 to 150 samples with 10% error on the data brought major differences between them. With only 25 samples analysis presented an error in the definition of the morphotypes boundaries ranging from 0.3µm to 1.0µm, much higher than the one given with 150 samples. For 150 samples, PCA presented much better results, with errors ranging from 0 to 0.3µm. (see Table 5.2).

Table 5.2 – Results for SPSS and Python on theoretical matrixes 25S_100m_10% and 150S_100m_10%

	25 Samples		**100 measurements**		**150 Samples**		**100 measurements**	
			REAL				**REAL**	
Predefined	4.3	8.7	10.5	13.6	4.3	8.7	10.5	13.6
			SPSS				**SPSS**	
	3.3	9.7	10.8	14.1	4.2	8.4	10.6	13.6
Difference for real	*-1*	*1*	*0.3*	*0.5*	*-0.1*	*-0.3*	*0.1*	*0*
Error %	*23.26*	*11.49*	*2.86*	*3.68*	*2.33*	*3.45*	*0.95*	*0.00*

5.3.3 25S_100m_40% and 150S_100m_40%

When increasing the error on the theoretical matrix, the lower number of samples performed better and achieved better results in the identification of the morphotypes boundaries, although not for all limits, as can been seen in Table 5.3.

Table 5.3 – Results for SPSS and Python on theoretical matrixes 25S_100m_40% and 150S_100m_40%

	25 Samples		**100 measurements**		**150 Samples**		**100 measurements**	
			REAL				**REAL**	
Predefined	4.3	8.7	10.5	13,6	4.3	8.7	10.5	13.6
			SPSS				**SPSS**	
	4.5	8.5	9.6	13.5	4.5	9.1	10.2	15.2
Difference for real	*0.2*	*-0.2*	*-0.9*	*-0.1*	*0.2*	*0.4*	*-0.3*	*1.6*
Error %	*4.65*	*2.30*	*8.57*	*-0.74*	*4.65*	*4.60*	*2.86*	*11.76*

5.3.4 150S_VARm_10%

The variable measurements were obtained using the 150S_100m_10% and running RAND() function in Excel. If the random number was below 0.5 it was be considered 0 (this limit was varied to 0.4 and 0.6 to generate higher variability). Above would equal 1. This was done in a total of 100 lines in 20 columns. This matrix of 0s and 1s was then multiplied by the morphometric data in the 150S_100m_10%. The result was a new

morphometric data with variable measurements in each sample, minimum of 34 and maximum of 64, with an average of 48.7 measurements per sample.

A PCA was applied to this matrix in SPSS. The results were similar to the results for 150S_100m_10% regarding the upper boundary of the smaller morphotype and the lower limit of the larger (Table 5.4). In the other boundaries the results were in between 25S_100m_10% and 150S_100m_10% for the lower limit of the smaller morphotype, and closer to 25S_100m_10% for the upper limit of the larger one.

Table 5.4 – SPSS results for theoretical matrix 150S_VARm_10%

	150 Samples		**VAR measurements**	
			REAL	
Predefined	4.3	8.7	10.5	13.6
			SPSS	
	3.8	8.5	10.6	14.4
Difference for real	*-0.5*	*-0.2*	*0.1*	*0.8*
Error %	*11.63*	*2.30*	*0.95*	*5.88*

5.4 Discussion

The use of Python improved the ability to produce theoretical matrixes, not only by predefining them with a specific statistical distribution but also by reducing the time expend in generating them.

These scenarios focused on morphotype limit determination by varying the number of samples and/or measurements. Pure matrixes were only performed with the IMMA current pattern of 100 measurements per slide, since this type of scenario is unreal and only serves for the purpose of testing the methodology. In that sense the number of samples appeared to have some influence, since there was a better performance with 150 samples in the determination of the lower limit of the smaller morphotype. But besides that limit, all the other three were determined equally by 25 and 150 samples.

When 10% error was introduced the set with 150 samples performed much better and the differences for the set with only 25 samples were significant. But with 40% error it is hard to select which one gave better results. 25 samples performed better in the upper limits of both morphotypes, while 150 samples was more accurate with the lower limit of the larger morphotype. The lower limit of the smaller morphotype was determined with the same error by both sets.

When variation was introduced in the number of measurements per slide to the 150S_100m_10% the error in the determination of the morphotypes increased. However this variation consisted only in reducing the number of measurements, with no sample over 64 measurements. These results pointed to the importance of the number of measurements. After all, just by decreasing the number of measurements the limits determination performed worst.

To understand the impact of measurements per sample a simulation was made by varying the number of measurements per sample and looking into the effects on variance extracted. This simulation was performed with 25, 75 and 150 samples to observe the combined effects of number of measurements and number of samples (Fig. 5.1, Fig. 5.2 and Fig. 5.3).

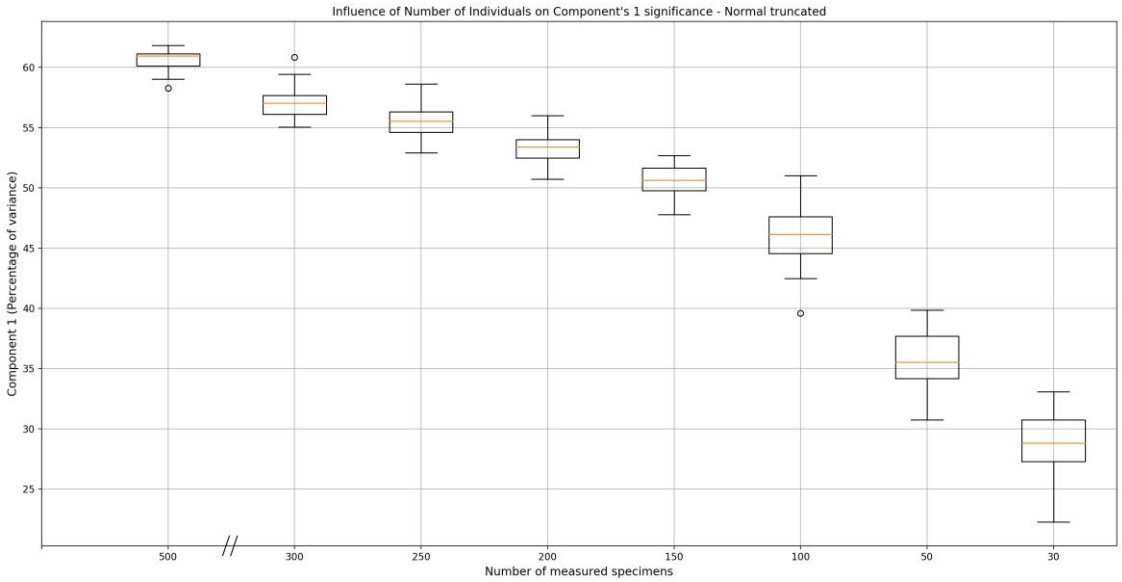

Figure 5.1 – Effect of number of measurements per sample in the percentage of variance extracted by component one in a normal truncated distribution with a total of 25 samples (note: there is a change in the scale of the abscissas - //).

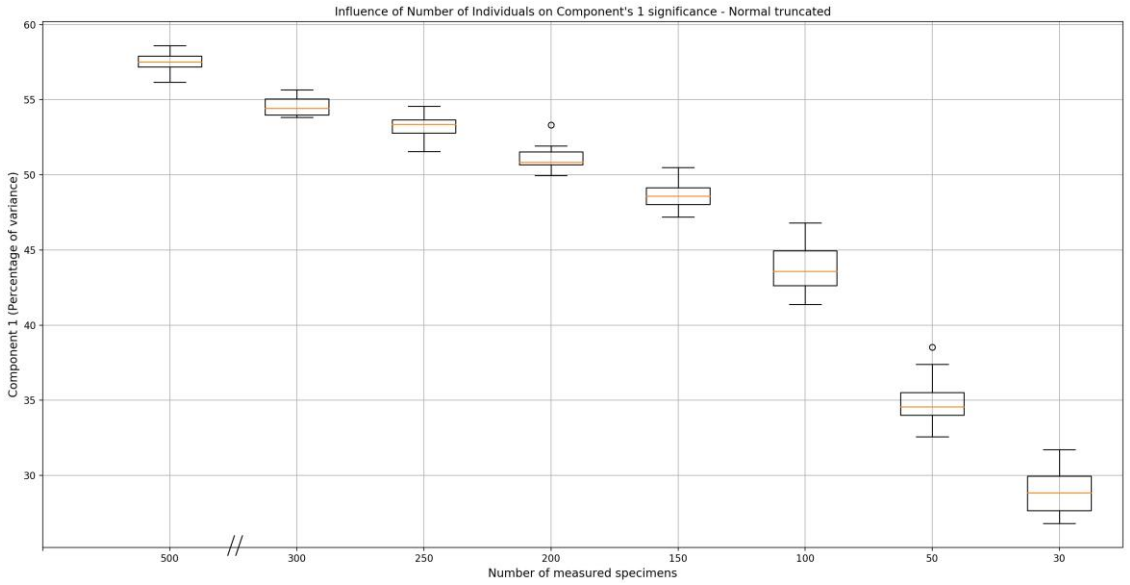

Figure 5.2 – Effect of number of measurements per sample in the percentage of variance extracted by component one in a normal truncated distribution with a total of 75 samples (note: there is a change in the scale of the abscissas - //).

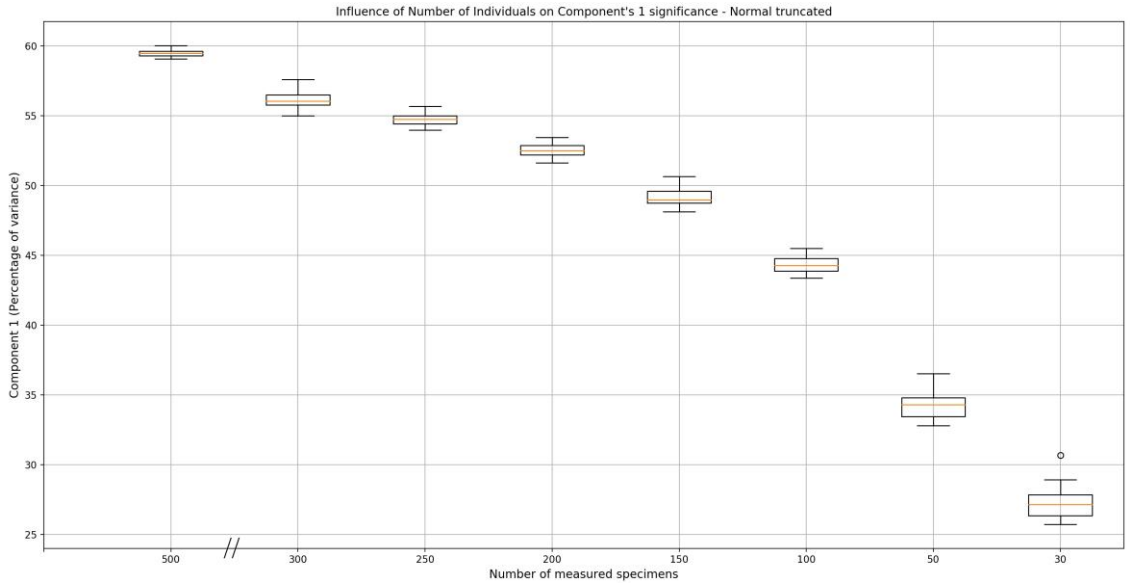

Figure 5.3 – Effect of number of measurements per sample in the percentage of variance extracted by component one in a normal truncated distribution with a total of 150 samples (note: there is a change in the scale of the abscissas - //).

The analysis brings two conclusions. The first one that it seems that 100 measurements per slide marks the point were variance extraction drops at a faster rate. The slope has a slower progression (declination) from 500 to 150 measurements. From 150 to 100 slightly increases its declination and from 100 below it drops quickly. So according to this test, 100 measurements per slide seem to be the minimum number of measurements to achieve reliable results.

The second conclusion regards the number of samples. Increasing the number of samples does not seem to improve the extraction of information. By the contrary, it progressively reduces the variance extracted, something already noticed by Henderiks & Törner (2006). However, as shown in Chapter 4 and commented in this chapter, increasing the number of measurements wont always result in better/more information extraction. Working with complex systems, which are ruled by biological and physical factors, forces to always look further. In the case of fossil coccoliths, we need to evaluate the palaeoenvironmental scenario, the sediment and depositional conditions, the resolution of the samples, the abundance of the species we are studying, among other factors that may be relevant for each particular case.

IMMA was born recently. It is still starting to crawl. It is showing a high potential for microevolutionary studies but it still needs to be tuned. To teach IMMA to walk we still need to run some tests, both with theoretical and real data. The next step would be to develop theoretical matrixes with size variability within the morphotypes, together with a simulated resolution, i.e., a stack of samples where the morphotypes vary their sizes according to certain parameters, with this variation being realistically oscillating throughout the samples. If a stack of, e.g., 150 samples were produced this way, IMMA could be tested for resolution by applying it to the entire set and to subsets of scattered samples.

One other relevant question is fixed number of measurements per sample or should the measurements be performed within a certain area of the slide? As seen above, measuring less than 100 coccoliths reduces the extraction of variance and thus reduces the morphometric information of the species under study. However a fixed number of coccoliths produce spurious negative correlations between morphotypes, since every time one increases its number of measurements, the other one must decrease.

The most likely solution for this issue would probably be defining a minimum area to obtain measurements and adjust it when coccolith counting's are low. For example, defining three rows of a slide as the total area where coccoliths will be measured. If by the end of these three rows the total of coccoliths measured is close or over 100, that slide is finished. If not, another row should be added. Although it may end up consuming more time and effort, it will also retrieve information on the abundance of the specie(s) being studied, which is also crucial information.

5.5 Conclusions

IMMA shows great potential for microevolutionary studies of coccolithophores, presenting it self as a new tool for micropalaeontology and palaeoceanography studies, as well as for improving our knowledge on coccolithophores evolution and behaviour.

Studying coccolithophore morphometry is a time demanding task. However it is clear that one should aim to a minimum of 100 measurements per slide, and that increasing the number of samples usually has no positive impact. Exceptions may be in cases where increasing the resolution is highly important or where characterizing previous and further periods is crucial.

There are still some aspects to be developed. It could be important to make IMMA the most automatized possible, by using open source software (like Spyder and with Python language), thus facilitating other researchers to work with microevolution of coccolithophores. Currently it is still a time consuming tool, since it demands the preparation of all data in Excel and then run it in SPSS, for example. Having it programed and able to import the morphometric data from an Excel or Text file, and run IMMA completely, saving the PCA data and producing graphics would make it not only more friendly but also more easy to share with other colleagues interested in looking for microevolution of coccolithophores.

The development of an automatized IMMA is already in motion, although, as seen in this chapter, there is still some work to be done.

References

Bornemann, A., Mutterlose, J., 2006. Size analyses of the coccolith species *Biscutum constans* and *Watznaueria barnesiae* from the Late Albian "Niveau Breistroffer" (SE France): taxonomic and palaeoecological implications. Geobios 39, 599–615. doi:10.1016/j.geobios.2005.05.005

Coxall, H.K., Wilson, P.A., Pälike, H., Lear, C.H., Backman, J., 2005. Rapid stepwise onset of Antarctic glaciation and deeper calcite compensation in the Pacific Ocean. Nature 433, 53–57. doi:https://doi.org/10.1038/nature03135

Daniels, C.J., Sheward, R.M., Poulton, A.J., 2014. Biogeochemical implications of comparative growth rates of *Emiliania huxleyi* and *Coccolithus* species. Biogeosciences 11, 6915–6925. doi:10.5194/bg-11-6915-2014

Diester-Haass, L., Zahn, R., 1996. Eocene-Oligocene transition in the Southern Ocean: History of water mass curculation and biological productivity. Geology 24, 163–166. doi:10.1130/0091-7613(1996)024<0163:EOTITS>2.3.CO

Diester-Haass, L., Zahn, R., 2001. Paleoproductivity increase at the Eocene - Oligocene climatic transition: ODP/DSDP sites 763 and 592. Palaeogeogr. Palaeoclimatol. Palaeoecol. 172, 153–170. doi:10.1016/S0031-0182(01)00280-2

Gerecht, A.C., Šupraha, L., Edvardsen, B., Langer, G., Henderiks, J., 2015. Phosphorus availability modifies carbon production in *Coccolithus pelagicus* (Haptophyta). J. Exp. Mar. Bio. Ecol. 472, 24–31. doi:10.1016/j.jembe.2015.06.019

Gerecht, A.C., Šupraha, L., Edvardsen, B., Probert, I., Henderiks, J., 2014. High temperature decreases the PIC / POC ratio and increases phosphorus requirements in *Coccolithus pelagicus* (Haptophyta). Biogeosciences 11, 3531–3545. doi:10.5194/bg-11-3531-2014

Goldner, A., Herold, N., Huber, M., 2014. Antarctic glaciation caused ocean circulation changes at the Eocene-Oligocene transition. Nature 511, 574–577. doi:10.1038/nature13597

Henderiks, J., 2008. Coccolithophore size rules — Reconstructing ancient cell geometry and cellular calcite quota from fossil coccoliths. Mar. Micropaleontol. 67, 143–154. doi:10.1016/j.marmicro.2008.01.005

Henderiks, J., Törner, A., 2006. Reproducibility of coccolith morphometry: Evaluation of spraying and smear slide preparation techniques. Mar. Micropaleontol. 58, 207–218. doi:10.1016/j.marmicro.2005.11.002

Houben, A.J.P., van Mourik, C. a., Montanari, A., Coccioni, R., Brinkhuis, H., 2012. The Eocene–Oligocene transition: Changes in sea level, temperature or both? Palaeogeogr. Palaeoclimatol. Palaeoecol. 335–336, 75–83. doi:10.1016/j.palaeo.2011.04.008

Katz, M.E., Miller, K.G., Wright, J.D., Wade, B.S., Browning, J. V., Cramer, B.S., Rosenthal, Y., 2008. Stepwise transition from the Eocene greenhouse to the Oligocene icehouse. Nat. Geosci. 1, 329–334. doi:10.1038/ngeo179

Lear, C.H., Bailey, T.R., Pearson, P.N., Coxall, H.K., Rosenthal, Y., 2008. Cooling and ice growth across the Eocene-Oligocene transition. Geology 36, 251. doi:10.1130/G24584A.1

Liu, Z., Pagani, M., Zinniker, D., Deconto, R., Huber, M., Brinkhuis, H., Shah, S.R., Leckie, R.M., Pearson, A., 2009. Eocene-Oligocene Climate Transition. Science (80-.). 323, 1187–1190.

Miller, K.G., Wright, J.D., Katz, M.E., Wade, B.S., Browning, J. V, Cramer, B.S., Rosenthal, Y., 2009. Climate threshold at the Eocene-Oligocene transition: Antarctic ice sheet influence on ocean circulation, in: Koeberl, C., Montanari, A. (Eds.), The Late Eocene Earth - Hothouse, Icehouse, and Impacts. Geological Society of America Special Paper 452, pp. 169–178. doi:10.1130/2009.2452(11).

Prista, G.A., Agostinho, R.J., Cachão, M.A., 2015. Observing the past to better understand the future: a synthesis of the Neogene climate in Europe and its perspectives on present climate change. Open Geosci. 7, 65–83. doi:10.1515/geo-2015-0007

Renaud, S., Klaas, C., 2001. Seasonal variations in the morphology of the coccolithophore *Calcidiscus leptoporus* off Bermuda (N . Atlantic). J. Plankton Res. 23, 779–795. doi:10.1093/plankt/23.8.779

Sheward, R.M., Daniels, C.J., Gibbs, S.J., 2014. Growth rates and biometric measurements of coccolithophores (*Coccolithus pelagicus*, *Coccolithus braarudii*, *Emiliania huxleyi*) during experiments, PANGAEA, http://doi.pangaea.de/10.1594/ PANGAEA.836841.

Sheward, R.M., Poulton, A.J., Gibbs, S.J., Daniels, C.J., Bown, P.R., 2016. Physiology regulates the relationship between coccosphere geometry and growth phase in coccolithophores. Biogeosciences Discuss. 14, 1493–1509. doi:10.5194/bg-14-1493-2017

Šupraha, L., Gerecht, A.C., Probert, I., Henderiks, J., 2015. Eco-physiological adaptation shapes the response of calcifying algae to nutrient limitation. Sci. Rep. 5, 16499. doi:10.1038/srep16499

Tsutsui, H., Takahashi, K., 2011. Cell size variation of *Anoplosolenia brasiliensis* (calcareous nannoplankton) in the central equatorial Pacific Ocean. 九州大学大学院理学研究院紀要 Ser. D, Earth Planet. Sci. XXXII, 27–38.

Tsutsui, H., Takahashi, K., Asahi, H., Jordan, R.W., Nishida, S., Nishiwaki, N., Yamamoto, S., 2016. Nineteen-year time-series sediment trap study of *Coccolithus pelagicus* and *Emiliania huxleyi* (calcareous nannoplankton) fluxes in the Bering Sea and subarctic Pacific Ocean. Deep. Res. Part II Top. Stud. Oceanogr. 125–126, 227–239. doi:10.1016/j.dsr2.2016.02.005

Zachos, J., Pagani, M., Sloan, L., Thomas, E., Billups, K., 2001. Trends, rhythms, and aberrations in global climate 65 Ma to present. Science 292, 686–93. doi:10.1126/science.1059412

Zachos, J.C., Dickens, G.R., Zeebe, R.E., 2008. An early Cenozoic perspective on greenhouse warming and carbon-cycle dynamics. Nature 451, 279–83. doi:10.1038/nature06588

The most important teaching of all scientific achievements is that all is interconnected in the Universe, and evolution is one of the most striking evidences of it.